

NS/rk

U. S. NAVAL TECHNICAL MISSION TO JAPAN
CARE OF FLEET POST OFFICE
SAN FRANCISCO, CALIFORNIA

31 January 1946

RESTRICTED

From: Chief, Naval Technical Mission to Japan.
To : Chief of Naval Operations.

Subject: Target Report - Characteristics of Japanese Naval
Vessels, Article 9 - Underwater Protection.

Reference: (a) "Intelligence Targets Japan" (DNI) of 4 Sept. 1945.

1. Subject report, dealing with Targets S-01 and S-05 of
Fascicle S-1 of reference (a), is submitted herewith.

2. The investigation of the target and the target report
were accomplished by Lieut. J. R. Morgan, RN.



C. G. GRIMES
Captain, USN

RESTRICTED

S-01-9

CHARACTERISTICS OF JAPANESE NAVAL VESSELS
ARTICLE 9
UNDERWATER PROTECTION

"INTELLIGENCE TARGETS JAPAN" (DNI) OF 4 SEPT. 1945
FASCICLE S-1, TARGETS S-01 AND S-05

JANUARY 1946

U.S. NAVAL TECHNICAL MISSION TO JAPAN

SUMMARY

SHIP AND RELATED TARGETS

CHARACTERISTICS OF JAPANESE NAVAL VESSELS ARTICLE 9 - UNDERWATER PROTECTION

This report is primarily concerned with experimental work done by the Japanese on underwater explosions.

In underwater side protection, the Japanese had developed empirical formulae for the thickness of protective bulkheads and bulge widths. These formulae were used with considerable confidence, since they were based on model and full scale experiments.

They had arrived at systems differing considerably from both U.S. and British with regard to methods of protection. When using liquid layers, which they considered to be the best, they placed them next to the protective bulkhead because their model experiments had shown this to be advantageous.

In some ships, such as YAMAMOTO, the air layer method was still used because the protection was essentially designed against diving shells. The bulges were then considered to be adequately strong without water layer protection.

A theory for the failure of submarine hulls, based on the relation between period of vibration of the hull and the duration of the pressure pulse, was developed. This theory was considered to have success practically, but was still some distance from the truth.

It should be noted that all charges used were of picric acid and the maximum charge against which protection had to be designed was considered about 500 kilograms.

TABLE OF CONTENTS

Summary	Page	I
List of Enclosures	Page	2
Introduction	Page	3
The Report		
Part I-A Summary of Reports on Experimental Side Protection (Translation)	Page	5
Part I-B Summary of Reports on Experimental Protection of Ships' Bottoms (Translation)	Page	79
Part II Strength of Submarines Against Depth Charges (Translation)	Page	121

LIST OF ENCLOSURES

(A) Part I Report of Mine and Torpedo Tests in Battleship TOSA ..	Page	191
Part II Announcement of Torpedo and Mine Tests	Page	202
(B) Summary of Tests on V Warheads	Page	211
(C) Charts of Developments of Tests on Underwater Defense (in Japan)	Page	217
(D) Discussion on the Use of Protective Plating Against Torpedo Attack	Page	221
(E) Experiments for Determining the Strength of Submarine Hull Models Against Depth Charges at Great Depths	Page	243
(F) The Effect of Opening and Closing of Kingston Valves on the Resistance of Submarine Pressure Hulls to Depth Charges	Page	251
(G) Testing Strength of Submarine Tanks Against Underwater Explosions	Page	263
(H) Model Experiments Testing the Strength of Submarine Hulls Against Underwater Explosions	Page	293
(I) Various Experiments Not Covered in the Translated Reports	Page	313
(J) List of Documents Forwarded Via ATIS to Washington Document Center	Page	315

INTRODUCTION

The main body of the report consists of the translation of three reports which are summaries of Japanese ideas and experiments. Since they contained much experimental evidence, it was considered advisable to include them wholly and without comment. In addition to these three principal reports, translations of various other reports on these subjects have been included. To avoid the verbosity which is present in all Japanese reports, parts have been summarized, but all experimental theoretical work has been included.

The Japanese had been working continuously with model experiments since 1935, and in having this organized they were several years ahead of the United States and Great Britain. Because of the limited personnel engaged in this work, they had not developed any very unusual methods, but their theoretical approach to submarine hull failure was essentially different from any the author has seen.

In the Japanese report on the strength of submarine hulls, a considerable portion has been devoted to the apparatus used in studying the phenomena associated with underwater explosions. The most significant of these was the cathode ray oscillograph and the electrical devices for its calibration.

PART I-A

SUMMARY OF REPORTS ON EXPERIMENTAL SIDE PROTECTION
(Translation)

TABLE OF CONTENTS

Chapter I	General Discussion of Contact Explosions and Protection of Ships' Sides	Page 8
Chapter II	Protective Methods Using Air Layers Only	Page 17
Chapter III	Protection Using Water Layers Only	Page 31
Chapter IV	Protective Methods Employing Protective Piping	Page 45
Chapter V	The Effect of the Volume of the Air Layer Outside the Protective Plate on the Protective Strength and the Size of the Experimental Target	Page 45
Chapter VI	Actual Examples of Area of Holes in Outer Skin and Amount of Leakage Caused by Underwater Explosions on a Ship's Side	Page 50
Chapter VII	Relation Between Depth of Explosive and Protective Strength	Page 53

LIST OF APPENDICES

Appendix I	Experimental Data Involving Air and Water Layers and Protective Piping	Page 55
Appendix II	Data for Calculation of Protective Strength	Page 67
Appendix III	Underwater Protection Systems in Various Combatant Ships	Page 71

LIST OF ILLUSTRATIONS

Figure 1	Results of Investigations and Experimentation of the Cause and Spreading of Splinters	Page 9
Figure 2	Splinter Dispersion and Damage to Protective Plate	Page 10
Figure 3	Protective Measures Utilizing a Water Layer	Page 11
Figure 4	Splinter Damage to Protective Plate - 200 kg Explosive	Page 12
Figure 5	Splinter Damage to Protective Plate - 400 kg Explosive	Page 13
Figure 6	Protective Methods Utilizing Protective Pipes	Page 14
Figure 7	Test Using Protective Pipes - 350 kg Explosive	Page 15
Figure 8	Holding Bulkhead Support	Page 16
Figure 9	Sharp Angle Connection	Page 16
Figure 10	Single Plate Protective Methods - Straight Type	Page 16
Figure 11	Single Plate Protective Methods - Straight Type	Page 16
Figure 12	Single Plate Protective Methods - Curved Type	Page 16
Figure 13	Multiple Thin Protective Plates	Page 18
Figure 14	Results of Comparative Experiments Between Single Plate and Multiple Plate Methods	Page 19
Figure 15	Standard Izod Test Values for Ducol Steel Plate	Page 20
Figure 16	Results of Comparative Experiments on CNC and DS	Page 21
Figure 17	Armored Joints with Butt Straps	Page 23
Figure 18	Thickness of Armor - Single and Multiple Plates	Page 28
Figure 19	Multiple Plate Test	Page 29
Figure 20	Correct and Incorrect Flooding of Voids	Page 32
Figure 21	Results of Correct and Incorrect Flooding of Voids	Page 32
Figure 22	Results of Various Percentages of Void Flooding	Page 32
Figure 23	Fuel Oil vs. Water in Voids	Page 32
Figure 24	Types of Protection Using Water Layers	Page 34
Figure 25	Relation of d_a and d_w	Page 34
Figure 26	Multiple Plate Arrangement Showing Minimum Plate Interval	Page 34
Figure 27	Explosion Vented to Atmosphere	Page 35
Figure 28	Single Plate Protective Bulkheads	Page 35
Figure 29	Calculation of C for Curved Type Bulkhead	Page 38

Figure 30	Water Layer Positions	Page 38
Figure 31	Graph of Defensive Strength (da/D vs. C)	Page 40
Figure 32	da and dw for Multiple and Single Layer Systems	Page 41
Figure 33	Multi-layer System - Oil Used from Outboard	Page 41
Figure 34	Multi-layer System - Increase of da with Use of Oil	Page 41
Figure 35	Liquid Layer Arrangements	Page 42
Figure 36	Air Layers Adjacent to Protective Bulkhead	Page 42
Figure 37	Results of Experiments Establishing Effectiveness of Air Layer Position	Page 43
Figure 38	Results of Experiments Establishing Effectiveness of Air Layer Position	Page 44
Figure 39	Air Only vs. Air with Oil Adjacent	Page 47
Figure 40	Scale Model Dimensions	Page 48
Figure 41	Comparison of 1/2.97 and Full-Scale Models	Page 49
Figure 42	TOSA - Typical Hole in Outer Skin	Page 52
Figure 43	TOSA - Length of Flooding	Page 52
Figure 44	Air Layers - Comprehensive Chart of Experimental Data	Page 58
Figure 45	Water Layers - Comprehensive Chart of Experimental Data ...	Page 62
Figure 46	Protective Piping - Comprehensive Chart of Experimental Data	Page 65
Figure 47	Curves for Calculation of Protective Strength When Using Air Layers Only	Page 67
Figure 48	Nomograph for Calculation of Protective Strength When Using Air Layers Only	Page 68
Figure 49	Curves for Determining Effective Thickness of Protective Plate When Water Layers Are Used	Page 69
Figure 50	Underwater Protection System - BB YAMATO	Page 71
Figure 51	Underwater Protection System - CV AKAGI (converted)	Page 72
Figure 52	Underwater Protection System - BB NAGATO	Page 73
Figure 53	Underwater Protection System - CV SHOKAKU	Page 74
Figure 54	Underwater Protection System - CV TAIHO	Page 75
Figure 55	Underwater Protection System - BISMARCK (German)	Page 76
Figure 56	Underwater Protection System - BB COLORADO (U.S.)	Page 77

CHAPTER I
GENERAL DISCUSSION OF CONTACT EXPLOSIONS AND PROTECTION OF SHIPS' SIDES

A. The Causes and Resultant Damage to Protective Bulkhead From Underwater Explosions

A contact side explosion causes the structure in the immediate vicinity to break up into various shaped fragments, some of which have knife-like edges. These strike the protective bulkhead, where those with high velocities may cause holes. Concentration of fragments, combined with the direct impact of explosion gases, destroys the protective bulkhead. (It has been confirmed by experiment that the fragments described above result from the destruction of the surrounding structure.)

Conclusions and results reached from a study of side protection against torpedoes carried out on 3 May 1932 by the Naval Technical Laboratory follow (see Figure 1):

Test No. 1 - to determine whether scratches on the surface of the protective bulkhead are caused by the flame produced at the time of the explosion: The head of the projectile was made of thin wood and the part of the outer bottom which the head of the projectile strikes was made of celluloid. No scars were found on the surface of the protective bulkhead.

Test No. 2 - to confirm that the head of the projectile breaks up into many small high velocity fragments: The head of the projectile was made of steel and the outer bottom of celluloid. After the explosion, the surface of the protective bulkhead had many small specks scattered over it having a luster-like appearance, but no large scars.

Test No. 3 - to determine whether the scars found on the protective bulkhead were due to fragments from the surrounding structure: The head of the projectile was made of wood and the outer bottom of steel. The protective bulkhead showed deeply scarred indentations and holes of wormwood appearance. These holes were scattered in a circular area around the center of the explosion. Some fragments of the outer bottom were embedded in the plate.

Test No. 4 - for comparison with Test No. 3 a steel hemisphere was attached to the projectile head and the outer bottom was made of steel: The resultant damage was only an indentation caused by the hemisphere. Scars from splinters were not found.

The formation of large fragments from the outer bottom was rare. When formed, they struck the protective bulkhead causing an impression of the hemisphere and a scale-like scar similar to the bark of a pine tree. In such cases no splinter scars could be found. Large fragments from the outer bottom were wrinkled, and, when flattened by pressure, were in one piece. Furthermore, their shape and size was impressed on the surface of the protective bulkhead.

The results of these tests clearly indicate that scars on the protective bulkhead are caused by splinters from the structure in the vicinity of the explosion. The speed of the splinters is unaffected materially by the width of the air space. The force of the explosion in the usual method of protection (about 10' wide) has considerable destructive power.

As protective measures, pipes or water layers may be used to stop these splinters. However the resistance of the bulge to a given attack is thereby increased because the concussion is distributed over a large area of the pro-

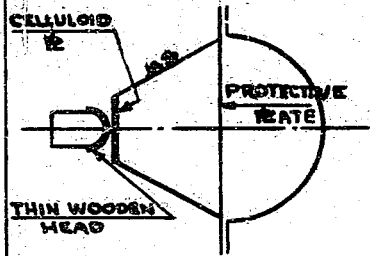
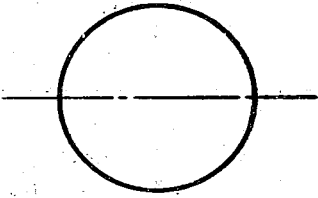
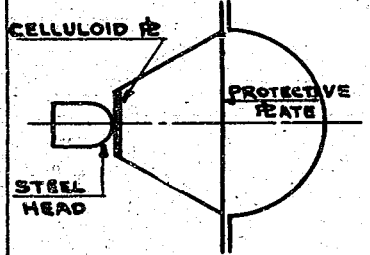
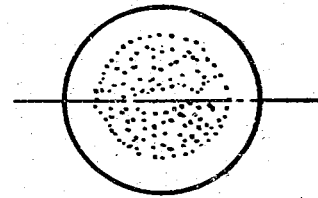
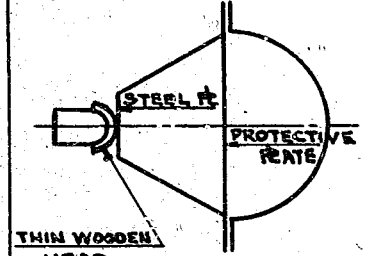

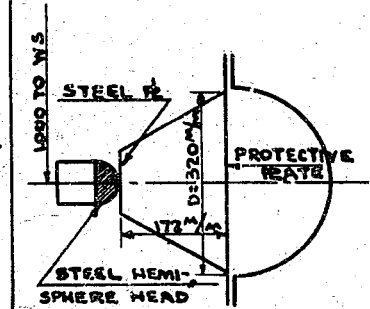
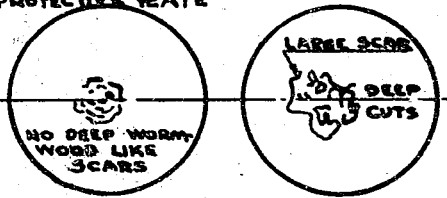
TEST NO.	MAIN POINTS OF TEST	CONDITION OF DAMAGED PROTECTIVE PLATE
NO. 1		 <p>NO DAMAGE</p>
NO. 2		 <p>SMALL SCATTERED SPECKS WITH PEARL-LIKE LUSTER CAUSED.</p>
NO. 3		 <p>SCARS OF WORM-WOOD LIKE APPEARANCE</p> <p>SMALL HOLES</p> <p>LACERATED SCAR</p> <p>LARGE SCAR OF WORM-WOOD LIKE APPEARANCE & SMALL HOLES WERE CAUSED & DEEP CUTS WERE APPARENT IN PLATE SURFACE.</p>
NO. 4		<p>NO DEEP WORM-WOOD LIKE SCARS. THE OUTER 2 SHOWS FOLDED SCARS & WHEN FLATTENED BECOMES A LUMP & COINCIDES EXACTLY WITH IMPRESSIONS IN PROTECTIVE PLATE</p> <p>DIAGRAM FRAG. OF OUTER PLATE</p>  <p>NO DEEP WORM-WOOD LIKE SCARS</p> <p>LARGE SCARS</p> <p>DEEP CUTS</p>

Figure 1

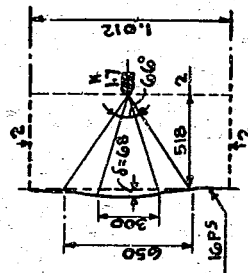
RESULTS OF INVESTIGATION AND EXPERIMENTATION
OF THE CAUSE AND SPREADING OF SPLINTERS

DIAGRAM NO. 1

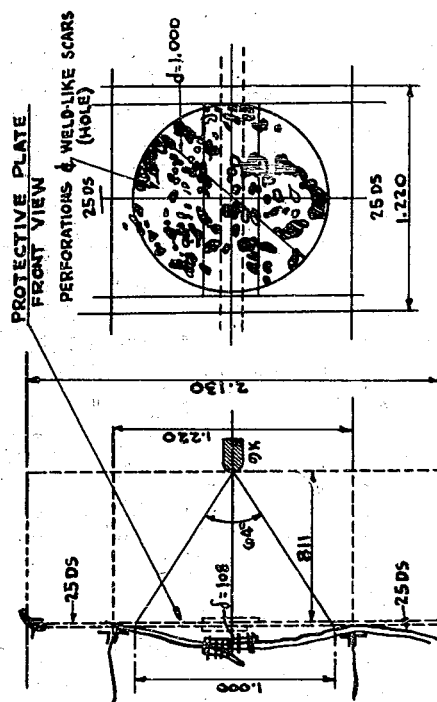
(1) 1/535 SCALE

A₁(3) (NO JOINT)

1.68 TWO KINDS OF HOLES (AT CENTER & WITHIN 150 RADIUS) DEEP HOLES IN RADIUS OF 150 FROM CENTER.
SHALLOW HOLES IN RADIUS OF 325 FROM CENTER.
THE AREA OF SPLINTER DISPERSION IS A CONE WITH A VERTICAL ANGLE OF 66° WHOSE APEX IS THE POSITION OF THE EXPLOSIVE.



- DIAGRAM NO. 2

(2) 1/297 SCALE C₃ (WITH 58.6% JOINT)

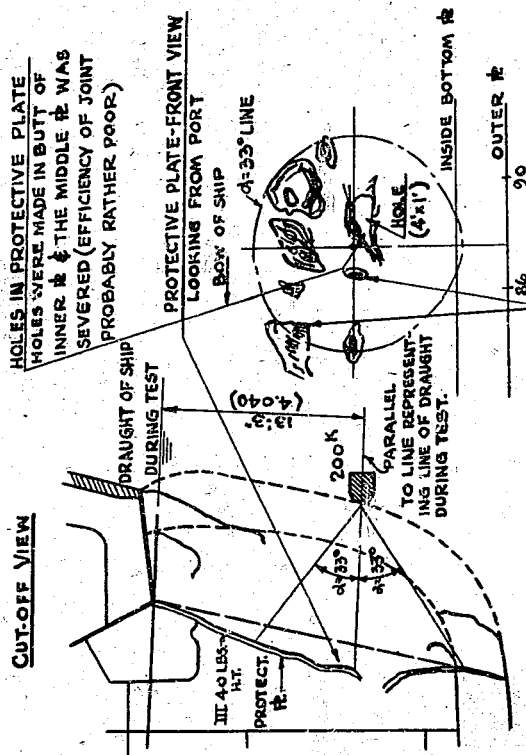
THE AREA OF SPLINTER DISPERSION IS A CONE WITH A VERTICAL ANGLE OF 66° WHOSE APEX IS AT THE POSITION OF THE EXPLOSIVE.

SLIP OF JOINT 12"/in, RIVETS ALMOST ALL DAMAGED.

DIAGRAM NO. 3

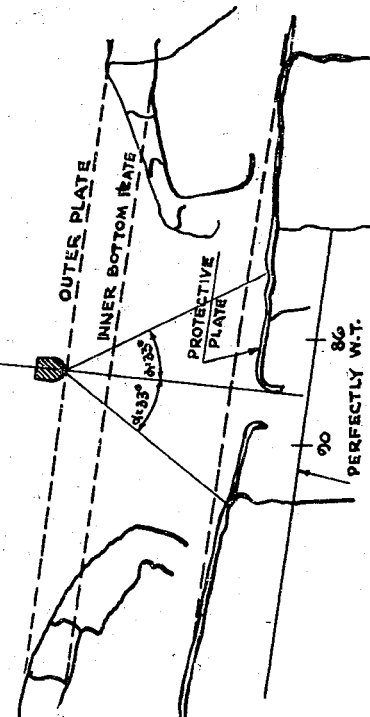
(3) LARGE SHIP (e.g. Tosa)

JOINT 47%



PLAN VIEW

CRACKS DUE TO SPLINTERS



THE AREA OF SPLINTER FLIGHT IN FULL SCALE IS GENERALLY THE SAME AS IN REDUCED SCALE

Figure 2

SPLINTER DISPERSION AND DAMAGE TO PROTECTIVE PLATE
(PROTECTIVE PLATE WITH ONLY VOID LAYER)

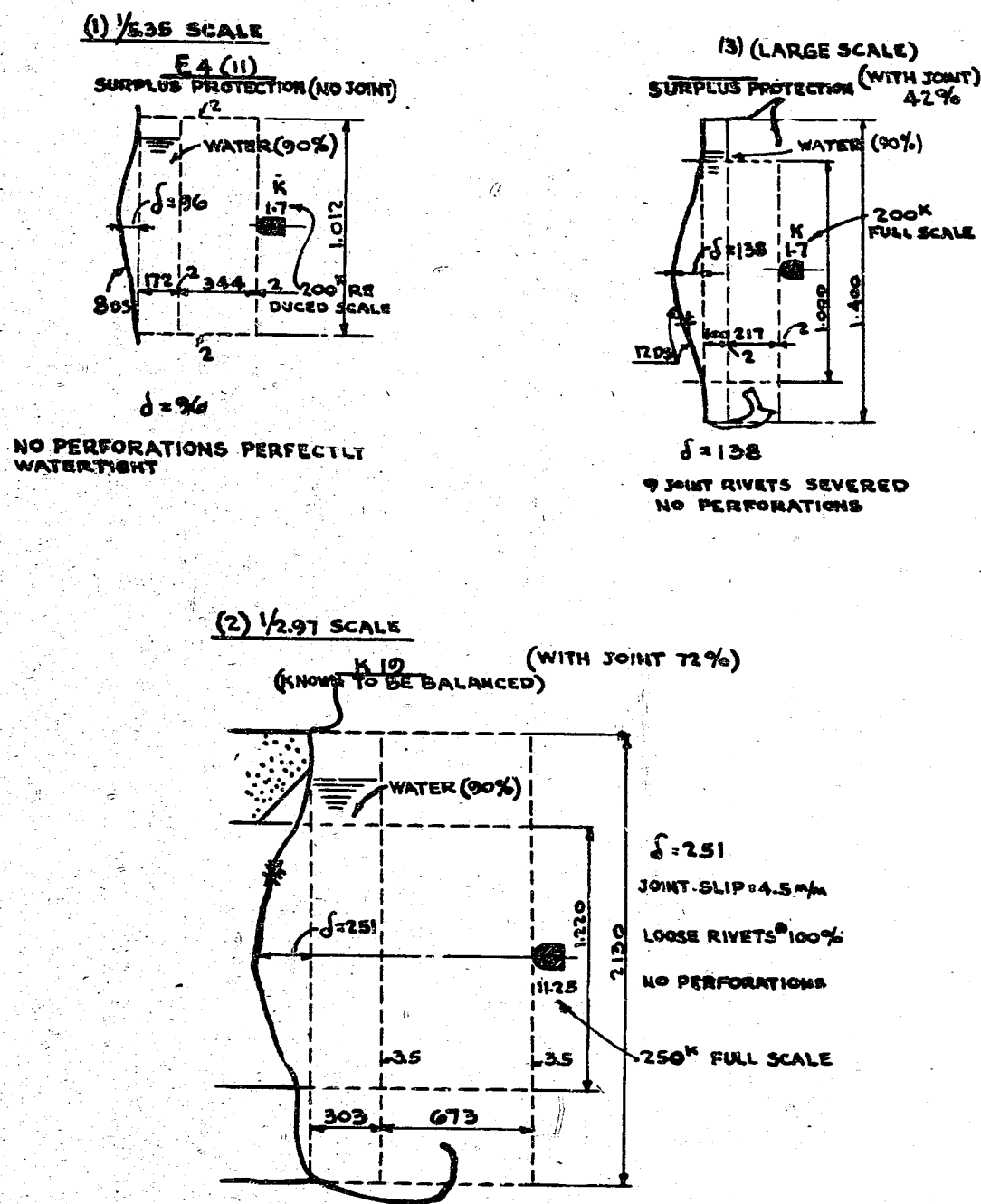
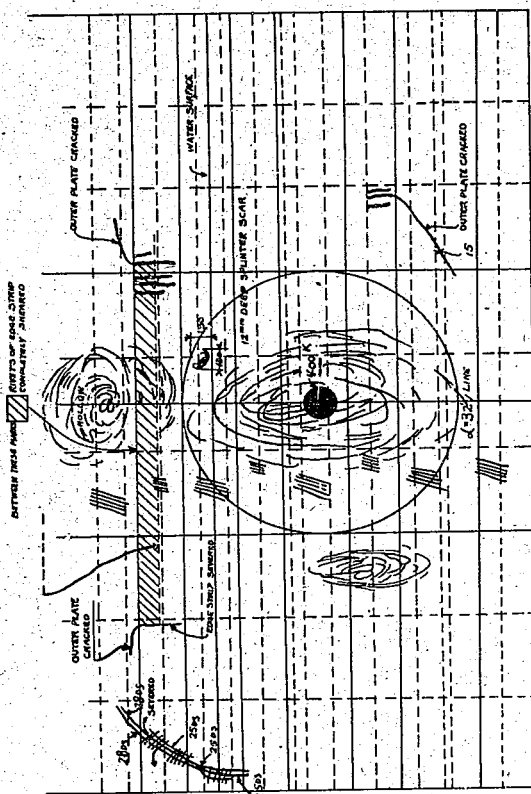


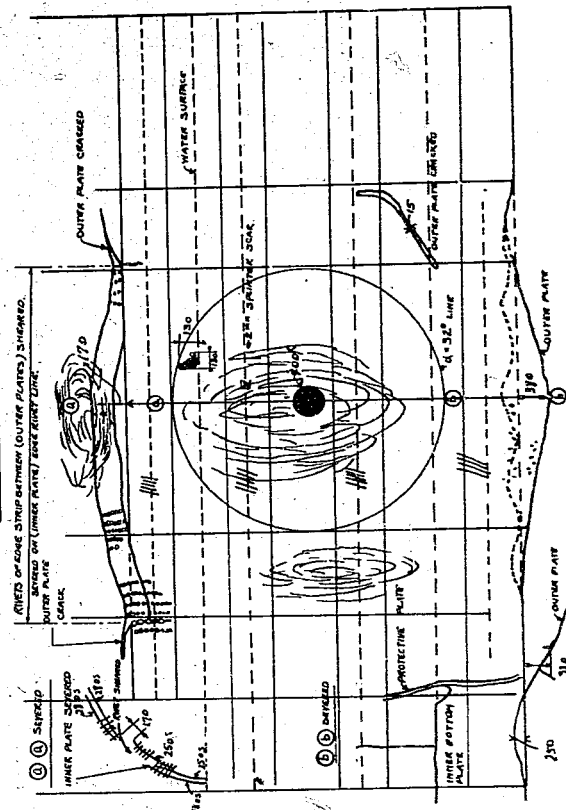
Figure 3
PROTECTIVE MEASURES UTILIZING A WATER LAYER

PROTECTIVE PLATE OUTSIDE SURFACE



DAMAGE HOLE IN PROTECTIVE PLATE

OUTER SURFACE



CUT-OFF VIEW CENTRAL PART PROTECTIVE PLATE
AND DAMAGE IN PROTECTIVE PLATE

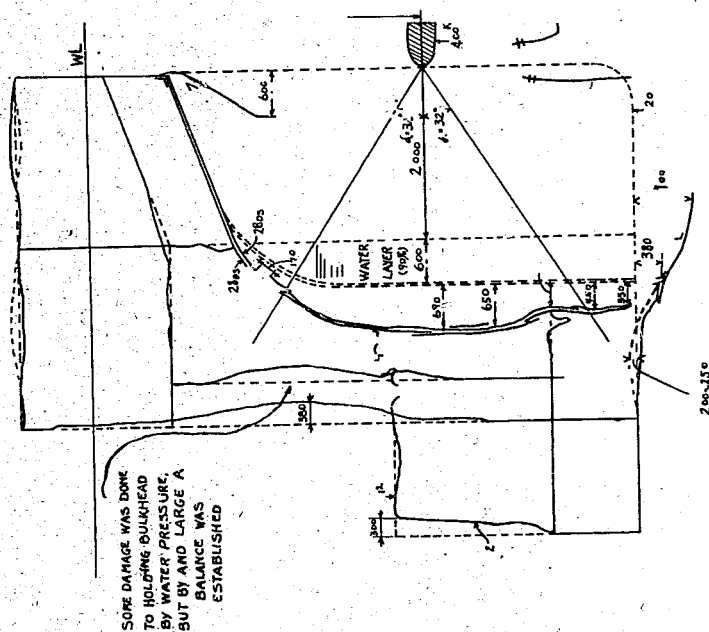


Figure 5
SPLINTER DAMAGE TO PROTECTIVE PLATE
(FULL SCALE TEST - 400g EXPLOSIVE)
(EFFICIENCY OF JOINT - 74.3%)

protective bulkhead. With this type protection, the protective bulkhead usually fails at the weakest point (often a joint), due to the fact that the plate is in tension.

The conditions described above are those occurring at the instant of the explosion, but the damage may be increased by the inrush of water through the hole caused by the explosion.

Figures 2 through 7 show the damage to protective plate by flying splinters.

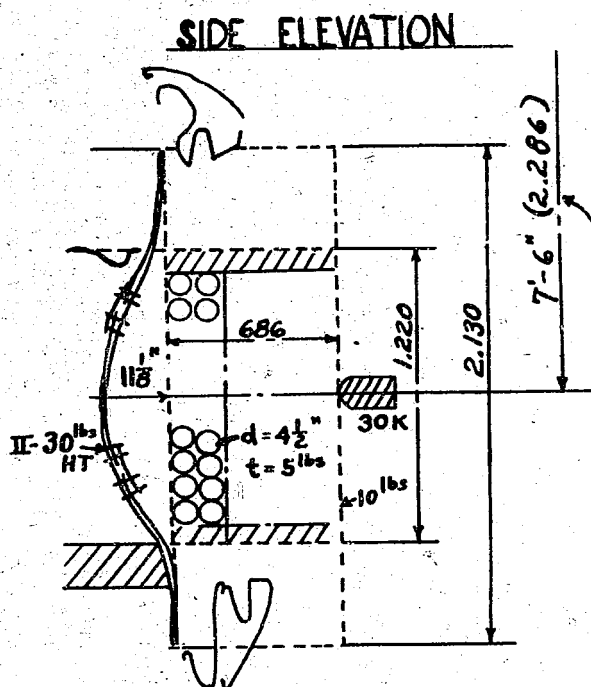
11 1/8

No perforations

Although the outer plate of II-39 lbs HT cracks in a diagonal line the inner plate is whole

1/37 SCALE

(WITH JOINT 57%)



If this target is conducted as 200K, even if it is made at 1/2 scale, the bursting charge is rather small. If 30K is made 1/2 scale of bursting charge, it becomes 215K at full scale. If 30K is made 1/2.97 of bursting charge, it becomes 667K at full scale

IF MODEL IS 1/2 FULL SCALE IS 4"570
IF MODEL IS 1/2.97 FULL SCALE IS 6"800

Figure 6

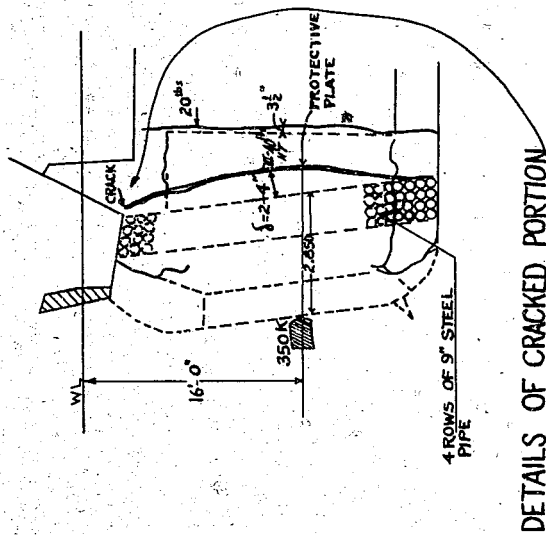
PROTECTIVE MEASURES UTILIZING PROTECTIVE PIPES

B. Chief Points of Underwater Protection

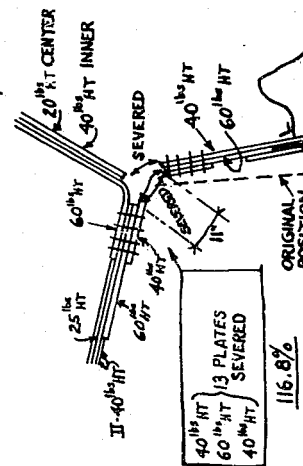
The following main types of protection are used:

1. Air layers only
2. Air and water layers
3. Protective piping

LARGE SHIP (TOSA),
47% JOINT EFFICIENCY

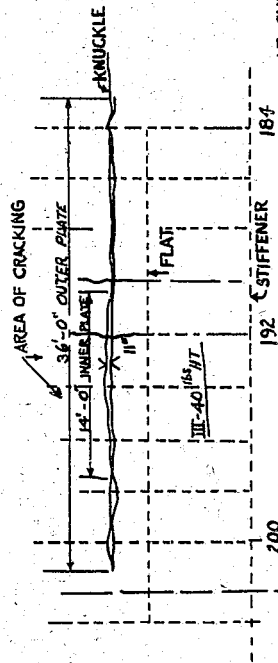


DETAILS OF CRACKED PORTION



Damage
No perforations on surface of protective plate because of piping.
Perhaps because the load concentrated on the knuckle line at the
top of the protective plate. Cracks appear over a 36\"/>

PROTECTIVE PLATE KNUCKLING - FRONT VIEW



IF SUITABLE IMPROVEMENT IN
THE CONSTRUCTION OF THE KNUCKLED
PART OF THE PROTECTIVE PLATE
WERE MADE, THE PROTECTIVE PLATE
WOULD APPARENTLY BE SOMEWHAT
THICKER THAN NECESSARY.

PLAN VIEW

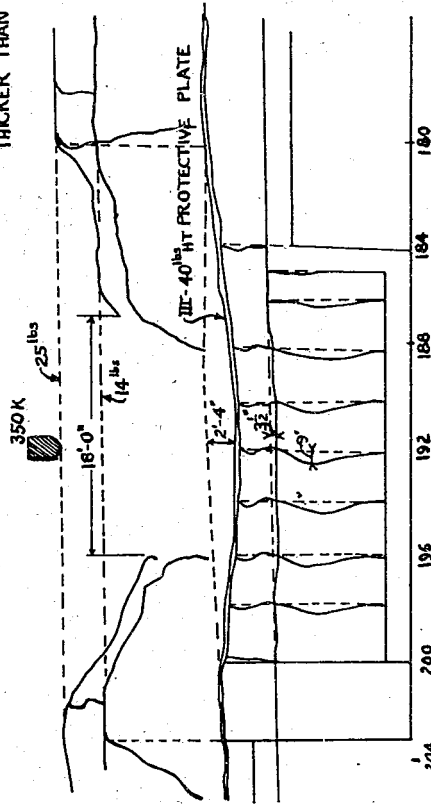


Figure 7

TEST USING PROTECTIVE PIPES
(FULL SCALE TEST - 350K & EXPLOSIVE)

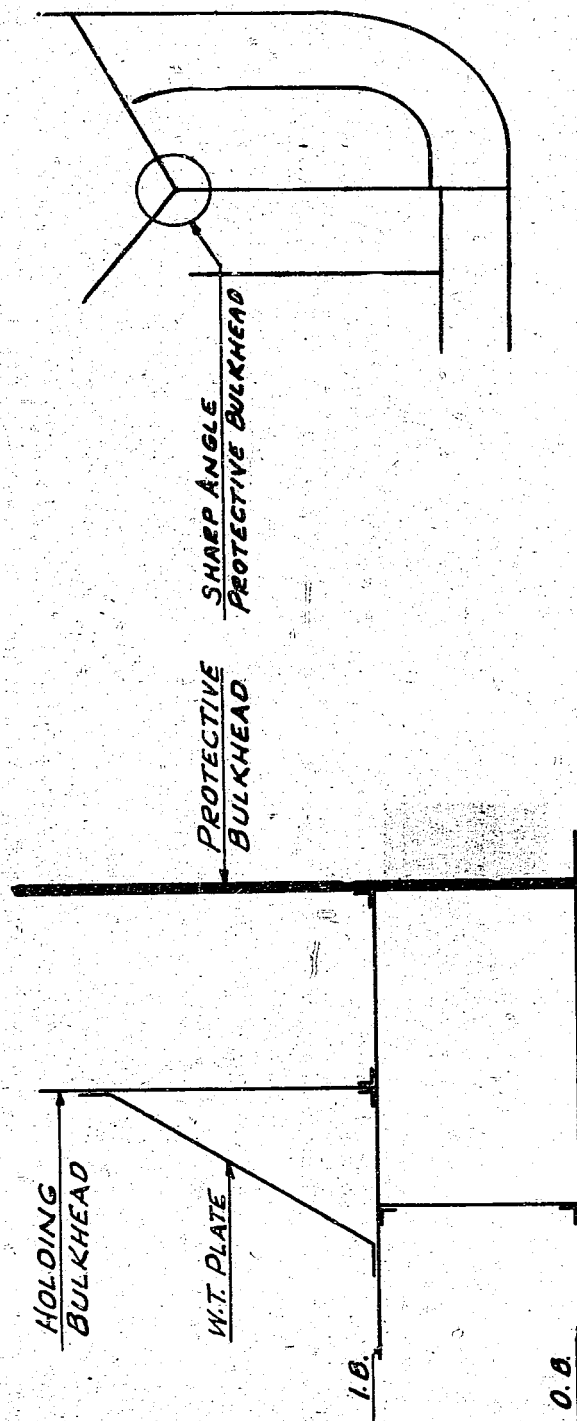


Figure 8
HOLDING BULKHEAD SUPPORT

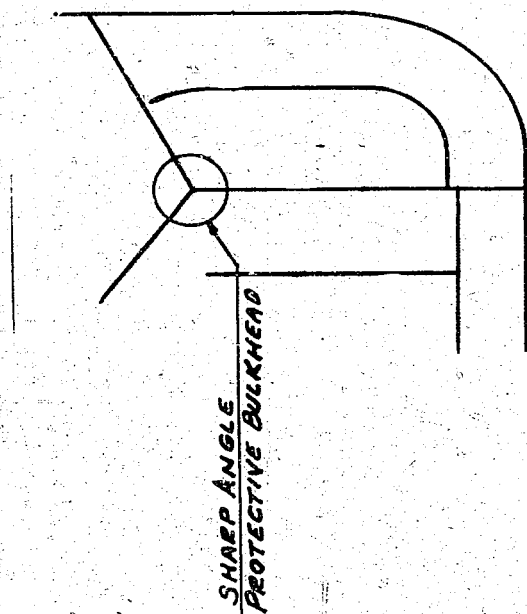


Figure 9
SHARP ANGLE CONNECTION

PROTECTIVE VERTICAL BULKHEAD

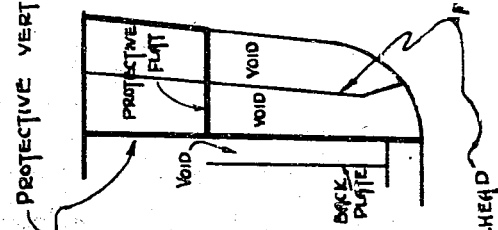


Figure 11
STRAIGHT TYPE

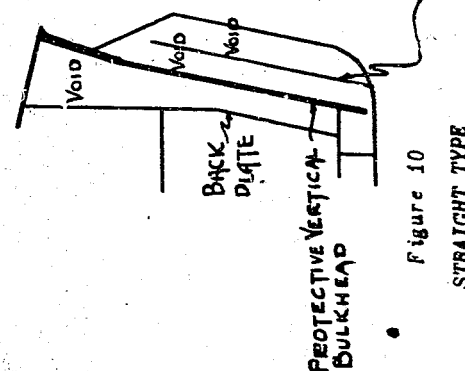


Figure 10
STRAIGHT TYPE

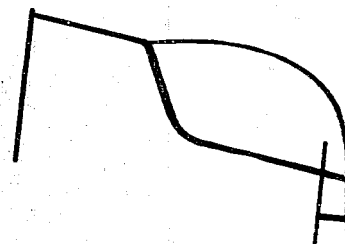


Figure 12
CURVED TYPE

The main purposes of such protection are:

1. Limitation of flooding by transverse bulkheads
2. Protection against flooding through protective bulkhead by building holding bulkheads.

Other important points are:

1. The bottom of the holding bulkhead is supported by a watertight plate as shown in Figure 8. (This plate may be incorporated with engine or boiler foundations.)
2. Sharp angular connections should be avoided where possible but unfortunately they may be necessary. Practical examples are shown in Figure 9.

C. Strength of Underwater Protection and Average Balanced Charge

The defensive strength or the balanced charge can be defined as "that charge which will cause flooding up to but not beyond the bulkhead next inboard to the protective bulkhead".

CHAPTER II PROTECTIVE METHODS USING AIR LAYERS ONLY

A. Classification of Protective Methods

Protective methods, using air layers only, can be divided into two groups; i.e., single plate and multiple plate methods. In the former the shape of the protective plate may be curved or straight; in the latter, however, it is always straight.

B. Single Plate Protective Method

1. Construction of single plate protective method: With the single plate method, two or three Ducol steel plates are attached together at a certain distance from the outer plate, or a vertical bulkhead is worked by a single plate covering all the protective parts. This system may be divided into two types according to its shape. (See Figures 10, 11, and 12.)

2. Characteristics of single plate protective method and its strength:

a. Straight type - in the straight type there are two patterns; in one the upper end of the armor is connected to a steel plate on the ship's side (Figure 10) and in the other it is connected to the upper armored deck (Figure 11). In the first case, the rush of water caused by the explosion is deflected to the upper part of the ship's side resulting in little damage inboard. For this reason, this type is very effective. In the second, the upper protective flat is liable to damage by the rush of water, in which case it becomes difficult to recover the ship's stability. With a particular type ship, it may be convenient to adopt this pattern, but in such case it is necessary to strengthen the protective flat and its fittings.

b. Curved type - in the curved type the upper end of the armor is curved and connected to a steel plate on the ship's side (Figure 12). In this type the rush of water is deflected to the ship's side along the armor. The effect is a little inferior to the pattern in Figure 10 and a little superior to the pattern in Figure 11. This method has two primary defects. First, the bulkhead is built-up of two or three plates which may not exactly fit, consequently they may be loosely joined. The construction of a well-fitting bulkhead is,

therefore, difficult. Secondly, the stress is concentrated on the curved part and weakens the protective value. The effect of this is not so marked with an air layer only, but it is considerable with the water layer type bulge.

C. Multiple Plate Method

1. Construction of multiple plate protective method: With this method a thick plate is not used as with the single plate method, and the ship is protected by several vertical bulkheads (Figure 13). Originally this device was planned for a water layer type bulge, and it is seldom used for the air layer type.



Figure 13

MULTIPLE THIN PROTECTIVE PLATES

2. Characteristics of multiple plate protective method and its strength:
The chief characteristics of the multiple plate protective method are:

- a. Construction is simple.
- b. Damage is comparatively small if the amount of explosion is below the balanced charge.
- c. The amount of flooding is small.

As previously mentioned, this method was used chiefly for the water layer type and few experiments have been made for an air layer type. Therefore, almost no difference in protective value is found between these two types. The results of the experiment are shown in Figure 14. In calculating the protective value, the relation between C , D and t is almost the same as in the case of the single plate method. This relation will be explained in Section 6.

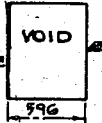
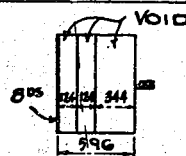
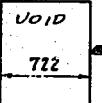
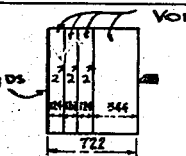
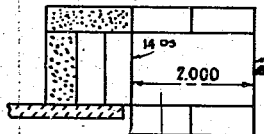
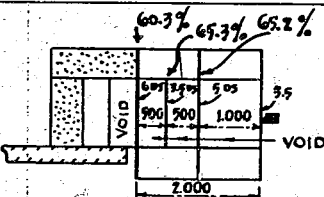
SCALE	TARGET	THICKNESS OF PLATE (mm)	CONDITION OF DAMAGE
$\frac{1}{5.35}$ (1.57)	NO EXPERIMENT THICKNESS OF PROTECTIVE PLATE IS BASED ON $t = 95.62 C^{0.469} d^{-\frac{1}{3}}$ 	14.6	BALANCE
	J, 38 	12.0	PERFECTLY WATER-TIGHT $\delta = 98$ THE BACK OF THE PLATE IS RAISED IN 4 PARTS - ONE PLATE WAS SLIGHTLY CRACKED
	NO EXPERIMENT THICKNESS OF PROTECTIVE PLATE IS BASED ON $t = 95.62 C^{0.469} d^{-\frac{1}{3}}$ 	13.7	BALANCE
	K, 39 	14.0	PERFECTLY WATER-TIGHT $\delta = 74$ FOUR CONVEX TRACES BEHIND
$\frac{1}{2.97}$ $(9K)$	EFFICIENCY OF JOINTS 61.7 % C, 5 	14.0	PERFORATION 10 CRACKS 3
	C, 6 	14.5	INSIDE PROTECTIVE PLATE PERFORATION 1 CRACKS 1
ABOVE EXPERIMENT WAS TRIED ONLY ONCE FOR EACH CASE; SO THAT IT IS NOT PROPER TO DECIDE THE PROTECTIVE VALUE BY IT. - BUT IF WE SYNTHESIZE THE RESULTS, NO DIFFERENCE IS FOUND BETWEEN THE TWO TYPES.			

Figure 14

RESULTS OF COMPARATIVE EXPERIMENT
 BETWEEN SINGLE PLATE AND MULTIPLE PLATE METHODS

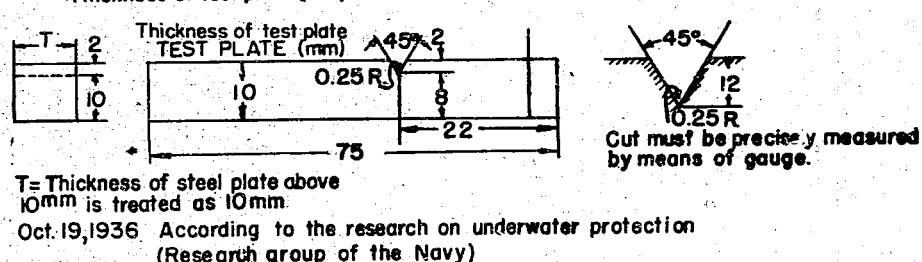
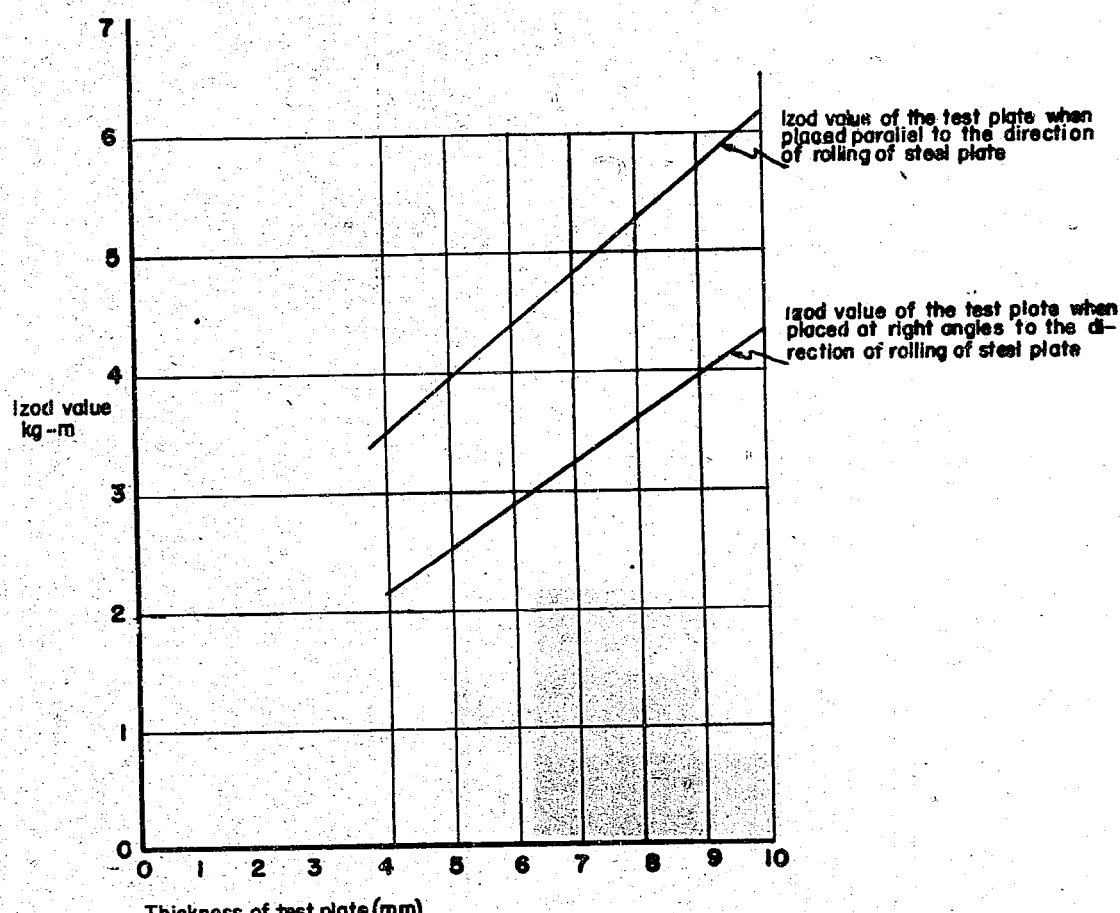


Figure 15

STANDARD IZOD TEST VALUE FOR DUCOL STEEL PLATE

D. Relation Between the Protective Value and the Quality of Plating and Riveting

1. Relation between the protective value and the quality of plate: The resistance of the protective plate against underwater explosion depends upon mechanical qualities of the plate. For example, Ducol steel is stronger than mild steel, and steel used for decks is the strongest. Among mechanical qualities, the Izod value is the most important. If this value is below a certain amount, the plate will be easily damaged. Ducol steel is used chiefly for the protective plate and, although the ultimate tensile strength and ductility of this steel are normal, its Izod value is often so low that sometimes it is dangerous to use. When Ducol steel of low impact value is used for a small scale model experiment, the results may be misleading.

For standard impact test values of Ducol steel see Figure 15.

A rough estimate of strength ratio of "Ducol" Steel, "Copper Non-Cemented", or "Vickers (New) Non-Cemented" against underwater explosions (air layer being used) is:

$$\frac{\text{CNC or NVNC}}{\text{DS}} \approx \frac{4}{3}$$

For results of comparative experiments on DS and CNC see Figure 16 and Table I.

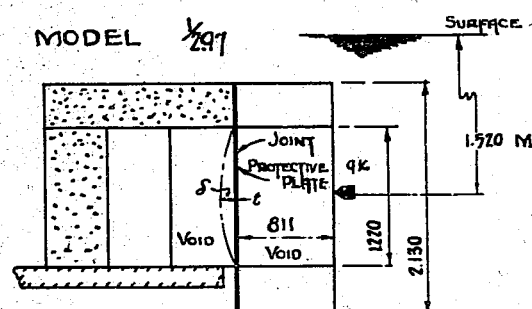


Figure 16

RESULTS OF COMPARATIVE EXPERIMENT ON CNC AND DS

Table I
RESULTS OF COMPARATIVE TESTS ON DS AND CNC

Target	Weight of Plate lbs/sq ft	Efficiency of Joints		Conditions of Damage on Protective Plate (Dimensions in mm)
		For Both Thicknesses	For 25mm (Rivet)	
C ₂ A	19 CNC	R-88.7% P-74.6%	67.4%	δ = 110, 600, Crack
C ₂ B	19 CNC	R-61.1% P-74.6%	46.4%	δ = 230, 700, Crack
C ₃ (A)	25 DS	R-58.6%	58.6%	δ = 900 x 640, Hole
C ₃ (B)	25 DS	R-42.2%	42.2%	δ = 280, Small Crack
C ₃ (C)	25 DS	R-58.6%	58.6%	δ = 108, Perforation
C ₄	19 Special Steel Plate	R-88.7% P-74.6%	58.6%	δ = 128, 500, Crack

Note: R - Rivet; P - Plate

C₂A, C₃(C), C₄ have the same protective strength.
C₂B, and C₃(B) have low joint efficiency and hence are much inferior.

1. 19 CNC and 25 DS are virtually equal that is, ratio of their strength is $\frac{DS}{CNC} = \frac{25}{19} = 1.32 = \frac{4}{3}$
2. The plate does not display maximum strength at less than 46.41% efficiency of joints.

This problem is further discussed in Chapter V.

2. The relationship between the protective strength and material of rivets: The material used must be strong in shear and tension, and must also have a high ductility. After riveting, large diameter HT rivets satisfy this condition; and although small diameter rivets have low ductility, their tensile strength remains high.

Rivets with diameters of 11mm, were of MS whose tensile strength and ductility are comparable to HT rivets.

The following rivets were therefore used in both full scale and model experiments:

Diameter greater than 13mm - HT
Diameter less than 11mm - MS

Hot riveting was used; cold riveting was found unsatisfactory.

Tables II and III, which show the mechanical properties of HT and MS rivets have been extracted from "A Study of Steel Rivet Material D, in Relation to the Knocking-Up Process", 30 April 1934, prepared by I. OHIRA of the Yawata Steel Works Laboratory.

E. Relation Between Armor Joint Efficiency and Protective Strength

Damage to armor provided only with a layer of air is due chiefly to splintering; if a butt strap is provided the efficiency of the joint may not be any greater, but this is made up for in protection. Since there is considerable effect exercised by concussion, however, tests were conducted (see Figure 17 and Table IV) and it was established that the minimum joint efficiency should be 50 to 60%.

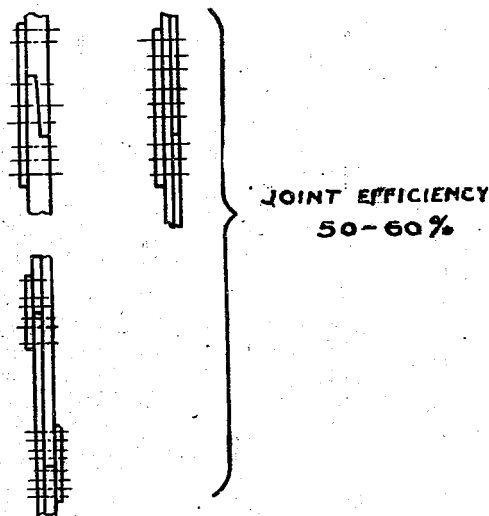


Figure 17

ARMOR JOINTS WITH BUTT STRAPS

Pitch of rivets
WT.....4.5d (4 ~ 4.5d)
OT.....4d (4 ~ 4.5d)
(Strength of steel plate when pitch is 4d is, in general, 70 - 73%)

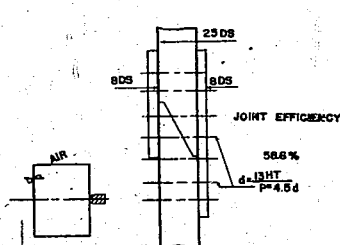
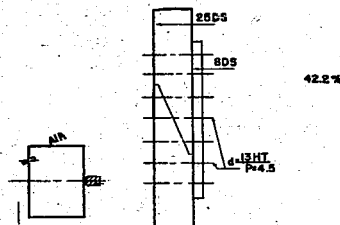
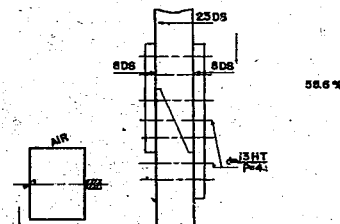
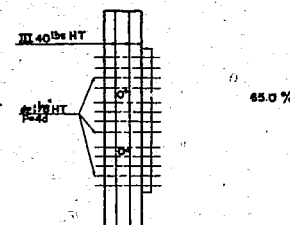
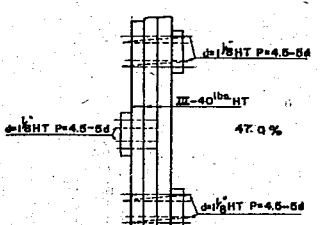
Table II
RELATION OF TYPE OF STEEL TO DIAMETER OF RIVET

Method of Manufacture	Basic Open Hearth Furnace															
	HT															
	C-0.25%, Mn-0.80%															
Steel																
Composition																
Diameter (mm)	37		28		22		19		16		13		11			
Test Fragment Position	A	B	A	B	A	B	A	B	A	B	A	B	A	B		
Proportional Limit (kg/mm ²)		22.7		22.4												
Yield Point (kg/mm ²)	34.8	34.3	37.4	38.0	37.0		39.1		37.6		43.1		46.7			
Tensile Strength (kg/mm ²)	59.9	55.2	54.5	55.9	53.6	56.4	56.1	57.0	55.8	56.7	57.8	58.5	57.7	60.2		
Ductility GL = 8d (%)	22.0	23.6	25.8	26.4	27.8		28.4		26.4		30.5		30.3			
GL = 1.2d (%)	(59.5)	56.2	(69)	55.4	(72)	54.7	(74)	57.3	(70.5)	59.6	(77)	63.2	(77)	57.2		
Reduction In Area (%)	48.9	64.4	51.5	64.2	51.5	61.6	50.6	63.8	53.3	62.9	56.6	64.3	55.8	62.9		
BHN	143		146		149		146		149		152		156			
Composition	Fe+P		Fe+P		Fe+P		Fe+P		Fe+P		Fe+P		Fe+P			
Proportional Limit (kg/mm ²)	30.0		31.3													
Yield Point (kg/mm ²)	39.7		42.8													
Tensile Strength (kg/mm ²)	62.5		62.3		70.0		71.9		78.6		89.6		92.8			
Ductility GL = 8d (%)	18.7		18.5													
GL = 1.2d (%)	61.5		61.3		49.1		48.8		39.4		41.0		24.8			
Reduction In Area (%)	65.4		66.7		61.9		64.6		56.9		52.8		37.6			
BHN	183		185		207		217		241		277		320			
Composition	Fe		Fe		SP+Fe		Fe		M+Fe		M+Fe		M+Fe			
Proportional Limit (kg/mm ²)	32		40													
Yield Point (kg/mm ²)	14		15													
Tensile Strength (kg/mm ²)	14		14		31		28		41		45		61		54	
Ductility GL = 8d (%)	-15		-28													
GL = 1.2d (%)	3		9		-32		-34		-44		-47		-68		-57	
Reduction In Area (%)	33		2		20		28		7		-7		-33		-40	
BHN	28		27		39		49		62		82		105			

Table II (Continued)
RELATION OF TYPE OF STEEL TO DIAMETER OF RIVET

Method of Manufacture		Basic Open Hearth Furnace											
Steel		MS											
Composition		C-0.22%, Mn-0.41%											
Diameter (mm)		37			28			22			19		
Test Fragment Position		A		B	A		B	A		B	A		B
Proportional Limit (kg/mm ²)		17.5		20.3	28.3		32.8	28.7		30.5	30.4		36.7
Yield Point (kg/mm ²)		26.6		32.5	41.0		46.2	43.4		43.1	43.9		48.7
Tensile Strength (kg/mm ²)		41.0		46.0	41.8		46.2	43.4		43.1	43.9		48.7
Ductility GL = 8d (%)		30.6		27.4	31.6		25.7	29.9		33.2	32.8		35.6
GL = 1.2d (%)		(77.3)		64.6	(80)		72.2	(76.5)		(89.3)	(83)		(88)
Reduction In Area (%)		57.4		61.1	62.8		65.4	63.2		66.3	65.7		69.1
BHN		123		123	123		123	131		131	130		131
Composition		Fe+P		Fe+P	Fe+P		Fe+P	Fe+P		Fe+P	Fe+P		Fe+P
Proportional Limit (kg/mm ²)		26.0		28.4	28.4		28.4	28.4		28.4	28.4		28.4
Yield Point (kg/mm ²)		33.0		36.2	36.2		36.2	36.2		36.2	36.2		36.2
Tensile Strength (kg/mm ²)		53.5		56.2	56.2		56.2	57.4		53.1	61.3		64.5
Ductility GL = 8d (%)		22.0		19.4	19.4		19.4	19.4		19.4	19.4		19.4
GL = 1.2d (%)		64.2		63.6	63.6		63.6	63.6		63.6	63.6		63.6
Reduction In Area (%)		64.6		70.5	70.5		70.5	69.8		71.1	70.4		72.3
BHN		143		152	152		152	166		174	183		215
Composition		Fe+P		Fe+P	Fe+P		Fe+P	SP+Fe		SP+Fe	SP+Fe		Type
Proportional Limit (kg/mm ²)		49		40	40		40	40		40	40		40
Yield Point (kg/mm ²)		24		28	28		28	26		37	40		33
Tensile Strength (kg/mm ²)		27		31	31		31	31		28	34		40
Ductility GL = 8d (%)		-28		-20	-39		-25	-25		-35	-17		-32
GL = 1.2d (%)		-17		-1	-20		-12	-4		-14	-36		-51
Reduction In Area (%)		13		6	11		7	15		7	7		5
BHN		16		16	16		16	27		33	41		63

Table IV
RESULTS OF TESTS ON RELATION OF JOINT EFFICIENCY TO PROTECTIVITY OF ARMOR

Test	Target	Joint and Damage
1/297 Scale Model (9 kg)	<p>C₃ (A)</p> 	Some rivets were loosened or scattered, but in general, no damage was done.
	<p>C₃ (B)</p> 	About 410mm of the butt strap was cut through and 23 rivets were sheared off.
	<p>C₃ (C)</p> 	A maximum slip of 12mm appeared, and rivets were almost loosened.
Full Scale Model (200 kg)	<p>Model G (NAGATO)</p> 	With δ of protective bulk-head 1/2" small cracks appeared in two places but almost no damage was done.
	<p>TOSA</p> 	The plate was concluded to be almost equal with Model G, but the appearance of two holes indicated that its strength was somewhat weak. That is, an opening appeared in the joint of the inner plate and the middle plate was cut away.

The minimum joint efficiency giving sufficient protection is shown to be 50-60%.

F. Calculation of Protective Strength

The computation of the protection of armor provided only with a layer of air is based on the following test formula:

$$T = 95.62C^{0.469} D^{-1/3}$$

(based on Study of Underwater Defense,
19 October 1936, Test Research Lab.)

T = total thickness of armor (including fore-plate) in millimeters.
C = balanced charge in kilograms.
D = distance between outer plate and protective armor in millimeters.

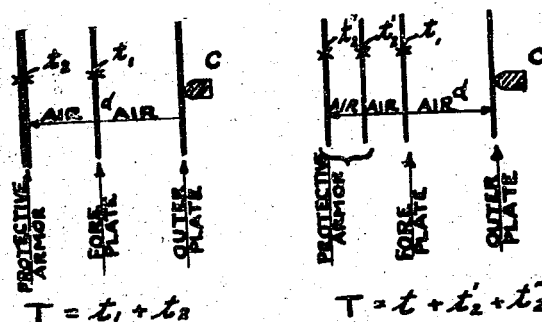


Figure 18

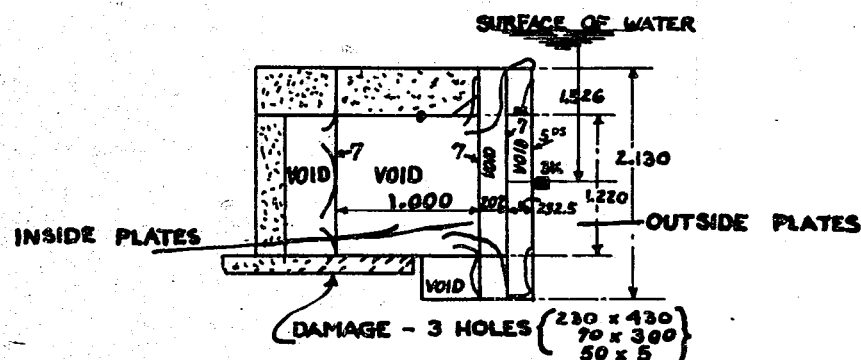
THICKNESS OF ARMOR, SINGLE AND MULTIPLE PLATE

Note: The above formula is a test formula based on a scale test using chiefly a 200 kg charge, and no inconvenience with regard to its application is found up to 400 kg. It must be remembered however, that further study is necessary for charges in excess thereof. In the case of an actual ship, no matter how large the charge against which protection is required, the unfortunate condition arises that the distance between the outer plate and the protective bulkhead cannot be increased, nor can the volume of empty space. (For results of tests on a protective bulkhead provided with only a layer of air and for tables used in computing protection given see appended Tables XII, XIII, XIV and Figures 44, 47 and 48.)

G. Relation of Position of Protective Bulkhead to Protection

1. Single plate, with protective bulkhead very close to outer plate:
On first consideration, the extreme case of making the outer plate serve as the protective bulkhead, i.e. bringing the latter close to the outer plate, results in the thickness of the protective bulkhead becoming infinitely large, but the results of a 1/2.97 scale test show that a thickness of 90mm HT balances a charge of 9 kg. The corresponding distance between the protective bulkhead and outer plate is the same as the value calculated for 27mm (see Figure 44).

This is thought to be due to the fact that even if the explosive is in contact with the protective bulkhead, the center of the explosion is somewhat separated from it. Since the explosive is in contact with the protective bulkhead, splinters from the outer plate, ribs, etc. do not strike the protective bulkhead through the air layer described above. However, since the center of the explosion is extremely close, the principal reason for the destruction of the protective bulkhead is simply the

K29 TARGET ($\frac{1}{2}$.97)

COMPUTATION OF PROTECTION
 THICKNESS OF PROT. BULK. $T = 9 \div (7 \div 7) \times \frac{21}{61} = 18.6$
 (TABLE 5) (CONVERSION OF MS TO DS AT RATIO OF TENSILE STRENGTH)

HYPOTHETICAL POSITIONS OF ARMOR		D	C
1	1.000	1.461.5	5.4
	D		
2		454.5	2.6
	D		
3		252.5	1.6
	D		
4	1.000	617	3.0
	D		

LOCATION OF CENTER OF GRAVITY OF PROTECTIVE BULKHEADS

Figure 19
 MULTIPLE PLATE TEST

violence of the concussion. Such would probably not be the case with a protective bulkhead provided with an ordinary air layer.

Therefore, considering the distance between the center of the explosion and the protective bulkhead as the ordinary distance (D), it is not proper to employ the formula given in the preceding section, both theoretically and practically. The center of gravity (the center of the explosion generally being considered as at the center of gravity of the charge) of the 9 kg explosive (a 1/2.97 scale reduction of the 200 kg torpedo warhead in use at present) used in tests thus far is located 134mm from the tip. When the results of this test are compared with the thickness of the protective bulkhead according to the formula in the preceding section, the distance between the outer plate and the protective bulkhead is found to be the same as for 27mm.

Consider a case where the air layer is extremely narrow. The results obtained in a test, where the distance between the outer plate and protective bulkhead was 100mm and the charge 9 kg, were in general the same as those obtained employing the formula. If the 100mm distance is decreased even further, the effect exercised by the distance between the outer plate and the center of the explosion on the distance (D) becomes greater. Therefore, there is no objection to the use of the formula.

To summarize, when the charge is 9 kg and the distance between outer plate and protective bulkhead is 100mm, or when the charge is 200 kg and the distance is 300mm or above, there seems to be no objection to using the formula. If the distance is any smaller, further study is required. It is not thought however, that any less protection is afforded than when the outer plate is made the protective bulkhead. In the latter case, all that can be done at present is to calculate on the basis of a 9 kg charge.

Note: A protective bulkhead provided with only an air layer, such that the distance between the outer plate and the protective bulkhead is 300mm, is not thought likely to arise as an actual problem.

2. Multiple plate, with outside protective bulkhead close to outer plate: If the protection is computed when the outside protective bulkhead is near the outer plate and when the distance between the outer plate and the inside protective bulkhead is the distance (D) of the formula in the following section, a value much greater than the actual protection is obtained. The chief reason for this is that the protective bulkhead near the outer plate is close to the center of the explosion, consequently it is believed scattered splinters destroy the inner protective bulkhead.

This problem has only been studied incidentally and no conclusions have been reached. However, if it is examined in the light of tests made with other objectives, the following statement can be made: "With regard to the D to be used in computing protection given, the distance from the outer plate to the center of gravity of the protective bulkheads seems the least erroneous".

The results of the above mentioned test and an illustration of the computation of protection follow:

A comparison of the test results and the example of computation indicates that, with a 3 kg charge, the inside protective bulkhead is punctured in three places, and the protection afforded against a 3 kg charge would appear to be insufficient, however, since hardly any damage was done to the holding bulkhead, this target may be said generally to be balanced for a 3 kg charge. The table of calculations (Figure 19) shows that when the protective armor is concentrated near the inside protective bulkhead, the charge required, 5.4 kg is excessive. Examples (2) and (3), in which it is

concentrated on the outside, give 2.6 kg and 1.6 kg which are insufficient. Example (4), in which it is concentrated at the center of gravity of the protective bulkheads, gives 3 kg. In other words, this last figure seems to come nearest the test results. This is merely an example, however, and since variations are expected to arise because of the mutual relationships of the distance between the outer plate and the inside protective bulkhead and the thickness of the latter, further study is required.

CHAPTER III PROTECTION EMPLOYING WATER LAYERS

A. The Function of the Water Layer

Protective armor employing water layers is provided with a layer of liquid over the face of the protective bulkhead. It is designed to prevent the destruction of the protective bulkhead by splinters described in Chapter II and to increase protective efficiency by distributing the force of the concussion over the entire surface of the protective bulkhead. Compared with protective armor provided only with an air layer, the thickness of the protective bulkhead may generally be reduced 50%, and at the same time flooding may be reduced 30% in the case of single plate and 50% in the case of multiple plate armor. The water layer is effective in neutralizing the force of the explosion, but it is necessary to leave a 10% space at the top of the voids.

1. Comparison of capacity flooding and 90% flooding: When the charge explodes and the splinters and concussion reach the fore-plate, in the case of capacity flooding, the impact is transmitted to the protective bulkhead unchanged. In the case of 90% flooding, the impact is somewhat neutralized because of the void space. Therefore 90% flooding affords greater protection than capacity flooding. Extensive experiments to establish the variation have not been conducted, and the ratio is not known at present. The following experiment has been performed, and it is offered in Figure 21 for its reference value.

2. Comparison of 90% flooding with less than 90% flooding: When tests were performed with a 70% water layer, better results were obtained than with 90% flooding. This was due to the checking of the impact of splinters on the protective bulkhead by the layer of water. If the explosive made contact at a spot so that splinters would pass through where there was no water, protection would be severely reduced. Therefore, it would seem better for practical purposes to have a 90% water layer. Results of a test are shown in Figure 22.

On an actual ship it would be uneconomical from the point of view of weight to carry water in the water layers, so fuel oil is used instead. If the fuel oil is consumed it must be replenished by water, so that protection is not lessened.

Possible damage due to the combustion of fuel near the point of explosion is a problem, but in scale experiments there was no such combustion and protection was thought to be no less than when water was used.

The results of the test were as shown in Figure 23.

Note: Instances of damage in the Great East Asia War are not lacking, but to date there has been no record of oil fires caused by underwater attacks.

B. Types of Protection and Construction of Armor

There are two systems of protective armor using water layers, single and multiple plate. Single plate armor may be subdivided into curved and straight types. Examples are given in Figure 24.

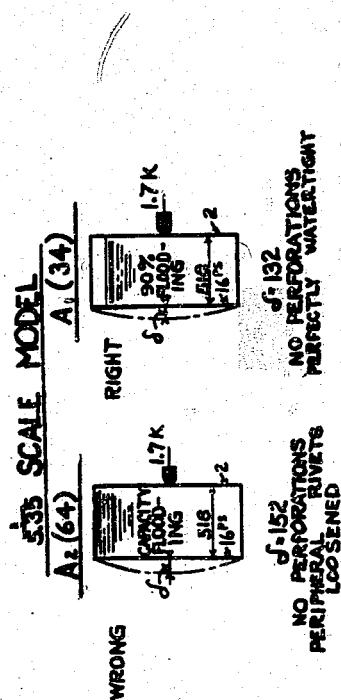


Figure 21

RESULTS - CORRECT AND INCORRECT FLOODING OF VOIDS

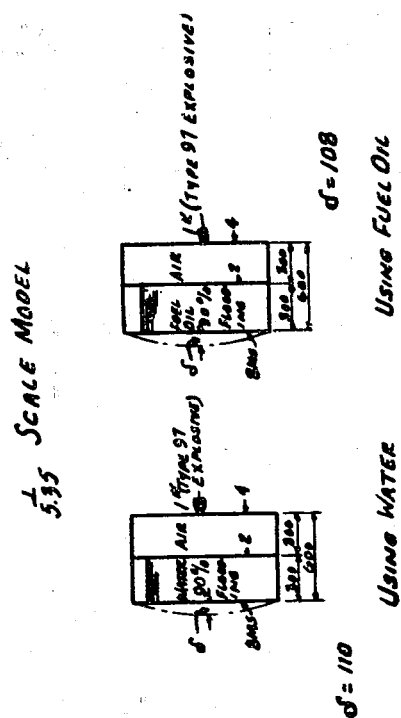


Figure 23

FUEL OIL vs. WATER IN VOIDS

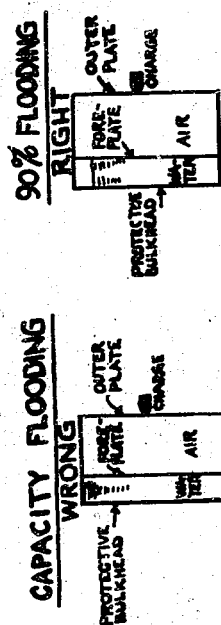


Figure 20

CORRECT AND INCORRECT FLOODING OF VOIDS

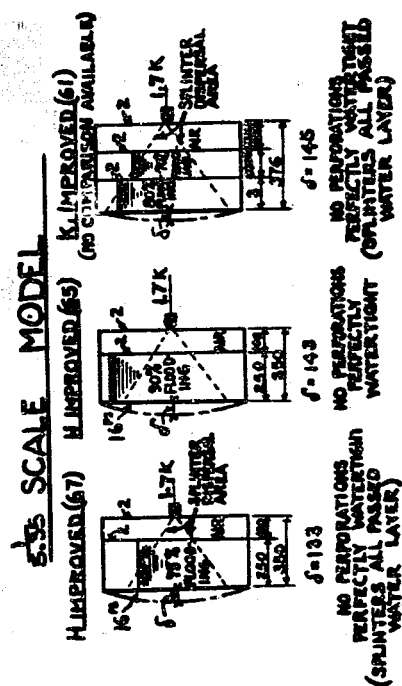


Figure 22

RESULTS WITH VARIOUS PERCENTAGES OF VOID FLOODING

Since the construction of these different types of armor was described in Chapter II, discussion is omitted here.

C. Relation Between Thickness of Water Layer and Protection

1. Single plate: The minimum thickness of water layer which will stop splinters was found by test to be 600mm (charge 400 kg). A comparative test was made with a 900mm water layer, with a view to improving distribution, but almost no difference in results was noted. It was wondered what the effect would be of reducing the width below 600mm, but since such a test would have involved practical difficulties, it was found convenient to take 600mm as a minimum.

Since protective efficiency with a wide air layer is great, it is most effective from the point of view of protection, to make the thickness of the water layer a minimum when the distance between the outer plate and the protective bulkhead is fixed. It must be remembered, however, that in such a case the volume of flooding increases.

When D is fixed, protection is greater where d_a is large than where d_a is small, but flooding is also greater.

Protection employing water layers does indicate a water layer directly before the protective bulkhead. It is desired to learn, however, the protection given when compartments outside the protective bulkhead are flooded or when the water and air layer are transposed. The operations performed in this sort of test, however, are very fundamental and the interrelations are not yet clearly understood. It is certain that such measures would be inferior to the normal water layer method.

2. Multiple plate: In this method the one water layer is increased to two or three, so the thickness of the water layer is sufficient to provide effective protection. If a case is considered in which the fuel oil is consumed first from the outboard tank, leaving only the one on the inside, the water layer of 600mm mentioned above is necessary, and therefore the minimum distance between protective bulkheads must be 600mm.

The multiple plate method was first adopted in the United States for underwater protection. A comparison between it and the single plate method follows:

Advantages

- a. Construction is somewhat simpler since the protective bulkheads are separate.
- b. The water layers are all filled 90% with fuel oil, and if the thickness of the protective bulkheads is fixed, the oil is used from the outside tank in, leaving only the inside tank. Protection is thus not lessened, but increased.
- c. If all the water layers are filled 90%, the volume of flooding is decreased considerably.

Disadvantages

- a. The greater the void layer thickness (d_a) the greater protective efficiency is. Therefore, if the distance (D) between the outer plate and protective bulkhead is fixed, the total thickness of protective bulkhead in the case of the multiple plate is greater than for the single plate method, and its weight is increased.

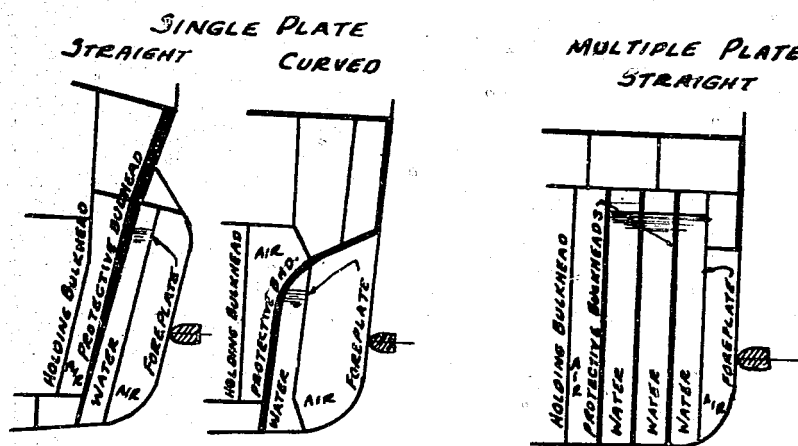
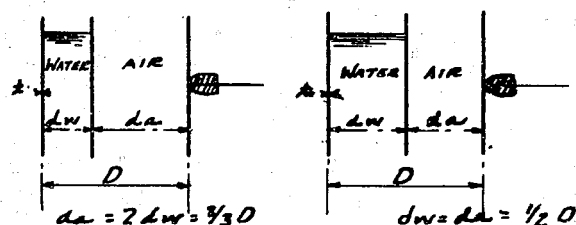
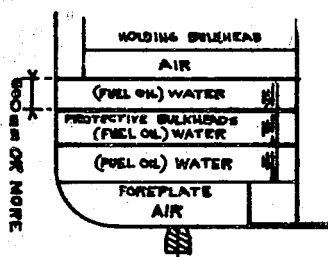


Figure 24

TYPES OF PROTECTION USING WATER LAYERS

Figure 25
RELATION OF d_a AND d_w Figure 26
MULTIPLE PLATE ARRANGEMENTS
SHOWING MINIMUM PLATE INTERVAL

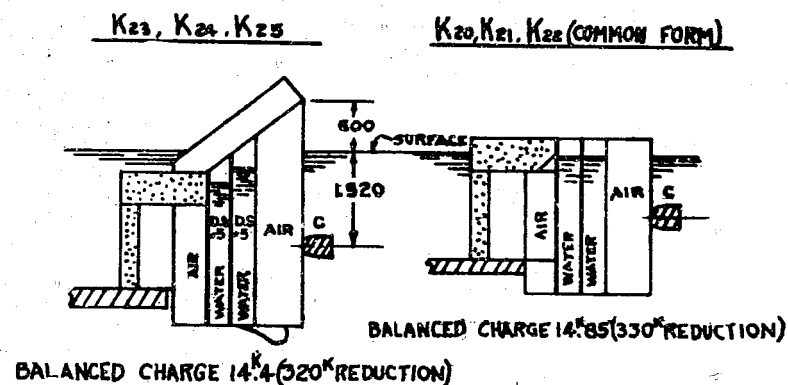


Figure 27

EXPLOSION VENTED TO ATMOSPHERE

(The K₂₅ target seems to be characterized by leakage from the water layer at the time of the test and more damage was done than anticipated. The balanced charge was lower than for the common form. It offered almost the same protection.)

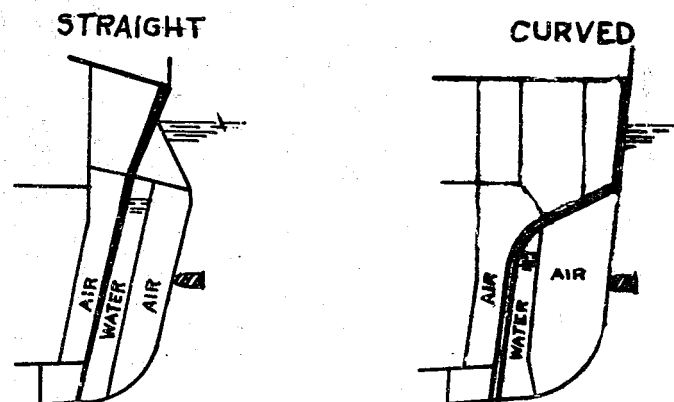


Figure 28

SINGLE PLATE PROTECTIVE BULKHEADS

b. If the weight of protective bulkhead is made equal to that in the single plate method, the distance (D) between outer plate and protective bulkhead is increased. Consequently, since ship sections become small forward and aft it is impossible to employ the same method of protection for the magazines as amidships.

D. Relation Between Joint Efficiency and Protection

The destruction of the protective bulkhead when water layers are used is due to the equalization of water pressure over its entire surface. The efficiency of the joints is directly related to the protection given and is, therefore, of paramount importance.

If 100% joints were made by welding, the protective bulkhead could be made much thinner.

At present DS (sometimes CNC or NVNC) is the material principally used for protective bulkheads as well as rivets. It is also used in the ship's main longitudinal structure, and all joints must be riveted. If the pitch of the rivet is made 4d (oil-tight), the maximum efficiency of the joint will be 70 to 73%. In other words "the efficiency of the joint is determined by the oil tight pitch of the rivets, and the standard is 70%".

Caution is necessary when using large type thick steel plates as underwater protective bulkheads. Since the rigidity of the deck structure against underwater explosions is great, the question as to whether or not 70% joints are absolutely essential is one requiring further study.

E. Protection With Explosion Vented to Sea Surface

Comparative tests of 1/2.97 scale model structures gave the results as shown in Figure 27.

When this construction was designed, it was expected that it would be somewhat superior, but test results showed almost no difference. If a direct comparison of the results is made, there is actually more damage, and there is no evidence that the concussion escaped through the air layer to the surface.

F. Relation of Form of Protective Bulkhead to Protective Strength

As stated before the single plate method includes the straight and curved types. DS plates in two or three courses are ordinarily used in the straight type against underwater explosions. Armor often in conjunction with bombproof protection can also be used. Armor cannot be used, however, with the curved type and two or three courses of DS plates are generally used. Therefore, the structural work is extremely difficult, and the courses of the protective bulkhead do not fit closely. A slight gap between the courses reduces the protective power. In the protective method employing water layers, the free surface of the water layer occurs just at the bend and the maximum shearing and bending stresses also occur there. The joints near the center of explosion, therefore, are not damaged, while those at the bend will be damaged.

The straight protective bulkhead affords more protection than the curved type, because the bending caused by the concussion is quite natural, and the top and bottom are securely fitted.

The ratio of the thickness of protective bulkheads of the straight and curved types for the same charge is as follows:

$$\frac{\text{Curved}}{\text{Straight}} = \frac{5}{4} = 1.25$$

In other words, the curved type must be 25% thicker, but there is much study yet to be done here.

Since the curved type must be thicker, its weight is also increased, but there are certain types of ships on which it is wise to use it. In such cases, some additional strength is to be obtained by observing the following points:

1. Make the radius of the curve at the bend as large as possible.
2. Avoid the bend in distributing the joints.

When this type has to be built, the efficiency of the joints must be especially large.

G. Computation of Protection Strength

The same test formula ($T = 95.620^{0.469D^{-1/3}}$) used with an air layer is also used for computation of protection with a water layer. The thickness of the protective plate is corrected according to the efficiency of the water layer, the efficiency of the joints of the protective plate, etc. and the computations are made in the following order, on this corrected thickness:

1. First the efficiency of the water layer in relation to an air layer is found:

With a straight type protective bulkhead: $K = 0.4 da^{-1/3} \phi (dw)$
 With a curved type protective bulkhead: $K = 0.5 da^{-1/3} \phi (dw)$

where:

K = efficiency as it differs with da
 da = thickness of air layer (in meters)
 $\phi (dw)$ = function of thickness of water layer = 1.0

Further study is necessary regarding $\phi (dw)$, and therefore, although it has been designated above, at present it is taken as 1.0. In other words, if $dw = 600\text{mm}$, the efficiency of the water layers will always be the same.

2. Next the effective thicknesses of the protective bulkhead and fore-plate is found.

$$\text{Effective thickness} = \Sigma t_1 + \Sigma t_2 y$$

where: Σt_1 = Total thickness of fore-plate (mm)

(Strength of joint in fore-plate not considered)

y = Efficiency of joint in protective bulkhead

$\Sigma t_2 y$ = Total effective thickness (mm) of protective bulkhead

3. Now the corrected thickness (T) of the protective bulkhead converted as for use with an air layer is determined.

$$T = \frac{\Sigma t_1 + \Sigma t_2 y}{K}$$

4. Next the distance (D) between the outer plate and the protective bulkhead is found as it would be with an air layer.

$$D = da + 600\text{mm}$$

When the thickness of the protective bulkhead with water layer, has been corrected as described above and its protective strength has been computed according to the corrected thickness as it would be with an air layer, the dw of the actual distance ($D = da + dw$) is always 600mm.

5. The protective strength is then computed with the T and D found in the manner described above by means of the following formula (for protective bulkhead with air layer):

$$T = 95.62C^{0.469}D^{-1/3}$$

Note: Apparently in the case of the single plate method, when $da/D < 0.55$ protective strength cannot be found by means of this method of computation. (For results of tests on protection using a water layer and efficiency curve for water layer, see Tables XV, XVI, XVII and Figures 45 and 49.)

Sample calculation - Curved Type Protective Bulkhead

1. Find efficiency of water layer (K).

According to Figure 49, $K = 0.372$

2. Find effective thickness of protective bulkhead and fore-plate.

$$\text{Effective thickness} = 8 + 50 \times 0.7 = 43\text{mm}$$

3. Find corrected thickness (T) of protective bulkhead converted as for air layer alone.

$$T = \frac{43}{0.372} \doteq 115.6\text{mm}$$

4. Find the balanced charge.

According to Figure 47 or 48, $C \doteq 400 \text{ kg}$

H. Relation Between Protection and Position of Water Layer

The position of the water layer affording maximum protective efficiency, as the method of computing protection given in the preceding section clearly shows, is that of a narrow water layer next to the protective bulkhead, with as large an air layer as possible next to the outer plate.

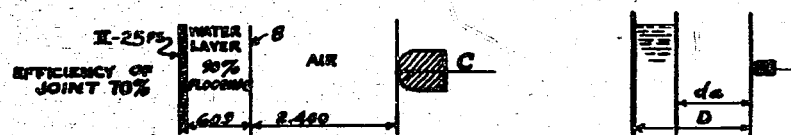
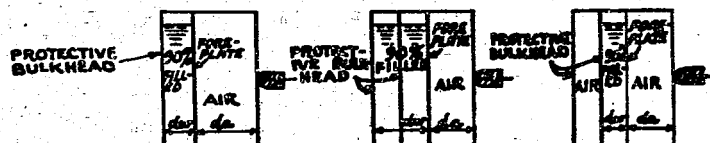


Figure 29

CALCULATION OF C FOR CURVED TYPE BULKHEAD



$$d_w \geq 600$$

Figure 30

WATER LAYER POSITIONS

Illustrations with water layer next to protective bulkhead and air layer next to outer plate (general procedure when using water layer) are shown in Figure 30.

Underwater protection employing water layers is designed to afford maximum protective strength; and, therefore, the thickness of the air layer in the single plate method (multiple plate method will be discussed later) is always greater than the water layer. The ratio between the thickness of the air layer and the distance (D), between the outer plate and protective bulkhead is generally 0.6 to 0.8.

In ships rebuilt to incorporate water layers, however, d_a/D may fall below 0.6. It does not seem to hold true that the formula given in the preceding section for computing protective strength is satisfactory no matter how small d_a/D may be.

If the curve of defensive strength for the type of protection shown in Figure 31 is plotted it appears as curve (1).

Transferring this to a scale $1/2.97$, experiments were carried out when $d_a/D = 0$ and $d_a/D = 0.69$ (Tanks 90% full, see Figure 38). These experiments show that when $d_a/D = 0$, the strength of the protection is 72% of that when $d_a/D = 0.69$; (When $d_w = 600\text{mm}$, $d_a/D = 0.79$ and the strength becomes 60% of this maximum); and that 155 kg is the balanced charge when using water layers.

On curve (1) when $C = 155\text{ kg}$, $d_a/D = 0.534$; i.e., at this point the actual strength is greater than the calculated strength.

As well as performing experiments in the range $d_a/D = 0.5-0.2$ if $\phi(w)$ were known, it would be possible to fix this point.

To summarize:

Single plate method:

1. When $d_a/D \geq 0.55$, the strength of the protection can be obtained from the above formula.
2. When $d_a/D < 0.55$, it is 60% of the maximum definitive strength.

(Since this 60% is accurate when $D = 2.900$ meters, it is thought that there will be some inaccuracy at the highest and lowest value of D.)

Until now, d_a has been 1.220 meters and $d_w = 900 \times 3\text{cm}$ (see Figure 32). This experiment shows, as the formula has previously indicated, that $d_w = 600\text{mm}$. That is, the multi-layer method has the same strength as the single layer method. $d_a/D = 0.667$, which means that the defensive strength as previously described is good.

As oil is used up from the outside, protection increases until only the in-board tank is full of oil.

The protective strength shown in Figure 34(a) is good. However, in Figure 34(b) and (c) if the outside tank is filled with air, $d_a = 2.120$ and, if the inboard tank only is filled with oil $d_a = 3.020$, respectively, and the remaining bulkheads become intermediate bulkheads only.

In the above method of calculation, 100% of the thickness of the intermediate bulkhead is taken as effective regardless of joints but this has not been confirmed by experiment.

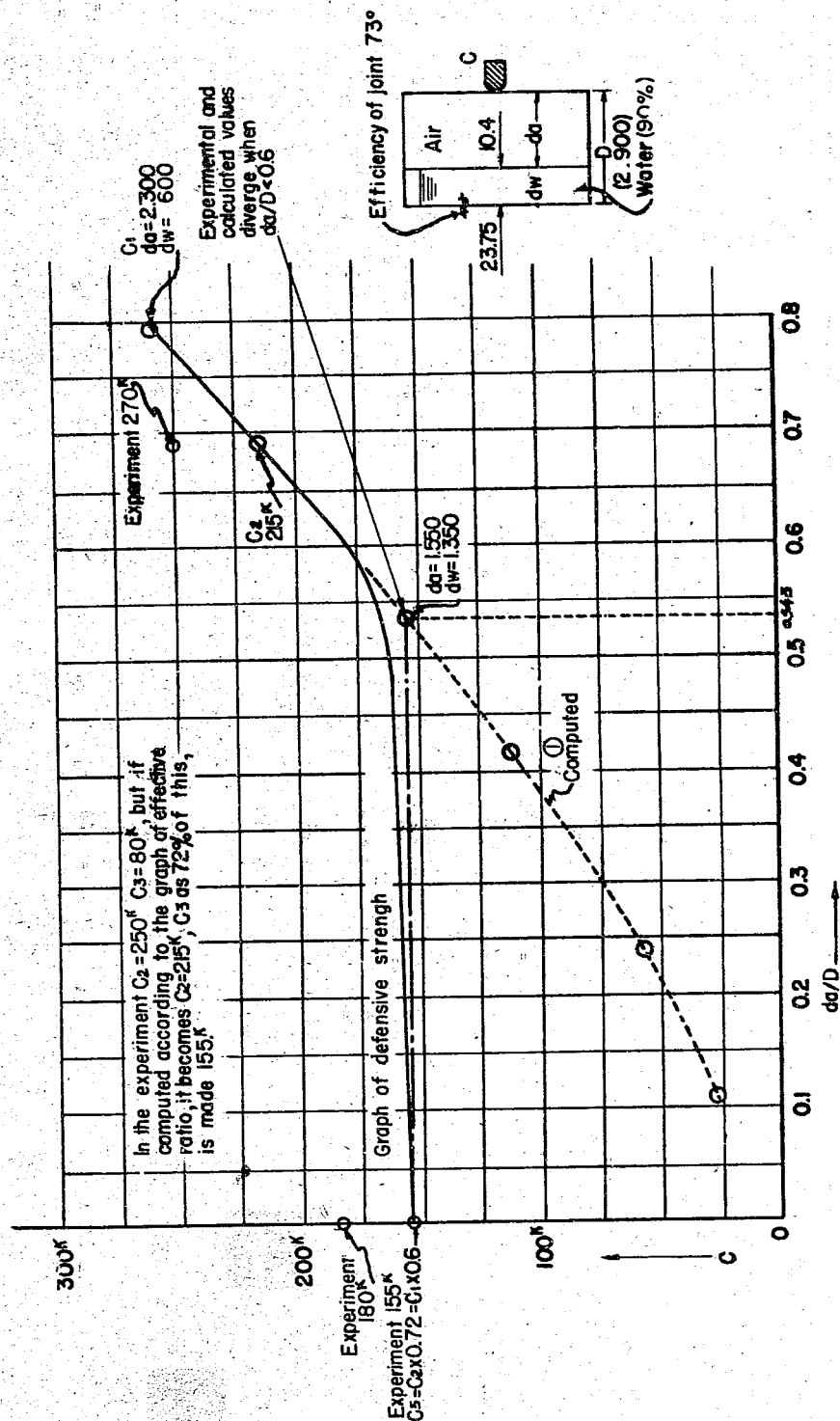


Figure 31
GRAPH OF DEFENSIVE STRENGTH (da/D vs C)

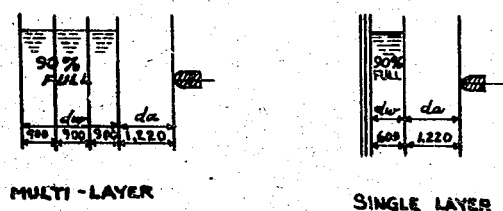


Figure 32

d_a AND d_w FOR MULTI- AND SINGLE LAYER SYSTEMS

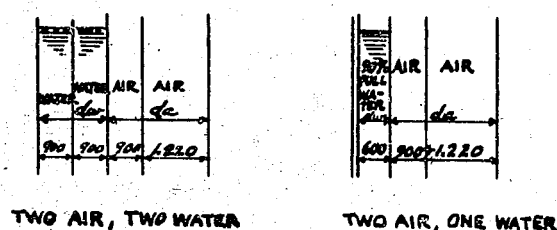


Figure 33

MULTI-LAYER SYSTEMS - OIL USED FROM OUTBOARD

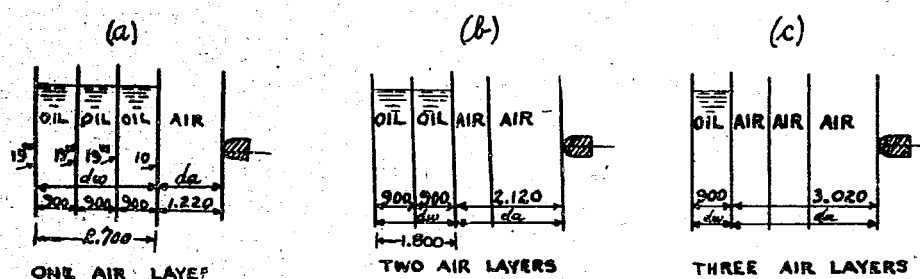


Figure 34

MULTI-LAYER SYSTEM - INCREASE OF d_a WITH USE OF OIL

The following ideas therefore are considered reasonable:

It is natural in the multi-layer method to depend on keeping the tanks full of oil and the effect of emptying the tanks in turn was calculated. The effective thickness of intermediate bulkheads has been calculated taking into account the efficiency of the joints. However, there are still points remaining to be investigated.

Usually in the multi-layer method the tanks are not worked at maximum efficiency and the usual efficiency is about 60% of the maximum. When the inboard tank only is filled with oil in these cases $D = d_a + 600\text{mm}$, and because of this it is considered reasonable for the efficiency to be 60% of single plate standard.

Hence it is thought that the systems in Figure 35 (b) and (c) are the same and that (c) has an efficiency of 60%. This, however, is yet to be confirmed by experiment.

It is difficult to formulate any rules for protection in which water layers are adjacent to the outer bottom and air layers adjacent to the protective bulkheads. Such systems are illustrated in Figure 36.

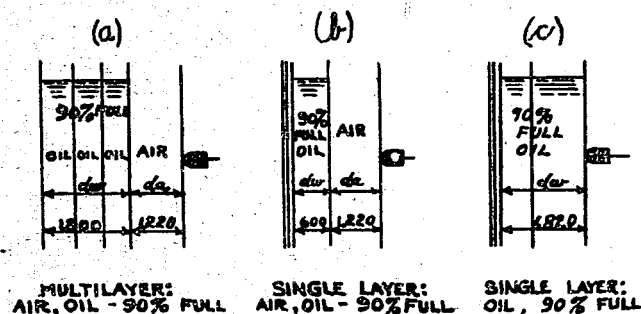


Figure 35

LIQUID LAYER ARRANGEMENTS

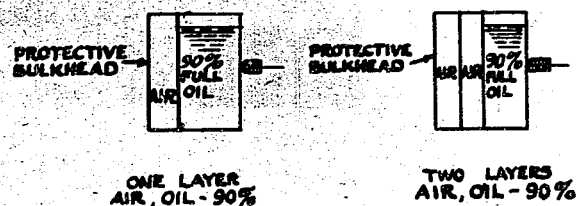
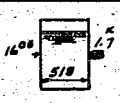
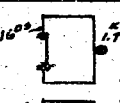

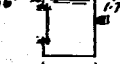

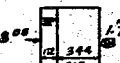

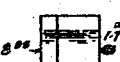

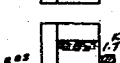
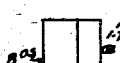

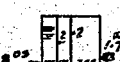






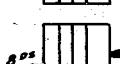



Figure 36

AIR LAYERS ADJACENT TO PROTECTIVE BULKHEAD

ORDER OF DEFENSIVE
STRENGTH

TARGET		TARGET		ORDER OF MERIT OF TYPES OF PROTECTION FROM THESE EXPER- IMENTS	
				TYPE	ORDER OF MERIT
A ₁ (34) A ₁ (45)		①	A ₂ (4)		①
A ₂ (64)		②	A ₂ (59)		②
A ₂ (2)		②			
E ₄ (11)		①	F (15) F (52)		①
E ₄ (23)		②	F (13)		②
E ₄ (26)		③	F (14)		②
E ₄ (12)		④			
J ₁ (31) J ₁ (54)		①	K ₁ (42)		①
J ₁ (22)		②	K ₁ (40)		②
J ₁ (32)		③	K ₁ (41)		③
J ₁ (25)		④	K ₁ (39)		④
J ₁ (38)		④			

THE WATER LAYER COMPARTMENTS
OVER 90% FULL

Figure 37

RESULTS OF EXPERIMENTS ESTABLISHING
EFFECTIVENESS OF AIR LAYER POSITION

It is thought, however, that it has a strength similar to that using air layers only. A detailed comparison is shown in Figures 37 and 38.

In these experiments the bulkheads had no joints; and, therefore, they only show trends.

From the results shown in Figures 37 and 38 we can make the following calculations, when ($D = 2.900$ meters, $da = 2.000$ meters and $dw = 900$ mm).

1. When the compartments outboard of the protective bulkhead are 90% full ($da/D = 0$), the defensive strength is 72% of that when the thickness of the outer layer is 900mm ($da/D = 0.69$).

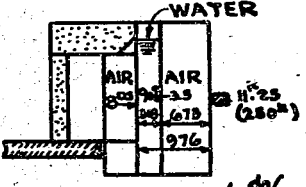
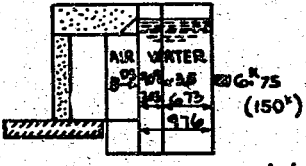
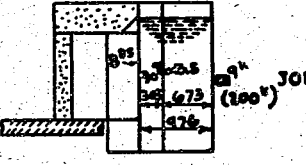
TARGET		REMARKS
K 19	 <p>EXTENT OF DAMAGE</p> <p>$S = 251$</p> <p>$(da/D = \frac{675}{976} = 0.69)$</p> <p>(JOINT EFFICIENCY 72%)</p>	INFERRED TO BE EQUAL
K 27	 <p>$S = 250$</p> <p>$(da/D = 0)$</p> <p>(JOINT EFFICIENCY 72%)</p>	BALANCED CHARGE 180°
K 28	 <p>$S = 334$</p> <p>JOINT FAILED IN 3 PLACES</p> <p>$(da/D = 0)$</p> <p>(JOINT EFFICIENCY 72%)</p>	

Figure 38

RESULTS OF EXPERIMENTS ESTABLISHING
EFFECTIVENESS OF AIR LAYER POSITION

2. The protective strength when the water layer is 900mm is 83% of that when the water layer is 600mm.
3. When the compartments outboard of the protective bulkhead are 90% full, the efficiency is 60% of the maximum (i.e. 600mm water layer).

CHAPTER IV PROTECTIVE METHOD EMPLOYING PROTECTIVE PIPING

In the protective method employing protective piping, from two to four rows of sealed metal pipes, 230mm in diameter and 6mm thick, are attached in the space before the protective plate. Like the water layer method described above, protective piping checks damage from splinters, distributes the concussion over the whole surface of the protective plate, causes a part of the explosive force to be absorbed by concussion on the protective piping, and increases the protective efficiency of the protective plate. Compared to the methods of employing air layers only, it has the advantages of reducing the thickness of the protective plate to 70% generally, and of reducing somewhat the amount of water used.

Experiments have been carried out with the protective piping attached in the space between the outer bottom and the protective plating; but, as in the case of the water layers, the only Japanese vessels employing piping are the NACHI class cruisers.

As piping will not be used from now on, only a brief statement of its potentialities will be given here.

1. Advantages of protective piping: It allows the protective plate to be made 30% thinner than when air layers only are used, thus curtailing the amount of Ducol steel used, and making the manufacture of protective plate easier.

2. Disadvantages of protective piping:

- a. The weight of the pipes is impractically high, and almost the same as the decrease in the weight of the protective plate, thereby making the weight of the ship about the same.

- b. The making of pipes and their installation requires considerable effort.

Note: Although the protective plate can be made 30% thinner when protective piping is used, it must be strong enough to support the pipes.

(Protective piping is illustrated in Tables XVIII, XIX and XX and Figure 46.)

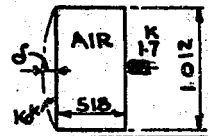
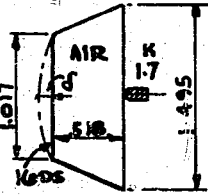
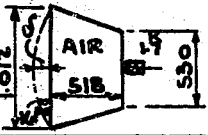

CHAPTER V EFFECT OF THE VOLUME OF THE AIR LAYER OUTSIDE THE PROTECTIVE PLATE ON THE PROTECTIVE STRENGTH, AND THE SIZE OF THE EXPERIMENTAL TARGET

A. General Remarks

In underwater explosions, damage done by splinters is related to the distance between the outer bottom and the protective plate, and it would seem to have almost no relation to the volume of the air layer. However, the damage by blast is greatly influenced by the volume of the air layer.

Table V shows the relation between the volume of air layer and the protective strength in experiments with a 1/5.35 scale model.

Table V
EFFECT OF AIR LAYER VOLUME ON PROTECTION

	TARGET (1/5.35 SCALE MODEL)	AIR LAYER VOLUME (V) CUBIC METRES	DEFLECTION OF PROTECTIVE PLATE (δ)	RATIO OF V	RATIO OF δ
(A)	(STANDARD MODEL) 	0.531	91 75 68 68 AVERAGE 75	1.0	1.0
(B)		0.815	69 57 AVERAGE 63	1.5	0.84
(C)		0.27	128 HOLE 128	0.5	1.71
(D)		0.515	81 66 AVERAGE 73	0.97	0.975

NOTE: THE ABOVE TARGETS ALL HAD 1~2
SPLINTER HOLES.

As Table V shows, the deflection of (B) with an air layer of large volume, is smaller than that of the standard model (A) while the deflection of (C), with an air layer of small volume is much larger than that of (A). Also, in (D), where the distance between outer bottom and protective plate is large, but the air layer volume the same, the results are almost similar to (A). Thus the relation between air layer volume and protective strength can be seen.

For example, in Figure 39, when the tanks are arranged as at (A), the thickness (calculated at 80mm) of the protective plate is generally sufficient to withstand the charge. In the case of (B), however, there are heavy oil tanks on both sides, so that the air layer in the area of explosion is decreased and dispersion in the adjoining compartments is restricted. Thus the blast transmitted to the protective plate is increased; and, as a result, the 80mm thickness sufficient in (A) is insufficient in (B). However, the relation between the air layer volume at which the calculated protective plate thickness manifests the expected protective strength, and the weight of the charge, is a matter which still requires research.

This relation has a very great influence on deciding the size of targets in scale experiments, but it would seem that there is no impediment to using a model of the size previously used in experiments with charges of 200 kilograms. However, much deliberation is necessary when deciding the size of models to be used with large charges.

B. Size of Models Used With 200 kg Charges

In experiments heretofore, 1/2.97 and 1/5.35 scale models have been chiefly used, and 1/2, 1/2.83, 1/3, 1/7.31 scale models only sparsely. The 1/2.97 and 1/5.35 models are discussed here.

The target size in experiments performed hitherto is as shown in Figure 40.

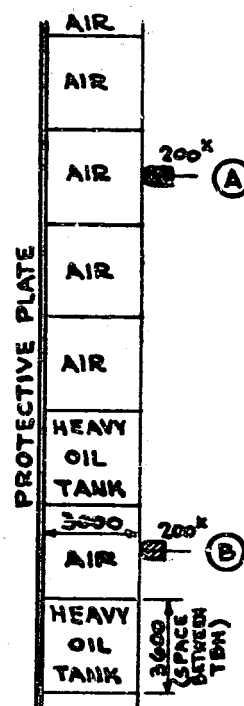


Figure 39

AIR ONLY vs. AIR WITH OIL ADJACENT

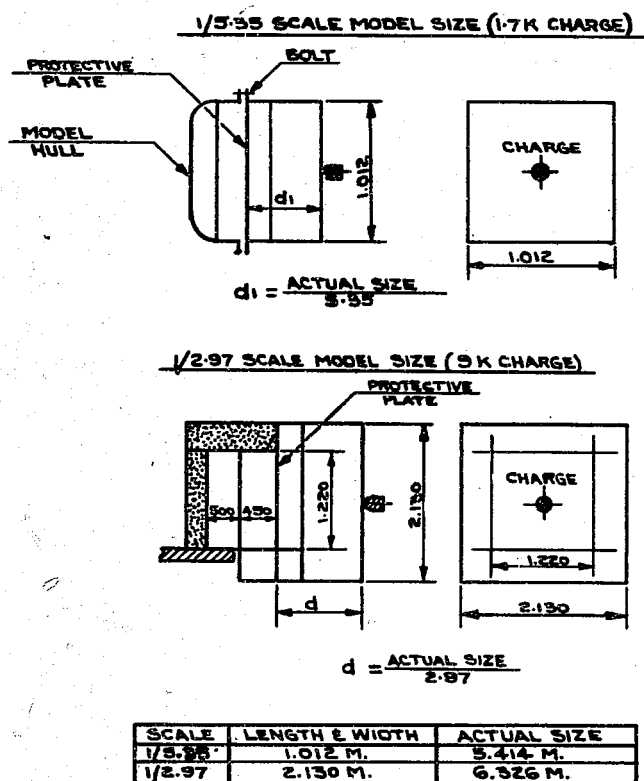


Figure 40
SCALE MODEL DIMENSIONS

The 1/5.35 scale model is a little smaller than the 1/2.97 scale model, but, as results in previous experiments have been almost the same, there is no impediment to using them in the future with less than 200 kg charges.

Also, there is no obstacle to making the 1/2.97 scale model full size, for a full-scale model. However, the air layers, water layers, and construction of a full-scale model must be almost the same as those of a real ship.

For example, in Figure 41 the width of a model on scale 1/2.97 is rather small, and the length is rather large, and it is usual to decide upon one with a decreased capacity.

Method of converting 1/2.97 scale to full-scale: $6.326 \times 6.326 \div$ Full-scale experimental model: 7.340×5.500

Also, the protective plate in the full-scale model is very similar to the actual ship, depending on the period of design.

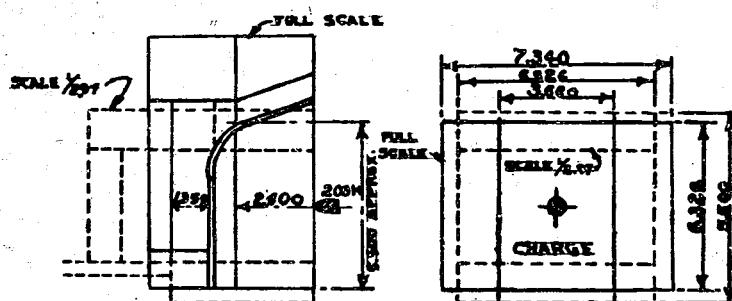


Figure 41

COMPARISON OF 1/2.97 AND FULL-SCALE MODELS

C. Size of Target for Large Explosive Charge

It can be said that the target for a large explosive charge can be considered as an enlarged target of 200 kg and its size decided upon. A 492 kg charge for a 1/2.97 scale model target and a 400 kg charge for a full size target will be examined.

Example 1. To find the size of 1/2.97 scale model target for 492 kg charge:

First, find the scaled explosive charge (C).

$$\text{Scale ratio} = \frac{\text{Model amount of explosive}}{\text{Actual amount of explosive}} = \frac{1}{2.843}$$

(According to research experiments on underwater defense 10/9/36)

$$C = 22.14 \text{ kg}$$

Next, find the scale ratio from the known charge 22.14 kg/200

$$\text{Scale ratio} = \left(\frac{22.14}{200} \right)^{2.843} = \frac{1}{2.16}$$

Therefore, the size of the target should be $1.37 - \left(\frac{2.97}{2.16} = 1.37 \right)$ times the 1/2.97 target.

In this case the capacity is $(1.37)^3$ or 2.57 times the 1/2.97 capacity.

Therefore, to make the distance between the outer bottom and protective plate equal to a scale of 1/2.97, (a charge of 9 kg) if the capacity is 9 kg x 2.57, the width and length are:

$$\sqrt{(1.37)^3} = \sqrt{2.57} = 1.6 \text{ times the 1/2.97 model}$$

The size and extent of the 1/2.97 scale model, 492 kg, experimented on in 1941 are given in Table VI.

Concerning the results in Table VI, the air capacity of a 22.14 kg target is 1.36 x 9 kg, and in view of the extent of the damage, the capacity seems to be suitably small.

However, the problem remains as to whether the capacity should be multiplied by 2.57 obtained by the above calculation.

Example 2. To find the size of a full-scale target for 400 kg

$$\text{Scale ratio} = \frac{400}{200} \sqrt[2.843]{1} = 1.276$$

i.e. a target 1.276 x 200 kg target.

The capacity is $(1.276)^3 = 2.07$ times the 200 kg target.

This time the distance between the outer skin and the protective plating is 1.276 x 200 kg target. To make this distance equal to the 200 kg, the width and length would be:

$$\sqrt{(1.276)^3} = \sqrt{2.07} = 1.44 \times 200 \text{ kg target}$$

The extent of damage to the 400 kg full-scale target experimented on in 1939 is given in Table VII.

From the results of Table VII, the air capacity of the 400 kg target is 1.63 x 200 kg target, and as the amount of damage was rather small there is apparently no necessity to increase it 2.07 times.

As the relation between amount of explosive and air capacity have not yet been settled, further research is necessary; but considering the results of the above experiments, in general it can be inferred that it is apparently possible to make a slight decrease in the calculated size of the target, when using a target with a large explosive charge on a scale increased from 200 kg.

In regard to the above problem, and those which should be studied in the future, it is thought that a decision can be reached by merely changing the thickness of the defensive plating on the same size of model, and carrying out experiments with various quantities of explosive.

CHAPTER VI ACTUAL EXAMPLES OF AREAS OF HOLES IN OUTER SKIN AND AMOUNT OF LEAKAGE CAUSED BY UNDERWATER EXPLOSIONS ON A SHIP'S SIDE

A. Examples of Areas of Holes In Outer Skin

Examples of the experiments carried out on TOSA are shown in Figure 42 and Table VIII.

Judging from Table VIII, the area of hole and the area of depression do not change appreciably when the charge of explosive is between 100 kg and 350 kg. They are generally 22.0m² and 120.0m² respectively.

B. Example of Flooding

It is necessary to carry out experiments on an actual ship to know the amount of leakage. In Japan, however, the only such data on hand are the results of experiments carried out on the scrapped ship TOSA.

Table VI
RESULTS OF TEST OF 1/2.97 MODEL WITH 492 AND 200 KG CHARGES

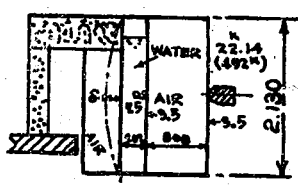
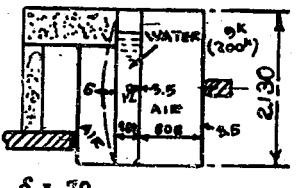
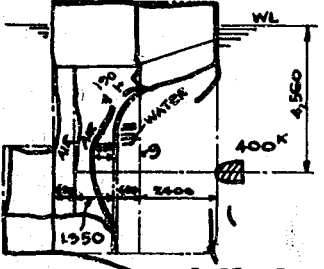
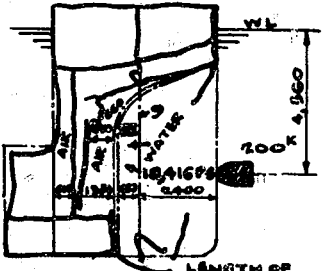
TARGET		RATIO OF VOID CAPACITY	DEGREE OF DAMAGE
(K11) 492K	 <p> $\delta = 200$ LENGTH OF TARGET = 2,200 AMOUNT OF CHANGE IN POSITION = 263 </p>	1.36	<p>LARGE</p> <p>THE THICKNESS OF THE PROTECTIVE PLATING, IN CONSEQUENCE OF THE EXPERIMENTAL TARGET, IS THICK IN COMPARISON TO K6 AND DAMAGE IS SLIGHT.</p>
(K6) 200K	 <p> $\delta = 70$ LENGTH OF TARGET = 2,130 AMOUNT OF CHANGE IN POSITION = 160 </p>	1.0	SMALL

Table VII
RESULTS OF EXPERIMENTS ON FULL SIZE TARGET USING 200 AND 400 KG CHARGES

TARGET		RATIO OF VOID CAPACITY	DEGREE OF DAMAGE
(B) 400K	 <p> LENGTH OF TARGET = 10,280 </p>	1.63	RATHER SMALL
(A) 200K	 <p> LENGTH OF TARGET = 7,940 </p>	1.0	RATHER GREAT

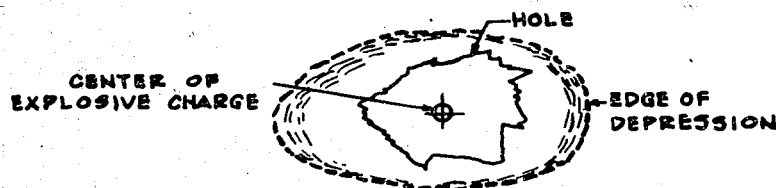


Figure 42

TOSA - TYPICAL HOLE IN OUTER SKIN

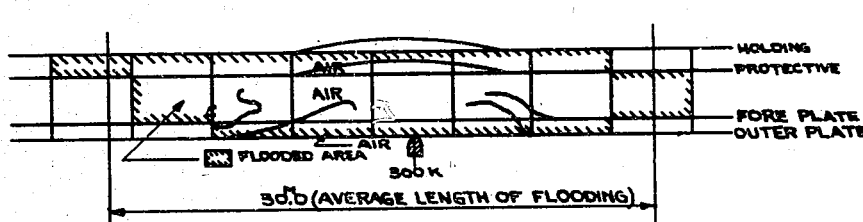


Figure 43

TOSA - LENGTH OF FLOODING

The flooding of this ship, when its protective strength was approximately 200 kg, is shown in Table IX.

It is estimated that the flooding due to 100 kg charge, if detonated inside the citadel, would be 500 to 600 tons. Also, when the charge and bulge are approximately balanced (200 kg), the amount of flooding is 1000 tons.

The following discussion considers water layer protection only, and the amount of water or oil in the flooded portion should be subtracted from the total flooding to give the amount of flooding.

The length of flooding for 200 to 300 kg given previously is 30 meters. It is considered reasonable to say that length of flooding is the same despite changes in the construction. Therefore, in flooding calculations in various ships the length of flooding is taken as the same.

Table VIII
TOSA - TYPICAL HOLES IN OUTER SKIN

Amount of Explosive(kg)	Thickness of Outer Skin(mm)	Area of Hole(m ²)	Area of Depression(m ²)
100	14	22.4	70.0
150	14	17.7	121.0
200	16	22.4	130.0
300	16	14.9	158.0
350	16	26.0	112.0
Average		21.7	118.0

Table IX
TOSA - FLOODING DATA

Charge(kg)	Amount of Flooding(tons)	Length of Flooding(m)	Remarks
100	995	19.0	Outside the citadel
150	726	23.0	Air layer only
200	1008	30.0	Air layer only
300	1203	30.0*	Air layer only
350	1160	31.0	Using pipes

*See Figure 43

Note: The lengths in Column 3 are average lengths of flooding.

$$\text{i.e. } \frac{\text{Amount of flooding}}{\text{Area of flooding at center of charge}}$$

CHAPTER VII CONNECTION BETWEEN DEPTH OF EXPLOSIVE AND PROTECTIVE STRENGTH

The protective plating splits at the instant of the explosion and the damage is caused by the shock wave. Such damage is increased by the rush of water through the holes in the outer bottom. Experiments carried out have made clear this fact for structures close to the charge.

Depth will have little effect on the pressure wave but the rush of water due to the expansion of the gas bubble may easily be affected.

From work already carried out, for other purposes, the following can be deduced: Depth settings for torpedoes are from 4-6 meters and previous experiments were carried out within these limits. Within these limits no difference could be observed.

Table X
DEPTH SETTINGS OF TORPEDOES

Target	Depth of Charge (m)	Calculated Depth for Full Size(m)
1/5.35 Model	1.000	5.350
1/2.97 Model	1.520 1.000	4.510 4.750
Full Size	4.570 4.750 6.096	4.570 4.750 6.096

To investigate the problem, a charge was placed at two or three times the normal depth and the following conclusions were reached:

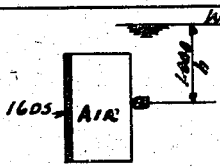
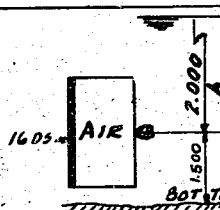
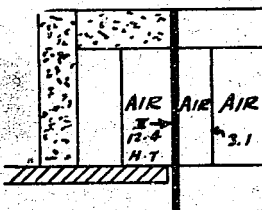
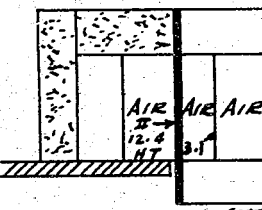
1. The sea-bed was quite close to the ship's bottom in these experiments and the effect of this was noticed. The greater the depth of the charge, the greater was its effect. The results are shown on Table XI.

2. As the depths used on these experiments were far greater than the draft of any ship, it can be said that the depth of charge has no effect on side protection.

According to the above, when the depth of the exploding charge is great, its destructive force is great. (Because when the sea bottom is near, its effect is increased.)

Note: The 2.000 meters depth of D2b (Table XI) at full scale would be 10.700 meters, and the 4.369 depth of G_A at full-scale would be 13.000 meters. Thus the latter depths would offer no protection to real ship hulls.

Table XI
RELATION OF DEPTH OF CHARGE TO RESISTING STRENGTH

REDUCED SCALE		TARGET	DAMAGE
$\frac{1}{5.35}$ (K)	D _{2a}		S=89 G HOLES
$\frac{1}{1.7}$ (K)	D _{2b}		S=120 CRACKING IN CENTER
$\frac{1}{2.97}$ (9K)	G _B		S=90 SCARRING IN CENTER
$\frac{1}{2.97}$ (9K)	G _A		S=92 PRODUCED 178±13 CRACKING IN CENTRAL PARTS

APPENDIX I

EXPERIMENTAL DATA INVOLVING AIR AND
WATER LAYERS AND PROTECTIVE PIPINGTable XII
EXAMPLES OF PROTECTIVE METHODS EMPLOYING AIR LAYERS

Target	Scale	Charge (kg)	Protective Plate Thickness (mm)	Fore-Plate Thickness (mm)	Total Thickness (mm)	Distance (D) (mm)	Damage (δ in mm)
A ₁ 1	1/5.35	1.7	16	DS	16	518	Tom perpendicular to welded line. 2 holes. $\delta = 91$
A ₂ 2	1/5.35	1.7	16		16	518	$\delta = 68$, 1 hole. Deep hole, $d = 300$ mm; shallow hole, $d = 650$ mm
A ₁ 3	1/5.35	1.7	16		16	518	$\delta = 68$, 2 holes. (Central hole, $d = 300$ mm peripherally); shallow hole, $d = 650$ mm peripherally.
A 4	1/5.35	1.7	16		16	518	$\delta = 65$, perfectly watertight. Deep hole, $d = 300$ mm; shallow hole, $d = 600$ mm
B 5	1/5.35	1.7	16		16	518	$\delta = 57$, 4 holes. Deep hole, $d = 350$; shallow hole, $d = 650$
C 6	1/5.35	1.7	16		16	518	Broken from the center.
D 7	1/5.35	1.7	16		16	843	$\delta = 66$, 3 holes ($d = 450$ peripherally)
E ₁ 12	1/5.35	1.7	8	2	10	518	$\delta = 100$, broken, 5 holes.
E ₂ 9	1/5.35	1.7	5 + 3	2	10	518	$\delta = 88$, flooded from holes in plates.
H 28	1/5.35	1.7	16	2	18	596	$\delta = 63$, 1 hole.
I 30	1/5.35	1.7	16	2	18	690	$\delta = 50$, perfectly watertight.
J ₁ 38	1/5.35	1.7	8	2 + 2	12	596	$\delta = 96$, perfectly watertight. Convex holes produced in inner - 4.
K ₁ 39	1/5.35	1.7	8	2 + 2 + 2	14	722	$\delta = 74$, perfectly watertight.
A ₁ 46	1/5.35	1.7	16		16	518	$\delta = 75$, 1 hole. Deep hole, $d = 300$
B 47	1/5.35	1.7	16		16	518	$\delta = 68$, Deep hole, $d = 350$; shallow hole, $d = 650$
C 48	1/5.35	1.7	16		16	518	$\delta = 128$, 1 hole. Deep hole, $d = 300$
D 49	1/5.35	1.7	16		16	843	$\delta = 81$, 10 holes. ($d = 400$ peripherally)
E ₁ 50	1/5.35	1.7	4 + 3	2	9	518	Great damage.
E ₂ 51	1/5.35	1.7	5 + 3	2	10	518	Great damage.
A ₁ 66 (Revised)	1/5.35	1.7	16		16	450	$\delta = 98$, 2 holes. Deep hole, $d = 250$ peripherally; shallow hole, $d = 450$ peripherally.
I 68 (Revised)	1/5.35	1.7	16		16	344	$\delta = 128$, 5 holes ($d = 200$ peripherally). Shallow hole, $d = 450$ peripherally. Central internal collapse.
I 69 (Revised)	1/5.35	1.7	16		16	344	$\delta = 124$, 8 holes ($d = 200$ peripherally). Shallow hole, $d = 450$ peripherally.
B ₁	1/5.35	1.7	20 _{PS}		20	224	Great damage.
B ₂	1/5.35	1.7	20 _{HT}		20	224	$\delta = 153$, 1 hole.
B ₃	1/5.35	1.7	16 _{PS}		16	224	Great damage.
B ₄	1/5.35	1.7	16 _{HT}		16	224	Great damage.
D ₁	1/5.35	1.7	16 _{HT}		16	450	$\delta = 92$, 3 holes.

Table XIII
EXAMPLES OF PROTECTIVE METHODS EMPLOYING AIR LAYERS

Target	Scale	Charge (kg)	Protective Plate Thickness (mm)	Core-Plate Thickness (mm)	Total Thickness (mm)	Distance (D) (mm)	Damage (δ in mm)
D _{2a}	1/5.35	1.7	16 DS		16	450	$\delta = 89$, 6 holes.
D _{2b}	1/5.35	1.7	16		16	450	$\delta = 120$, central cracking (great because of 2m depth).
E ₁	1/5.35	1.7	6 + 4 + 6		16	450	$\delta = 98$, 2 holes.
E ₂	1/5.35	1.7	8 + 8		16	450	$\delta = 96$, 4 holes.
E ₃	1/5.35	1.7	outside hull		16	450	$\delta = 87$, scarring, but no holes.
E ₄	1/5.35	1.7	inside hull		16	450	$\delta = 98$, 2 holes.
F ₁	1/5.35	1.7	16		16	450	$\delta = 104$, 12 holes.
F ₂	1/5.35	1.7	16		16	450	$\delta = 115$, 8 holes.
F ₃	1/5.35	1.7	16		16	450	Cracking, 4 holes (supporting bulkhead weak).
HEI	1/2.97	9	12.4 _{HT} + 24.85 _{HT}	NS	37.3	419	$\delta = 222.3$, $d = 228$ in center. Holes producing cracking.
HEI A	1/2.97	9	II 18.65 _{HT}		37.3	419	$\delta = 190.2$, $d = 228$ in center, scarring.
C _{TA}	1/2.97	9	II 12.4 _{HT}	3.1	27.9	991	$\delta = 92.1$, (12.7 x 177.8 damage area in center: great because of water depth of 14 1/4").
C _{TB}	1/2.97	9	II 12.4 _{HT}	3.1	27.9	991	$\delta = 88.9$, scarring in center.
3 - 1	1/2.97	9	II 28.1 _{HT}		56.2	Contact	900.6 x 990.6 hole.
3 - 2	1/2.97	9	II 21.75 _{HT}		43.5	210	$\delta = 165.1$, scarring in center.
3 - 3	1/2.97	9	21.75 _{HT}	3.1	24.9	1289	$\delta = 47.6$, more or less scarring in center.
3 - 4	1/2.97	9	16.8 _{HT}	3.1	19.9	1610	$\delta = 54$, numerous scarrings and holes in center.
4 - 1	1/2.97	9	II 28.1 _{HT}		56.2	102	Great damage.
4 - 2	1/2.97	9	III 24.85 _{HT}		74.6	Contact	Great damage.
4 - 3	1/2.97	9	II 18.65 _{HT} + 24.85 _{HT}		62.2	102	$\delta = 241.3$
4 - 4	1/2.97	9	IV 28.45 _{HT}		113.8	Contact	$\delta = 171.5$
Standard Type	1/2.97	9	24.85 _{HT}	3.1	28	1016	$\delta = 90$, holes, rear plates damaged.
Standard Type (30°)	1/2.97	9	24.85 _{HT}	3.1	28	1016	$\delta = 90$, holes, rear plates generally concave.
Large Type (60°)	1/2.97	9	24.85 _{HT}	3.1	28	1016	$\delta = 75$, holes, rear plates damaged.
Standard Type (90°)	1/2.97	9	24.85 _{HT}	3.1	28	1016	Great damage. Rear plates heavily damaged.

Table XIV
EXAMPLES OF PROTECTIVE METHODS EMPLOYING AIR LAYERS

Target	Scale	Charge (kg)	Protective Plate Thickness (mm)	Fore-Plate Thickness (mm)	Total Thickness (mm)	Distance, D (mm)	Damage (δ in mm)
C _{2A}	1/2.97	9	19 x 25/19 (19CNC), Joint Eff - 67.4%		25	811	δ = 110, 600 Cracking.
C _{2B}	1/2.97	9	19 x 25/19 (19CNC), Joint Eff - 46.4%		25	811	δ = 230, 700 Cracking.
C _{3T}	1/2.97	9	25 _{DS} , Joint Eff - 58.6%		25	811	900 x 640 hole.
C _{3s}	1/2.97	9	25 _{DS} , Joint Eff - 42.2%		25	811	δ = 280, small Cracking.
C _{3n}	1/2.97	9	25 _{DS} , Joint Eff - 58.6%		25	811	δ = 106, 2 holes.
C ₄	1/2.97	9	19 x 25/19 (19 Special Deck) Joint Eff - 58.6%		25	811	δ = 128, 500 Cracking.
C ₅	1/2.97	9	14 _{DS}		14	2000	δ = 68, 18 holes.
C ₆	1/2.97	9	5 _{DS} +3.5 _{DS} +6 _{DS}		14.5	2000	δ = 88, 1 hole.
5 - 1	1/2.97	9	II 24.85 _{DS} + II 18.65 _{DS}		87.0	Contact	Great damage.
5 - 2	1/2.97	9	63.5 x 25/19 (24"NVNC)		83.6	Contact	Damage.
5 - 3	1/2.97	9	II 10.57 _{DS}	6.22	27.4	1000	δ = 73, 2 small holes.
HEI B	1/2	30	III 18.65 _{HT}		56.0	628.4	d = 1.1 Cracking around circumference of holes, and numerous scarrings.
2nd Time*	1/1	200	88.9 x 25/19 (34"KNC)		117	Contact	Great damage, five feet circular hole produced, plate split in tr-
3rd Time*	1/1	200	88.9 x 25/19+19 (34"KNC)+19 _{HT}	7.45 _{MS}	143.5	2134	Greatest bend in plate, 1 1/2"; no other unusual change.
E (Provisional)*	1/1	200	II 43.5 _{HT}	7.45	94.5	2134	Greatest bend in protecting plate 8 1/2"; no other damage.
F (Provisional)*	1/1	200	II 37.3 _{HT}	7.45	82.1	2134	Hole - 8" x 10"
G (Provisional)*	1/1	200	III 24.85 _{HT}	8.7	83.3	2772	Although cracking was produced in one part, protection seemed perfect.
TOSA (6th Year Type Torpedo)*	1/1	200	III 24.85 _{HT} , Joint Eff - 47%	8.7	83.3	2850	In the vicinity of the center of explosion, a 4' x 1' hole occurred.
TOSA (9th Year Type Torpedo)*	1/1	150	III 24.85 _{HT} , Joint Eff - 47%	8.7	83.3	2850	In the vicinity of the center of explosion, a hole and scarring occurred.
TOSA (8th Year Type Torpedo)*	1/1	300	III 24.85 _{HT} , Joint Eff - 47%	8.7	83.3	2850	Damage in the outermost plate in the vicinity of the center of explosion producing cracking.

* Full Scale Model.

Note: Depths

TOSA (6th Year Type Torpedo) 4.050 meters
TOSA (9th Year Type Torpedo) 6.330 meters
TOSA (8th Year Type Torpedo) 4.880 meters

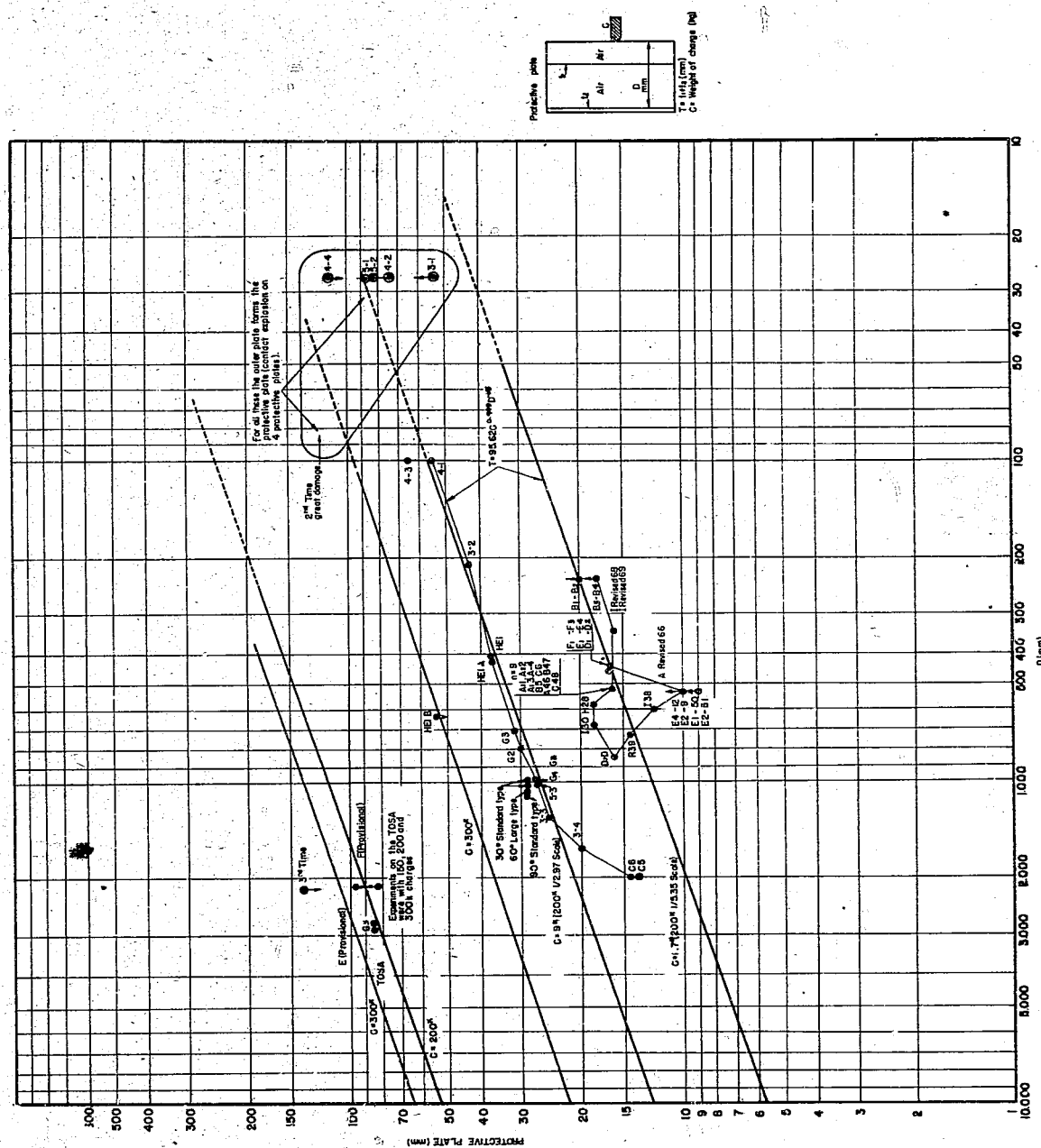


Figure 44

AIR LAYERS - COMPREHENSIVE CHART OF EXPERIMENTAL DATA

Table XV
EXAMPLES OF PROTECTIVE METHODS EMPLOYING WATER LAYERS. (THE NUMERICAL VALUES IN THIS CHART
ARE CONVERTED TO FULL SCALE, BUT THE DAMAGE STATISTICS ARE FOR A 1/5.35 SCALE MODEL)

Target and Scale	da (m)	dr (m)	D (da+600) (m)	Σt_1 MS (mm)	Σt_2 MS (mm)	Protective γ Plate Eff. γ	$\Sigma t_2 \gamma$ (mm)	$\Sigma t_1 + \Sigma t_2 \gamma$ (mm)	T (mm)	K	C (kg)	Damage	Single or Multiple Layers
Basic Model (no protective plates)	E ₁ (8), 1/5.35	1.840	0.920	2.440	10.7	37.5	1.00	37.5	48.2	0.567	200	Circular tear	Single
	E ₂ (10), 1/5.35	1.840	0.920	2.440	10.7	48.2	1.00	48.2	58.9	0.693	200	Circular tear	Single
	E ₃ (11), 1/5.35	1.840	0.920	2.440	10.7	42.8	1.00	42.8	53.5	0.630	200	Complete bend = 96	Single
	F (15), 1/5.35	0.920	1.840	1.520	10.7	42.8	1.00	42.8	53.5	0.535	200	Complete bend = 133	Single
	J ₁ (21), 1/5.35	2.500	0.664	3.100	21.4	42.8	1.00	42.8	64.2	0.823	200	Complete bend = 83	Single
	H (29), 1/5.35	1.840	1.340	2.440	10.7	85.6	1.00	85.6	96.3	1.130	200	Complete bend = 77	Single
	J ₁ (32), 1/5.35	1.840	1.330	2.440	10.7	42.8	1.00	42.8	64.2	0.756	200	Complete bend = 103	Single
	K ₁ (41), 1/5.35	1.840	1.990	2.440	10.7	64.2	1.00	64.2	74.9	0.883	200	Complete bend = 108	Multiple
	K ₁ (42), 1/5.35	2.500	1.330	3.100	21.4	53.5	1.00	53.5	74.9	0.961	200	Complete bend = 75	Multiple
	F (52), 1/5.35	0.920	1.840	1.520	10.7	42.8	1.00	42.8	53.5	0.535	200	Complete bend = 145	Single
	J ₁ (54), 1/5.35	2.500	0.664	3.100	21.4	42.8	1.00	42.8	64.2	0.823	200	Complete bend = 95	Single
	K ₁ revised	1.330	0.664	1.930	21.4	42.8	1.00	42.8	64.2	0.698	200	Complete bend = 142	Single
	K ₁ revised	0.664	1.264	1.264	10.7	42.8	1.00	42.8	53.5	0.504	200	Complete bend = 203	Single
	H revised	0.535	1.340	1.135	10.7	53.5	1.00	53.5	64.2	0.605	200	Complete bend = 165	Multiple
	H revised	0.535	1.340	1.135	10.7	85.6	1.00	85.6	96.3	0.876	200	Complete bend = 143	Single
	No. 1, 1/5.35	0.985	1.070	1.585	10.7	58.9	0.66	38.9	49.6	0.433	200	Complete bend = 144	Multiple
Large Model (equipped with protective plates)	No. 2, 1/5.35	0.985	1.070	1.585	10.7	64.2	0.605	38.9	49.6	0.433	200	Complete bend = 125	Multiple
	No. 3, 1/5.35	1.520	0.535	2.055	10.7	58.9	0.66	38.9	49.6	0.552	200	Complete bend = 131	Single
	No. 4, 1/5.35	1.520	0.535	2.055	10.7	64.2	0.42	27.0	37.7	0.418	200	Complete bend = 138	Single
	No. 5, 1/5.35	0.625	1.070	1.225	10.7	69.5	0.61	42.4	53.1	0.394	200	Complete bend = 145	Multiple
	No. 6, 1/5.35	0.985	1.070	1.585	10.7	48.1	0.70	33.7	44.4	0.383	200	Complete bend = 159	Multiple
	No. 6, 1/5.35	0.985	1.070	1.585	10.7	48.1	0.70	33.7	44.4	0.383	200	Complete bend = 159	Multiple

*Water layer completely full.

Notes:

1. The basic models are not equipped with protective plates. The results of water layer protection are shown, but the extent of its usefulness is not clear, because of the lack of protective plates.
2. The working models are all equipped with protective plates. The results of water layer protection can be clearly seen from the standard model. The same results are obtainable with a 1/2.97 scale model.

Table XVI
EXAMPLES OF PROTECTIVE METHODS EMPLOYING WATER LAYERS
(Numerical Values Converted to Full Scale; Damage Statistics for 1/5.35 Scale Model.)

Target	Scale	σ_{da} (m)	d_w (m)	P (kgf/cm^2)	Σx_1 MS (mm)	Σx_2 MS+RS (mm)	γ	Σt_{27}	$\Sigma x_1 + \Sigma x_2$ (m)	T (mm)	K	C (kg)	Damage (δ in mm)
C_{T1} 16	1/5.35	1.840	1.840	2.440	10.7	48.1	0.5	24.0	34.7	85.0	0.408	200	Cracking
C_{T1} 17	1/5.35	1.840	0.920	2.440	10.7	48.1	0.5	24.0	34.7	85.0	0.408	200	Cracking
C_{T2} 18	1/5.35	1.840	1.840	2.440	10.7	53.5	0.5	26.8	37.5	85.0	0.431	200	Cracking
C_{T2} 19	1/5.35	1.840	0.920	2.440	10.7	53.5	0.5	26.8	37.5	85.0	0.431	200	Cracking
C_{T3} 20	1/5.35	1.840	1.840	2.440	10.7	59.0	0.5	29.5	40.2	85.0	0.473	200	Cracking
C_{T3} 35	1/5.35	1.840	0.920	2.440	10.7	59.0	0.5	29.5	40.2	85.0	0.473	200	Cracking
C_{T4} 36	1/5.35	1.840	1.840	2.440	10.7	53.5	0.5	26.8	37.5	85.0	0.431	200	$\delta = 144$ Cracking
C_{T4} 37	1/5.35	1.840	0.920	2.440	10.7	53.5	0.5	26.8	37.5	85.0	0.431	200	$\delta = 144$ Cracking
C_{T4} 53	1/5.35	1.840	1.840	2.440	10.7	53.5	0.5	26.8	37.5	85.0	0.431	200	$\delta = 122$ Cracking

Note: Installation of four layers of protective plating is insufficient (estimated 50% efficiency). It is presumed that the innermost layer of protective plate is unable to show the estimated resisting strength because it is too thin.

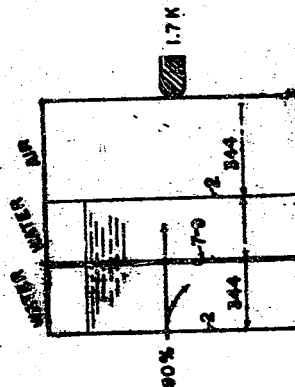


Table XVII
EXAMPLES OF PROTECTIVE METHODS EMPLOYING WATER LAYERS
(Numerical Values Corrected To Full Scale Damage Statistics for 1/2.97 Scale Model)

Target	Scale	ds (m)	dw (m)	D (dist 600) (m)	Σk_1 18° (mm)	Σk_2 18° (mm)	γ	$\Sigma k_1 + \Sigma k_2$ (mm)	$\Sigma k_1 + \Sigma k_2$ (mm)	T (mm)	K	C (kg)	Damage (δ in mm)	
K ₁	1/2.97	1.200	0.600	1.800	10.4	47.5	0.667	31.7	42.1	94.0	0.448	200	$\delta = 110$	Single Layer
K ₂	1/2.97	1.200	1.200	1.800	10.4	47.5	0.667	31.7	42.1	94.0	0.448	200	$\delta = 63$	Single Layer
K ₃	1/2.97	1.200	1.200	1.800	10.4	47.5	0.688	32.7	43.1	94.0	0.459	200	$\delta = 76$	Multiple Layer
K ₄	1/2.97	1.200	1.800	1.800	10.4	47.5	0.680	32.3	42.7	94.0	0.454	200	$\delta = 93$	Multiple Layer
K ₅	1/2.97	1.200	1.800	1.800	10.4	47.5	0.715	33.6	44.0	94.0	0.468	200	$\delta = 70$	Multiple Layer
K ₆	1/2.97	2.400	0.600	3.000	10.4	35.6	0.675	24.0	34.4	88.0	0.430	200	$\delta = 70$	Single Layer
K ₇	1/2.97	2.400	0.600	3.000	10.4	23.75	0.694	16.5	26.9	80.0	0.336	200	$\delta = 102$	Single Layer
K ₈	1/2.97	3.600	0.600	4.200	10.4	23.75	0.694	16.5	26.9	71.0	0.379	200	$\delta = 98$	Single Layer
K ₉	1/2.97	2.400	0.600	3.000	10.4	23.5	0.780	41.7	52.1	110.0	0.474	400	$\delta = 65$	Single Layer
K ₁₀	1/2.97	2.400	0.600	3.000	10.4	23.5	0.780	41.7	52.1	110.0	0.474	400	$\delta = 50$	Single Layer
K ₁₁₋₁₄	1/2.97	2.400	0.600	3.000	10.4	74.3	0.728	54.0	64.4	122.0	0.527	482 (470)	$\delta = 200$	Single Layer
K ₁₅	1/2.97	2.400	0.600	3.000	10.4	32.7	0.734	24.0	34.4	80.0	0.430	200	Water layers decreased to 64% by leakage.	Single Layer (arc shaped)
K ₁₆	1/2.97	2.400	0.600	3.000	10.4	35.6	0.670	23.8	34.2	80.0	0.427	200	$\delta = 145$	Single Layer
K ₁₇₋₁₉	1/2.97	2.000	0.900	2.600	10.4	23.75	0.720	17.1	27.5	92.0	0.299	250	$\delta = 251$	Single Layer
K ₂₀₋₂₂	1/2.97	2.000	1.800	2.600	10.4	29.7	0.709	21.0	31.4	107.0	0.293	330	Presumed to be balanced.	Multiple Layer
K ₂₃₋₂₅	1/2.97	2.000	1.800	2.600	10.4	29.7	0.709	21.0	31.4	105.0	0.290	320	Presumed to be balanced. Water layers in K-25 to be completely flooded.	Multiple Layer
K ₂₆₋₂₈	1/2.97 (Flooded)		2.900		10.4	23.75	0.720	(described elsewhere)				180	Presumed to be balanced.	Single Layer
American Warship	1/2.97	1.200	2.700	1.800	10.0	57.0	0.7	39.9	49.9	132.0	0.375	400	Downer plates broken	Multiple Layer
American Warship	1/2.97	1.200	2.700	1.800	10.0	57.0	0.7	39.9	49.9	140.0	0.359	450	From the results of the above, presumed to be balanced.	Multiple Layer
A*	1/1	2.400	0.600	3.000	9.0	34.0	0.740	25.2	34.2	80.0	0.427	200	Presumed to be balanced.	Single Layer (arc shaped)
B*	1/1	2.400	0.600	3.000	9.0	50.0	0.720	36.0	45.0	110.0	0.409	400	Presumed to be balanced.	Single Layer (arc shaped)

* Full Scale Target

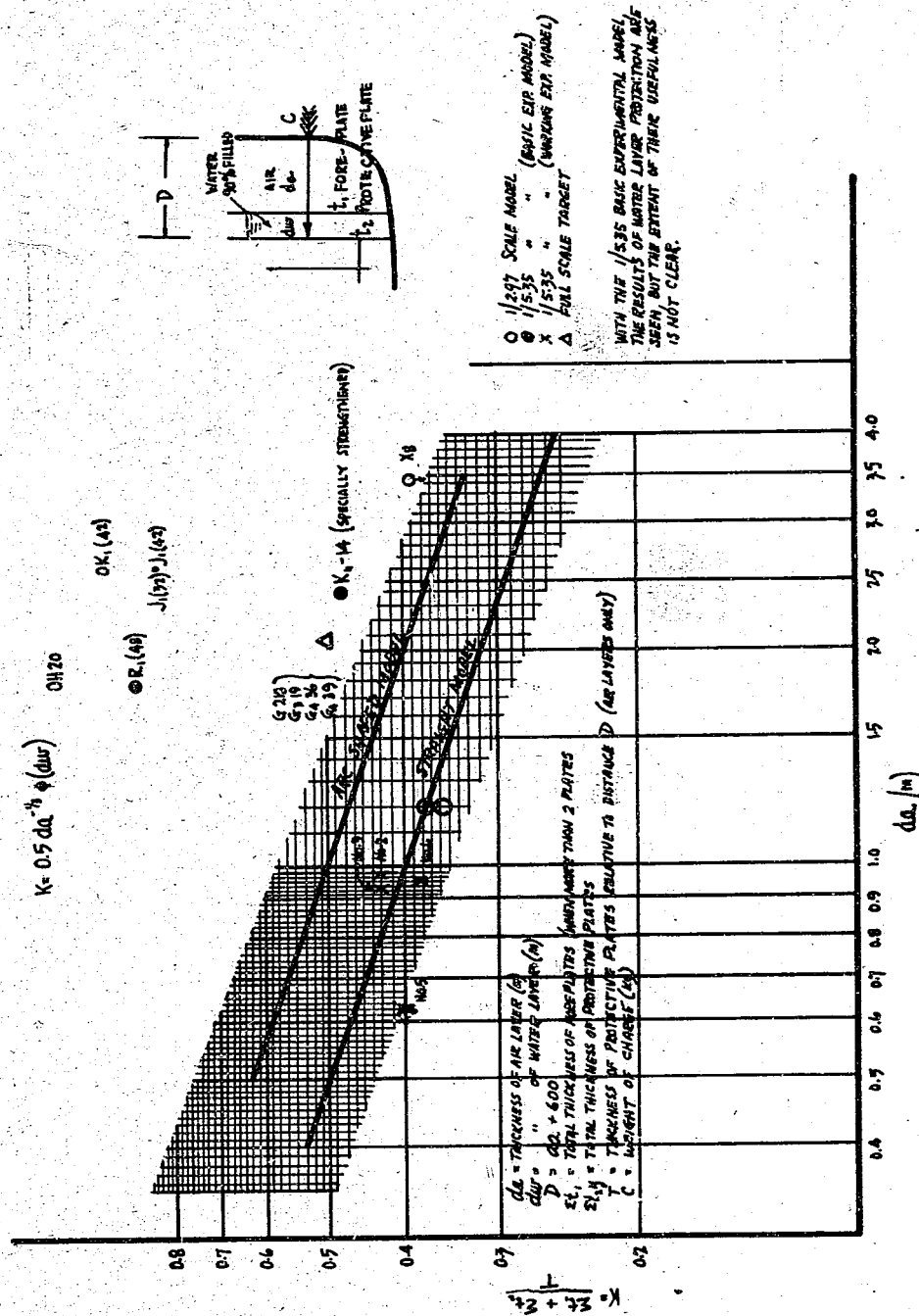


Figure 45
WATER LAYERS - COMPREHENSIVE CHART OF EXPERIMENTAL DATA

Table XVIII
EXAMPLES OF PROTECTIVE METHODS EMPLOYING PROTECTIVE PIPING

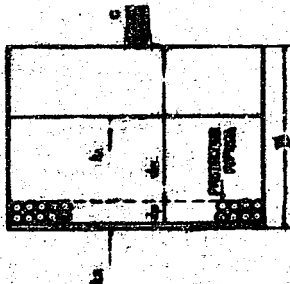
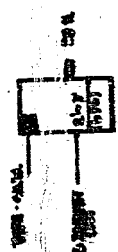
Target (scale)	da	D	Σt	τ	$K = \frac{\Sigma t}{\tau}$	Damage
	1.935	2.850	83.3	106	0.786	Good.
						No local damage but a 36' damage area along the upper part of the curved area.
In the following table: (da, D, Σt , τ , $K = \frac{\Sigma t}{\tau}$ are converted to full scale; target size and damage are for a 1/2 scale model.)						
Target (h)	da	D	Σt	τ	$K = \frac{\Sigma t}{\tau}$	Damage
	1.357	2.037	110	160	0.687	Damage
						Cracking produced diagonally in the outer plate of the II - 30 in HT metal plates, but inner plates undamaged. Maximum deflection 11"

Table XIX
EXAMPLES OF PROTECTIVE METHODS EMPLOYING PIPING

Target (1/2.97)	da (mm)	D (in)	St MS, DS (mm)	T (mm)	$K = \frac{St}{T}$	Damage
	451	1.357	74.3	104	0.715	Great damage. Three of the 20 lb HT plates were broken at the edge of the angle section attachment and part of the lower one was broken at the edge of the attachment and almost torn off.
	64	1.357	74.3	104	0.715	Great damage. Three of the 20 lb HT plates were broken and only one of the rear plates was left.
	451	1.357	37	104	0.358	Great damage. The circumference of the 20 lb HT plate was broken, and the 17 lb plates of the rear wall were broken and blown into the cement wall. The circumference of the 20 lb HT plate was broken and bent, and cracking occurred.
	906	1.357	74.3	104	0.715	Good. Greatest deflection of the 20 lb HT plate 6". It was observed that this deflection was arc-shaped because the pipes distributed the force of the explosion.
	2.566	3.018	46	79	0.582	Great damage. A 2' vertical by 2'9" horizontal hole was produced in the 20 lb HT plate.
	1.604	2.055	55	91	0.604	Great damage. A large hole, 2' vertical by 1'9" horizontal, was produced in the 30 lb HT plate. On the upper edge of the inner part, cracking occurred, extending the width of the plate.
	1.396	2.076	55	90	0.611	Good. Maximum deflection of the 30 lb HT plate 4". Although a hole was not produced, the rivets were loosened. A crack, width 1/8", length 8" was produced in the 25 lb HT plate.
	906	1.586	74	99	0.748	Good. Greatest deflection of 40 lb HT plate, 4-9/16". Although there was no damage, the rivets were loosened.
	2.260	3.165	40.7	78	0.521	Good Protective plate be.

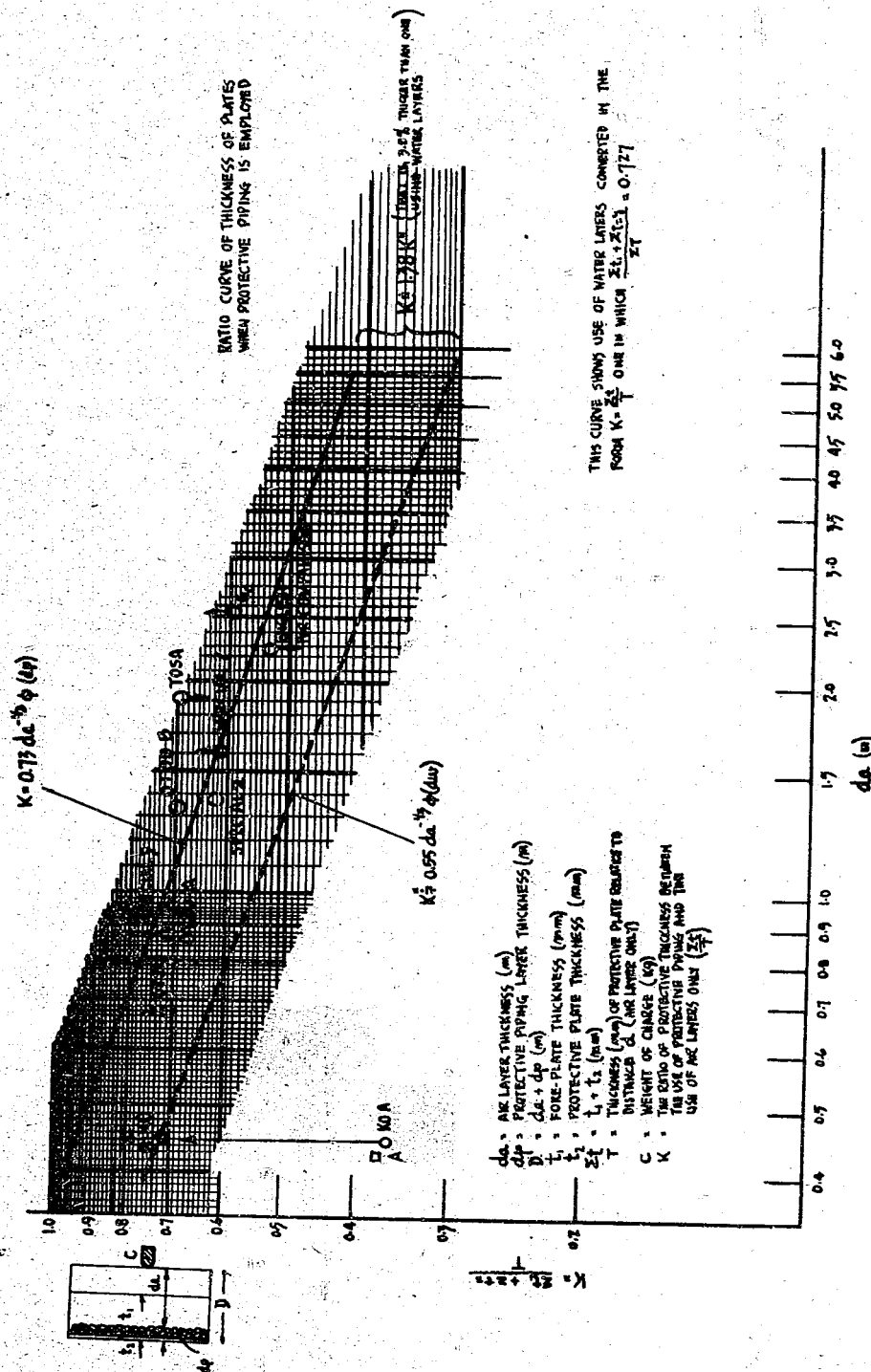
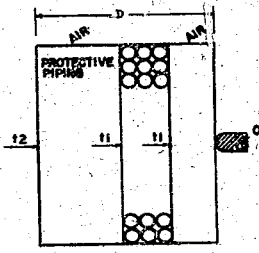
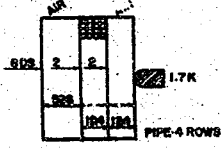
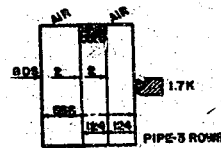
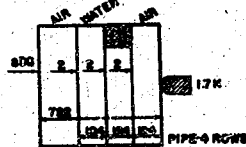

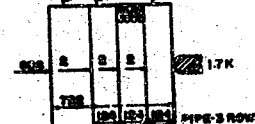


Figure 46

PROTECTIVE PIPING - COMPREHENSIVE CHART OF EXPERIMENTAL DATA

Table XX
PROTECTIVE METHODS WITH PROTECTIVE PIPING ARRANGED IN CENTRAL AREA

		D = Air layer thickness (m)				
		t_1 = Total fore-plate thickness (mm)				
		t_2 = Protective plate thickness (mm)				
		$\Sigma t = t_1 + t_2$ (mm)				
		T = Protective plate thickness (mm) relative to distance D (air layer only)				
		C = Weight of charge (kg)				
(D, Σt , T , $K = \frac{\Sigma t}{T}$ are all converted to actual size; target and damage statistics for 1/5.35 model.)						
Target ($\frac{1}{5.35}$)		D (m)	Σt (mm)	T (mm)	$K = \frac{\Sigma t}{T}$	Damage
J_2		3.189	64.2	78	0.824	Perfectly watertight No perforation
(24)						Deflection 96mm
J_2		3.189	64.2	78	0.824	Perfectly watertight No perforation
(55)						Deflection 100mm
J_3		3.189	64.2	78	0.824	One part cracked
(33)						Deflection 103mm
J_3		3.189	64.2	78	0.824	Perfectly watertight No perforation
(56)						Deflection 113mm
E_2		3.863	75	73	1.03	Perfectly watertight No perforation
(27)						Deflection 92mm
E_2		3.863	75	73	1.03	Perfectly watertight No perforation
(43)						Deflection 109mm
K_3 (44)		3.863	75	73	1.03	Perfectly watertight
						No perforation
						Deflection 110mm
						Perfectly watertight
K_3 (58)		3.863	75	73	1.03	No perforation
						Deflection 101mm

APPENDIX II

DATA FOR CALCULATION OF PROTECTIVE STRENGTH

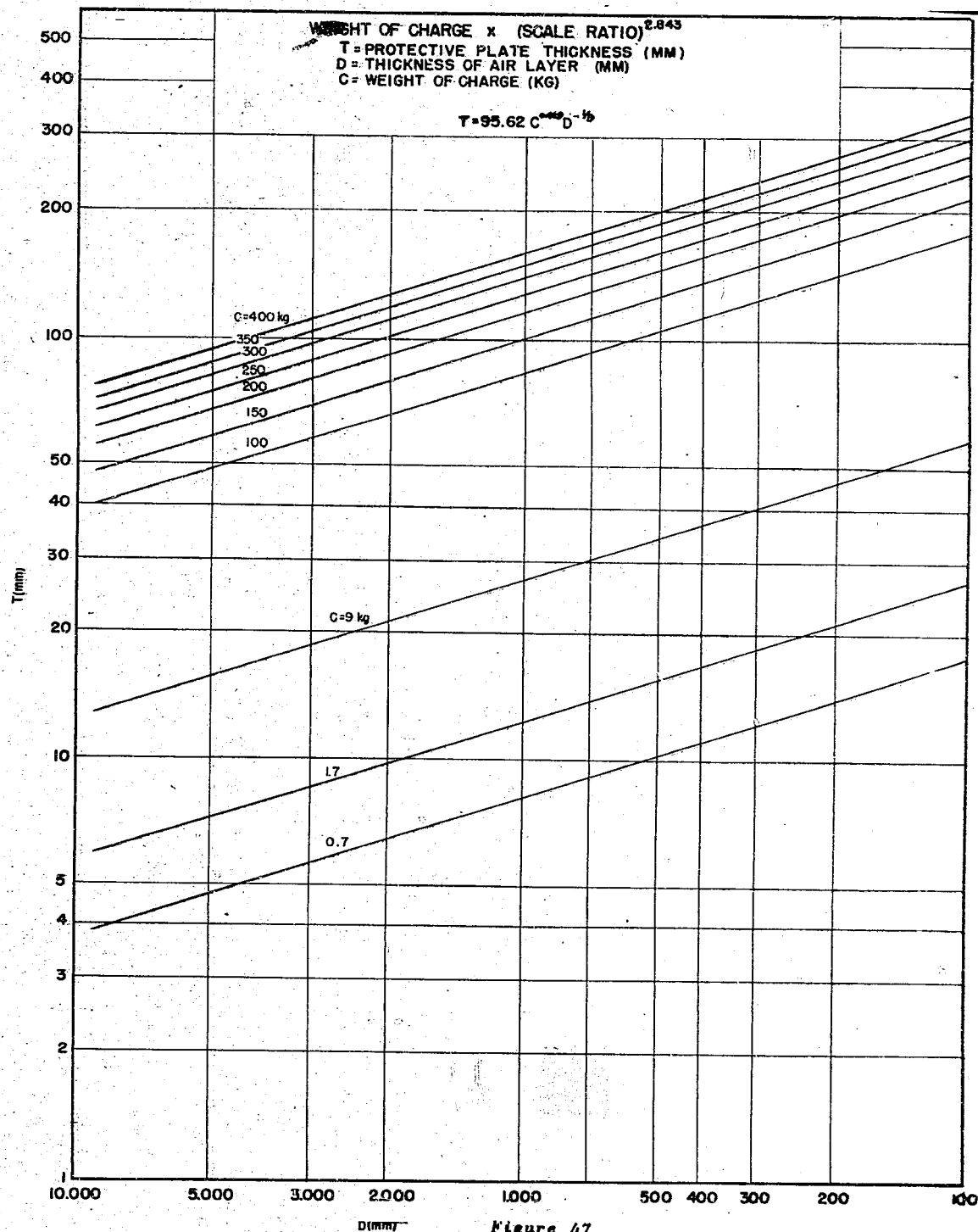


Figure 47

CURVES FOR CALCULATION OF PROTECTIVE STRENGTH
 WHEN USING AIR LAYERS ONLY D (mm)

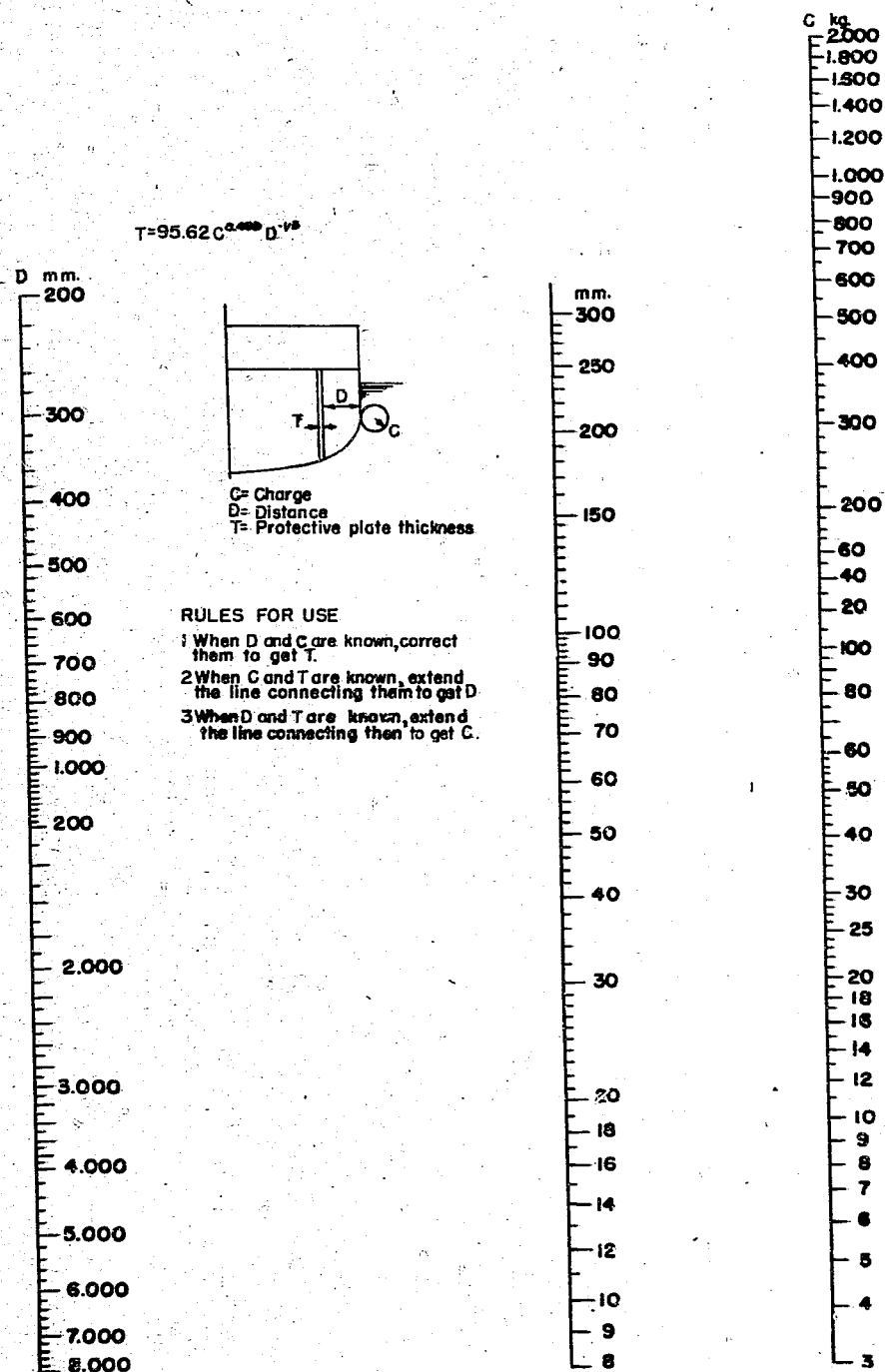


Figure 48

NOMOGRAPH FOR CALCULATING PROTECTIVE STRENGTH
WHEN USING AIR LAYERS ONLY

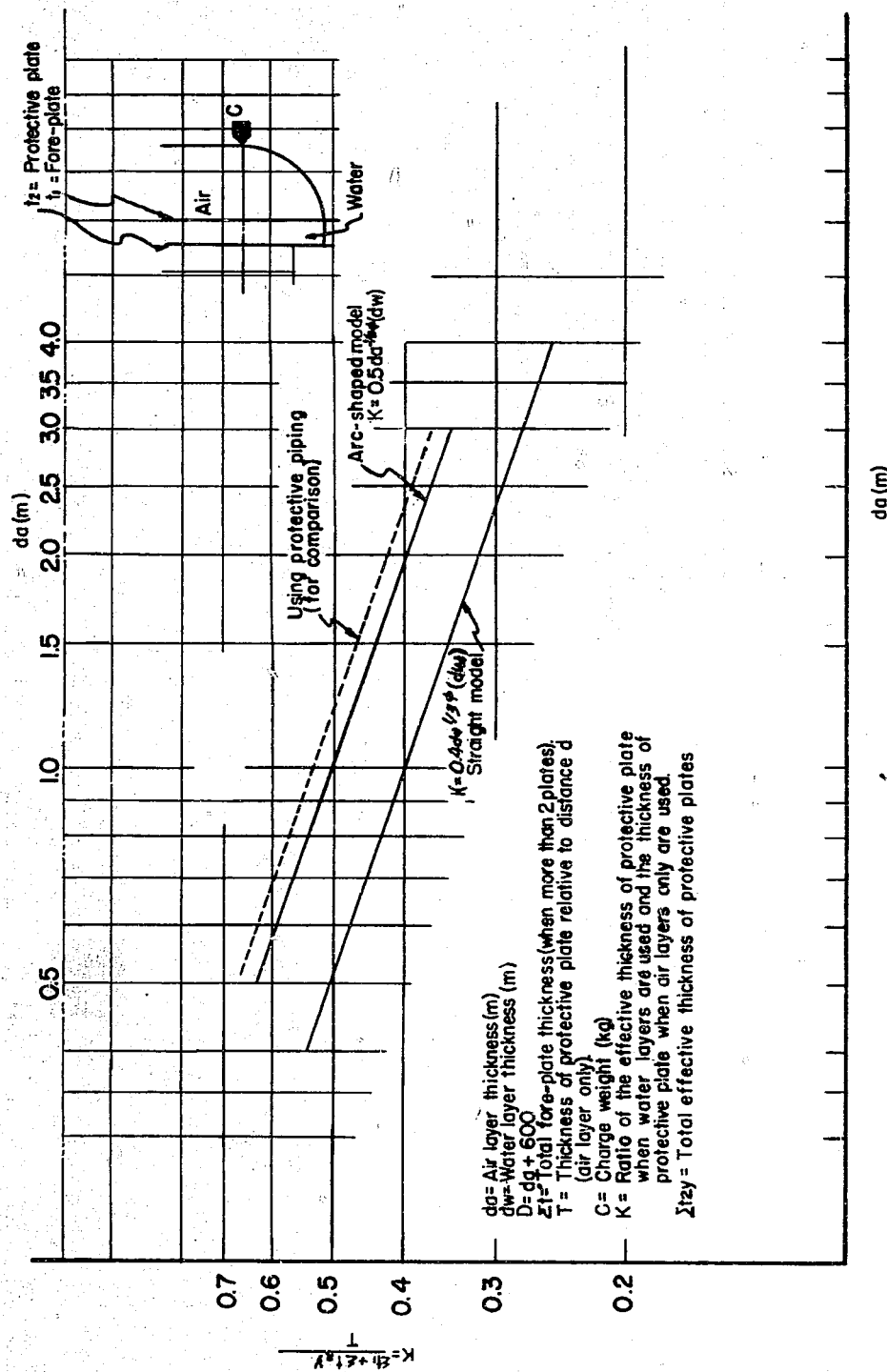


Figure 49
CURVES FOR DETERMINING EFFECTIVE THICKNESS OF PROTECTIVE PLATE
WHEN WATER LAYERS ARE USED

Table XXI
CHARGES USED IN SCALE MODEL EXPERIMENTS

Full Scale Charge (kg)	1/2.97 Scale Charge (kg)	1/5.35 Scale Charge (kg)	1/7.31 Scale Charge (kg)
600	27.1	5.1	2.1
550	24.75	4.675	1.925
500	22.5	4.25	1.75
450	20.25	3.825	1.575
400	18.0	3.4	1.4
350	15.75	2.975	1.225
300	13.5	2.55	1.05
250	11.25	2.225	0.875
200	9.0	1.7	0.7
150	6.75	1.275	0.525
100	4.5	0.85	0.35
50	2.25	0.425	0.175

$$\text{Scale ratio} = \left(\frac{\text{Model Charge}}{\text{Full Scale Charge}} \right) \frac{1}{2.843}$$

APPENDIX III

UNDERWATER PROTECTION SYSTEMS IN VARIOUS COMBATANT SHIPS

Air Layers Only

Single Layer Protection Method - Straight Model

Protective Strength = 520 kg Joint Efficiency = 45%

Weight of Water About 970 Tons (Shaded Area on Diagram)

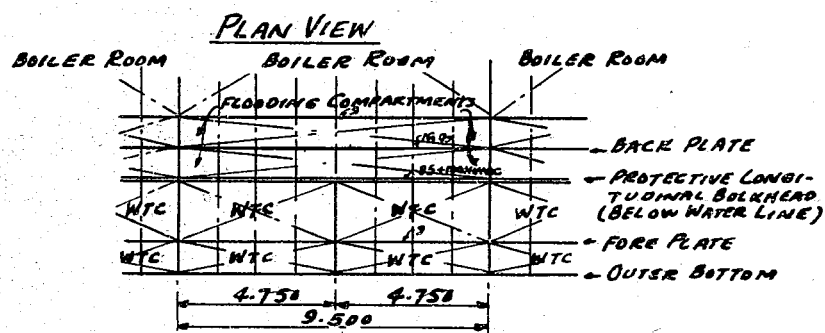
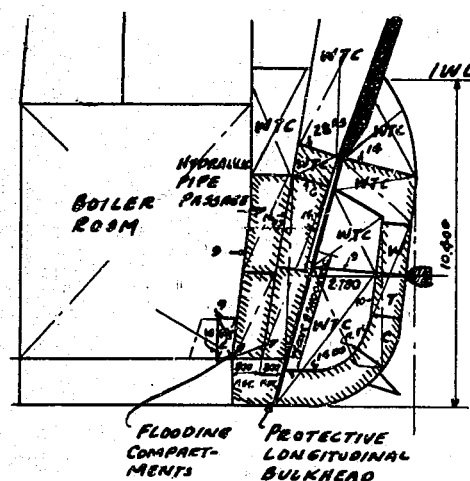


Figure 50

UNDERWATER PROTECTION SYSTEM - BB YAMATO

Air Layers Only

Single Layer Protection Method - Arc Shaped Model

Protective Strength = 500 kg (With Air Layers) Joint Efficiency = 65%

Weight of Water About 1600 Tons (When all outside protective plating is air layer)

About 1000 Tons (When outer tank is as shown in Figure 52)

(Shaded Area on Diagram)

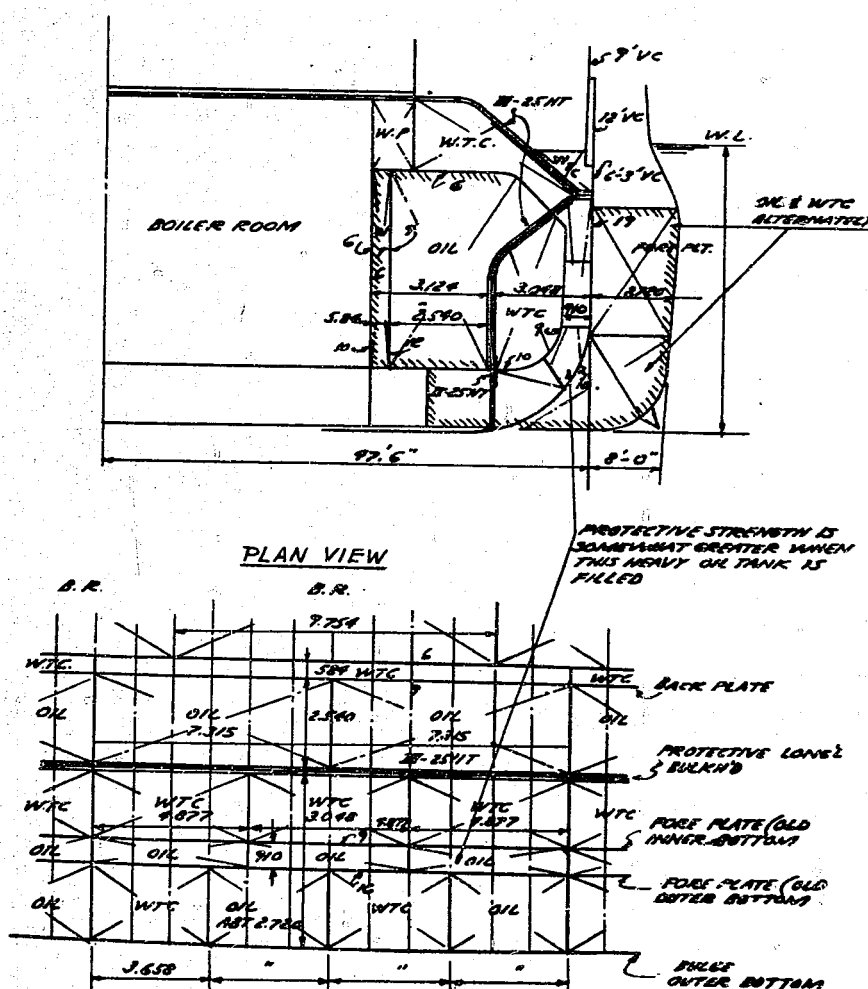


Figure 52

UNDERWATER PROTECTION SYSTEM - BB NAGATO

Water Layers

Single Layer Protection Method - Straight Model

Protective Strength = 450 kg (Engine Room Area) Joint Efficiency = 53%

Weight of Water About 900 Tons (Shaded Area on Diagram)

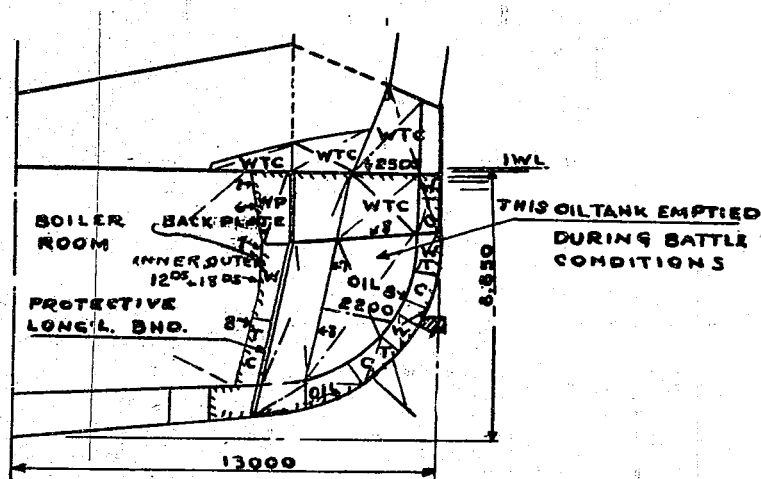
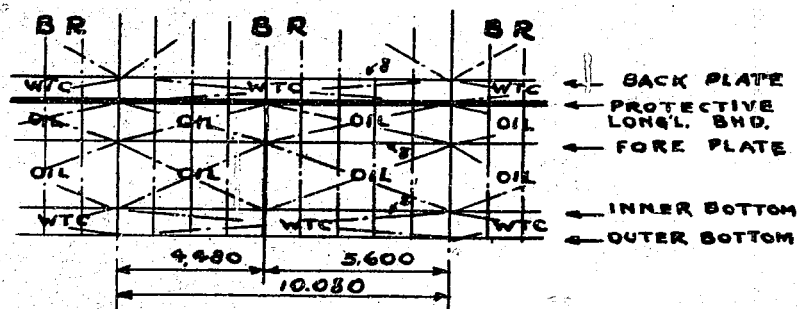
PLAN VIEW

Figure 53

UNDERWATER PROTECTION SYSTEM - CV SHOKAKU

Water Layers

Single Layer Protection Method - Arc Shaped Model

(a) Construction No. 130 (CV - TAIHO)

(b) Revised Construction No. 130

Protective Strength = (a) 300 kg
(b) 350 kg

Joint Efficiency = 72%

Weight of Water About (a) 730 Tons, (b) 770 Tons (Shaded Area on Diagram)

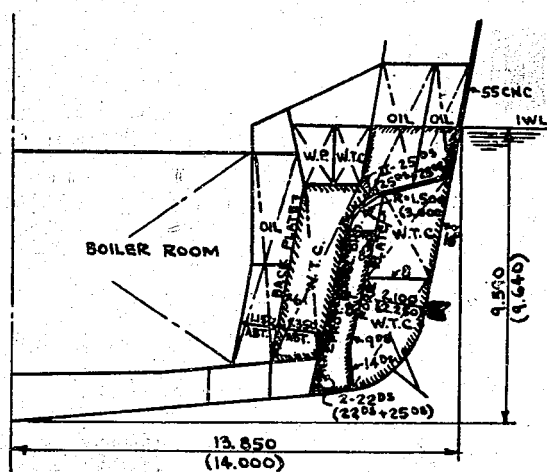
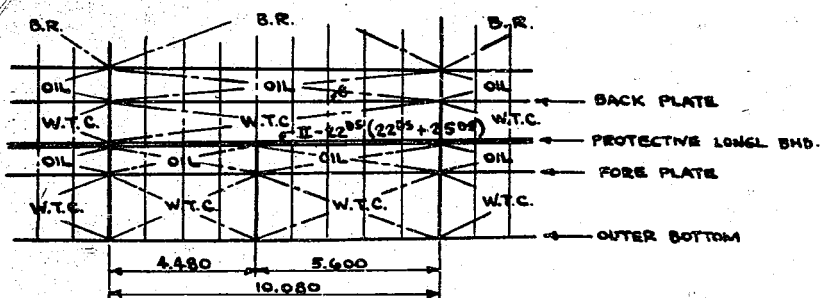
PLAN VIEW

Figure 54

UNDERWATER PROTECTION SYSTEM - CV TAIHO

Water Layers

Single Layer Protection Method - Straight Model

Protective Strength = 900 kg

Joint Efficiency = 85% (Est.)

Weight of Water About 90 Tons

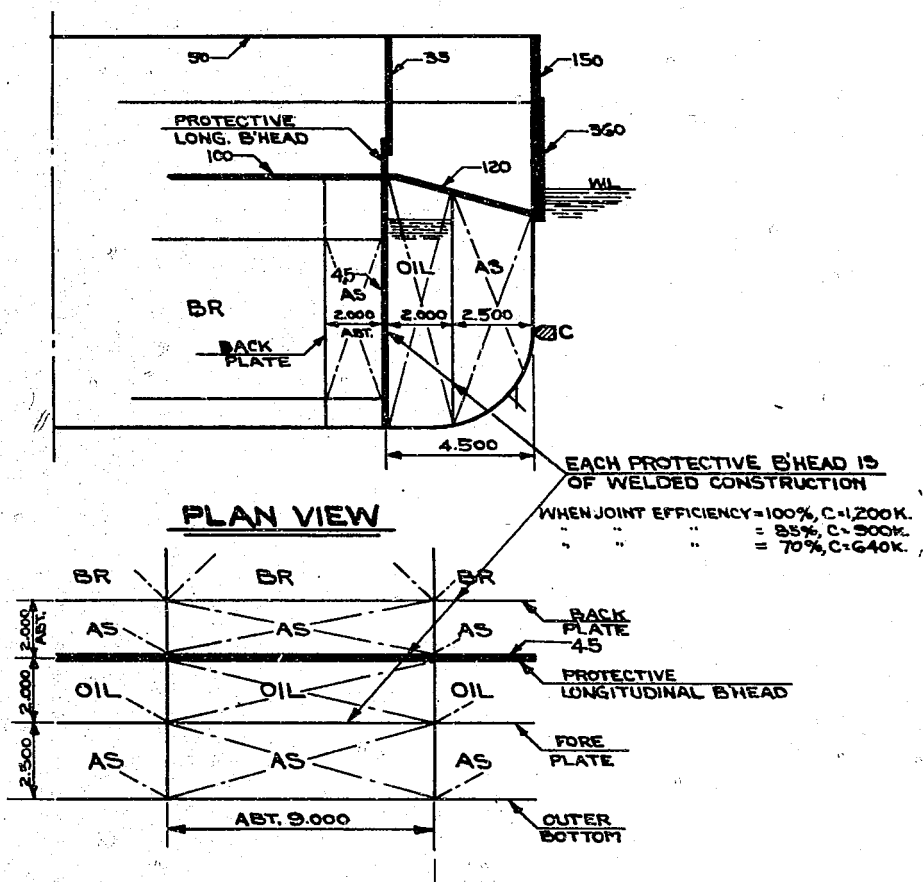


Figure 55

UNDERWATER PROTECTION SYSTEM - BISMARCK (German)

Water Layers

Multiple Layer Protection Method - Straight Model

Protective Strength = 400 kg (Est.) Joint Efficiency = 70% (Est.)

Weight of Water About 730 Tons

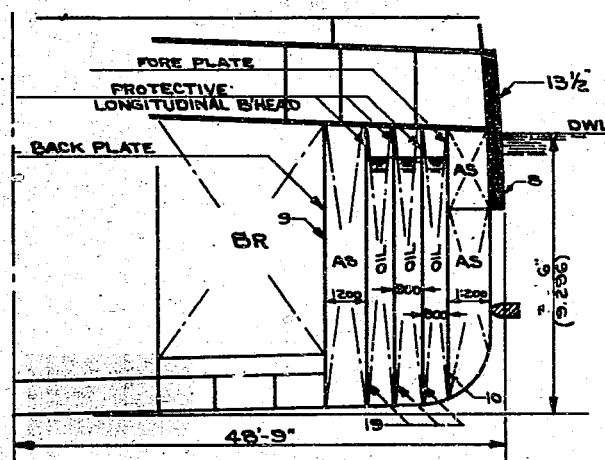
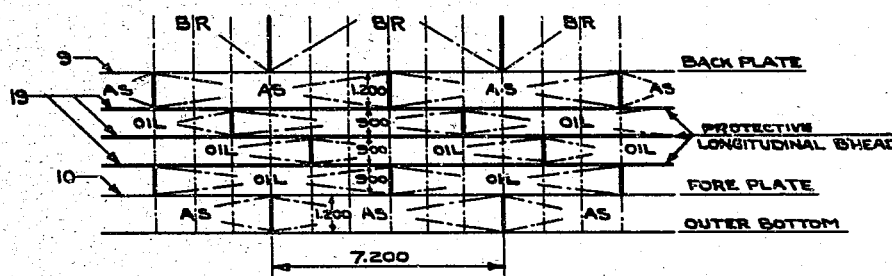
PLAN VIEW

Figure 56

UNDERWATER PROTECTION SYSTEM - BB COLORADO (U.S.)

PART I-B

SUMMARY OF REPORTS ON EXPERIMENTAL PROTECTION OF SHIPS' BOTTOMS
(Translation)

TABLE OF CONTENTS

Chapter I	General Discussion	Page 82
Chapter II	Methods of Bottom Protection	Page 82
Chapter III	Examination of Experimental Results	Page 86
Chapter IV	Method of Calculating Protective Strength	Page 99
Chapter V	Relationship of Model Size to Protective Strength	Page 103

LIST OF APPENDICES

Appendix I	Tabulations of Experimental Results	Page 105
Appendix II	Sketches Illustrating Actual Damage to Models	Page 110
Appendix III	Graph Showing Relation of Protective Strength to Distance Between Center of Explosive Charge and Outer Skin of Ship's Bottom	Page 120

LIST OF ILLUSTRATIONS

Figure 1	Typical Triple Bottom Layout	Page 83
Figure 2	Water Layer Replaced by Protective Plate	Page 83
Figure 3	Position of Liquid Layer Used Against Contact Explosion	Page 85
Figure 4	Test Set-up for Non-contact Explosion - Double Bottom 60% Flooded	Page 85
Figure 5	Proposed Set-up for Non-contact Explosion	Page 85
Figure 6	Contact Explosion Model No. 2 - Scale 1/7.31	Page 87
Figure 7	Contact Explosion Model U - Scale 1/2.97	Page 87
Figure 8	Contact Explosion Model V - Scale 1/2.97	Page 87
Figure 9	Non-contact Explosion Model P - Scale 1/5.35	Page 90
Figure 10	Non-contact Explosion Model Q - Scale 1/5.35	Page 90
Figure 11	Non-contact Explosion Model S - Scale 1/2.97	Page 90
Figure 12	Contact Bottom Explosion Model □ - Scale 1/2.97	Page 95
Figure 13	S ₂ Model - Scale 1/2.97	Page 98
Figure 14	Distance of Charge Center to Point of Contact	Page 98
Figure 15	Distance of Charge Center to Point of Contact (Torpedo) ..	Page 98
Figure 16	Calculation of C for S ₂ Model	Page 101
Figure 17	Calculation of C for M ₃ Model	Page 101
Figure 18	Calculation of C for M ₈ Model	Page 101
Figure 19	Schematic Showing B x L	Page 104
Figure 20	Contact Explosion - Air Layer Protective System - 1/5.35 Scale, Model D ₃	Page 110
Figure 21	Contact Explosion - Air Layer Protective System - 1/2.97 Scale, Model O	Page 111
Figure 22	Contact Explosion - Water Layer Protective System - 1/7.31 Scale, Model No. 2	Page 112
Figure 23	Contact Explosion - Water Layer Protective System - 1/2.97 Scale, Model V	Page 113
Figure 24	Non-contact Explosion - Air Layer Protective System - 1/2.97 Scale, Model M ₅	Page 114
Figure 25	Non-contact Explosion - Water Layer Protective System - 1/5.35 Scale, Model P	Page 115
Figure 26	Non-contact Explosion - Water Layer Protective System - 1/2.97 Scale, Model M ₉	Page 116

- Figure 27 Non-contact Explosion - Water Layer Protective System -
1/2.97 Scale, Model S₂ Page 117
- Figure 28 Non-contact Explosion - Water Layer Protective System -
1/7.31 Scale, Model M₃ Page 118
- Figure 29 Non-contact Explosion - Water Layer Protective System -
1/2.97 Scale, Model M₃ Page 119
- Figure 30 Graph Showing Relation of Protective Strength to
Distance Between Center of Explosive Charge and Outer
Skin of Ship's Bottom Page 120

CHAPTER I
GENERAL DISCUSSION OF EXPLOSIONS UNDER A SHIP'S BOTTOM
AND PROTECTION AGAINST THEM

Contact explosions, while common against a ship's side, are fairly rare against a ship's bottom. Non-contact explosions usually affect the bottom before the sides. Although it is necessary to study both, non-contact explosions are of primary importance.

Experiments to date have indicated that less damage is caused by effects similar to those described in Part I A, that is, by splinters and blast. If triple bottoms are used, the upper layer being water-filled, damage will be similar to that caused by side contact explosions. Damage may be slightly increased by the fact that the explosive gases vent into the ship instead of the water.

In non-contact explosions, damage is caused only by the shock-wave. Triple bottoms with upper layer filled with water give the best protection. Generally they should be layed out as shown in Figure 1.

The watertight plate should be placed at the bottom of the bulkhead in each compartment since the construction of such a plate within the triple bottoms is virtually impossible.

As the longitudinal strength may be largely concentrated in the triple bottom plates, the connections must be well made.

Balanced charge and degree of protection is defined as, "that charge which will not cause leakage into the main portion of the ship faster than the ship's pumps can discharge it".

CHAPTER II
METHODS OF BOTTOM PROTECTION

A. Classification of Bottom Protection Methods

Bottom protection methods may be classified as:

1. Air layers only
2. Liquid layers

The classifications may be subdivided according to types of explosion, thus:

1. Air layer protection

a. Contact explosions. The water layer can be replaced by a suitable thickness of protective plate, as shown in Figure 2. The triple bottom is not essential.

The degree of protection given by this method may be calculated as described in Chapter IV.

b. Non-contact explosions. In this case also the triple bottom is not essential. The main damage is caused by blast and not by splintering as in the case of contact explosions. Only one experiment has so far been made on air layer protection, and it indicated that the protection afforded could be calculated in the same way as that given by liquid layer protection. When the charge was 4.75 meters from the outer bottom, the efficiency was above 85% of that of the water layer type.

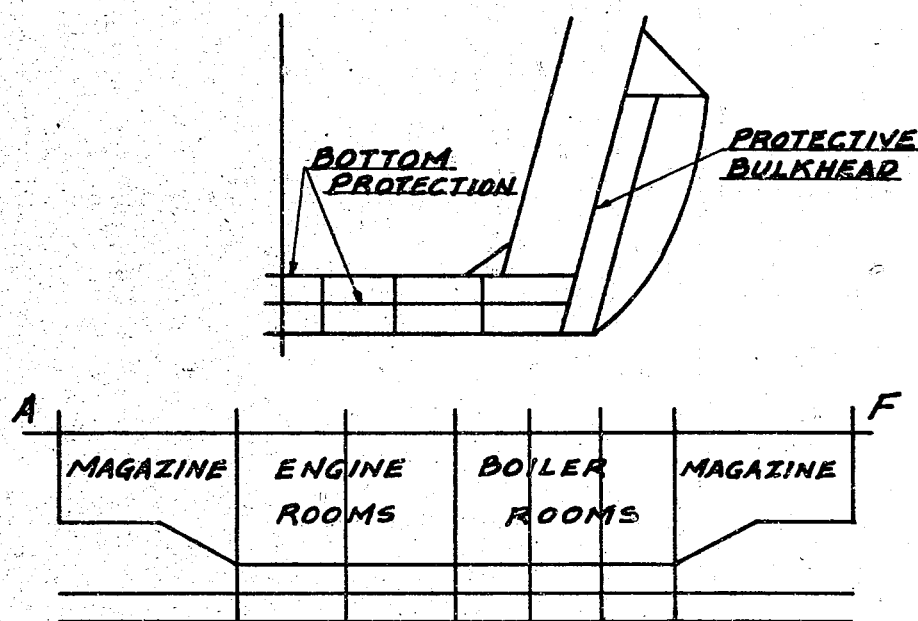


Figure 1
TYPICAL TRIPLE-BOTTOM LAYOUT

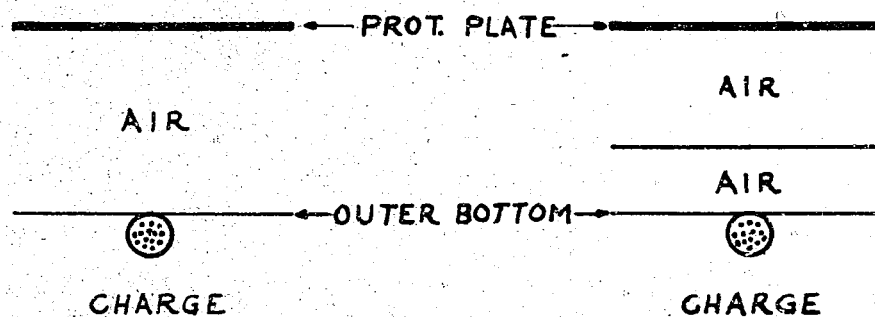


Figure 2
WATER LAYER REPLACED BY PROTECTIVE PLATE

2. Liquid layer protection

a. Contact explosions. The triple bottom is now essential. In addition to the triple bottom, a further layer of watertight plating is theoretically desirable, but as this is impractical the discussion assumes this further layer not fitted.

For contact explosions the liquid layer should be above the air layer and a thick plate should be used for the innermost bottom (Figure 3).

The degree of protection can be calculated as for side protection.

b. Non-contact explosions. The triple bottom is superior to the 60% flooded double bottom as appears from the following experiment, using a flooded double bottom.

Model M₃, scale: 1/2.97

Where: Σt = 21.24mm
 C = 15.75 kg
 δ = 535mm, no holes

Calculation using the method of Chapter IV showed that the balanced charge should be 2.88 kg. Actual charge used was 3.25 kg (Figure 4). The damage was so extensive that it was estimated the balanced charge was about 1.5 kg. It is thought that if the structure is changed to that shown in Figure 5, protection may be improved, but further experiments are required.

A discussion of the relative advantages of flooding top or bottom layers follows.

With contact explosions it is advantageous to have the liquid layer immediately below the protective plate, whether this is fitted as the middle or innermost bottom.

However, in the case of non-contact explosions, it can be seen from the following experimental results that for maximum protection the three bottoms should be of equal thickness and the lower space should contain the liquid layer.

a. The Effect of Composition of Protective Plates

The problem is generally the same as in side protection. In the case of non-contact explosions, damage is by blast rather than by splinters; and, consequently, the effectiveness of the plate, even if it is an armor material stronger than DS, is limited by the efficiency of the riveted connections.

C. The Influence of Efficiency of Riveted Joints in the Protective Plate

The problem is generally the same as in side protection.

1. Contact Explosions. As for side protection, for maximum protection rivet efficiencies must be:

Air layer - 50 to 60%
 Liquid layer - about 70%

2. Non-contact explosions. The maximum efficiency possible is desirable, namely, about 70%.

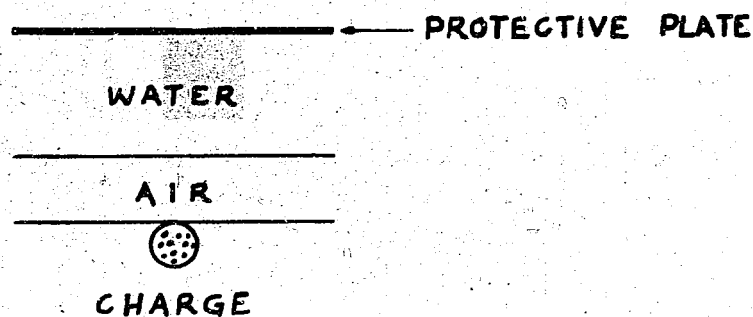


Figure 3
POSITION OF LIQUID LAYER USED
AGAINST CONTACT EXPLOSION

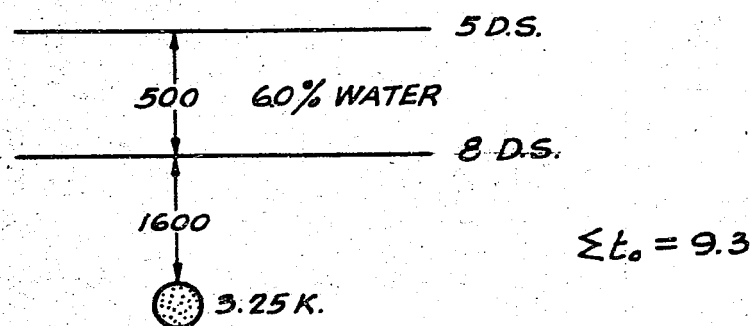


Figure 4
TEST SET-UP FOR NON-CONTACT EXPLOSION -
DOUBLE BOTTOM 60% FLOODED

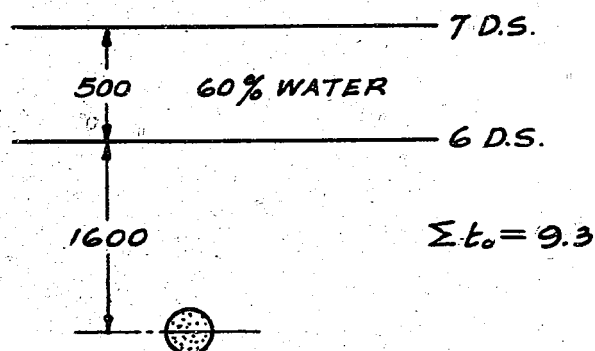


Figure 5
PROPOSED SET-UP FOR NON-CONTACT EXPLOSION

Table I
NON-CONTACT EXPLOSION TESTS

MODEL	S_2	M_3	M_9	M_8
ARRANGEMENT	8 ds + 9 ds	5 ds	9 ds	9 ds
	WATER	AIR	WATER	AIR
	5 ds	8 ds + 9 ds	10 ds	10 ds
	AIR	WATER	AIR	WATER
	7 ds	7 ds	9 ds	9 ds
	1.600 M	1.600 M	1.600 M	1.600 M
	15.75 K (SCALE 350 K)	15.75 K	18.00 K (SCALE 400 K)	18.00 K
$\sum t_e$ (mm)	21.24	20.68	19.81	19.81
DEFLECTION δ (mm)	535	495	554	445
DAMAGE	NO HOLES	SMALL HOLES	NO HOLES	NO HOLES

CHAPTER III EXAMINATION OF EXPERIMENTAL RESULTS

A. Scale Effect

1. Contact Explosions. Only one scale (1/5.35) was used for air layer experiments, so the scale effect could not be studied.

Two scales (1.731 and 1/2.97) were used for the liquid layer experiments, so that a comparison of the results can be used as a guide to the scale effect. Figures 6, 7, and 8 give details of the models used and Table II gives the results. From these it can be seen that, as in the case of side protection, the thickness of the outer bottom has little influence upon protection against contact explosions, but the thickness of the middle bottom has considerable influence.

2. Examination of results

a. Distance between outer and protective plates

For Model No. 2 this distance = $93 + 2 + 93 = 188\text{mm}$
 Converting to the scale of U and V, this gives 462mm
 Corresponding distance in U and V is 476.5mm

Hence, U and V are slightly more advantageous.

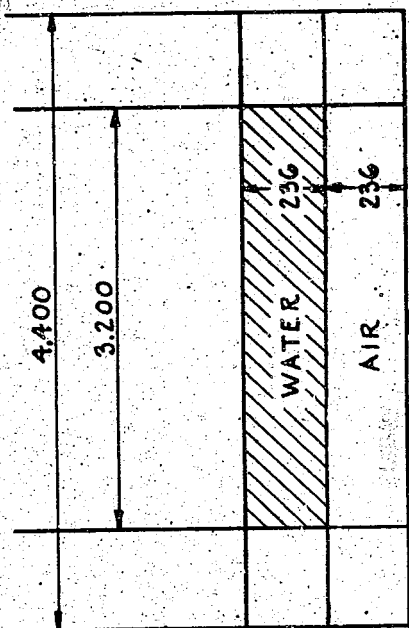


Figure 7
CONTACT EXPLOSION MODEL U -
SCALE 1/2.97

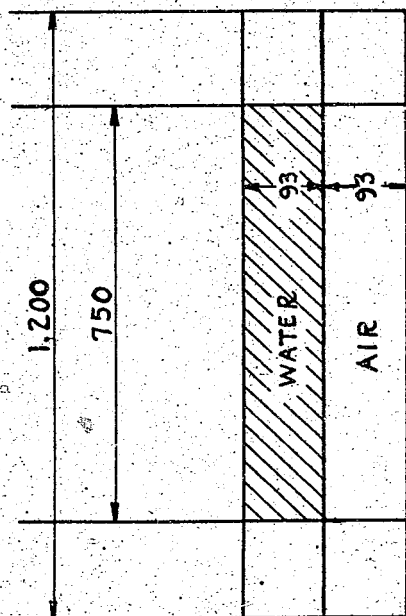


Figure 6
CONTACT EXPLOSION MODEL NO. 2 -
SCALE 1/7.31

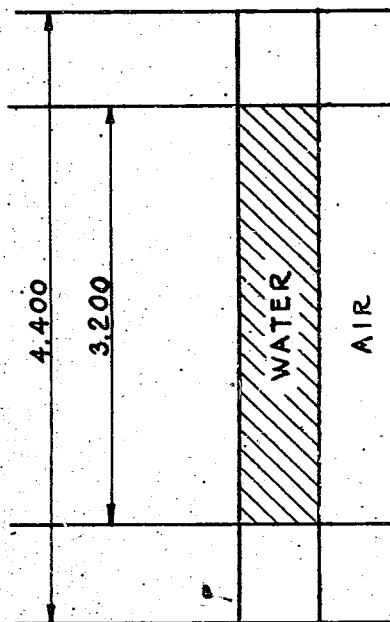
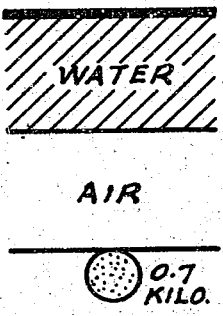
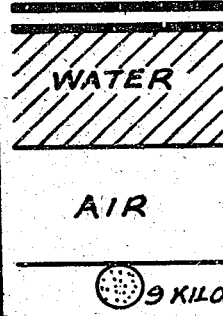
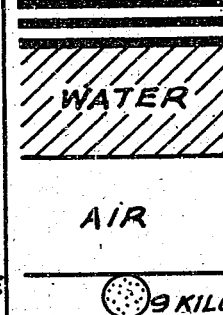


Figure 8
CONTACT EXPLOSION MODEL V -
SCALE 1/2.97

Table II
RESULTS OF MODEL TESTS

MODEL	DIAGRAM	THICKNESS OF PLATE	RIVET EFFICIENCY	EFFECTIVE THICKNESS t_e	STATE OF DAMAGE
NO. 2		6	76	4.56	INTACT $\frac{d}{L} = 0.086$
		2		2.00	
		2		—	
SCALE $\frac{1}{7.31}$				$\Sigma t_e = 6.56$	
U		8+8	63	10.10	RIVETS INTACT RIVETS SHEARED PERFORATED $\frac{d}{L} = 0.106$
		4.5		4.5	
		7		—	
SCALE $\frac{1}{2.97}$				$\Sigma t_e = 14.60$	
V		9+9+9	673	18.2	INTACT $\frac{d}{L} = 0.06$
		4.5	—	4.5	
		7	—	—	
SCALE $\frac{1}{2.97}$				$\Sigma t_e = 22.7$	

b. Width of models, measured between inside walls

Width of U and V = 3,200mm
 Width of No. 2 on same scale = 1,850mm

Hence the damage conditions favor No. 2.

c. Effective thickness of protective plating

Thickness of U and V is 18.6mm with a 9 kg balanced charge
 Thickness of No. 2 to the same scale is 16.4mm

This difference is not thought large enough to matter.

3. Non-contact explosions. Only one experiment was made with air layer protection, consequently, scale effect could not be determined.

Water layer experiments were carried out with two separate scales, namely 1/5.35 and 1/2.97, and hence a scale effect study was possible. The models used were as shown in Figures 9 to 11 with the results given in Table III.

4. Examination of resultsa. Distance between outer plate and protective plate

Distance in S = 476.5mm
 Distance in P and Q to same scale = 477mm

Difference negligible.

b. Width between inside walls

Distance in S = 3200mm
 Distance in P and Q to same scale = 3200, exactly the same

c. Effective thickness of protective plating

In Model P with charge 1.7 kg, Σt_0 was 10.357 and protection was successful. In Model Q, with same charge, Σt_0 was 8.989 and protection failed. Hence, we assumed a charge of 1.7 kg was balanced by $\Sigma t_0 = 9.5$. Converting this to the scale of Model S we obtain $\Sigma t_0 = 17.1$ for balance. Actual Σt_0 in Model S was 15.2. The 12% difference is considered negligible.

5. Conclusions

From results of above experiments it was deduced that the law established for side explosions, namely,

$$\text{Model ratio} = \frac{(\text{Wt. of charge against model}) \frac{1}{2.843}}{(\text{Wt. of charge against ship})}$$

is applicable to all underwater explosions, whether they be side explosions or bottom explosions.

B. Relationship between Σt_0 and Size of Balanced Charge

Only one experiment was made with contact explosions; therefore, only non-contact explosions can be discussed.

1. A comparison of the experiments conducted on P and Q (1/5.35 models)

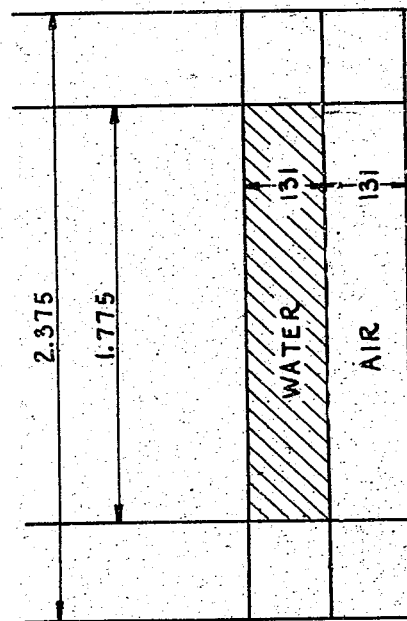


Figure 9
NON-CONTACT EXPLOSION MODEL P -
SCALE 1/5.35

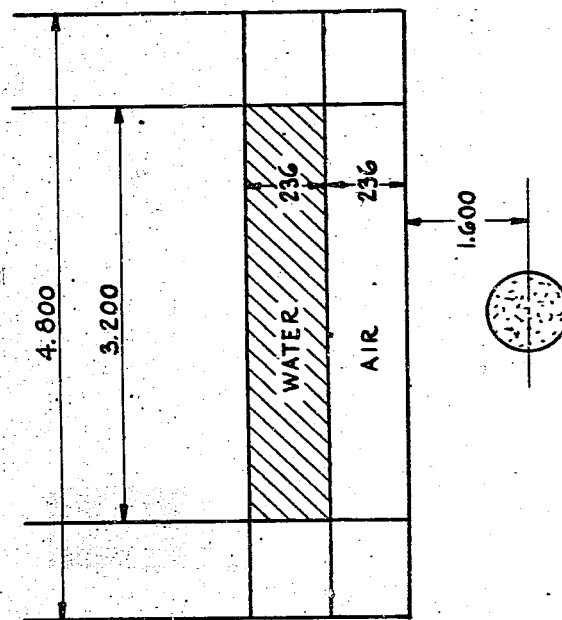
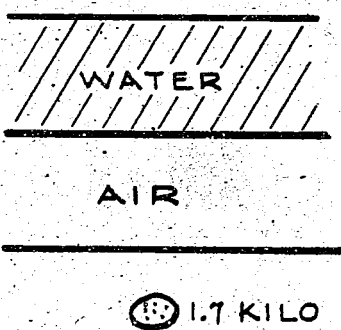
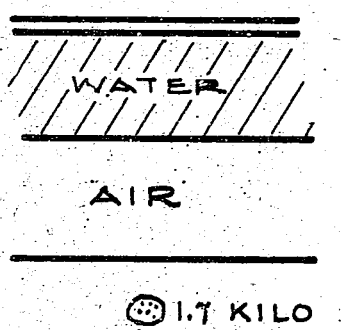
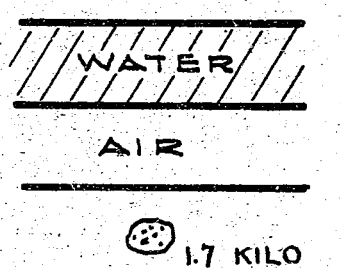


Figure 10
NON-CONTACT EXPLOSION MODEL Q -
SCALE 1/5.35



Figure 11
NON-CONTACT EXPLOSION MODEL S -
SCALE 1/2.97

Table III
TEST RESULTS MODELS P, Q, AND S

MODEL	DIAGRAM	THICKNESS OF PLATE t	RIVET JOINT EFFICIENCY	EFFECTIVE THICKNESS t_e	DAMAGE
P	<p>SCALE $\frac{1}{5.35}$</p> 	8 2.9 4	0.754 0.706 0.57	6.032 2.065 2.28 $\Sigma t_e = 10.357$	ALL INTACT $\frac{\delta}{L} = 0.081$
Q	<p>SCALE $\frac{1}{5.35}$</p> 	8 2.9 4	0.583 0.706 0.57	4.666 2.065 2.28 $\Sigma t_e = 8.989$	INTACT RIVETS SHEARED PERFORATED
S	<p>SCALE $\frac{1}{2.97}$</p> 	14 4.5 7	0.128 0.568 0.402	10.200 2.560 2.820 $\Sigma t_e = 15.58$	ALL INTACT $\frac{\delta}{L} = 0.073$

with 9 kg charge, 200 kg to scale) and with $S_2(1/2.97$ model with 15.75 kg charge, 350 kg to scale) was made.

In P and Q Models, $\Sigma t_0 = 17.1$ and is balanced by a 9 kg charge.

Results of the S_2 test were as shown in Table IV. Assuming $\Sigma t_0 = 17.1$ to balance a 9 kg charge in the first model, we calculate the theoretical balanced charge C for the second model.

$$\left(\frac{C}{9}\right)^{0.469} = \frac{21.2}{17.1} \text{ where } C = 15 \text{ kg}$$

The actual test showed the balanced charge = 15.75 kg. This is considered a good approximation.

2. Comparison of experiments on $S(1/2.97$ target, 9 kg, 200 kg reduction) with those on $S_2(1/2.97$ target, 15.75 kg, 350 kg reduction):

The average of Σt_0 in the S target is, as explained in the previous paragraph, generally 15.2. In the S_2 target, when $\Sigma t_0 = 21.20$, the bursting charge is 15.75 kg.

When $\Sigma t_0 = 15.2$ compared with 9 kg

$$\text{if } \Sigma t_0 = C^{0.469}$$

$$\text{then } \left(\frac{21.20}{15.2}\right) = \left(\frac{C}{9}\right)^{0.469}$$

$$C^{0.469} = 9^{0.469} \times \left(\frac{21.2}{15.2}\right)$$

$$\therefore C = 16.4 \text{ kg}$$

As previously explained, in the results of the S_2 target the charge was 15.75 kg therefore, this is considered a good approximation.

3. Comparison of $M_3(1/7.31$ target with 1.75 kg charge, 500 kg to scale) and $M_3(1/2.97$ target, with 15.75 kg charge, 350 kg to scale) experiments:

Comparing these results with other tests on Model M_3 which gave an average Σt_0 of 23.9mm for a 22.5 kg charge we have,

$$\text{if } \Sigma t_0 \sim C^{0.409}$$

$$\left(\frac{20.68}{23.9}\right) = \left(\frac{C}{22.5}\right)^{0.409} \text{ where } C = 16.7 \text{ kg}$$

Results of M_3 Model gave balanced charge = 15.75 kg. An M_4 Model, of the same construction, was destroyed by a charge of 18 kg.

The error of 4% is considered negligible.

4. Conclusions

As shown above, the law of proportionality followed by bottom explosions is generally the same as for side explosions.

$$\text{i.e. } \Sigma t_0 \propto C^{0.469}$$

a. Air layers only. If the strength of the joints of the protective plating is greater than necessary, the joint efficiency is not considered, i.e., actual protective plating thickness varies as $C^{0.469}$.

Table IV
S₂ MODEL TEST RESULTS

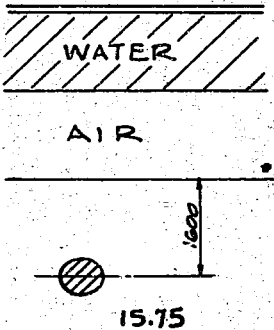
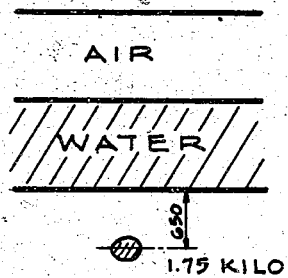
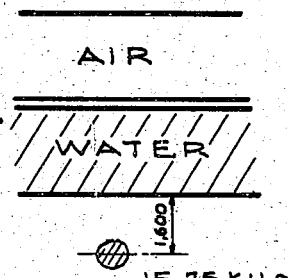
DIAGRAM	THICKNESS OF PLATE t	CORRECTION EFFICIENCY	EFFECTIVE THICKNESS t_e	DAMAGE
	8+9	.749	12.10	$\frac{\delta}{L} = .111$ INTACT
	5	.703	3.51	
	1	.713	4.99	
			$\Sigma t_e = 21.20$	

Table V
MODEL M₃ TEST RESULTS

MODEL	DIAGRAM	THICKNESS OF PLATE t	RIVET JOINT EFFICIENCY	EFFECTIVE THICKNESS t_e	DAMAGE
M ₃		2	0.787	1.57	$\frac{\delta}{L} = 0.097$ SMALL CRACKS
		6	0.75	5.25	
		2.9	1.00	2.9	
				$\Sigma t_e = 9.72$	
M ₃		5	0.698	3.99	$\frac{\delta}{L} = 0.101$ SMALL HOLES
		8+9	0.718	12.20	
		1	0.713	4.99	
				$\Sigma t_e = 20.68$	

b. Water layers. Here also, as in the case of side protection, the joint efficiency of the water layer front plate is not considered, i.e., effective thickness of protective plating and actual front plate thickness varies as $C^{0.469}$.

C. Comparison of Defensive Strength of Side Protection and Bottom Protection

No non-contact work was done with side protection, so the discussion will cover only contact explosions.

1. Water layers only

a. $\frac{1}{2.97}$ Model experiment and results.

Converting to full scale, the sum of protective plate thicknesses is 65.4mm. The distance between outer bottom and protective plate is 4.600 meters. Hence, using the side protection formula,

$$T = 95.62 C^{0.469} D^{-1/3}$$

we find $C = 180 \text{ kg}$

In the actual experiment a charge corresponding to 200 kg full scale caused two holes in the model. It is considered that the calculated value is a good approximation to the balanced charge.

The depth of immersion of the charge corresponded to 9.44 meters on the full scale, compared with depths of 4 to 6 meters used in the side protection work, but it is not considered that depth has a large influence.

b. $D_3(1/5.35)$ Model experiments and results.

Models D_{2a} and D_3 were of the same construction, but were used in the side and bottom positions, respectively, as shown in Table VI. From the results shown in Table VI it is seen that damage to the bottom was slightly less than the damage to the side. However, in actual practice it frequently happens that watertight plating is not fitted inside the protective plate. Accordingly, it is considered that on the whole bottom protection is inferior to side protection.

2. Model experiments

a. $1/7.31$ Model experiments and results

Using the formula for side protection, the following results had been predicted for a charge of 0.7 kg.

Model a - Large damage
Model b - Balance
Model c - Reserve of protection

The calculated results agree well with the actual experimental results.

As previously stated these models are narrow in comparison with the $1/2.97$ scale models.

b. $1/2.97$ Model experiments and results

If the balanced charges for U and V are calculated by the side protection formula, we get:

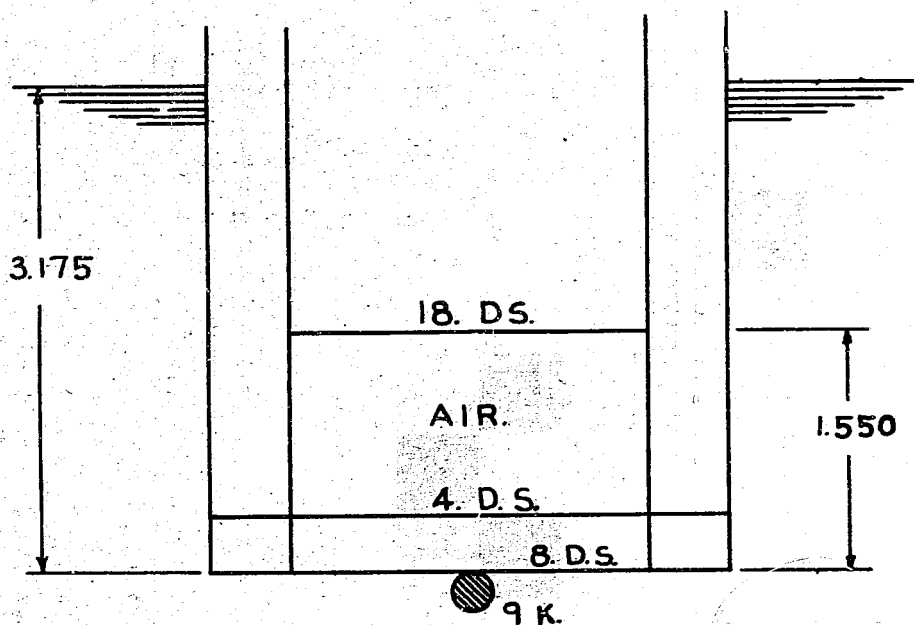


Figure 12
CONTACT BOTTOM EXPLOSION MODEL
SCALE 1/2.97

Table VI
TEST RESULTS, MODEL D_{2a} AND D₃

		D ₃	D _{2a}
MODEL			
DAMAGE	DISTORTION	82 mm	89 mm
	PUNCTURES	I = 3	N = 6
	AREAS OF TOTAL DAMAGE ON BACK.	N = 2	N = 2

Table VII
TEST RESULTS, 1/7.31 SCALE MODELS

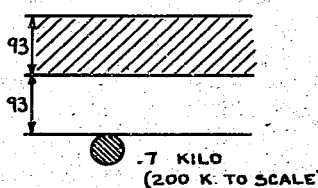
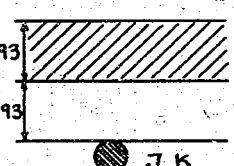
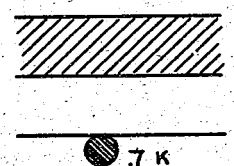
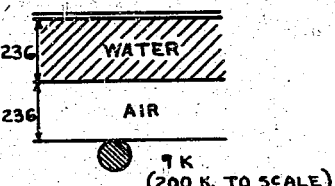
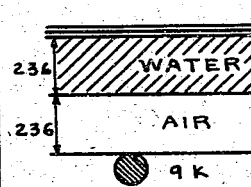
MODEL	DIAGRAM	PLATE THICKNESS	DEFLECTION δ/L	DAMAGE	REMARKS
a.		5. DS. 2. 2.	—	LARGE DAMAGE	
b.		6 DS. 2. 2.	.086	INTACT	NEAR BALANCE
c.		7 DS. 2. 2.	.077	INTACT	RESERVE

Table VIII
TEST RESULTS, 1/2.97 SCALE MODELS

MODEL	DIAGRAM	PLATE THICKNESS	DEFLECTION δ/L	DAMAGE	REMARKS
U		8 DS + 8 DS 4.5 DS. 7 DS.	0.106	ONE HOLE	PROTECTION INADEQUATE
V		9 DS + 9 DS + 9 DS 4.5 DS 7 DS.	0.06	INTACT	RESERVE OF PROTECTION

Charge for U = 7.2 kg (160 kg to scale)
 Charge for V = 17.1 kg (380 kg to scale)

from which it would be expected that U would fail against 9 kg while V would stand up to 9 kg. This is roughly what was found in the experiments, though the extent of damage actually experienced was greater than that expected from the calculation. It was estimated from the experimental results that balanced charge for U = 5.85 kg (130 kg to scale) and balanced charge for V = 13.5 kg (300 kg to scale). From the results it may be tentatively assumed that protective strength of the bottom is 20% less than that of the side.

3. Conclusions

Whether air or water layers are used, it seems generally true to say that bottom protection is 20% inferior to side protection in terms of charge.

Expressing this in terms of effective thickness of protective plating,

$$\begin{aligned} \text{In general} \quad \Sigma t_b &\propto C^{0.469} \\ \text{Therefore} \quad \Sigma t_b &= \left(\frac{1.0}{0.8}\right)^{0.469} \times \Sigma t_s \\ \Sigma t_b &= 1.11 \Sigma t_s \end{aligned}$$

i.e., for bottom protection to equal side protection, about 20% decrease in charge or about 10% increase in plate thickness is necessary.

D. Relation between Charge, Distance, and Protective Power

Observations on S_2 Model (Scale $\frac{1}{2.97}$):

In S_2 Model, $d = 1600\text{mm}$, $C = 15.75$(1)

i.e., in full scale, $d = 4750\text{mm}$, $C = 350$

In S_4 Model, $d = 800\text{mm}$, $C = 135$(2)

i.e., in full scale, $d = 2375\text{mm}$, $C = 300$

A contact explosion test was not made with S_2 , therefore the strength is estimated using the results of U, V, (1/2.97) and No. 2 (1/7.31) Models as a basis. We have

for U and V, (1/2.97) $\Sigma t_b = 18.6$ and $C = 9\text{ kg}$

for No. 2, (1/7.31) $\Sigma t_b = 16.4$ and $C = 9\text{ kg}$ on scale of 1/2.97

Because S_2 (1/2.97) has $\Sigma t_b = 17.7$ it may be assumed for contact explosion the balanced charge is 9 kg (200 kg on full scale).....(3)

Even in the case of contact explosions, we must consider the distance from charge center to outer bottom plate. In Models U and V this distance was 134mm representing 377mm on the full scale.....(4)

In the case of torpedo contact with the hull, d is indefinite, depending upon the angle of impact. To cover the indefinite cases, we assume the charge spherical (see Figure 15) and determine d as follows. For a charge of 200 kg.

$$\frac{4}{3} \pi d^3 = \frac{200}{1.6} \times 10^3$$

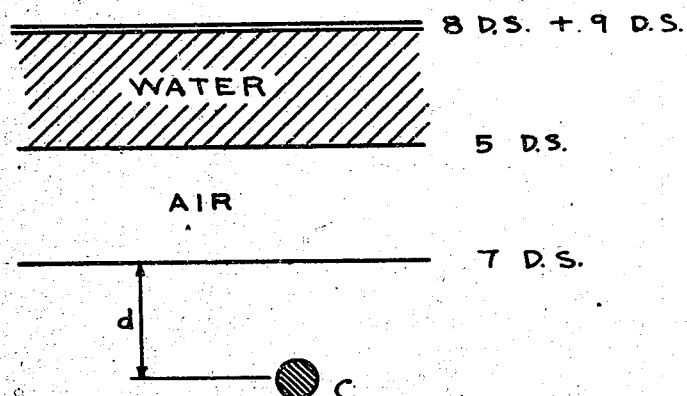


Figure 13
 S_2 MODEL - SCALE 1/2.97

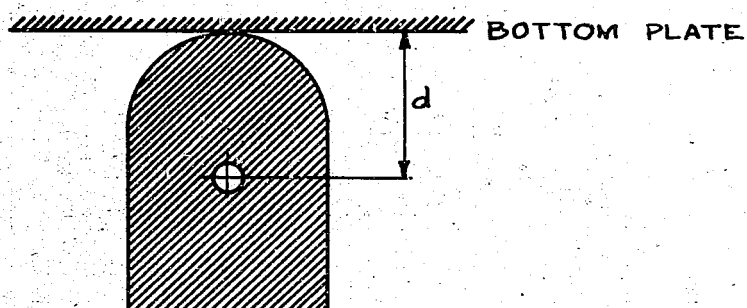


Figure 14
 DISTANCE OF CHARGE CENTER TO POINT OF CONTACT

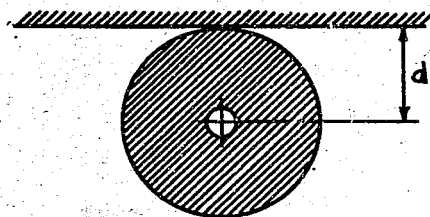


Figure 15
 DISTANCE OF CHARGE CENTER TO
 POINT OF CONTACT (TORPEDO)

where 1.6 = density of the explosive

where d = 310mm

Using the results of (1), (2), (3) and (4) above, the curve of Figure 30 was plotted. From this graph it can be seen that $C \propto d^{0.238}$. Using this, a law connecting T, d, and C can be found as follows:

$$T \propto C^{0.469} \text{ for constant d} \dots\dots\dots(5)$$

$$\text{and } C \propto d^{0.238} \text{ for constant T}$$

$$C^{0.469} \propto d^{0.238 \times 0.469}$$

$$C^{0.469} \propto d^{0.1116} \dots\dots\dots(6)$$

$$\text{Combining (5) and (6) } T \propto C^{0.469} \times d^{-0.116}$$

This law is based upon a very small number of tests and more experimental work is necessary.

CHAPTER IV

METHOD OF CALCULATING PROTECTIVE STRENGTH

A. Contact Explosions on Ship's Bottom

1. Air layer type

As this is the same as an explosion on the ship's side, it may be done according to the following equation:

$$T = 95.62 C^{0.469} D^{-1/3} \dots\dots\dots(1)$$

T = Total thickness of protective plating (mm)

C = Balanced charge quantity (kg)

D = Distance between outer skin and protective plating (mm)

However, as previously stated, the thickness of the protective plating of the ships' bottom must be increased by 10%. It follows, therefore, that

$$T = 95.62 C^{0.469} D^{-1/3} \times 1.1$$

$$= 105.182 C^{0.469} D^{-1/3}$$

$$= 105 C^{0.469} D^{-1/3} \dots\dots\dots(2)$$

The protective strength can be calculated by equation (2). However, as we already have the calculated data from (1) above, it would be simpler to correct from equation (1), i.e., it is sufficient to increase T by 10% and to decrease C by 20%.

As the above equations were developed from scale experiments with 200 kg charges, it should be noted that, as in the case of the ship's side defense, further research with larger quantities of explosive is necessary.

2. Water layer type

In the water layer type also, using the same method as the ship's side, it is sufficient to increase T by 10% and decrease C by 20%; but the

method of calculation is explained also in this paragraph.

- a. First calculate the effective ratio (K) in relation to the thickness of the air layer.

$$K = 0.4 da^{-1/3} \phi(dw)$$

where K = effective ratio which varies as da .

da = thickness of air layer (meters)

$\phi(dw)$ = function of thickness of water layer = 1.0

There is a need for further research into $\phi(dw)$, and even though it is included in the above K equation, at present it is calculated as 1.0.

That is to say, when $dw = 600$ the effective ratio of the water layer is thought always to be the same.

The calculation of the ship's bottom protection is based upon the straight type of side protection.

- b. To calculate effective thickness of protective plating and middle bottom.

Effective thickness $\Sigma t_1 + \Sigma t_2 y$ where

Σt_1 = Total thickness of plating other than protective plating (mm)

(The strength of joints in the forward plating not considered)

Σt_2 = Total thickness of protective plating (mm)

y = Efficiency of joints in the protective plating

- c. To calculate the revised thickness (T) of the protective plating as corrected for air layer type of protection,

$$T = \frac{\Sigma t_1 + \Sigma t_2 y}{K}$$

- d. To calculate the distance (D) between the outer skin and the protective plating as in the air layer protection type,

$$D = da + 600\text{mm}$$

The thickness of the water layer is assumed to be 600mm since any increased thickness does not increase the protection. It is also assumed that the D obtained by this means can be used in the air layer formula.

- e. T and D being known, C can be calculated from

$$T = 95.62 C^{0.469} D^{-1/3}$$

- f. This then is corrected as follows to apply to the bottom:

T is increased by 10%
C is decreased by 20%

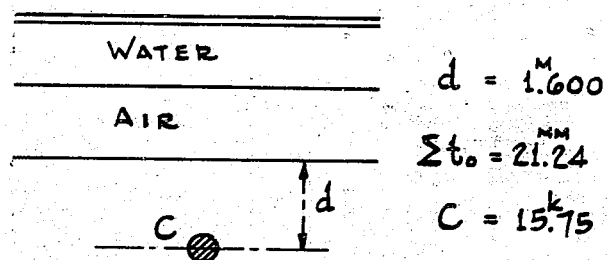


Figure 16
CALCULATION OF C FOR S_2 MODEL

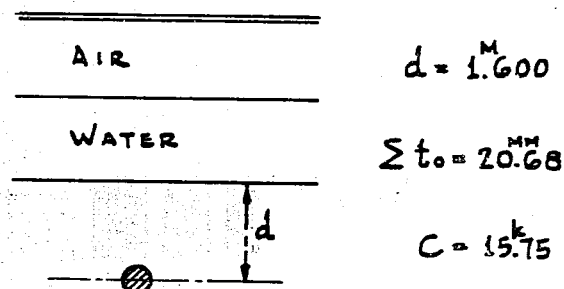


Figure 17
CALCULATION OF C FOR M_3 MODEL

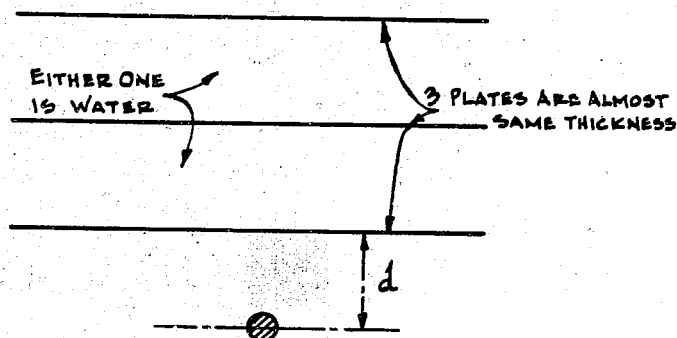


Figure 18
CALCULATION OF C FOR M_8 MODEL

Table IX
RESULTS OF M_5 EXPERIMENTS

DIAGRAM	t	JOINT EFFICIENCY	EFFECTIVE THICKNESS t_o	DAMAGE
	5 DS	.698	3.49	HOLE 730 x 4.800
	8 DS + 9 DS	.728	12.20	
	7 DS	.713	4.99	
			$\Sigma t_o = 20.68$	

in ship's bottom protection, there is an inherent difficulty in increasing d_s and d_w , generally, and d_s and d_w are each taken to be 600 - 800mm, therefore:

$$d_s = d_w, \text{ i.e. in many cases}$$

$$d_s = \frac{1}{2}D$$

In ship's side protection, when $d_s/d < 0.55$, the above calculation cannot be used, but in the case of the ship's bottom, when $d_s/d = 0.5$, there is no difficulty.

However, when $d_s/d < 0.5$ it may not be used, and it is easily understood that the side protection has a somewhat greater protective strength than calculated as above.

B. Non-Contact Explosions on Ship's Bottom

1. Air layer type

Experiments were made with Model M_5 , scale 1/2.97, only. Results were widely scattered and only rough conclusions could be drawn.

Assuming the balanced charge of M_5 was the same as for M_3 and M_4 which were similar in construction.

M_3 --- C = 15.75 kg (Scale 350 kg) Intact

M_4 --- C = 18.0 kg (Scale 400 kg) Hole torn

M_5 --- C = 15.75 kg (Scale 350 kg) Hole torn

From this it was estimated that the balanced charge for M_5 was 13.5 kg (scale 300 kg), when

$$d = 1600$$

$$\Sigma t_0 = 20.68$$

This agrees roughly with the law

$$\Sigma t_0 \propto C^{0.469} d^{-0.1116}$$

2. Water layer type

Experiments were made on models of scale 1/7.31, 1/5.35, and 1/2.97. The most accurate results can be expected from the largest scale models, of which the results of S_2 , M_3 and M_8 , using different arrangements of protective plating, are studied below.

Figures 16, 17 and 18 are based on the equation

$$\Sigma t_0 \propto C^{0.469} d^{-0.1116}$$

In the case of non-contact explosions against bottom protection, the protective strength is thought to vary with the distance between outer bottom and protective plate. The effect does not appear to be so great in the case of contact explosions; earlier experiments comparing distances of 1.4 and 1.5 meters showed negligible difference in the results. Also, except in the case of protection under magazines, practical considerations limit the distance to about 1.6 meters, and it is not thought necessary to investigate larger distances.

CHAPTER V
RELATIONSHIP OF MODEL SIZE TO PROTECTIVE STRENGTH

The size of experimental models may be discussed by a comparison of lengths and widths of the interior walls.

B X L of experiments to date are shown on the following table:

Table X
SIZES OF EXPERIMENTAL MODELS

Scale	Model	B X L (mm x mm)	B X L (Corrected to Actual Size) (mm x mm)	Size of Com- partment of boiler rooms in Capital ships. B'xL' (mm x mm)	L/L'
1/7.31	No. 1-No. 3	675x750	4,930x5,480	6,800x9,500	1/1.73
	M ₁ - M ₃	680x984	4,970x7,190	6,800x9,500	1/1.32
1/5.35	P Q R	1,270x1,775	6,800x9,500	6,800x9,500	1
	A B (TD)	1,800x2,000	5,450x5,940	6,800x9,500	1/1.52
1/2.97	U V				
	S	2,290x3,200	6,800x9,500	6,800x9,500	1
	S - S ₄				
	M ₃ - M ₇				
	D ₃ - D ₄	1,012x1,012	5,420x5,420	6,800x9,500	1/1.75
1/5.35	G ₁	2,024x2,024	10,840x10,840	6,800x9,500	1.14
	G ₂	3,036x3,036	16,250x16,250	6,800x9,500	1.71
	G ₃	4,048x4,048	21,610x21,610	6,800x9,500	2.28

Models D₃, D₄, G₁, G₂, G₃, were attached to frameworks in order to test the effect on adjoining compartments (these tests were in air only).

The 1/5.35 scale P, Q, and R Models and the size of 1/2.97 scale U, V, S, S₂, S₃, S₄, M₃, M₄, M₅, M₆, M₇, M₈ and M₉ Models were made to correspond to the proportions of a boiler room compartment in a capital ship. Where water layer ship's bottom protection is used it is considered necessary that such proportions be used. The extent to which the proportions affect the protective strength has a direct influence upon the results of the tests, and considerable attention must be paid this point.

The results of the test of the small scale (1/7.31) No. 2 Model (ratios L/L' ratios shown in Table X) are considerably better than those of the 1/5.35 P, Q, and R Models. Moreover, the results of the 1/7.31 M₃ Model are somewhat superior to those of the 1/2.97 M₃ Model.

However, where air layers only are used, it does not seem necessary to use a model representing as large a piece of structure. Results of 1/5.35 scale models D₁, D₂, G₁, G₂ and G₃ were consistent. Thus it seems that for this work models such as 1/5.35 D₃ and 1/2.97 B are satisfactory.

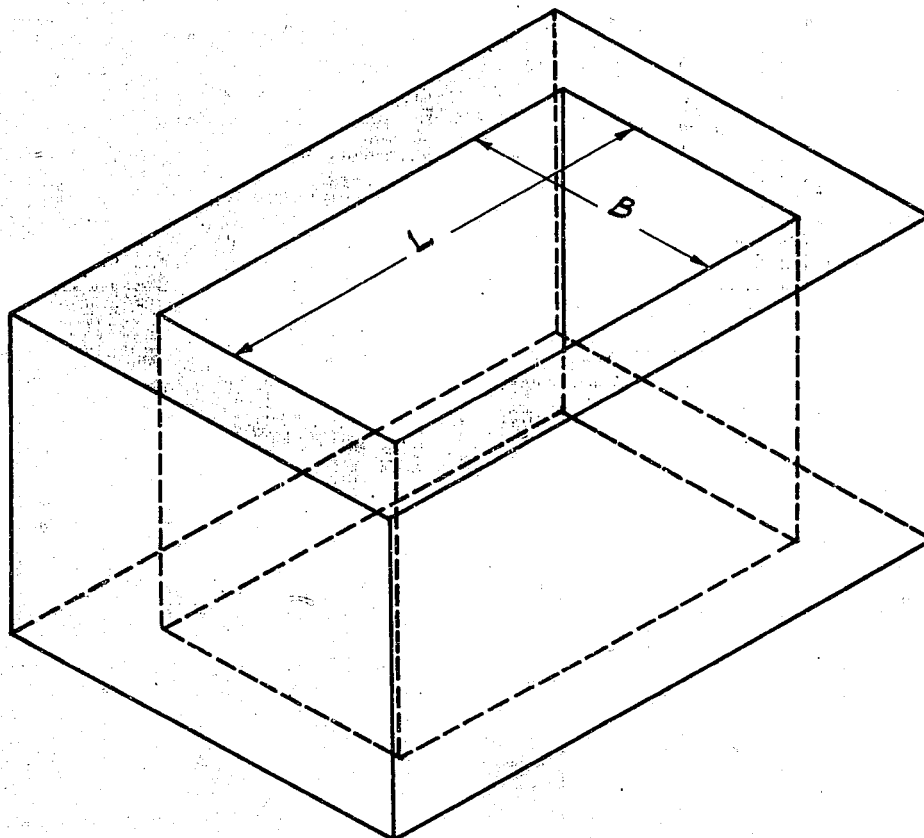
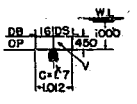
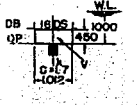
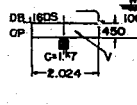
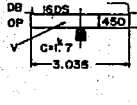
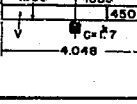
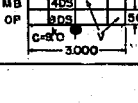


Figure 19
SCHEMATIC SHOWING $B \times L$

APPENDIX I

TABULATIONS OF EXPERIMENTAL RESULTS

Table XI
AIR LAYER TYPE PROTECTION OF SHIPS' BOTTOMS AGAINST CONTACT EXPLOSIONS

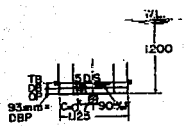
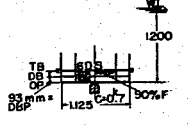
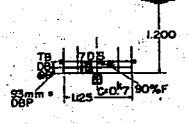
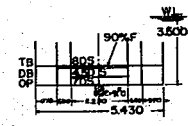
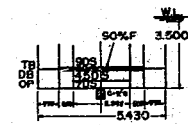
Model	Scale	d (mm)	Thickness of Protective Plate (mm)		Charge (kg)	Results of Experiments	Assumed Balance Charge (kg)
			Actual Thickness	Effective Thickness			
	1/5.35	Contact	DB 16 DS (85.6)	16 (85.6)	1.7 (200)	deflection = 81 3 holes	(200)
	1/5.35	Contact	DB 16 DS (85.6)	16 (85.6)	1.7 (200)	deflection = 83 1 hole	(200)
	1/5.35	Contact	DB 16 DS (85.6)	16 joint efficiency 43.8% (85.6)	1.7 (200)	deflection = 76 no holes	(200)
	1/5.35	Contact	DB 16 DS (85.6)	16 joint efficiency 43.8% (85.6)	1.7 (200)	deflection = 80 no holes	(200)
	1/5.35	Contact	DB 16 DS (85.6)	16 joint efficiency 43.8% (85.6)	1.7 (200)	deflection = 75 no holes	(200)
	1/2.97	Contact	IB 16 DS DB 4 DS (65.4)	22 joint efficiency 58.4% MB 71.5% (65.4)	9.0 (200)	deflection = 80 50 x 350 torn hole 50 x 200	(180)

Note: The numerals in () show those for actual size.

Legend

V - Void
DB - Double Bottom
DS - Dual Steel
IB - Inner Bottom
MB - Middle Bottom
OP - Outer Plating
WL - Water Line

Table XII
WATER LAYER TYPE PROTECTION OF SHIPS' BOTTOMS AGAINST CONTACT EXPLOSIONS

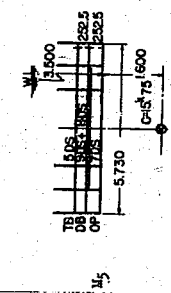
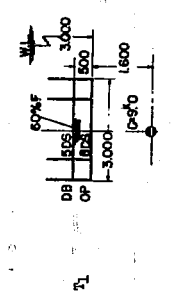
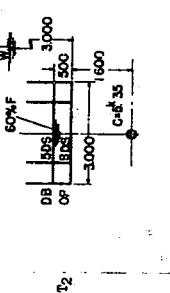
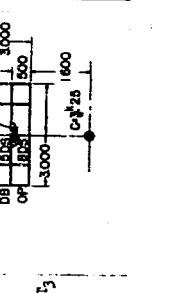
Model	Scale	d (mm)	Thickness of Protective Plate (mm)		Charge (kg)	Results of Experiments	Assumed Balance Charge (kg)
			Actual Thickness	Effective Thickness			
	1/7.31	Contact	TB 5 ^{DS} DB 2 } = 7	$5 \times 0.76 = 3.8$ $2 \times 0.75 = 1.5$ } = 5.3	0.7	Great damage	(140)
			(51.17)	(38.74)	(200)		
	1/7.31	Contact	TB 6 ^{DS} DB 2 } = 8	$6 \times 0.76 = 4.56$ $2 \times 0.75 = 1.5$ } = 6.06	0.7	deflection = 103 no hole	(200)
			(58.5)	(44.3)	(200)		
	1/7.31	Contact	TB 7 ^{DS} DB 2 } = 9	$7 \times 0.76 = 5.32$ $2 \times 0.75 = 1.5$ } = 6.82	0.7	deflection = 93 no hole	(250)
			(65.8)	(49.85)	(200)		
	1/2.97	Contact	TB 9 ^{DS} + 9 ^{DS} DB 4.5 ^{DS} } = 20.5	$(8+8) \times 0.63 = 10.1$ $4.5 \times 0.568 = 2.56$ } = 12.66	9.0	deflection = 70 torn hole 170 x 280	(130)
			(60.88)	(37.6)	(200)		
	1/2.97	Contact	TB 9 ^{DS} + 9 ^{DS} + 9 ^{DS} DB 4.5 ^{DS} } = 31.5	$(9+9+9) \times 0.673 = 18.2$ $4.5 \times 0.568 = 2.56$ } = 20.76	9.0	deflection = 265 no hole	(300)
			(93.55)	(61.66)	(200)		

Note: The numerals in () show those for actual size.

Legend

F - Flooded
DB - Double Bottom
DS - Duol Steel
OP - Outer Plating
TB - Triple Bottom
WL - Water Line
DBS - Distance Between Plates

Table XIII
AIR LAYER TYPE PROTECTION OF SHIPS' BOTTOMS AGAINST NON-CONTACT EXPLOSIONS

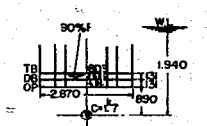
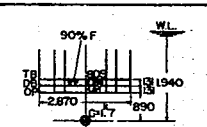
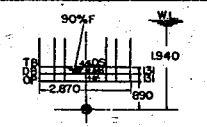
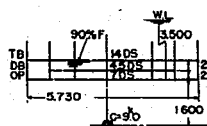
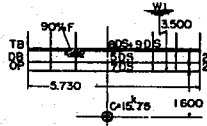
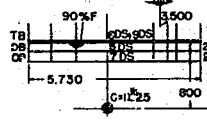
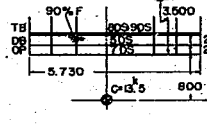
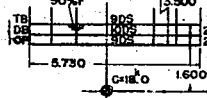
Model	Scale	d (mm)	Thickness of Protective Plate (mm)	Charge (kg)	Results of Experiments	Assumed balance Charge (kg)
	$\frac{1}{2.97}$	1600 (4750)	Actual Thickness DB 5DS = 29 Bott. plating 7DS (61.42)	15.75 (350)	destroyed torn hole = 770 x 4,800	(300)
	$\frac{1}{2.97}$	1600 (4750)	DB 5DS = 13 OP 8DS (38.6)	9.0 (200)	DB torn hole = (approx.) 1,500 x 1,500	
	$\frac{1}{2.97}$	1600 (4750)	Double plating 5DS = 13 OP 8DS (38.6)	5.35 (119)	DB torn hole = (approx.) 1,500 x 1,500	
	$\frac{1}{2.97}$	1600 (4750)	DB 5DS = 13 OP 8DS (38.6)	3.25 (72)	DB torn hole = (approx.) 1,500 x 1,000	

Note: The numerals in () show those for actual size.

Legend

P - Flooded
DB - Double Bottom
DS - Decks Steel
OP - Outer Plating
WB - Triple Bottom
WL - Water Line

Table XIV
WATER LAYER TYPE PROTECTION OF SHIPS' BOTTOMS AGAINST NON-CONTACT EXPLOSIONS

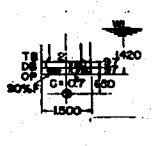
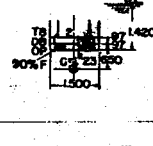
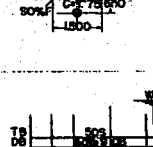
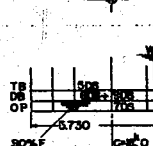
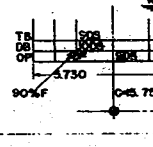
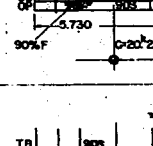
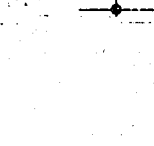
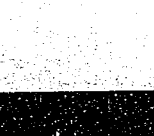
Model	Scale	d (mm)	Thickness of Protective Plate (mm)		Charge (kg)	Results of Experiments	Assumed Balance Charge (kg)	
			Actual Thickness	Effective Thickness				
P		$\frac{1}{5.35}$	890 (4750)	$\left. \begin{array}{l} \text{TB } 8\text{DS} \\ \text{DB } 2.9\text{DS} \\ \text{OP } 4\text{DS} \end{array} \right\} = 14.9$ (79.7)	$\left. \begin{array}{l} 8 \times 0.754 = 6.03 \\ 2.9 \times 0.706 = 2.05 \\ 4 \times 0.57 = 2.28 \end{array} \right\} = 10.36$ (55.41)	1.7 (200)	deflection no hole	(250)
Q		$\frac{1}{5.35}$	890 (4750)	$\left. \begin{array}{l} \text{TB } 8\text{DS} \\ \text{DB } 2.9\text{DS} \\ \text{OP } 4\text{DS} \end{array} \right\} = 14.9$ (79.7)	$\left. \begin{array}{l} 8 \times 0.583 = 4.66 \\ 2.9 \times 0.706 = 2.05 \\ 4 \times 0.57 = 2.28 \end{array} \right\} = 8.99$ (48.1)	1.7 (200)	deflection, hole	(180)
R		$\frac{1}{5.35}$	890 (4750)	$\left. \begin{array}{l} \text{TB } 4.5\text{DS} \\ \text{DB } 2.9\text{DS} \\ \text{OP } 4\text{DS} \end{array} \right\} = 11.4$ (60.99)	$\left. \begin{array}{l} 4.5 \times 0.502 = 2.26 \\ 2.9 \times 0.725 = 2.11 \\ 4 \times 0.57 = 2.28 \end{array} \right\} = 6.64$ (35.52)	1.7 (200)	Great damage	(100)
S		$\frac{1}{2.97}$	1600 (4750)	$\left. \begin{array}{l} \text{TB } 14\text{DS} \\ \text{DB } 4.5\text{DS} \\ \text{OP } 7\text{DS} \end{array} \right\} = 25.5$ (75.74)	$\left. \begin{array}{l} 14 \times 0.728 = 10.2 \\ 4.5 \times 0.568 = 2.56 \\ 7 \times 0.402 = 2.82 \end{array} \right\} = 15.58$ (46.27)	9.0 (200)	deflection no hole	(200)
S ₂		$\frac{1}{2.97}$	1600 (4750)	$\left. \begin{array}{l} \text{TB } 8\text{DS} + 9\text{DS} \\ \text{DB } 5\text{DS} \\ \text{OP } 7\text{DS} \end{array} \right\} = 29$ (86.13)	$\left. \begin{array}{l} (8+9) \times 0.749 = 12.73 \\ 5 \times 0.703 = 3.52 \\ 7 \times 0.713 = 4.99 \end{array} \right\} = 21.24$ (63.08)	15.75 (350)	deflection no hole	(350)
S ₃		$\frac{1}{2.97}$	800 (2376)	$\left. \begin{array}{l} \text{TB } 8\text{DS} + 9\text{DS} \\ \text{DB } 5\text{DS} \\ \text{OP } 7\text{DS} \end{array} \right\} = 29$ (86.13)	$\left. \begin{array}{l} (8+9) \times 0.749 = 12.73 \\ 5 \times 0.703 = 3.52 \\ 7 \times 0.713 = 4.9 \end{array} \right\} = 21.15$ (63.08)	11.25 (250)	deflection no hole	(300)
S ₄		$\frac{1}{2.97}$	800 (2376)	$\left. \begin{array}{l} \text{TB } 8\text{DS} + 9\text{DS} \\ \text{DB } 5\text{DS} \\ \text{OP } 7\text{DS} \end{array} \right\} = 29$ (86.13)	$\left. \begin{array}{l} (8+9) \times 0.749 = 12.73 \\ 5 \times 0.703 = 3.52 \\ 7 \times 0.713 = 4.9 \end{array} \right\} = 21.15$ (63.08)	13.5 (300)	deflection no hole	(300)
M ₉		$\frac{1}{2.97}$	1600 (4750)	$\left. \begin{array}{l} \text{TB } 9\text{DS} \\ \text{DB } 10\text{DS} \\ \text{OP } 9\text{DS} \end{array} \right\} = 28$ (83.16)	$\left. \begin{array}{l} 9 \times 0.706 = 6.35 \\ 10 \times 0.71 = 7.1 \\ 9 \times 0.706 = 6.35 \end{array} \right\} = 19.8$ (58.84)	18.0 (400)	deflection no hole	(400)

Note: The numerals in () show those for actual size.

Legend

F - Flooded OP - Outer Plating
 DB - Double Bottom TB - Triple Bottom
 DS - Ducol Steel WL - Water Line

Table XV
WATER LAYER TYPE PROTECTION OF SHIPS' BOTTOMS AGAINST NON-CONTACT EXPLOSIONS

Model	Scale	d (mm)	Thickness of Protective Plate (mm)		Charge (kg)	Results of Experiments	Assumed Balance Charge (kg)
			Actual Thickness	Effective Thickness			
	1/7.31	650	$\left. \begin{array}{l} TB \text{ 2} \\ DB \text{ 2DS} \\ OP \text{ 2, 9DS} \end{array} \right\} = 9.9$	$\left. \begin{array}{l} 2 \times 0.787 = 1.57 \\ 5 \times 0.75 = 3.75 \\ 2.9 \times 1.0 = 2.9 \end{array} \right\} = 8.22$	0.7	deflection = 61 no hole	(330)
		(4750)	(72.37)	(60.08)	(200)		
	1/7.31	650	$\left. \begin{array}{l} TB \text{ 2} \\ DB \text{ 2DS} \\ OP \text{ 2, 9DS} \end{array} \right\} = 10.9$	$\left. \begin{array}{l} 2 \times 0.787 = 1.57 \\ 6 \times 0.75 = 4.5 \\ 2.9 \times 1.0 = 2.9 \end{array} \right\} = 8.97$	1.23	deflection = 89 no hole	(400)
		(4750)	(79.68)	(65.57)	(350)		
	1/7.31	650	$\left. \begin{array}{l} TB \text{ 2} \\ DB \text{ 2DS} \\ OP \text{ 2, 9DS} \end{array} \right\} = 11.9$	$\left. \begin{array}{l} 2 \times 0.787 = 1.57 \\ 7 \times 0.75 = 5.25 \\ 2.9 \times 1.0 = 2.9 \end{array} \right\} = 9.72$	1.75	deflection = 126 cracked along rivet line	(500)
		(4750)	(86.99)	(71.05)	(500)		
	1/2.97	1600	$\left. \begin{array}{l} TB \text{ 2DS} \\ DB \text{ 2DS + 9DS} \\ OP \text{ 7DS} \end{array} \right\} = 29$	$\left. \begin{array}{l} 5 \times 0.698 = 3.49 \\ (8+9) \times 0.718 = 12.27 = 20.68 \\ 7 \times 0.713 = 4.99 \end{array} \right\}$	17.75	deflection = 485 torn 50 x 150-1 hole 100 x 100-1 110 x 100-1	(350)
		(4750)	(86.13)	(61.42)	(350)		
	1/2.97	1600	$\left. \begin{array}{l} TB \text{ 2DS} \\ DB \text{ 2DS + 9DS} \\ OP \text{ 7DS} \end{array} \right\} = 29$	$\left. \begin{array}{l} 5 \times 0.698 = 3.49 \\ (8+9) \times 0.718 = 12.27 = 20.68 \\ 7 \times 0.713 = 4.99 \end{array} \right\}$	18.0	damaged torn hole = 630 x 4,800	(350)
		(4750)	(86.13)	(61.42)	(400)		
	1/2.97	1600	$\left. \begin{array}{l} TB \text{ 9DS} \\ DB \text{ 10DS} \\ OP \text{ 9DS} \end{array} \right\} = 28$	$\left. \begin{array}{l} 9 \times 0.706 = 6.354 \\ 10 \times 0.71 = 7.1 \\ 9 \times 0.706 = 6.354 \end{array} \right\} = 19.81$	15.75	deflection = 425 no hole	(350)
		(4750)	(83.16)	(58.84)	(350)		
	1/2.97	1600	$\left. \begin{array}{l} TB \text{ 9DS} \\ DB \text{ 10DS} \\ OP \text{ 9DS} \end{array} \right\} = 28$	$\left. \begin{array}{l} 9 \times 0.706 = 6.354 \\ 10 \times 0.71 = 7.1 \\ 9 \times 0.706 = 6.354 \end{array} \right\} = 19.81$	20.25	damaged torn hole = 760 x 4,800	(400)
		(4750)	(83.16)	(58.84)	(450)		
	1/2.97	1600	$\left. \begin{array}{l} TB \text{ 9DS} \\ DB \text{ 10DS} \\ OP \text{ 9DS} \end{array} \right\} = 28$	$\left. \begin{array}{l} 9 \times 0.706 = 6.354 \\ 10 \times 0.71 = 7.1 \\ 9 \times 0.706 = 6.354 \end{array} \right\} = 19.81$	18.0	deflection = 445 no hole	(400)
		(4750)	(83.16)	(58.84)	(400)		

Note: The numerals in () show those for actual size.

Legend

F - Flooded OP - Outer Plating
DB - Double Bottom TB - Triple Bottom
DS - Ducol Steel WL - Water Line

APPENDIX II

SKETCHES ILLUSTRATING ACTUAL DAMAGE TO MODELS

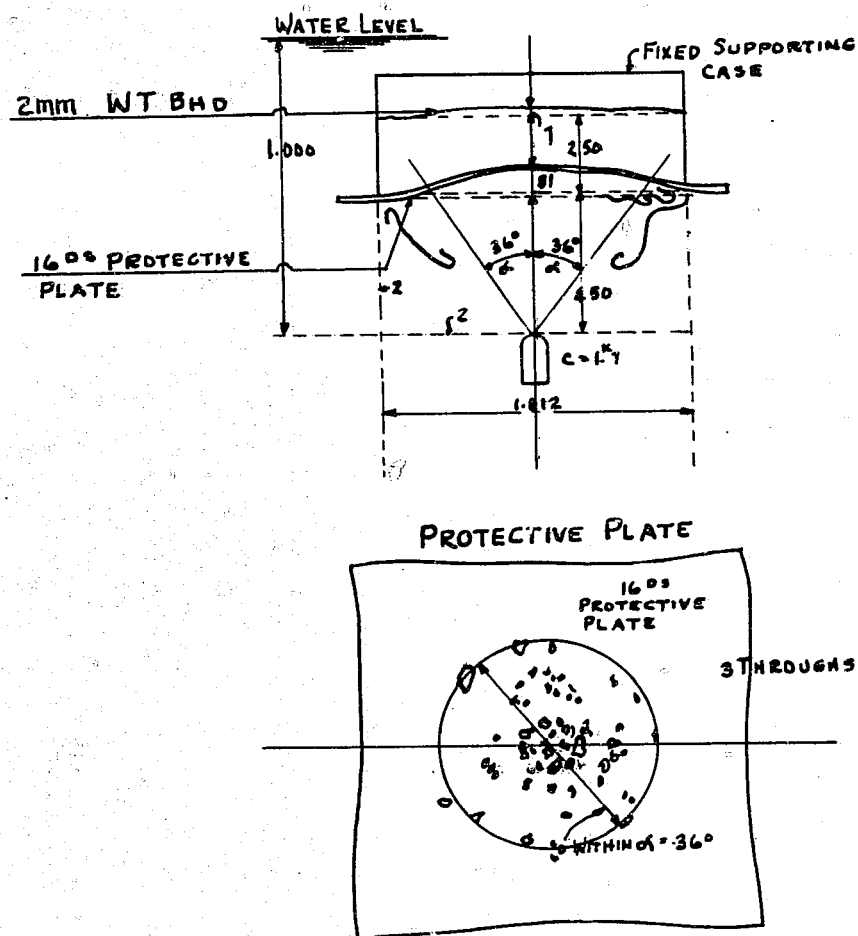


Figure 20
CONTACT EXPLOSION - Al^P LAYER PROTECTIVE
SYSTEM - 1/5.35 SCALE, MODEL D₃

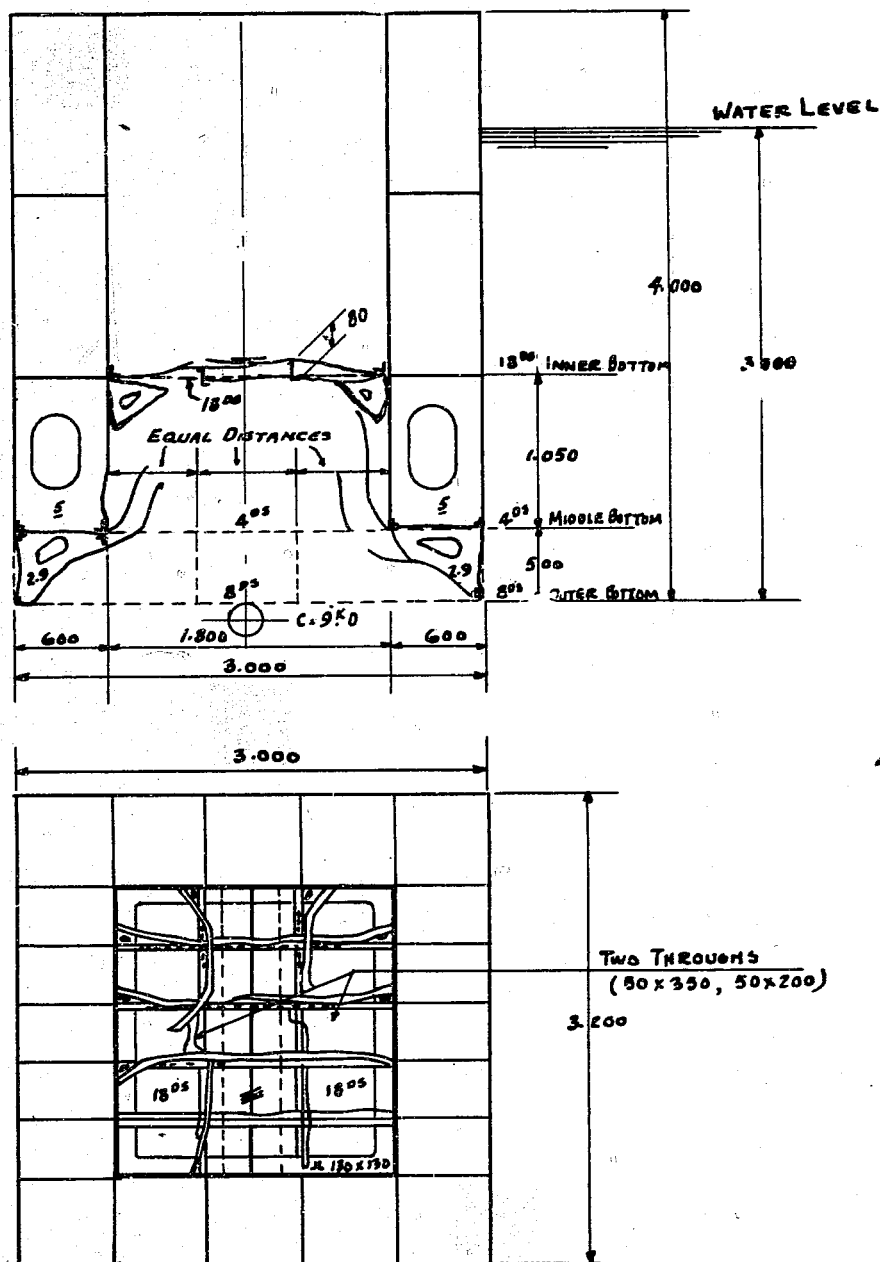


Figure 21
CONTACT EXPLOSION - AIR LAYER PROTECTIVE
SYSTEM - 1/2.97 SCALE, MODEL O

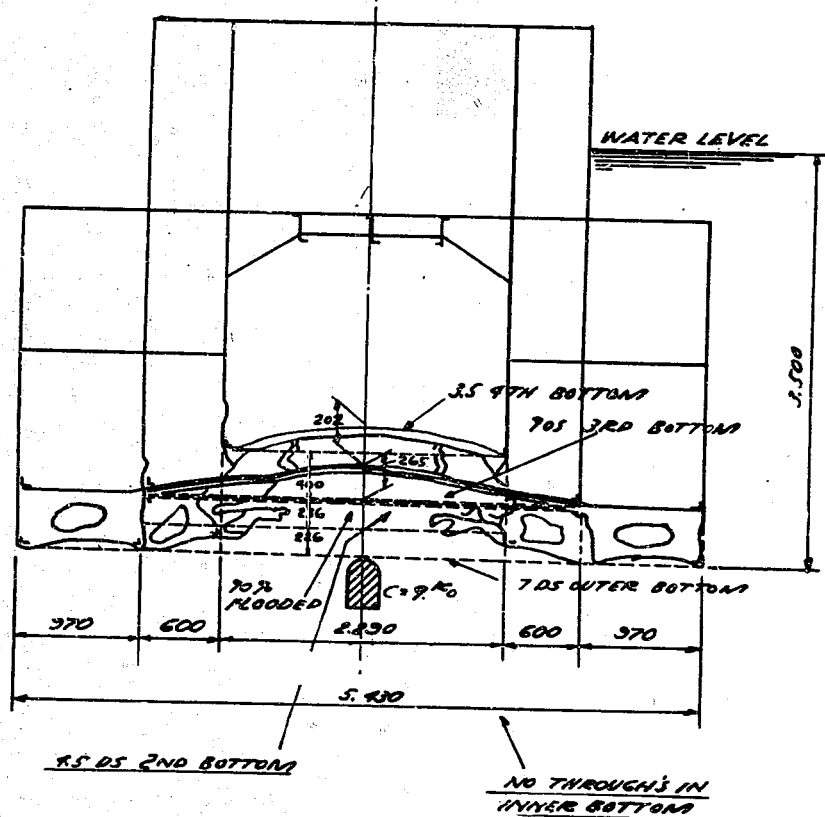


Figure 23
CONTACT EXPLOSION - WATER LAYER PROTECTIVE
SYSTEM - 1/2.97 SCALE, MODEL V

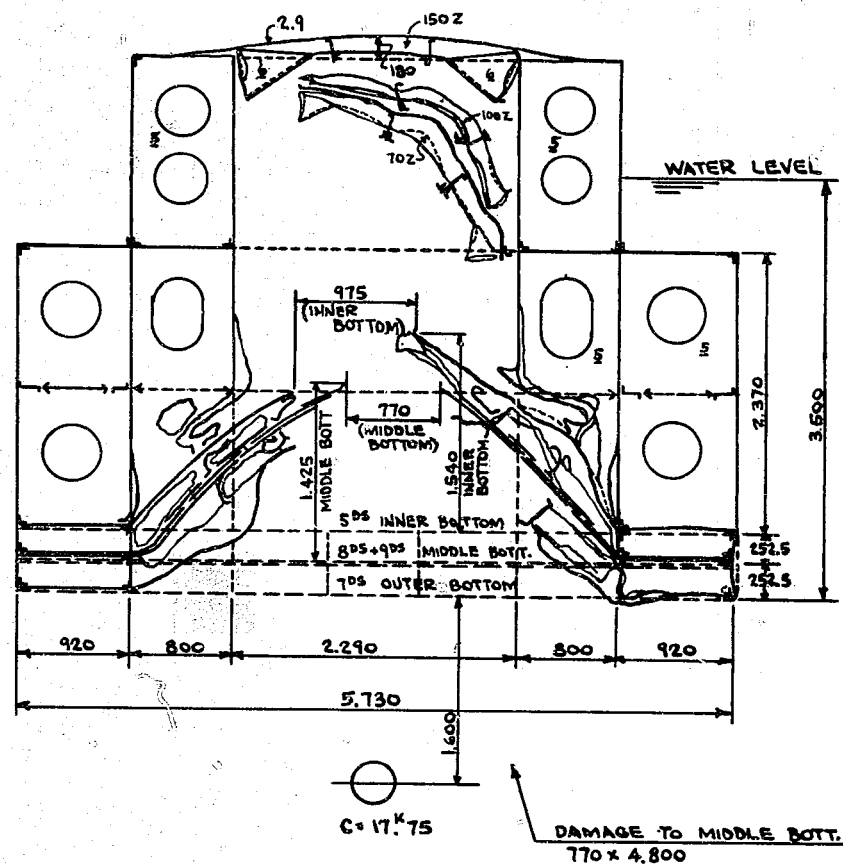


Figure 24
NON-CONTACT EXPLOSION - AIR LAYER PROTECTIVE
SYSTEM - 1/2.97 SCALE, MODEL M₅

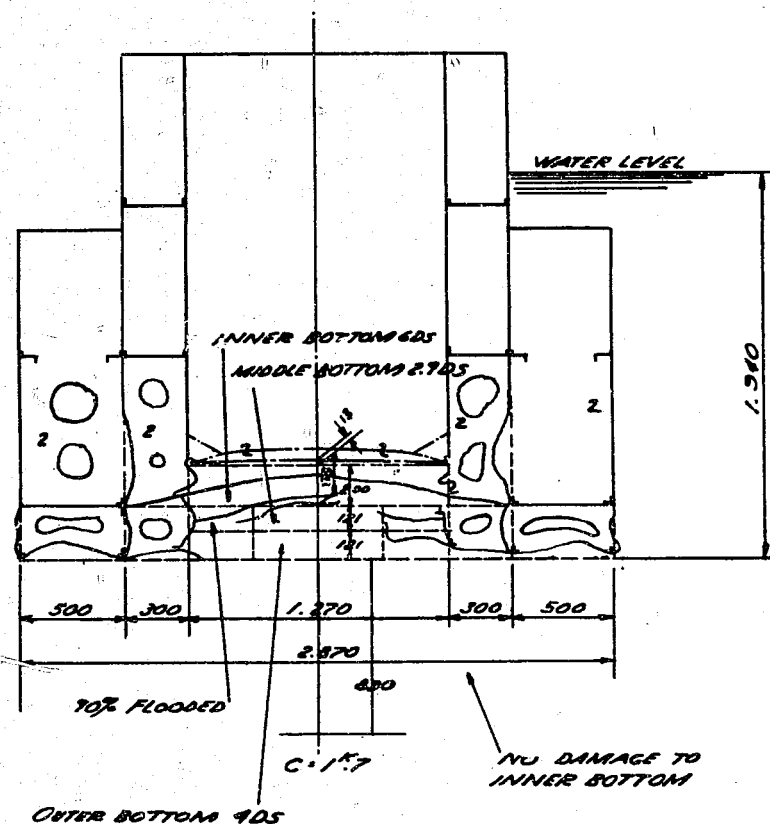


Figure 25
NON-CONTACT EXPLOSION - WATER LAYER PROTECTIVE
SYSTEM - 1/5.35 SCALE, MODEL P

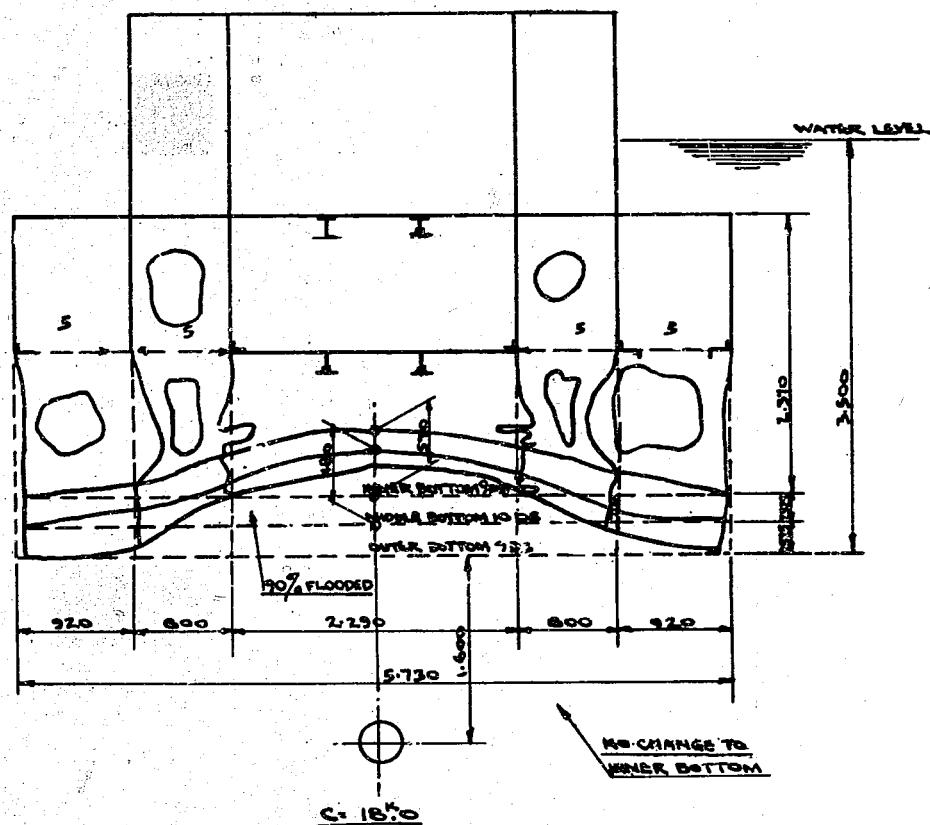


Figure 26
 NON-CONTACT EXPLOSION - WATER LAYER PROTECTIVE
 SYSTEM - 1/2.97 SCALE, MODEL N₉

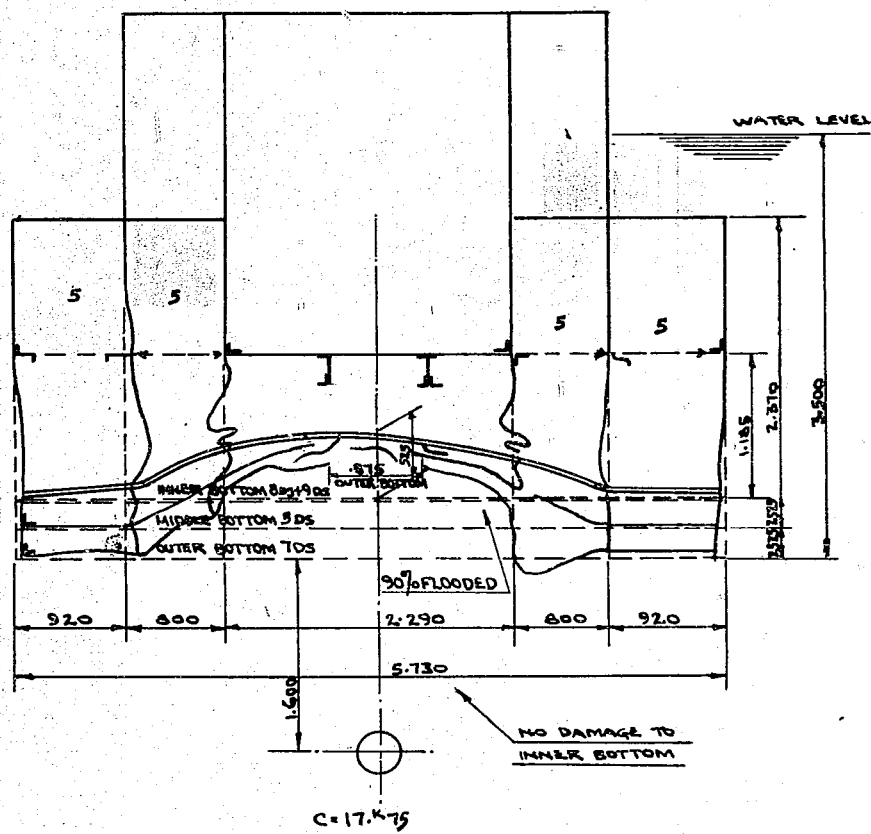


Figure 27
NON-CONTACT EXPLOSION - WATER LAYER PROTECTIVE
SYSTEM - 1/2.97 SCALE, MODEL S₂

APPENDIX III

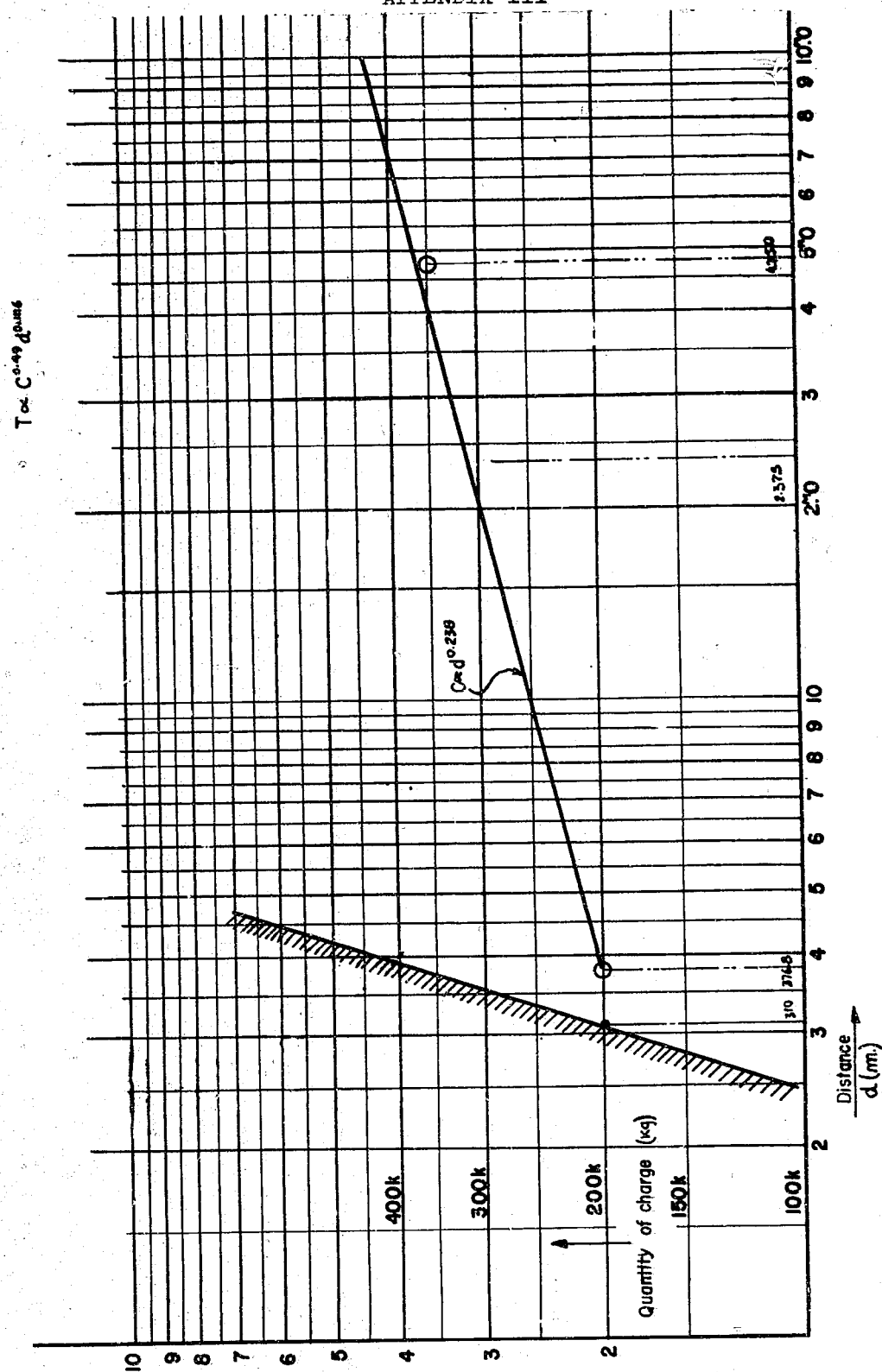


Figure 30
GRAPH SHOWING RELATION OF PROTECTIVE STRENGTH
TO DISTANCE BETWEEN CENTER OF EXPLOSIVE
CHARGE AND OUTER SKIN OF SHIP'S BOTTOM

PART II
STRENGTH OF SUBMARINES AGAINST DEPTH CHARGES
(Translation)

TABLE OF CONTENTS

Chapter I	Preface	Page 124
Chapter II	Measurement of Underwater Explosion Pressures	Page 126
Chapter III	Vibration of an Elastic Body Under Explosive Loading	Page 133
Chapter IV	Crusher Gauge Readings	Page 135
Chapter V	Strength of a Cylindrical Shell Supported at Both Ends and Subjected to Underwater Explosions	Page 136
Chapter VI	Blast Resistance of Pressure Hull of Submarines to Underwater Explosions	Page 141
Chapter VII	Proposals for Increasing the Power of Depth Charges ..	Page 146
Chapter VIII	Conclusion	Page 147

LIST OF APPENDICES

Appendix I	Propagation of Underwater Explosive Pressure Wave ...	Page 148
Appendix II	Underwater Pressure Gauges	Page 151
Appendix III	Approximate Calculation of the Flexural Vibration of Thin Cylindrical Shell Supported on Both Ends	Page 153
Appendix IV	Tables and Illustrations	Page 156

LIST OF ILLUSTRATIONS

Figure 1	Saw-Tooth Explosion Wave	Page 124
Figure 2	Crystal Pressure Receiver Calibration Graph	Page 129
Figure 3	Relation Between Weight of Charge and Weight of Frequency	Page 129
Figure 4	X vs. w_i/w Curve for Independent Sine Wave Impulse	Page 134
Figure 5	$T_i(t)$ vs. t Curve for Single Sine Wave Impulse	Page 134
Figure 6	Indentation Curve for Crusher Gauges	Page 135
Figure 7	Revised Graph for Determining Underwater Explosive Pressure from Pressure Gauge Readings	Page 139
Figure 8	Static Collapsing Pressure vs. Dynamic Critical Pressure	Page 145
Figure 9	Critical Pressure Ratio vs. Dimension Ratio	Page 145
Figure 10	Peak Pressure vs. Wave Duration	Page 147
Figure 11	Saw-Tooth Explosion Wave	Page 150
Figure 12	Thin Cylinder with End Support	Page 153
Figure 13	Construction of Crusher Gauges	Page 158
Figure 14	Graph Summarizing Results of Experiments with Brass Models	Page 160
Figure 15	Graph Summarizing Results of Experiments with Mild Steel	Page 161
Figure 16	Experimental Apparatus for Underwater Explosions	Page 164
Figure 17	Wiring Diagram for Underwater Explosion Test Apparatus ..	Page 165
Figure 18	Trigger Amplifier Circuit	Page 166
Figure 19	Trigger Switch	Page 167
Figure 20	Frequency Curve of Amplifier	Page 168
Figure 21	Relationship of Frequency and Phase Lag	Page 169
Figure 22	Wiring Circuit of Artificial Explosion Signal Generator	Page 170
Figure 23	Diagram of Explosive Charges	Page 171
Figure 24	Pressure Damping Curve	Page 172
Figure 25	Pressure Damping Curve	Page 173
Figure 26	Graph of X vs. w/w_0	Page 174
Figure 27	Construction of Brass and Mild Steel Models	Page 175

Figure 28	Correction Factor "A"	Page 176
Figure 29	Curve of Weight of Charge vs. Destruction Radius	Page 177
Figure 30	Nomograph - Radius of Destruction	Page 178
Figure 31	Graph - S vs. 1	Page 179
Figure 32	GIKEN Type Model A Pressure Gauge	Page 180
Figure 33	GIKEN Type Model B Pressure Gauge	Page 181
Figure 34	Wiring Diagram of Amplifiers	Page 182
Figure 35	Method of Suspension of Pressure Gauges and Arrange- ment of Recording Instruments	Page 183
Figure 36	Static Calibration of Quartz Pressure Gauge	Page 184
Figure 37	Traces on C.R. Tube of Single Saw-Tooth Wave	Page 185
Figure 38	Traces on C.R. Tube of Single Sine Wave	Page 186
Figure 39	Photographs of Pressure Waves - Model A Pressure Gauge	Page 187
Figure 40	Photographs of Models	Page 188
Figure 41	Photographs of Models	Page 189
Figure 42	Photographs of Models	Page 190

CHAPTER I PREFACE

Before experimenting with the resistance of a submarine hull to underwater explosions, it is first necessary to know the characteristics of the pressure wave. A gauge was developed for this, and, after experiments with thin cylindrical tubes, a tentative theory of failure was developed. This theory related the period of vibration of the tube to the duration of the explosion, and from this the probable damage was estimated. This theory has proved to be fairly practicable.

A. The Characteristics of a Shockwave from an Underwater Explosion

1. The pressure wave: Assume that when $t = 0$, there is a sphere with radius "A" having an external pressure P_0 , and a distribution as follows:

$$P = \frac{P_0}{2R} (R - CT) \quad (R - A) < CT < R$$

$$P = \frac{P_0}{2R} (R - CT) \quad R < CT < (R + A)$$

$$P = 0 \quad \text{For other values of } CT$$

where:

R = Distance from center of explosion
 C = Speed of sound in water

i.e. The explosion wave can be represented as a single saw-toothed wave with maximum and minimum values (see Figure 1).

$$\frac{AP_0}{2R} \quad \text{and} \quad -\frac{AP_0}{2R}$$

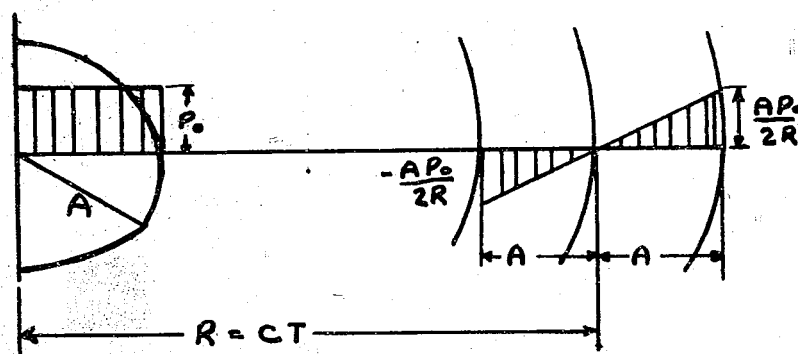


Figure 1
SAW-TOOTH EXPLOSION WAVE

2. Relation between pressure, wave length, and frequency:

When:

G = Amount of charge (grams)

 δ = Specific weight of charge (grams/cm³)

a = Radius of charge (cm)

N = Frequency (cycles/sec)

 λ = Wave length (cm)

C = Speed of sound (underwater) (cm/sec).

The following is obtained:

$$a = \lambda/2 = \left(\frac{4\pi G}{\delta} \right)^{1/3}$$

$$N = \frac{C}{2a} = \frac{C}{\lambda} = \frac{C}{\left(\frac{6}{\pi} \cdot \frac{G}{\delta} \right)^{1/3}}$$

The relations of amount of charge, wave length, and frequency, are roughly as follows in Table I where:

$$C = 150,000 \text{ cm/sec and } \delta = 1.6 \text{ grams/cm}^3$$

Table I
RELATION BETWEEN CHARGE, WAVE LENGTH AND FREQUENCY

G (grams)	$\frac{\lambda}{2} = a$ (cms)	N (cycles/sec)
400	3.9	19,200
1,700	6.3	10,900
18,000	13.9	5,400
200,000	31.0	2,420
400,000	39.1	1,920

Because the bulk modulus of the water will change when the pressure (P_0) increases, the speed of sound (C) will change. Therefore, a correction must be made using the formula:

$$C = C_0 (1 + \delta)$$

F the above results the following conclusions were made:

a. A "saw-toothed" wave is the ideal for an underwater shockwave. Its wave length is proportional to the size of charge.

b. The negative explosive pressure can never exceed the vapor pressure, and therefore it is assumed that the positive portion will exist.

c. The larger the charge, the longer the pressure continues. Therefore, although the pressure amplitude is equal to that of a small charge, it will have more energy for destruction.

d. The wave length is an important factor in pressure distribution around obstacles. In model experiments the wave length had to be decreased in the ratio of the model charge to the full-size charge.

e. For measuring the shape of an explosion wave a very high frequency meter is necessary, as the wave length of the explosion is very short. It is now known what standard is required.

CHAPTER II MEASUREMENT OF UNDERWATER EXPLOSION PRESSURES

A. Apparatus for the Measurement of Explosion Pressure

About one kg charge was used for the experiment, and in this case the basic frequency of the explosion pressure was 10,000 to 20,000 cycles/sec. Because a higher frequency was expected to be measured, a pressure gauge was adopted using piezo-electric effect as a means for measurement. This is the only method by which the mechanical power of pressure is converted into electric power, and the result is recorded on an oscillograph. This apparatus is the result of various improvements, and although its efficiency is not ideal, it may be very helpful for the solution of problems.

The apparatus consists of the following parts:

1. Quartz pressure gauge
2. Feeder line
3. Amplifier
4. Wave recorder
5. Measuring instrument

For the whole instrument see Figure 34.

1. Quartz pressure gauge: As an experiment A-type and B-type gauges were manufactured, both of Giken pattern. Details of their construction are explained in Appendix II. Screw or steel support is not fixed to these new instruments; for this reason the vibration frequency of the gauge is raised, and the phenomena of reflection and penetration are easily observed. In the B-type especially, pressure is applied from both sides of the quartz, and thus exceedingly high vibration frequency is obtained without being affected by the quartz support. However, since the surface of the gauge is parallel to the direction of pressure wave, it is not affected by the reflection on the quartz surface. But, these instruments are not free from defects, since the surface of the gauge is parallel to the direction of pressure wave, and the results of the measurement show the average value at every moment.

However, in the case of a large charge, the error is only slight.

2. Feeder line: The feeder line leads voltage from the piezo-electric gauge to the first amplifier. Since the voltage is static, the insulation of the conductor must be perfect, and completely protected from magnetic influences.

Hitherto no cable suitable for the purpose was available, and a steel pipe containing a single-wire line with amberoid insulators at both ends was used.

The feeder line must be straight; if too long it is difficult to set a lead-wire in the water. However, a special cable called "the high-frequency code" was manufactured at the Furukawa Electric Company, and found to be very effective.

The new wire is a twisted copper wire covered with tin, and insulated by "steatite" insulators. About 112 meters of this wire was used, having a static capacity of $38 \mu\text{f}/\text{km}$ and an inductance of $0.48 \text{ mh}/\text{km}$. The whole wire was contained in a steel tube to be protected from the underwater explosion pressure.

3. Amplifier: If the pressure gauge is placed near the charge when the pressure is measured, a sufficient distance must be put between the gauge and the observer. The voltage caused by the quartz is static, and it is difficult to send it long distances without being affected by leakage and magnetic influences.

For this reason an amplifier was put near the gauge, which converted this voltage into a form easily transmittable. The output from this amplifier was led by a wire to the second amplifier.

The two amplifiers were connected by a capture cable. The diameter of this wire is 12mm and its length is 100 meters, having $100 \mu\text{f}/\text{km}$ of static capacity. In order to make the frequency of the gauge satisfactory and to make the amplification factor small, we used a battery as a source.

For the construction of the first and second amplifiers see Appendix II.

4. Wave recorder:

a. Cathode ray oscillograph - in recording the transient wave train of 144 cycles in this experiment, a cathode ray oscillograph should be used. However, a "Braun" tube type oscillograph was used because of the simplicity of its handling.

b. Time base - when the phenomenon with the cathode ray oscillograph is observed it is necessary to apply voltage on the X-plate fixed at right-angles to the Y-plate, and thus the time scale is applied on the cathode ray tube.

However, if the phenomenon is transient as in the case of underwater explosion, it is necessary to apply only one time scale, and thus measure and record the phenomenon. Generally the discharge current of a capacitor is used for such purpose, and the time is adjusted by the combination of capacity and resistance.

5. Trigger: Since the explosion pressure propagates speedily and the wave length is short, it is difficult to catch the wave at a particular point. This time it was caught on the cathode ray tube, and this method, though simple, can be said to be almost ideal.

The velocity of propagation of an underwater sound wave is about 1,500 m/sec, and frequency of the pressure wave in the present experiment is 15,000 cycles/sec; i.e., in $1/30,000$ second it goes from 0 to maximum and back to 0.

Accordingly, the wave length in water is about 50mm. An attempt was made to catch and photograph this wave over a distance of 80mm, while the fluorescent screen was effective. When trying to record the wave which lasts $1/30,000$ second (length of about 7mm), it must be deflected on the time deflection plate at the speed of: $0.007 \div 1/30,000 = 210 \text{ m/sec}$, so that it needs about $1/2600$ second for the wave to move 80mm on the screen.

Figure 18 shows the construction of a trigger amplifier. First, the spot is fixed at the right side of the fluorescent screen by controlling its position, and then it is moved to the left side for a moment by closing the trigger. After that the spot returns to the right side, and then goes off the screen at the speed controlled by adjustment of the condenser

and resistance.

a. Oscillator - an oscillator was used in order to investigate the sweep speed of the pressure wave and regulate its length. After photographing the pressure phenomenon, voltage of a certain frequency was applied on the axis, and the wave form recorded on the time axis adjusted at the time of photographing. This time a wave of 10,000 cycles/sec was recorded.

b. Camera - the wave form on the fluorescent screen was recorded by a camera, Contax Sonnar f 1.5. As a result of various tests, Sakura Röntgen film was found to be comparatively good.

If the spot, i.e.; the zero, is fixed on the screen of the cathode ray tube from the first, halation appears on the whole photograph. It is desirable that some new method should be invented by which the zero is first off the screen and the spot of light moved to a certain position on the screen just before the appearance of the wave.

If the zero is 20 to 30mm off the screen and an endeavor made to represent the wave about 30mm from the center of the screen, the spot must move for 1/3000 second before the wave reaches the quartz pressure gauge. Taking into account the speed of underwater sound, a time axis trigger was placed 0.5 meters from the center of the screen and this proved successful.

Figure 19 is an outline drawing of this equipment. "T" indicates an insulated terminal, and "R" a copper plate (20.1mm thick). When the pressure pulse strikes the pressure plate it strikes the terminal, closing the trigger circuit.

6. Calibration: Previous to the experiment the crystal is calibrated by means of a static pressure. This static pressure is applied prior to every test by means of an Amsler testing machine. The expected peak pressure is estimated and the sensitivity condenser is adjusted. The electrical apparatus was designed so that it could be tuned to frequencies of pressure wave produced by charges of up to 200 kg of explosive charge.

In this test only a few stages were necessary to go from zero to a maximum load, and errors from the leakage of piezo electricity were practically nil. Figure 2 shows a typical calibration wave.

B. Capacity of Apparatus to Respond to Explosion Impulses

The frequencies which were required to be maintained were of the order of 10,000 to 20,000 cycles/sec, and this will indicate the capacities of various parts of the equipment.

1. Quartz receiver: The two types A and B, described above were devised because of the lowering of the natural periods of previous gauges by various attachments. Type B has good following qualities as its natural frequency is 270,000 cycles/sec.

In type A the steel support to the back of the crystal is not perfectly rigid, and reflection occurs at the boundaries. Hence the natural frequency is not as good as the type B model.

Table II shows a comparison of steel and quartz, giving the sonic propagational properties; while Table III compares reflection characteristics.

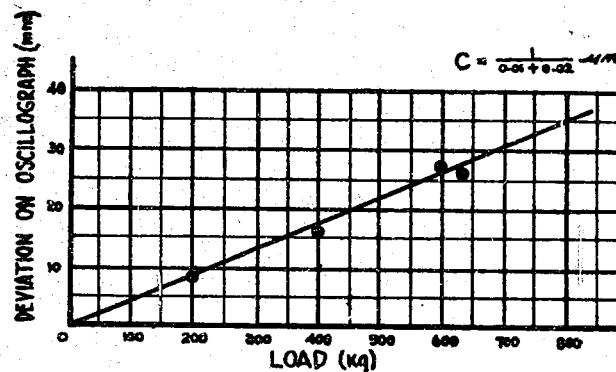


Figure 2
CRITICAL PRESSURE RECEIVER CALIBRATION GRAPH

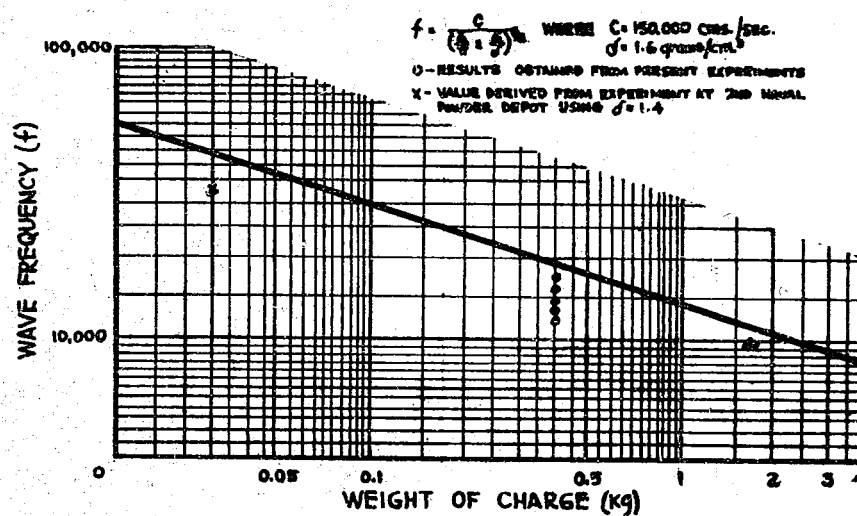


Figure 3
RELATION BETWEEN WEIGHT OF CHARGE AND WAVE FREQUENCY

Table II
SONIC PROPERTIES - WATER, QUARTZ AND STEEL

Material	Bulk Modulus (dynes/cm ²)	Density (gm/cm ³)	Velocity of Propagation (m/sec)
Water (15°C)	2.04×10^{10}	1.0	1430
Quartz	7.85×10^{11}	2.65	5440
Steel	2×10^{12}	7.85	5040

Table III
REFLECTION CHARACTERISTICS - WATER, QUARTZ AND STEEL

Material and Direction of Propagation of Wave	Transmitted Pressure *	Reflected Pressure
Water \longrightarrow Quartz	$1.82 P_0$	$0.82 P_0$
Quartz \longrightarrow Water	$0.18 P_0$	$-0.82 P_0$
Water \longrightarrow Steel	$1.93 P_0$	$0.93 P_0$
Steel \longrightarrow Water	$0.07 P_0$	$-0.93 P_0$
Quartz \longrightarrow Steel	$1.46 P_0$	$0.46 P_0$
Steel \longrightarrow Quartz	$0.54 P_0$	$-0.46 P_0$

*Incident Pressure - P_0

In type A the pressure recorded was 1.82 times the actual pressure at that point.

When a nearly saw-toothed wave form containing up to the third harmonic was incident, it was calculated that the recorded pressure was 2.2 times the incident at 10,000 cycles/sec and 2.4 times at 15,000 cycles/sec.

2. Amplifier:

a. Special frequency characteristics - the frequency response of the amplifiers in range 10 to 20 kilocycles, which is beyond the flat frequency response of the gauge, was determined. The results are shown in Figure 20.

b. Relationship of frequency and phase lag - it was again hoped that a flat curve would be obtained, but the results are shown in Figure 21.

c. Transient response - in addition to the above two characteristics, the amplifiers must have a suitable transient response. To check this a special circuit was produced which gave a saw-toothed wave of about 10,000 cycles. This was led to the cathode ray tube directly through the amplifier, and the performance was compared. (Figure 22.)

The cathode ray oscillograms shown in Figures 37 and 38, indicate the type that is accepted in practice.

Table IV shows its amplification sensitivity.

Table IV
AMPLIFIER SENSITIVITY

Wave Form	Amplitude on CR Tube (mm)		Amplification Ratio*	Sensitivity
	Directly	Through Amplifier		
Low frequency 1000 cycles	12.5	14.0	1.12	100
Single saw-toothed form	9.5	9.5	1.00	90
Single sine wave	17.2	18.6	1.08	96

*Amplitude through amplifier \div amplitude direct

C. Experimental Procedure

The explosive pressure at points along a horizontal line through the center of the charge was measured for a given weight of charge.

Charges of 1.7 kg and 0.4 kg in special containers were hung vertically with the explosive at the bottom. They were detonated at depths of 2 meters and 1.2 meters respectively. (See Figure 23.)

The disposition of the charges and pressure gauges is shown in Figure 16. The gauge was fixed and the charges were placed at 3, 5, 7, and 10 meters away. The electric circuit of the gauges is shown in Figure 17.

Photographs were taken in a dark room with the shutter opened one second before detonation.

D. Experimental Results

1. Pressure wave form: A typical oscillogram is shown in Figure 39 as obtained by an A and B type pressure gauge. It also shows a 10,000 cycle sine wave at the same sweeping velocity.

As seen in the photograph, the pressure wave formation is a greatly reduced sine wave, a single wave being distinct. With the A gauge, a small vibration accompanied to the end of the principal wave and thereafter; this however, is believed to be due to constructional peculiarities of this gauge. With the B gauge, this phenomenon was not noted. Mathematically speaking, the discrepancy between the saw-tooth wave and the sine wave is thought to be due to the fact that the detonation velocity is finite, and to the damping of high harmonics. Wave differences due to distance from the explosion and to size of pressure vibrations were expected, but in this experiment were not noted.

2. Relation between amount of explosive (charge) and length of pressure wave (frequency): The frequency of the pressure wave is given in Figure 1.

Frequencies, thus, are 10,000 cycles for 1.7 kg and 14,000 for 0.4 kg. If the velocity of propagation of underwater pressure waves is 1500 m/sec, the wave lengths are respectively 15cm and 107cm.

According to the experiment conducted by the Research Division of the No. 2 Powder Depot, the frequency of the pressure wave, when 35 grams of powdered tetryl were used as an explosive, was approximately 32,000 cycles.

This experimental value is shown in the same chart in comparison with the A value computed using a ball charge. In this regard, the tendency for pressure wave frequency to decrease in proportion to the diameter of the explosive charge produces a result in agreement with the result previously stated. This circumstance is a phase of the problem of explosive loading of structures which will require further research for clarification.

3. Pressure amplitude: The maximum pressure amplitude obtained by the statically calibrated value of the maximum amplitude shown in the oscillogram is given in Figures 24 and 25.

Generally speaking, when sound waves pass the boundaries of different media, they are either reflected or else they pass on through. Thus, true pressure amplitude is not shown in underwater measurements obtained through the use of an A type pressure gauge.

In Figure 24, the ratio of pressure values obtained through the use of A and B type pressure gauges is 2.57. The principal reason for this is the fact, as stated above, that pressure increases 1.89 times upon passing from water to quartz. Concerning this increase, it must be noted that the quartz section of an A type pressure gauge is imperfect. On the other hand, the pressure surface of a B type gauge is of such size that pressure wave lengths cannot be reduced, and therefore gradually lower values are shown. In Figure 25 a comparison between the modified value obtained from both of these instruments is given and apart from the above-mentioned considerations, it is believed that the modified value obtained from an A type pressure gauge extends only to third-order harmonics and errors may therefore be present.

4. Decrease in amplitude: The following formula expresses the decrease of pressure amplitude which accompanies the increase of distance from the center of the explosive charge:

when: P_0 = Initial pressure
 d = Distance from center of explosive charge
 $P = P_0 d^{-1.07}$

E. Effects of Water Pressure Due to Expansion of Detonation Gases

Until now, concern has been given only to the elastic impulse waves created by the explosive charge; however, inasmuch as there is also a change of water pressure created by the gases formed in the area of the explosion, the influences of this pressure as it concerns depth charges and submarines must be investigated. For this problem, KIYOMIGU'S research efforts provide a clear answer. According to his results, the effects of water pressure at a distance of about 10 times the diameter of the explosive charge may be safely disregarded; he shows elastic impulse waves as the principal element of explosive force.

In calculating these distance limits, the following is true:

<u>Explosive Weight</u>	<u>Approximate Distance</u>
1.7 kg	120cm
150 kg	560cm
200 kg	620cm

In view of the above figures on pressure propagation, it is clear that the effects of water pressure, insofar as the limits of this discussion are concerned, may be disregarded.

F. Conclusions

The length of the elastic impulse waves, which are produced by underwater detonation or the explosive charge, is established as increasing with the size

of the explosive; that is to say, the wave length is proportional to the cube root of the weight of the explosive.

When the weight of an explosive charge runs into tens of kilograms, the impulse wave frequencies are 10,000 cycles more or less. It is believed necessary that the "following potential" of the apparatus used to record pressure wave formations be capable of handling frequencies in excess of those mentioned above.

CHAPTER III VIBRATION OF AN ELASTIC BODY UNDER EXPLOSIVE LOADING

A. General

When an elastic body is acted on by a transitory force, as in an explosion, a forced and natural vibration are simultaneously generated. After the external force ceases to act, only the induced natural vibration remains. This natural vibration will consist of fundamental and various harmonics including those of very high frequency.

The displacement can be represented by:

$$\delta = \sum_{n=1}^{n=\infty} S_n(X) T_n(t) \dots\dots\dots (III-1)$$

if the body has been acted on by a transient force 3.1.1. which is a function of time; n represents the harmonics in which it may be vibrating.

The factors controlling the high-frequency vibration, induced by a transient explosive force of a plate as a whole, may be verified by investigating the convergence of this infinite series. The quantity $\sum S_n(X)$, obtained by making $T_n(t) = 1$, gives the static deflection of the whole body when the peak value of this force is applied slowly. $T_n(t)$ is the parameter which indicates the ratio of the displacement at any instant to the static displacement by an equal force. Its characteristics are determined by the type of impulsive force, the natural frequency of the body, and the damping characteristics of the system.

Calculations on the vibration of a rectangular plate already exist (Rayleigh, MUTO, and KAMI), but some further calculations were made.

B. Amplitude Coefficient

If consideration is given the i^{th} frequency of vibration from formula (III-1)

$$\delta_i = S_i(X) T_i(t)$$

and the maximum value of δ_i occurs when $T_i(t)$ is at a maximum. The maximum value of $T_i(t)$ is called the amplitude coefficient and will be denoted by X. The value of X differs according to the external force wave shape and the natural period of the elastic body. The results when an independent sine wave impulse is applied are shown in Figures 4 and 5.

In Figure 4 when $\omega \doteq 0.62\omega_1$, by means of the curve, $X = 1.77$.

Figure 5 shows the displacement for various values of $\frac{\omega}{\omega_1}$ for a body acted on by sinusoidal impulse.

In Figure 5 it can be seen that when ω_1 which is a function of the period of the applied force, is small $T(t) \rightarrow 1$. This is similar to static loading. When $\omega \doteq 0.62\omega_1$ $T(t)$ reaches a maximum value of about 1.77. At this stage the shockwave is severe. As ω increases, the maximum value of $T(t) \rightarrow 0$. This shows that an applied force of small duration rarely affects the body as a whole.

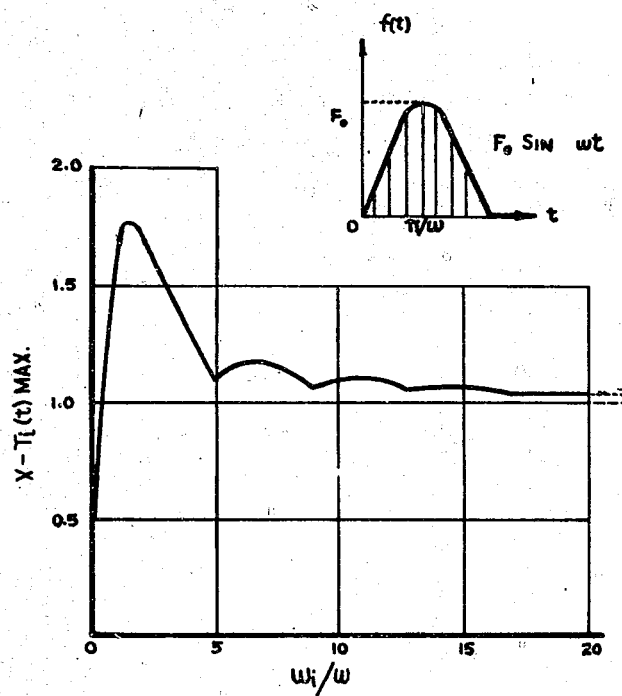


Figure 4
 X vs. ω_i/ω CURVE FOR INDEPENDENT SINE WAVE IMPULSE

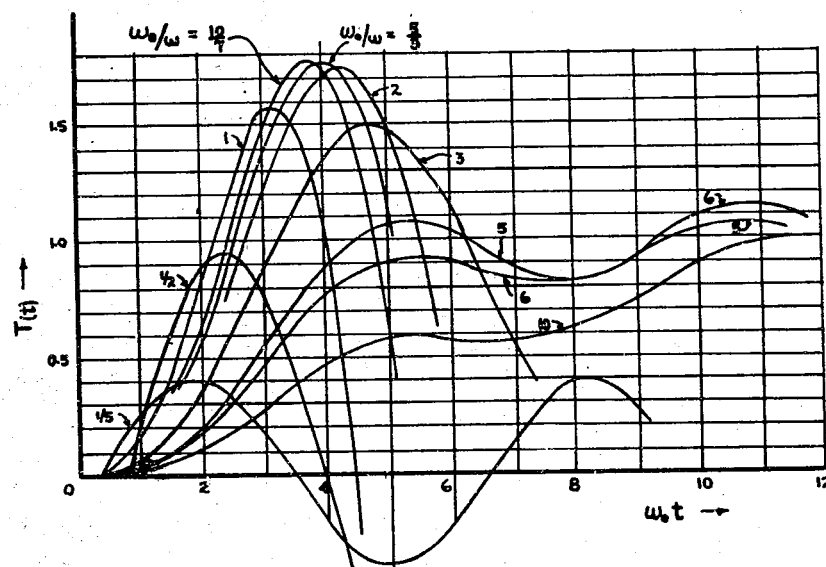


Figure 5
 $T_i(t)$ vs. t CURVE FOR SINGLE SINE WAVE IMPULSE

CHAPTER IV CRUSHER GAUGE READINGS

A. Theoretical Examination

A crusher gauge is frequently used in explosive experiments, but it does not record the correct shape of the pressure wave. Variations in readings occur as has been explained in Chapter III.

The crusher gauge may be considered as an elastic body with one degree of freedom. It is made up of a shock-absorbing piston; a movable mass, consisting of a ball; and an elastic spring in the form of a copper rod. The depth of indentation due to a static load of the copper rod and the load are in direct proportion. Using this (Figure 6), it is possible to determine the elastic force of the spring restraining the load which creates unit indentation.

Therefore, the reading of the copper rod will probably be dependent upon the relation between the period of the explosive wave and the natural frequency of the gauges.

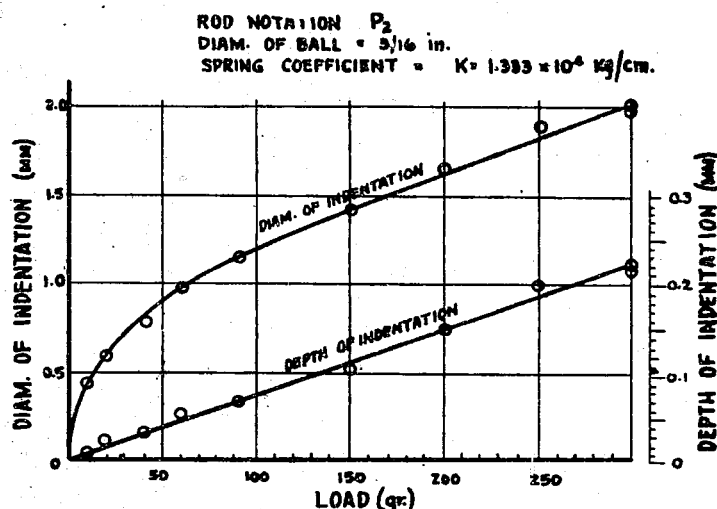


Figure 6
INDENTATION CURVE FOR CRUSHER GAUGES

B. Experimental Results

To verify the above conclusions, experiments were conducted with 1.7 kg of picric acid. The effect of varying the following was tried:

1. The mass of the "shock-absorbing piston" of the crusher gauge.
2. The frequency of natural vibration of several gauges by using lead as well as copper for the rods.

The readings of the various crusher gauges at a given peak pressure (measured by quartz gauge) were obtained. Figure 26 shows the variation of X with ω/ω_0 where:

- ω_0 = Angular frequency of vibration of crusher gauge
 ω = Angular frequency of explosive defined from its wave length

Details of the gauges are given in Table IX.

Figure 27 includes many scattered points, but as the friction of the movable part of the gauge and the internal resistance of the copper rod were not taken into account, this is not considered unreasonable.

C. Conclusion

The crusher gauge can be considered as a vibrating system. The displacement, when acted on by explosive pressure, is in the ratio of the displacement amplitude to that displacement given by an equal static load. It is dependent on the relation of the natural frequency of the gauge to that of the explosion.

The crusher gauge may be read by converting the indentation to its equivalent static load, although it still does not indicate the maximum value of the explosive pressure. With the same type and amount of explosive, if the physical characteristics of the rod and piston vary, readings will vary. Even with the same gauge using different charges (or different frequencies of explosion), the ratio of its reading to the peak pressure will not be constant. This relation has been quantitatively obtained.

Large indentations of the ball of a gauge will give inaccurate readings.

CHAPTER V STRENGTH OF A CYLINDRICAL SHELL, SUPPORTED AT BOTH ENDS AND SUBJECTED TO UNDERWATER EXPLOSIONS

A. Introduction

The problem consists in first, studying the distribution of pressure over the surface; secondly, obtaining the mode of vibration and relating this to the statical collapsing pressure.

B. Hypothesis

In general, when an elastic body is subjected to a transient force of $f(t)$, the vibration shown in equation III-(1) is induced. When the amplitude of the initial impulse of $f(t)$ remains constant and the fundamental vibration frequency increases, the equation will tend to become fixed, and depend mainly on the initial impulse amplitude. At the same time, the effect of the natural frequency is still evident to a minor degree.

The pressure hull of a submarine may be treated as this, and it is thought that the vibration causing damage may be based on such a relation.

The distribution of pressure is not constant even for a simple sine wave and the treatment becomes very complex.

The following assumptions are made:

1. The total surface of the cylinder is subjected to explosive pressure of the same phase and wave length.
2. The wave length is constant and the same as at a point remote from the cylinder.
3. The cylinder develops a constant form of vibration and the predominant harmonic is the one which gives the maximum value of X .
4. Dividing the static collapsing pressure for this mode by the efficiency of vibration inducement, we obtain the peak pressure of the explosion at which the shell will just begin to collapse.

5. Since the force acting on the shell changes suddenly, the elastic limit and yield point of the material is unimportant.

6. The wave form of the explosion is a simple sine wave.

C. Vibration of the Cylindrical Shell Supported At Both Ends

There are many instances of treatment of the vibration of a cylindrical shell, but no explanation for one which is fixed or supported at both ends. In the approximate explanation in this case, neglecting displacement in radial direction and the change on longitudinal and circumferential direction; and considering only the bending vibration in the case of a thin cylinder shell, the following equation is possible.

$$f_n = \frac{1}{\pi} \sqrt{\frac{E}{3\rho(1-\sigma^2)} \frac{S}{D^2}} (\alpha^2 + n^2) \dots\dots\dots (V-1)$$

$$\alpha = \frac{\mu D}{2L} \text{ where } \mu = 1, 3, 5, \dots\dots\dots$$

provided that: D = Diameter of cylindrical shell
S = Thickness
L = Unsupported length
 ρ = Density of material
 σ = Poisson's ratio
n = No. of half wave lengths of circumferential direction
 μ = No. of half wave lengths of longitudinal direction

Next it is necessary to consider the virtual mass of water. Approximately, the part surrounded by the nodal line is considered to be a flat plate, and the calculation for the decrease of vibration frequency is used when an oblong plate is vibrating under water according to the graph of the sine wave displacement i.e.;

$$f_w = \frac{f_a}{\sqrt{1+\epsilon}} \dots\dots\dots (V-2)$$

$$\epsilon = \frac{\rho_w}{\rho_m} \frac{2}{S\pi} \frac{ab}{\sqrt{a^2+b^2}} \dots\dots\dots (V-3)$$

f_w = Underwater frequency
 f_a = Frequency in air
 ρ_w = Density of water
 ρ_m = Density of flat plate
S = Thickness of plate
a, b = Distances between nodal lines

In the above formula, ϵ is the value when water is present on both sides of the plate. This value is one-half when water is on one side only.

D. Static Collapsing Pressure of the Cylindrical Shell

When the cylindrical shell is subjected to static pressure, the critical pressure may be calculated in accordance with the following TOKUGAWA formula:

$$P_{cr} = \frac{E S}{(n^2 - 1 + \frac{1}{2}\alpha^2)} \left[\frac{2\alpha^4}{(n^2 + \alpha^2)^2} + \frac{2}{3} \frac{1}{1-\sigma^2} \left(\frac{S}{D} \right)^2 \left\{ (n^2 + \alpha^2)^2 - \frac{n^4(2n^2 - 1)}{(n^2 + \alpha^2)^2} \right\} \right] \dots\dots\dots (V-4)$$

provided that: P_{cr} = Collapsing pressure
S = Thickness of cylindrical shell
D = Mean Diameter of cylinder
L = Unsupported length

- E = Young's modulus
 σ = Poisson's ratio
 n = No. of lobes
 $a = k \frac{\pi D}{2L}$
 k = Correction factor for end conditions

At present, the value of n is extremely large compared to a , and therefore, the above equation can be expressed as:

$$P_{cr} = 2/3 \frac{E}{1-\sigma} (S/D)^3 \psi(na)$$

provided that:

$$\psi(na) = \frac{1}{(n^2 - 1 + \frac{1}{2} a^2)} \left\{ (n^2 + a^2)^2 - \frac{n^4 (2n^2 - 1)}{(n^2 + a^2)^2} \right\} \dots\dots\dots (V-5)$$

$$\approx n^2 + 3.3 (D/L)^{2.06}$$

Further, when the hoop stress exceeds the limit of proportionality and the yield point, this is not valid.

E. Calculation of Critical Pressure Against Explosion of Cylindrical Shell

1. Vibration mode of critical pressure against explosion of cylindrical shell, which gives the maximum efficiency in relation to the frequency of the explosive pressure wave.

In practice the underwater explosion pressure wave may be considered to be an exponential single sine wave; therefore, the frequency $f(m)$ of the cylindrical shell which gives the maximum efficiency X , in relation to the pressure frequency N , may be attained by $N/f_n = 0.167$.

Consequently, when the weight of charge is given, the pressure frequency N may be obtained by the formula shown in Chapter I, Section 2. From this, the mode n , which should give the required frequency of the underwater cylindrical shell is calculated by formula shown in Chapter V, Section C. This gives the number of half wave lengths-- M --at the time of the collapsing pressure, when the cylindrical shell is subject to an explosion pressure of frequency N .

2. Limiting explosive pressure: P_{cr} , the critical statical collapsing pressure for the mode of vibration (n) calculated above, can be found as shown above. This pressure multiplied by the amplitude coefficient gives the critical explosive peak pressure for the frequency N .

F. Results of Model Experiments

1. Main points of experiments:

- a. Brass cylinder machined from solid brass
- b. Mild steel cylinder
- c. Pressure hull model

See
Figure 27
and Table X

Charges: 0.4 kg and 1.7 kg picric acid.

The experiment was conducted at the testing tank at the Naval Technical Research Institute. The majority of experiments were conducted in a depth of two meters with the explosive wave normal to the axis of the cylinder.

Additional experiments at sea off YOKOSUKA used 18 kg and 400 kg charges.

2. Results: Results are shown in Figures 14 and 15. \odot indicates the estimated critical (balanced) distance and also the estimated balanced explosion pressure. The balance pressure is defined as that which will just cause a slight permanent set (for convenience of conclusiveness).

The deformation, to be assumed in this case, is 0.1 to 0.05% of the diameter of the cylinder. Photographs of models damaged at the critical distance are shown in Figures 40, 41, and 42.

3. Comparison of experiment and theory: The comparison of calculated and actual pressures and distances, are shown in Tables XI and XII and Figure 28.

For large charges, no quartz gauge readings are available; and crusher gauge readings were corrected by the revised method shown in Chapter VI, Section C. The formula to be revised was $P = KG^{0.45} d^{-1.07}$ (See Figure 7)

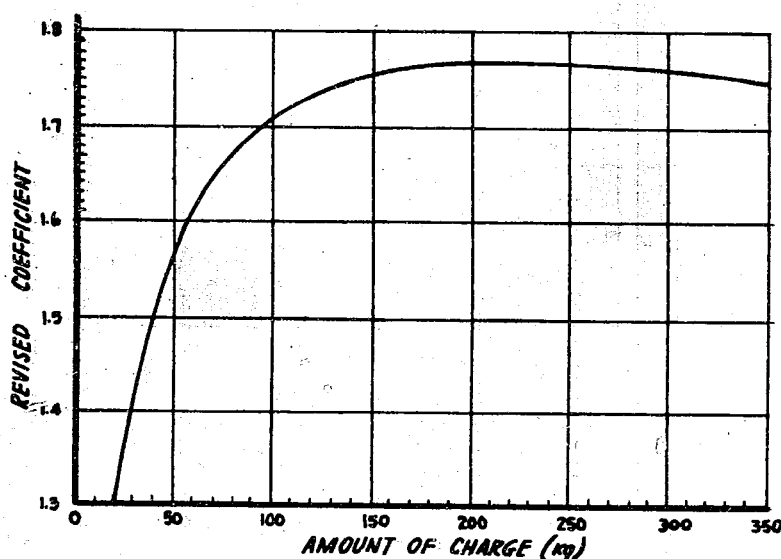


Figure 7
REVISED GRAPH FOR DETERMINING UNDERWATER EXPLOSIVE PRESSURE
FROM PRESSURE GAUGE READINGS

It appears that:

- a. There are differences between the calculated and experimental values for the number of lobes in the mode of failure, but high frequency modes are predominately induced.
- b. If D/λ is constant, the ratio of experimental, to theoretical value is approximately constant (see Figure 28).

As the calculation of critical explosive pressure is based on a simple and bold hypothesis, the results are fair. The differences are due to the fact that as D/λ varies there is no fixed distribution of pressure.

Therefore, calling the ratio of experimental to theoretical values A , the ratio may be plotted against D/λ and used as a correction factor in future calculations.

Table V
CALCULATION OF RADIUS OF DAMAGE

	Experiment	
	Full Scale Model	Model for Depth
Model dimensions (outside diameter x plate thickness x frame spacing)	550cm x 1.4cm x 70cm	83.4cm x 0.29cm x 9.8cm
Wt. of explosive (Picric acid)	148 kg	100 kg
Pressure wave frequency, N	2670	3045
Pressure wave length λ	56.1cm	49.3cm
η (number of lobe) at X max	103	37
X	1.7685	1.7681
P_{cr} at n	259 kg/cm ²	101.2 kg/cm ²
Critical Pressure (calculated P_{cal} $= P_{cr}/X$)	146.5 kg/cm ²	57.2 kg/cm ²
D/λ	9.80	1.69
Correction factor, A	0.315	0.692
Required Critical pressure P_k	46.1 kg/cm ²	39.6 kg/cm ²
Angular frequency of copper crusher gauge	2.39×10^4 cycles/sec	2.39×10^4 cycles/sec
Angular frequency of pressure wave ω_0 ($-2\pi N$)	1.68×10^4 cycles/sec	1.91×10^4 cycles/sec
ω_0/P_0	0.703	0.800
Correction factor to copper crusher gauge	1.754	1.710
P_k at copper crusher gauge	80.9 kg/cm ²	67.7 kg/cm ²
Critical pressure (copper crusher gauge)	82.5 kg/cm ²	67.7 kg/cm ²
Lethal radius (measuring from outside of model)	39.0 m	38.4 m
Correction for outer hull *	0.98	

G. Conclusions

A correction factor A was obtained depending on the ratio of diameter of shell (D) to the wave length of explosion (λ).

Tables X, XI, and XII show that the relation between statical collapsing pressure and critical explosive pressure is irregular.

Increase in size increases critical explosive pressure without necessarily raising statical collapsing pressure.

CHAPTER VI

BLAST RESISTANCE OF PRESSURE HULL OF SUBMARINES TO UNDERWATER EXPLOSIONS

A. Introduction

A submarine's inner pressure hull is made of one layer or thin circular material. By using the data noted in Chapter V the blast resistance of the pressure hull to various types of explosive charges can be determined. Since in submarines there is a thin steel plate which is outside the pressure hull and which is separated from it by sea-water or heavy oil, the blast effect will be diminished by having to pass through this outer hull. In this discussion, calculations will be presented for blast resistance against the pressure hull of a submarine and the results of a practical application of the data obtained.

B. Comparison of Previous Experimental Results and New Methods of Calculation

At the Kure Navy Yard, blast pressure limits were calculated from experiments on large-scale models and special models for depth tests. The A coefficient based on the experiment explained in Chapter V, Section F, Sub-section 3 was modified; thereby making it possible to calculate the radius of damage by a pressure formula derived by means of a copper crusher gauge. The results of this calculation are given in Table V.

In Table V asterisk represents the permeability of explosive blast waves on the outer hull; in the experiment on the full-scale model, plate thickness of the outer hull was 5mm.

Table VI
RESULTS OF TEST SUBSTANTIATING CALCULATION OF LETHAL RADIUS

Distance from Charge to the Outer Surface of Pressure Hull	Pressure Exerted on Outer Plate (as registered by Copper Crusher gauge)	Conditions of Damage
48.3 meters	0.72 kg/mm ²	No permanent set on pressure hull. 10 leaking rivets, but no penetration of water was observed.
16.5	2.09	Produced permanent set on pressure hull. (Maximum set 15mm.)
7.7		Considerable damage to outer hull. (Maximum deflection 560mm.)

Although it was difficult in this experiment to ascertain the critical distance, 39 meters is considered reasonable by the new system of computation.

The results of model tests at various depths are as shown in Table VII.

As shown in Table VII, there were discrepancies at various depths; the direct distance between depth charge and target was between 32 and 47 meters. For the new calculation, this distance is considered as 38.4 meters.

C. Formulae for Lethal Radius of Submarines

In the new method of calculation critical pressure for the various scantlings of a submarine pressure hull was obtained as follows:

$$P_k = \frac{8.4 S^{1.97}}{C^{0.162} D^{1.46} l^{0.03}}$$

Where:

- P_k = Critical pressure (kg/mm²)
- C = Weight of explosive (kg)
- D = Diameter of pressure hull (m)
- S = Thickness of pressure hull (mm)
- l = Frame spacing (mm)

It was decided that the above formula could be used practically. The relation between lethal radius and weight of explosive is shown in Figure 29.

When there is more than 120 kg of explosive, $d \propto C^{0.545}$
 When there is less than 120 kg of explosive, $d \propto C^{0.405}$

Thus, lethal radius is given approximately by the following formulae:

$$d = 51 C^{0.405} D^{1.36} S^{-1.84} l^{0.028} ; C \leq 120 \text{ kg}$$

$$d = 26.5 C^{0.545} D^{1.36} S^{-1.84} l^{0.028} ; C \geq 120 \text{ kg}$$

Since this calculation is made only under set circumstances, care must be taken in the use of the above formulae. In view of the fact that certain errors can appear; when the pressure hull is made of material other than mild steel, when the dimensions of the pressure hull are either particularly great or small, when the type of explosive varies, or when the weight of explosive varies, etc., at least one check must be made.

D. Definition of Lethal Radius

For the sake of convenience in a theoretical analysis of critical pressure and lethal radius, it is assumed that only a very small permanent deformation will be created.

Therefore, even though leaking rivets appeared and caulking was damaged within the lethal radius, no vital damage was sustained.

The distance at which a submarine would be disabled under battle conditions was assumed to be half of the distance defined here as the critical (lethal) distance. (This is based on full scale trials at KURE.)

E. Relation Between Explosive and Statical Strength

As previously stated, the effect of a shockwave depends upon its frequency and the elastic properties of the structure subjected to an explosion.

Table VII
RESULTS OF EXPERIMENTS FOR ESTABLISHING CRITICAL DISTANCE

Position of Depth Charge		Position of Model		Mean Pressure (indicated by Copper Crusher Gauge) (kg/mm ²)	Maximum Deformation (mm)	Condition of Damage
Horizontal Distance (meters)	Depth (meters)	Depth (meters)	Vertical Distance of Depth Charge (meters)			
50	40	20	54	70	<div style="display: flex; align-items: center;"> <div style="font-size: 2em; margin-right: 5px;">}</div> <div style="display: inline-block; vertical-align: middle; text-align: center;"> 0.4 0.4 0.4 </div> </div>	No damage noted
		60	54	41		
		100	78	30		
50	60	20	64	52	<div style="display: flex; align-items: center;"> <div style="font-size: 2em; margin-right: 5px;">}</div> <div style="display: inline-block; vertical-align: middle; text-align: center;"> 0.4 0.6 0.3 </div> </div>	No damage noted
		60	50	66		
		100	64	60		
25	40	20	32	112	1.0	68 indentations on plate; very slight 100 indentations on plate; very slight 10 indentations on plate; very slight
		60	32	87	10.0	
		100	65	97	1.0	
25	60	20	47	130	1.0	43 indentations on plate; very slight Indentations appeared on the whole surface. Though maximum was 18mm, there were many of 2mm. 123 indentations on plate; all slight
		60	25	154	18.0	
		100	47	58	1.0	
12	60	40	23	114	65	Collapsed. 16 rivets came out.
		80	23	129		Collapsed elliptically
12	40	20	23	148		Large damage; half remained intact.
		60	23	135		Collapsed from circular cross-section to kidney-shaped cross-section
23	40	40	23	154	35	Entire surface collapsed slightly
23	80	80	23	114	23	Entire surface collapsed slightly

A structure of large static strength is not, therefore, necessarily strong against explosion. In other words, the ratio of static strength to dynamical strength is not constant. The value of static collapsing pressure can be obtained from the following formula:

$$P_{st} = 0.602 E \left(\frac{D}{L}\right)^{0.85} \left(\frac{S}{D}\right)^{2.275}$$

(Hoop stress being lower than the limit of proportionality)

$$P_{st} = 0.0418 E \left(\frac{D}{L}\right)^{0.46} \left(\frac{S}{D}\right)^{1.69}$$

(Hoop stress being over the limit of proportionality)

Calculating the value of critical pressure against explosion from the formula in Section C, the relation of the two strengths is obtained: i.e.: static collapsing pressure and dynamic critical pressure against explosion, as shown in Figure 8.

Changing the above formulae:

$$P_{st} \propto \frac{S^{2.275}}{D^{1.425} L^{0.85}}$$

Hoop stress being lower than the limit of proportionality

$$P_{st} \propto \frac{S^{1.69}}{D^{1.23} L^{0.46}}$$

Hoop stress being over the limit of proportionality

Considering the case when each parameter D, S, or L, changes its magnitude, the curves shown in Figure 9 are obtained in which abscissa and ordinate indicate respectively dimension ratio and strength ratio; that is, ratio of P_{st} to a given standard. From these curves the following results can be concluded:

1. The effects of diameter and wall thickness upon the static strength and the strength against explosion are nearly the same, and in order to increase both of these together, an increase of wall thickness is most efficient.

2. Decrease of the frame spacing is comparatively efficient for increasing static strength but has little effect on the strength against explosion.

F. Determination of the Dimensions of the Pressure Hull of Submarines

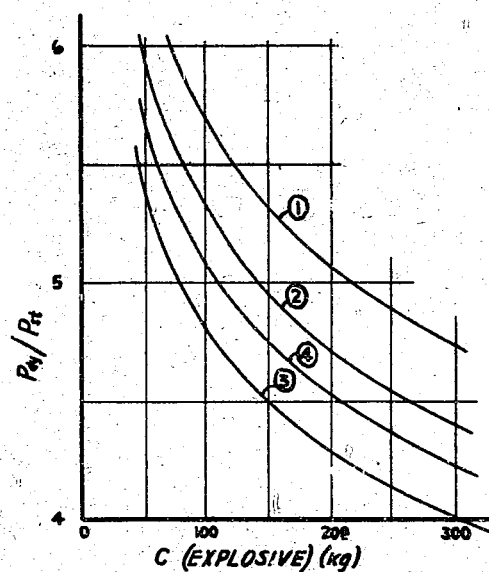
An applied example of the lethal radius is shown when the method of determining the appropriate thickness and frame spacing when the diameter of inner hull and the safe diving depth are given. Putting D (diameter) = 5.3 meters and H (depth) = 80 meters for simplicity, the manner of calculation is as follows:

1. S-L curve: If D = 5.3 meters and H = 80 meters, using 1.5 as a safety factor, from the formula for static collapsing pressure described above, the relation between same L can be found and the curves shown in Figure 31 obtained. But here, L can be selected freely; S, however, is determined as 14, 18, and 20mm by the limit of materials available, and so the curves must be corrected as shown by the dotted lines.

2. Dimension of frame: By the formula for the strength of frames:

$$P_k = \frac{3EI}{R^3L}$$

P_k (determined as 1.2 times the static collapsing pressure as is customary) and R (the radius of pressure hull) being assumed, I can be calculated as a function of L. Thus, for four kinds of bulb angle sections in service, the range of effective scantlings can be determined from the table



Notation	Dimension of Cylindrical Shell			Static Collapsing Pressure (kg/cm ²)
	D(m)	S(mm)	l(mm)	
①	5.0	18	600	16.5
②	5.0	14	600	10.8
③	5.0	18	400	9.8
④	6.0	14	600	8.6

Figure 8
STATIC COLLAPSING CURVE VS. DYNAMIC CRITICAL PRESSURE

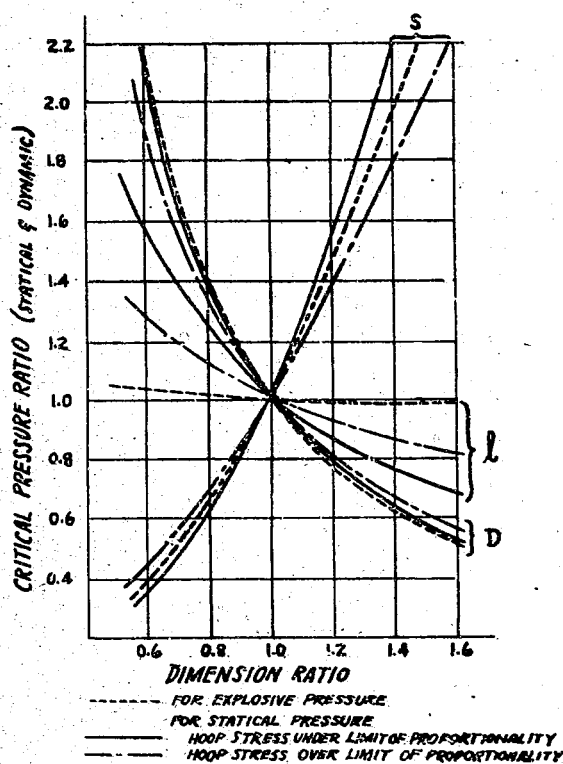


Figure 9
CRITICAL PRESSURE RATIO VS. DIMENSION RATIO

of standard size of sections for hulls of warships and merchant ships.

3. Weight curve: S and dimensions of frame being determined as above, weights may be expressed and distributed for the frame and pressure hull plate as shown by the formulae below.

In these formulae, detailed items like weight of butt straps and the difference of weight corresponding to the various methods of attachment were neglected since the main purpose is to check the weight ratio.

The weight of the pressure hull plate:

$$W_p = \rho \pi DSL$$

The weight of the frame:

$$W_f = \pi w D \frac{L}{\ell}$$

here: ρ = Density of steel material
 w = Weight of angle section per meter.

On putting L = one meter, both formulae will give the weight per unit length.

The curve W in Figure 31 is the sum of these W_p and W_f .

4. Curve of lethal radius: The lethal radius can be obtained by the formula shown in Chapter VI, Section C using the relation between S and ℓ described above. For example, the curve d was drawn for the lethal radius when the charge weight was 150 kg.

After obtaining all the curves in Figure 31 in this manner, the following can be examined:

The dimension for which the weight may be least is (1) $\ell = 320$, $S = 14$ and (2) $\ell = 635$, $S = 16$. The former is slightly better than the latter against statical pressure, but far worse against explosive pressure. Moreover, considering the method of construction, the latter is thought more adequate. In addition, the case of $\ell = 960$, $S = 18$ may be worth considering because of the increase in resistance to explosion, with only a small increase in weight.

G. Conclusions

In applying the result of the cylindrical model tests to actual submarine construction, the method of calculating the lethal radius of submarine for the depth charge was obtained.

Having determined the relation between static strength and lethal radius, a method was found for designing a pressure hull to resist depth charge attack. It should be noted that the frame spacing has no effect on resistance to depth charges.

CHAPTER VII PROPOSALS FOR INCREASING THE POWER OF DEPTH CHARGES

Damage depends on the duration of the shockwave or rather on peak pressure and duration. Improvement can result by increasing either of these or both.

In general, an increase in peak pressure increases sensitiveness and decreases the stability of the explosive. It is proposed that an explosive be found with increased duration. The writer not being an expert on explosives is unable to discuss further details, but feels that an explosive with a slower rate of detonation might be useful provided the peak pressure is maintained.

Figure 10 shows the peak pressure which will cause the same damage with varying durations of wave.

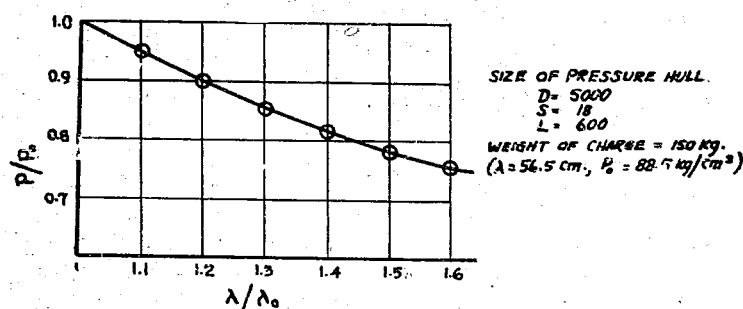


Figure 10
PEAK PRESSURE VS. WAVE DURATION

CHAPTER VIII CONCLUSIONS

The required conditions for the performance of a pressure gauge were determined from the theoretical study of the strength of a submarine pressure hull.

This research related the pressure formed to the weight of the charge.

The momentary change of elastic displacement in the case of a structure subjected to explosive pressure depends on the duration of the impulse and the period of natural vibration of the structure. As a simple example of this, the precise readings of the copper crusher gauge as described above were recorded.

The simple theory or crusher gauge readings have been expanded experimentally to the calculation of critical strength of thin cylindrical shells. The method of calculating critical strength was determined by first obtaining the correction factor due to the relationship of the damage to the size of the cylinder and wave length of the explosion.

This theory was expanded to the pressure hull of a submarine and the lethal radius calculated which compared reasonably with full scale tests done previously.

The correct materials for the construction of the pressure hull were determined after relating the statical collapsing pressure to the critical pressure in explosion.

From the knowledge gained, improvements for future depth charges are recommended.

APPENDIX I

PROPAGATION OF UNDERWATER EXPLOSION PRESSURE WAVE

On firing an underwater charge, a certain pressure (P_0) is generated which propagates spherically. The problem should be approached as follows:

"What is the pressure at any point at time t ?"

The initial condition being that there exists uniform condensation S_0 inside the sphere and $S = 0$ outside the sphere at the time $t = 0$, then

$$c^2 = \frac{K}{\rho_0} = \left[\frac{dP}{d\rho} \right]_{P=P_0}$$

where: P = Pressure at a point at time t
 K = Bulk modulus of water
 S = Degree of condensation
 C = Propagation velocity of underwater sound wave
 ρ_0 = Density of water at statical condition

$$K = \left[\rho \frac{dP}{d\rho} \right]_{P=P_0}$$

$$S = \frac{\rho - \rho_0}{\rho_0}$$

By the formula of elasticity

$$P = KS \dots \dots \dots (1)$$

The equation of motion for the sound wave is

$$\begin{aligned} \rho_0 \frac{\partial \mu}{\partial t} &= - \frac{\partial P}{\partial X} \\ \rho_0 \frac{\partial v}{\partial t} &= - \frac{\partial P}{\partial Y} \\ \rho_0 \frac{\partial w}{\partial t} &= - \frac{\partial P}{\partial Z} \end{aligned} \dots \dots \dots (2)$$

Denoting the velocity potential by ϕ

$$\begin{aligned} \mu &= - \frac{\partial \phi}{\partial X} \\ v &= - \frac{\partial \phi}{\partial Y} \\ w &= - \frac{\partial \phi}{\partial Z} \end{aligned} \dots \dots \dots (3)$$

Also by formula (2)

$$\phi = C^2 \int_0^t S \, dt + \phi_0 \dots \dots \dots (4)$$

The equation of continuity is

$$\frac{\partial S}{\partial t} = - \left(\frac{\partial \mu}{\partial X} + \frac{\partial v}{\partial Y} + \frac{\partial w}{\partial Z} \right) \dots \dots \dots (5)$$

Putting the formulas (3) and (4) into this

$$\frac{\partial^2 \phi}{\partial t^2} = C^2 \left(\frac{\partial^2 \phi}{\partial X^2} + \frac{\partial^2 \phi}{\partial Y^2} + \frac{\partial^2 \phi}{\partial Z^2} \right) = C^2 \nabla^2 \phi \quad \dots\dots\dots (6)$$

Since the phenomenon is symmetrical about the origin, formula (6) may be written as follows:

$$\frac{\partial^2}{\partial t^2} (\gamma \phi) = C^2 \frac{\partial^2}{\partial \gamma^2} (\gamma \phi) \quad \dots\dots\dots (7)$$

Here

$$\gamma = \sqrt{X^2 + Y^2 + Z^2}$$

the general solution of equation (7) has the form

$$\gamma \phi = f(ct - \gamma) + F(ct + \gamma) \quad \dots\dots\dots (8)$$

Since there is no source at the origin $\gamma = 0$

$$\lim_{\gamma \rightarrow 0} \left(-\frac{\partial \phi}{\partial \gamma} \gamma^2 \right) = 0$$

Consequently it is necessary

$$f(ct) + F(ct) = 0$$

Using this we can write formula (8) as follows:

$$\gamma \phi = F(ct + \gamma) - F(ct - \gamma) \quad \dots\dots\dots (9)$$

Since $\phi = 0$ at $t = 0$, by formula (9)

$$F(\gamma) - F(-\gamma) = 0$$

or

$$\begin{aligned} F(\gamma) &= F(-\gamma) \\ F'(\gamma) &= -F'(-\gamma) \end{aligned}$$

and next by formula (9)

$$\begin{aligned} S &= \frac{1}{c^2} \frac{\partial \phi}{\partial t} = \frac{1}{\gamma c^2} [CF' (ct + \gamma) - CF' (ct - \gamma)] \\ &= \frac{1}{\gamma c} [F' (ct + \gamma) - F' (ct - \gamma)] \quad \dots\dots\dots (10) \end{aligned}$$

also

$$\left. \begin{aligned} S &= S_0, \gamma < a \\ S &= 0, \gamma > a \end{aligned} \right\} \quad \text{at } t = 0.$$

Therefore, by formula (10)

$$\begin{aligned} S &= \frac{1}{\gamma c} [F'(\gamma) - F'(-\gamma)] = \frac{2F'(\gamma)}{\gamma c} = S_0, \gamma < a \\ S &= \frac{1}{\gamma c} [F'(\gamma) - F'(-\gamma)] = \frac{2F'(\gamma)}{\gamma c} - 0, \gamma > a \end{aligned}$$

$$\left. \begin{aligned} F'(\gamma) &= \frac{S_0}{2} \gamma c, \gamma < a \\ F'(\gamma) &= 0, \gamma > a \end{aligned} \right\} \quad \dots\dots\dots (11)$$

substituting to equation (10)

$S = 0$ ----- for other values of ct except those listed below.

$$S = \frac{S_0}{2\gamma} (\gamma - ct); (\gamma - a) < ct < \gamma$$

$$S = \frac{S_0}{2\gamma} (\gamma - ct); \gamma < ct < (\gamma + a)$$

.. (12)

As $P = KS$, we obtain the value of p at any time t , which is shown graphically as follows:

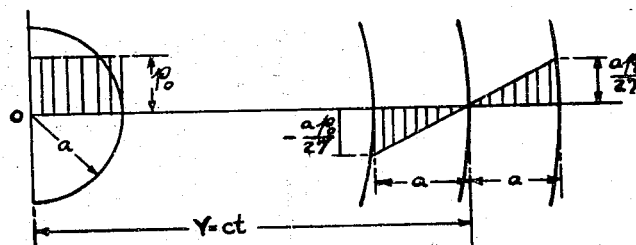


Figure 11
SAW-TOOTH EXPLOSION WAVE

Thus the pressure P_0 expands as a spherical wave which consists of positive and negative pressure $\pm a P_0 / 2\gamma$, respectively.

APPENDIX II

UNDERWATER PRESSURE GAUGES

A. Quartz Pressure Gauges

1. GIKEN Type A receiver (Figure 32): This gauge has a receiver made of quartz cut to generate piezo-electricity. In Figure 32, Q_1 , Q_2 are the quartz crystals, cut along the plane normal to the electric axis. They are 25mm in diameter and 10mm thick. Each is plated with silver on both plane surfaces. The two pieces lie against each other with opposite polarities touching. They are separated by a circular sheet of aluminum foil ($d = 25\text{mm}$ and $t = 0.5\text{mm}$). This foil is insulated from the earth and the opposite surfaces are connected with the earth.

M is a finished steel holder designed for quick removal. B is an insulating material of beeswax and pine resin which insulates the quartz and fixes it to the steel holder. D is a covering piece protecting the insulation from the explosion. C_1 is a thin wire connected to the aluminum foil and has amberoid insulators as well as normal insulation. It leads the piezo voltage to the feeder line C_2 . This is shielded by a steel pipe (SP) 35mm in diameter and three meters long which takes the feeder line to the surface of the water. P is a waterproof packing.

The receiver is also fixed by bolts to a large iron weight when in use. (See Figure 35.)

The feature of this receiver is the amplifier used to raise the natural frequency. One surface only of the quartz is exposed to the water, the other beams directly on the finely ground surface of the holder. This device does not use a plunger on the receiving surface as a means of fixing, such as steel balls and springs, in order to maintain its high natural frequency.

On the other hand reflection and transparency at the boundary may affect this gauge. The edge of the quartz surface has to be carefully packed with wax and pine resin.

2. GIKEN Type B receiver (Figure 33): The quartz unit is 5mm in diameter and 5mm thick. The two pieces are oriented on top of one another in series with both surfaces exposed to the water. The lead wires are water-proofed with wax in the same manner as Type A. (See Figure 33.)

The quartz unit receives the pressure wave simultaneously on both surfaces. It has a natural resonant frequency of 270 kilocycles and a flat response curve to pressure waves acting on it. Since the receiving surface of the crystal unit is parallel to the direction of the propagated pressure wave, there is no reflection from the receiving surface. The value recorded by the crystal unit is the mean value of the pressure wave striking the receiving surface at any one instant, but this inaccuracy is negligible and may be ignored, because the receiving surface is only one fourteenth of the pressure wave caused by a 1.7 kg charge. The chief value of this unit is that it is small, light and simple to operate.

B. First Amplifier (Figure 34)

In the first stage there is a UX-54, in the second stage a "Phillips" 615 and in the third stage six UX-171 tubes are used in parallel. Since the UX-54 has a high input impedance, it is used to measure small changes in current and as an amplifier for piezo-electricity measurement. It does have a low trans-

conductance and poor frequency characteristics. There are six UX-171 tubes connected in parallel in the third stage as a final amplifier. The terminal voltage is decreased to lower the static capacity of the inter-amplifier coupling. The plate or load resistance is decreased as much as possible to improve the frequency characteristics by lowering the mutual capacitance.

The plate supply of the last stage is placed on the plate side of the load resistor, since one deflection plate of the cathode ray oscilloscope is grounded. For that reason each amplifier requires its own power supply.

C is the tuning capacitor connected in parallel with the quartz unit. This capacitor has to have a very high insulating resistance (TN: high Q) to match the properties of the quartz unit. It is made from waxed copper plates set in "micadon" (insulator).

C. Second Amplifier (Figure 34)

The function of the second amplifier is to amplify the voltage from the first amplifier to a point necessary to operate the cathode ray oscilloscope. The two stages are made up from a UY-76 and a UY-47B. Although the UY-47B draws a large plate current, nothing better could be found for the purpose.

The plate supply batteries are connected in the same way as in the first amplifier. The output is connected to the oscilloscope. One side of the amplifier is grounded while the other side is connected to the intermediate terminal on the plate supply battery in order to counteract the DC voltage drop across the load resistor, and thereby centering the image of the oscilloscope. The power supply is furnished by a battery similar to the one in the first amplifier.

D. Cathode Ray Type Oscilloscope

This oscilloscope was made by the TOKYO DENKI. Characteristics are as follows:

Type	BG-140-V
Total length of tube	535mm
Maximum diameter	14.0mm
Fluorescence substance	zinc silicate
Filament voltage	2.5 v
Filament current	2.1 amps
No 2 anode	maximum, 5000 v
Grid	negative

APPENDIX III

APPROXIMATE CALCULATION OF THE FLEXURAL VIBRATION OF
A THIN CYLINDRICAL SHELL SUPPORTED ON BOTH ENDS

Determining notations as follows:

D = Diameter of cylindrical shell
S = Thickness
L = Unsupported length

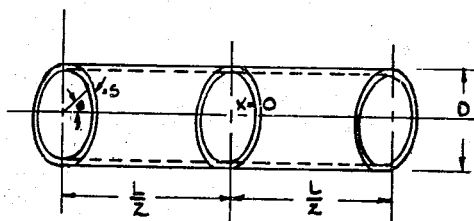


Figure 12
THIN CYLINDER WITH END SUPPORT

and assuming a solution of the form -

$$\begin{aligned} u &= u \sin mx \sin n \theta \cos (pt + \epsilon) \\ v &= v \cos mx \cos n \theta \cos (pt + \epsilon) \\ w &= w \cos mx \sin n \theta \cos (pt + \epsilon) \end{aligned}$$

where $m = \frac{\mu \pi}{L}$ and $\mu = 1, 3, 5, \dots$

u = Axial displacement of an element
v = Peripheral displacement of an element
w = Radial displacement of an element

For end conditions, $v = w = 0$ at $x = \pm \frac{L}{2}$ and the equation of motion of the elements is as follows:

$$\begin{aligned} & - \left\{ m^2 + \frac{1-\sigma}{2} \frac{n^2}{\left(\frac{D}{2}\right)^2} - \frac{\rho S}{c} p^2 \right\} U + \left\{ \frac{\sigma}{\left(\frac{D}{2}\right)} mn + \frac{1-\sigma}{D} mn + \frac{1-\sigma}{6} \frac{\left(\frac{S}{2}\right)^2}{\left(\frac{D}{2}\right)^3} mn \right\} V \\ & + \left\{ \frac{\sigma}{\left(\frac{D}{2}\right)} m + \frac{1-\sigma}{6} \frac{\left(\frac{S}{2}\right)^2}{\left(\frac{D}{2}\right)^3} mn^2 \right\} w = 0 \\ & \left\{ \frac{1-\sigma}{2} \frac{mn}{\left(\frac{D}{2}\right)} + \frac{\sigma}{\left(\frac{D}{2}\right)} mn \right\} U - \left\{ \frac{1-\sigma}{2} m^2 + \frac{n^2}{\left(\frac{D}{2}\right)^2} + \frac{1-\sigma}{2} \frac{\left(\frac{S}{2}\right)^2}{3\left(\frac{D}{2}\right)^2} m^2 + 1/3 \frac{\left(\frac{S}{2}\right)^2}{\left(\frac{D}{2}\right)^4} n^2 - \frac{\rho S}{c} p^2 \right\} V \end{aligned}$$

$$\begin{aligned}
& - \left\{ \frac{n}{\left(\frac{D}{2}\right)^2} + \frac{1-\sigma}{2} \frac{\left(\frac{S}{2}\right)^2}{\left(\frac{D}{2}\right)^2} m^2 n + \frac{n^3}{3} \frac{\left(\frac{S}{2}\right)^2}{\left(\frac{D}{2}\right)^4} + \frac{\sigma}{3} m^2 n \frac{\left(\frac{S}{2}\right)^2}{\left(\frac{D}{2}\right)^2} \right\} W = 0 \\
& \frac{\sigma}{\left(\frac{D}{2}\right)} m U - \left\{ \frac{\sigma}{3} \frac{\left(\frac{S}{2}\right)^2}{\left(\frac{D}{2}\right)^2} m^2 n + \frac{2(1-\sigma)}{3} \frac{\left(\frac{S}{2}\right)^2}{\left(\frac{D}{2}\right)^2} m^2 n + \frac{1}{3} \frac{\left(\frac{S}{2}\right)^2}{\left(\frac{D}{2}\right)^4} n^3 + \frac{n}{\left(\frac{D}{2}\right)^2} \right\} V \\
& - \left\{ \frac{1}{3} \frac{\left(\frac{S}{2}\right)^2}{\left(\frac{D}{2}\right)^2} m^4 + \frac{\sigma}{3} \frac{\left(\frac{S}{2}\right)^2}{\left(\frac{D}{2}\right)^2} m^2 n^2 + \frac{2}{3} (1-\sigma) \frac{\left(\frac{S}{2}\right)^2}{\left(\frac{D}{2}\right)^2} m^2 n^2 + \frac{\sigma}{3} \frac{\left(\frac{S}{2}\right)^2}{\left(\frac{D}{2}\right)^2} m^2 n^2 \right. \\
& \left. + \frac{1}{3} \frac{\left(\frac{S}{2}\right)^2}{\left(\frac{D}{2}\right)^4} n^4 + \frac{1}{\left(\frac{D}{2}\right)^2} - \frac{\rho S}{c} p^2 \right\} W = 0
\end{aligned}$$

where: $c = \frac{ES}{1-\sigma^2}$

ρ = Density of material
 σ = Poisson's ratio
 E = Young's modulus

The determinant for each coefficient must be zero so that the simultaneous equation above is satisfied. Therefore, we obtain a third order equation for p^2 . Simplifying the calculation by neglecting U and V , we obtain the following equation for p .

$$-\frac{\rho S}{c} p^2 + \left(\frac{D}{2}\right)^2 m^4 \xi + 2m^2 n^2 \xi + \frac{n^4}{\left(\frac{D}{2}\right)^2} \xi + \frac{1}{\left(\frac{D}{2}\right)^2} = 0$$

$$\xi = \frac{S^2}{3D^2}$$

where:

Now take the solution

$$p^2 = \frac{E}{\rho(1-\sigma^2)} \frac{1}{\left(\frac{D}{2}\right)^2} \left[1 + \frac{S^2}{3D^2} \left\{ \left(\frac{D}{2}\right)^2 m^2 + n^2 \right\}^2 \right]$$

and put

$$\left(\frac{D}{2}\right)^2 m^2 = \left(\frac{\mu \pi D}{2L}\right)^2 = \alpha^2$$

From this we obtain

$$p^2 = \frac{4E}{\rho(1-\sigma^2) D^2} + \frac{4E}{3\rho(1-\sigma^2)} \frac{S^2}{D^4} (\alpha^2 + n^2)^2$$

In the equation above, the first term shows the extensional vibration and the second term the flexural vibration. As S/D is very small we consider the flexural vibration only, thus

$$p^2 = \frac{4E}{3\rho(1-\sigma^2)} \frac{S^2}{D^4} (\alpha^2 + n^2)^2$$

and the expression for frequency is.

$$fn = \frac{1}{\pi} \sqrt{\frac{E}{30(1 - \sigma^2)}} \frac{S}{D^2} (\alpha^2 + n^2)$$

where:

$$\alpha = \frac{\mu \pi D}{2L} \text{ and } \mu = 1, 3, 5, \dots$$

In this equation n is the number of lobes and μ is the number of half wave lengths in the axial direction.

APPENDIX IV
TABLES AND ILLUSTRATIONS

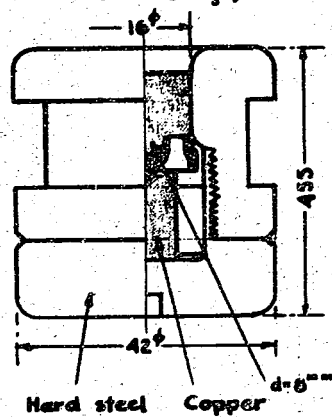
Table VIII
RESULTS OF MEASUREMENTS OF PRESSURES IN UNDERWATER EXPLOSIONS

Pressure Gauge	Wt. of Charge (kg)	Distance (m)	Depth (m)	Temp. of Water (°C)	Frequency (cycles/sec)	Amplitude on Cathode Ray Tube (mm)	Pressure (kg/cm)
Type A	0.4	2.0	1.2	6	14,000	21.0	390
		2.0		17	16,000	24.0	408
		2.0		17	14,000	25.0	416
		3.0		8	17,000	45.6	235
		5.0		8	14,000	26.5	133
		7.0		8	12,000	12.0	92
		7.0		7	13,000	18.0	98
		7.0		7	14,000	34.8	104
		10.0		4	16,000	21.6	64
		10.0		4	14,000	23.5	69
		10.0		19	13,000	25.0	62
		10.0		20	12,000	22.5	62
Type B	1.7	3.0	2.0	16	10,000	30.0	474
		3.0		17	10,000	27.6	470
		5.0		12	10,000	21.0	266
		7.0		11	10,800	26.1	160
		7.0		11	10,000	26.0	160
		10.0		11	10,000	28.2	124
		10.0		16	10,000	24.6	114
		10.0		17	10,000	18.0	108
		9.0		18		6.0	52
		5.0		18		13.0	94
		5.0		18		14.0	98

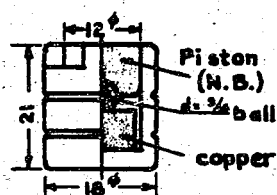
Table IX
PRINCIPAL DIMENSION OF COPPER CRUSHER GAUGE

Designation of Case	Bx	B	G	Y	Ry	Bs	Bs1
Wt. of piston and ball (gr)	8.5	4.29	1.71	20.0	7.0	6.0	3.9
Area receiving pressure (cm ²)	1.131	1.131	1.131	2.0	0.95	0.866	0.263
Dia. of ball (inches)	3/16	3/16	3/16	8.0mm	3/16	3/16	3/16
$\mu \left(\frac{\text{kg sec}^2}{\text{cm}} \right)$	8.67×10^6	4.38×10^6	1.75×10^6	20.4×10^6	7.14×10^6	6.12×10^6	3.96×10^6
Designation of copper (lead)	P1	P2	P3	P4	P5	P6	P7
$k \left(\frac{\text{kg}}{\text{cm}} \right)$	0.750×10^4	1.333×10^4	0.750×10^4	1.410×10^4	0.972×10^4	1.165×10^4	0.0776×10^4
Designation of copper (lead)	B x P1	BP1	GP1	B x P2	BP2	GP2	
$\omega_0 = \sqrt{\frac{k}{m}} \left(\frac{1}{\text{sec}} \right)$	2.94×10^4	4.14×10^4	6.56×10^4	3.92×10^4	5.52×10^4	8.73×10^4	
Designation of crusher gauge	B x P3	BP3	GP3	B x P4	BP4	GP4	
$\omega_0 = \sqrt{\frac{k}{m}} \left(\frac{1}{\text{sec}} \right)$	2.94×10^4	4.14×10^4	6.56×10^4	4.33×10^4	5.68×10^4	8.99×10^4	
Designation of crusher gauge	B x P5	BP5	GP5	YP6	BP7	BaP7	Bs1P7
$\omega_0 = \sqrt{\frac{k}{m}} \left(\frac{1}{\text{sec}} \right)$	3.35×10^4	4.71×10^4	7.46×10^4	2.39×10^4	1.04×10^4	1.13×10^4	1.41×10^4

Y Crusher Gauge

(YOKOSUKA Type Copper
Crusher Gauge)

Bx Crusher Gauge



B & G Crusher Gauge

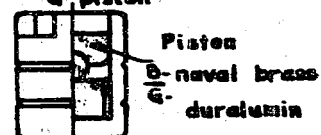
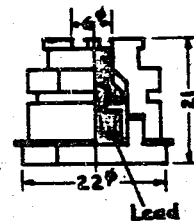
The same as Bx except
a pistonBy Crusher
GaugeBz Crusher
GaugeBz Crusher
Gauge

Figure 13
CONSTRUCTION OF CRUSHER GAUGES
(See Table IX.)

Table X
LIST OF SCANTLINGS AND THE STATICAL STRENGTH OF THE MODELS

Material of Model	Designation	Outer Dia. (cm ²)	Thickness of wall (cm)	Unsupported length (cm)	$\frac{D}{\lambda} \times 10^3$	$\frac{D}{\lambda}$	Statcal Strength Calculated (kg/cm ²)	n	Remarks
Brass	β_1	10.0	0.1	12.0	10	0.833	25.6	4	
	β_{II}	5.0	0.05	6.0	10	0.833	25.6	4	
	β_{III}	2.4	0.025	3.4	10.4	0.705	23.5	4	
	γ_1	10.0	0.05	12.0	5	0.833	4.5	6	
	γ_{II}	5.0	0.025	6.0	5	0.833	4.5	6	
	μ	10.0	0.1	5.0	10	2.0	48	7	
	μ^A	10.0	0.1	2.5	10	4.0	75	9	
	μ^H	10.0	0.1	1.25	10	8.0	105	9	
	ν	10.0	0.05	5.0	5	2.0	110	8	
	ν^A	10.0	0.05	2.5	5	4.0	18.6	11	
	ν^H	10.0	0.05	1.25	5	8.0	30.5	13	
	γ_{II}^H	20.0	0.1	20.0	5	1.0	5.0	6	
Mild steel	A	100	1.0	120	10	0.833	28.4	5	outer framing ∠ 60 x 50 x 7
	C	60	0.6	72	10	0.833	28.4	5	
	D	100	0.8	120	8	0.833	17.2	5	
	E	62.5	0.5	75	8	0.833	17.2	5	
	F	100	0.7	120	7	0.833	11.7	5	
	F (modified)	100	0.7	40	7	2.50	28.7	8	
	G	57.1	0.4	68.6	7	0.833	11.7	5	outer framing ∠ 40 x 20 x 3
	H	100	0.35	13.5	3.5	7.41	14.7	15	
	I	100	0.35	13.5	3.5	7.41	14.7	15	inner framing ∠ 40 x 20 x 3
	J	100	0.35	15.5	3.5	6.45	13.8	15	

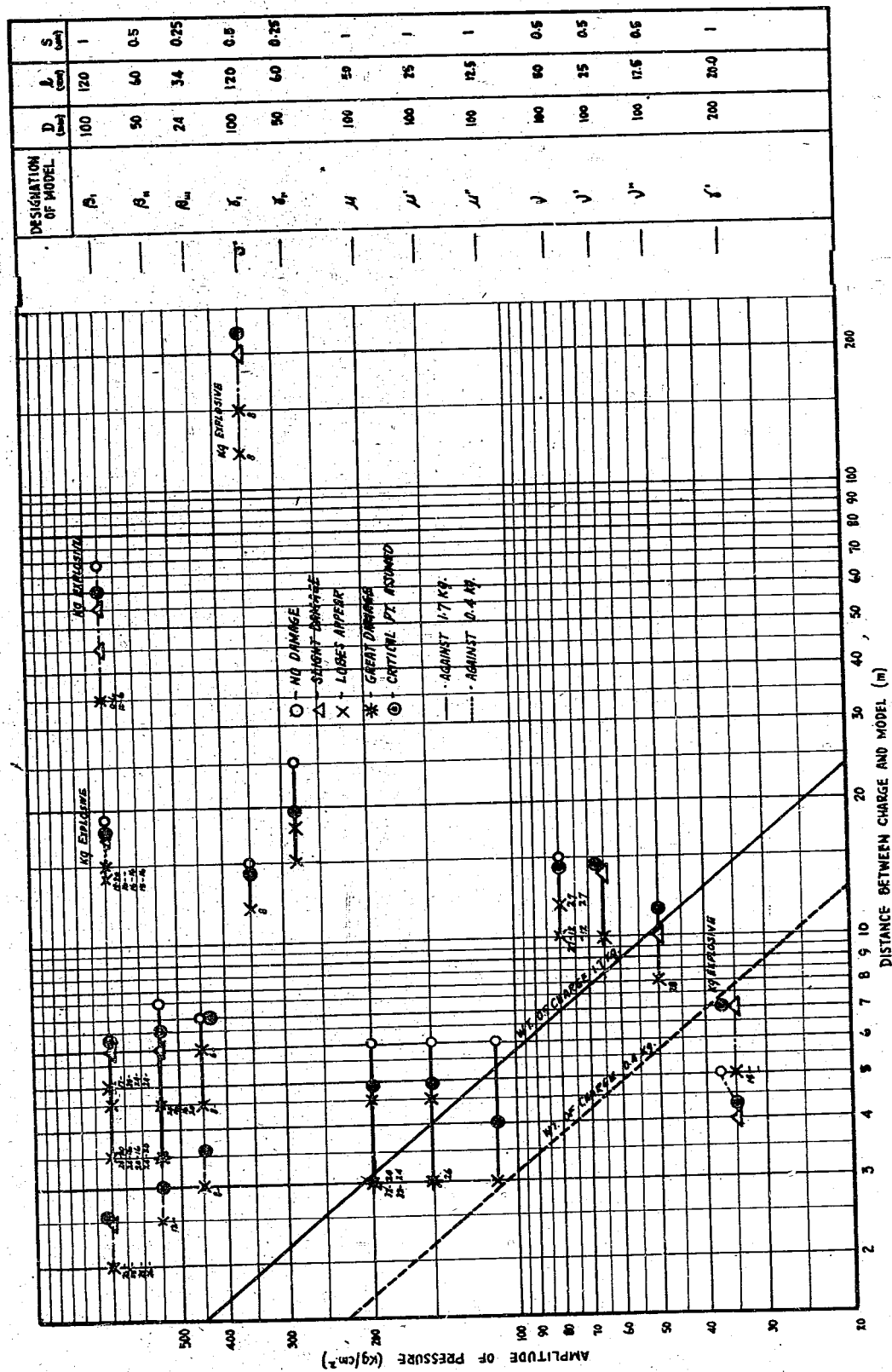


Figure 14
GRAPH SUMMARIZING RESULTS OF EXPERIMENTS WITH BRASS MODELS

Table XII
COMPARISON OF CALCULATED AND EXPERIMENTAL CRITICAL PRESSURES

Weight of Charge	Designation	Calculated Value				Experimental Value		$A = \frac{Q}{\lambda}$	D/λ	L/D
		n^* at X_{max}	X_{max}	Per (st) at n (kg/cm ²)	λ Per (st) (kg/cm ²)/ X	n	Q Per (dy) (kg/cm ²)			
0.4 kg P.A. (cast)	β_1	19	1.7667	257.5	145.8	26 25 25 26	125	0.858	0.935	1.20
	β_2	14	1.7684	156.4	88.4	12	105	1.188	0.467	1.20
	β_3	10	1.7653	90.3	51.2	8	85	1.660	0.224	1.42
	γ''	39	1.7684	150.3	85.0	?	69	0.812	1.869	1.00
	γ'	46	1.7684	1.060	899.4	20	250	0.417	5.336	1.20
0.8 kg P.A. (cast)	γ'	36	1.7684	128.1	72.4	14	55	0.760	1.600	1.00
18 kg P.A. (cast)	β_1	12	1.7645	114.6	64.9	18 16 16 15	65	1.002	0.360	1.20
400 kg Type 97 Explosive	β_1 γ'	8 11	1.7610 1.7656	52.3 12.1	29.7 6.85	6-10 8	46 11.6	1.549 1.693	0.128 0.128	1.20 1.20

* n = number of lobes

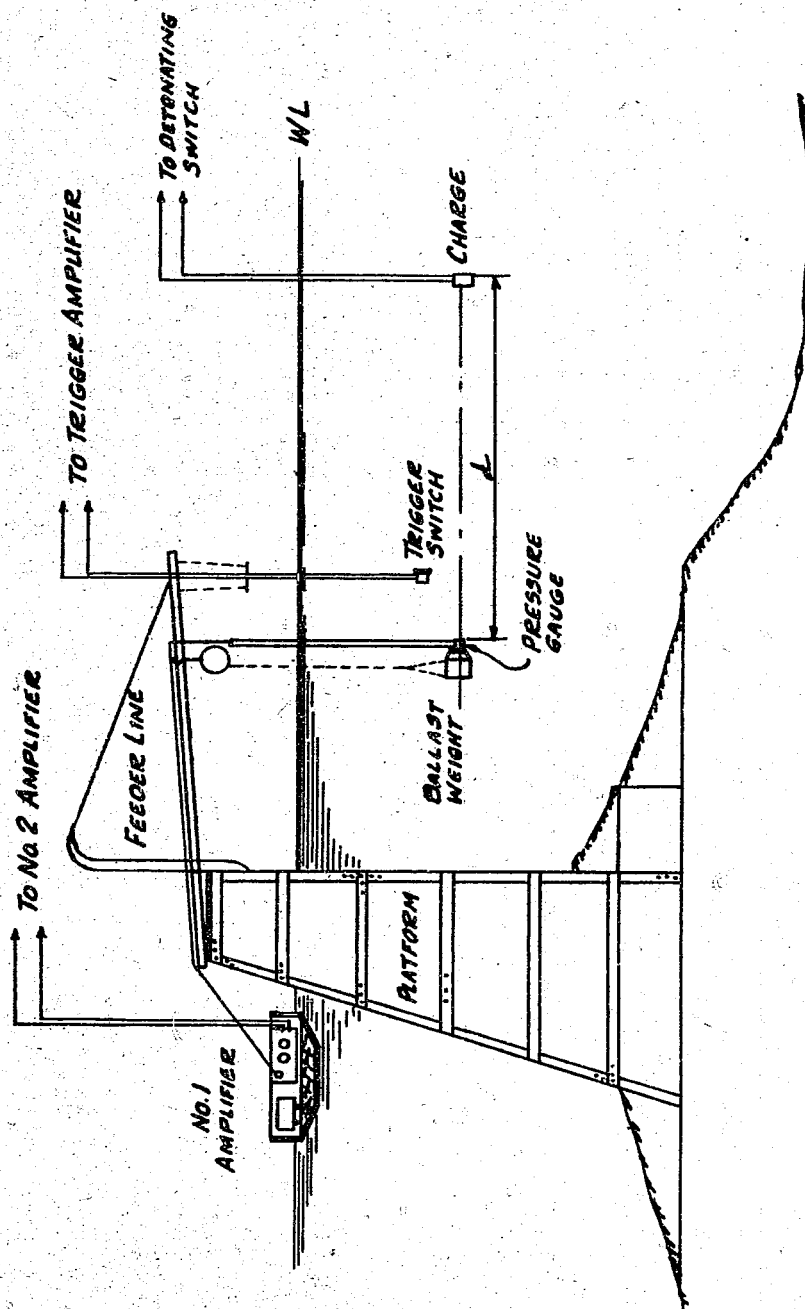


Figure 16
EXPERIMENTAL APPARATUS FOR UNDERWATER EXPLOSIONS

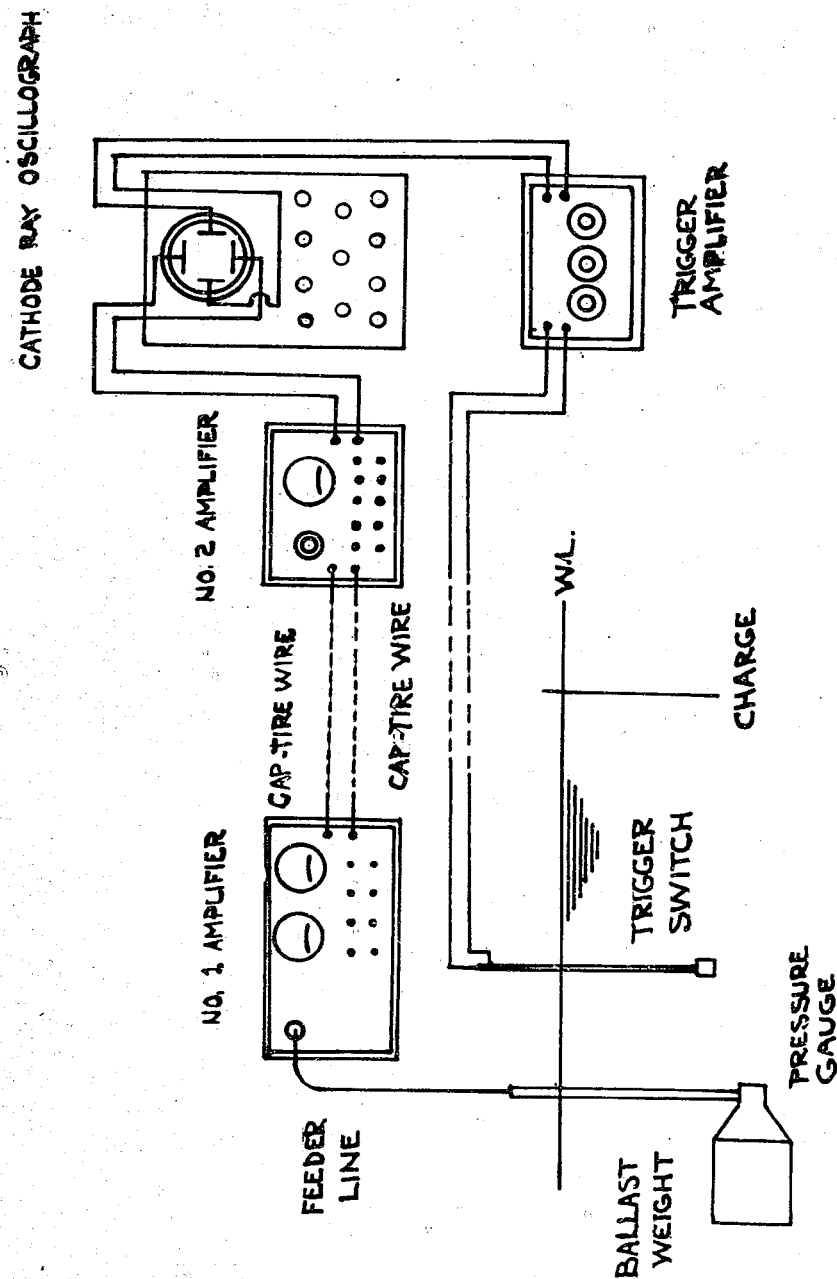
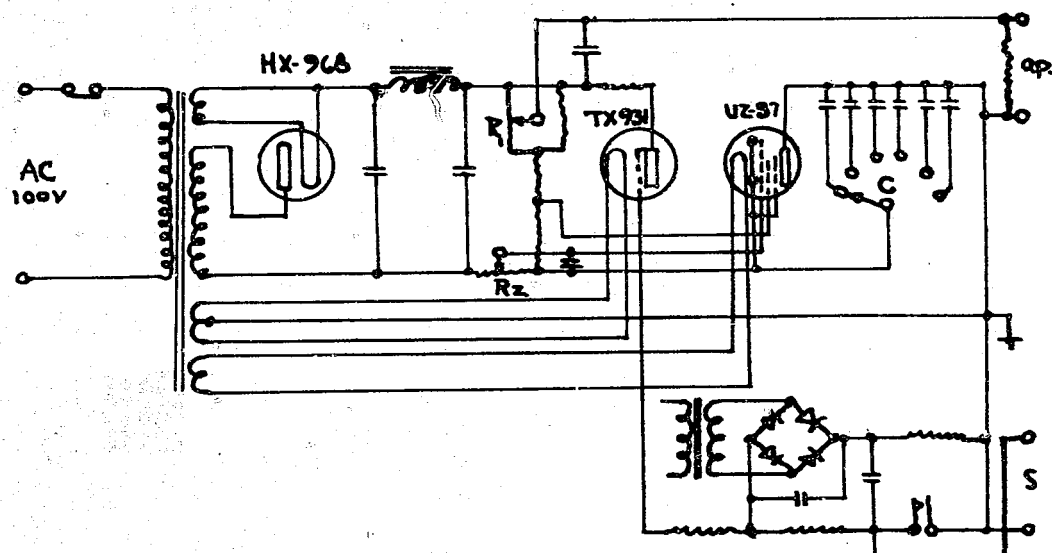


Figure 17
WIRING DIAGRAM FOR UNDERWATER EXPLOSION TEST APPARATUS



R₁-CONTROLS POSITION OF SPOT
 R₂-CONTROLS SPEED OF SWEEP
 C-CONTROLS LARGE CHANGES IN
 SPEED OF SWEEP
 S- TERMINALS TO TRIGGER SWITCH
 O.P- OUTPUT VOLTAGE

Figure 18
 TRIGGER AMPLIFIER CIRCUIT

T TERMINAL
R COPPER PLATE WHICH
RECEIVES EXPLOSION
PRESSURE
I INSULATOR
C LEAD WIRE
P STEEL PIPE

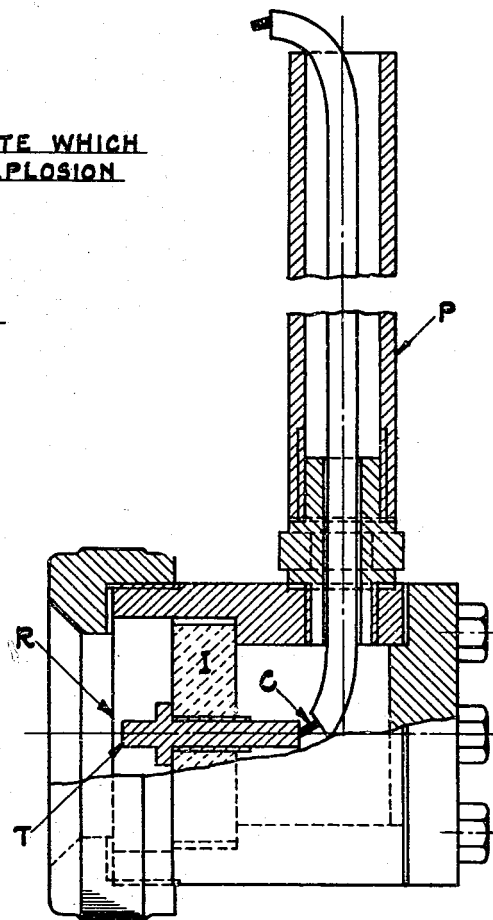


Figure 19
TRIGGER SWITCH

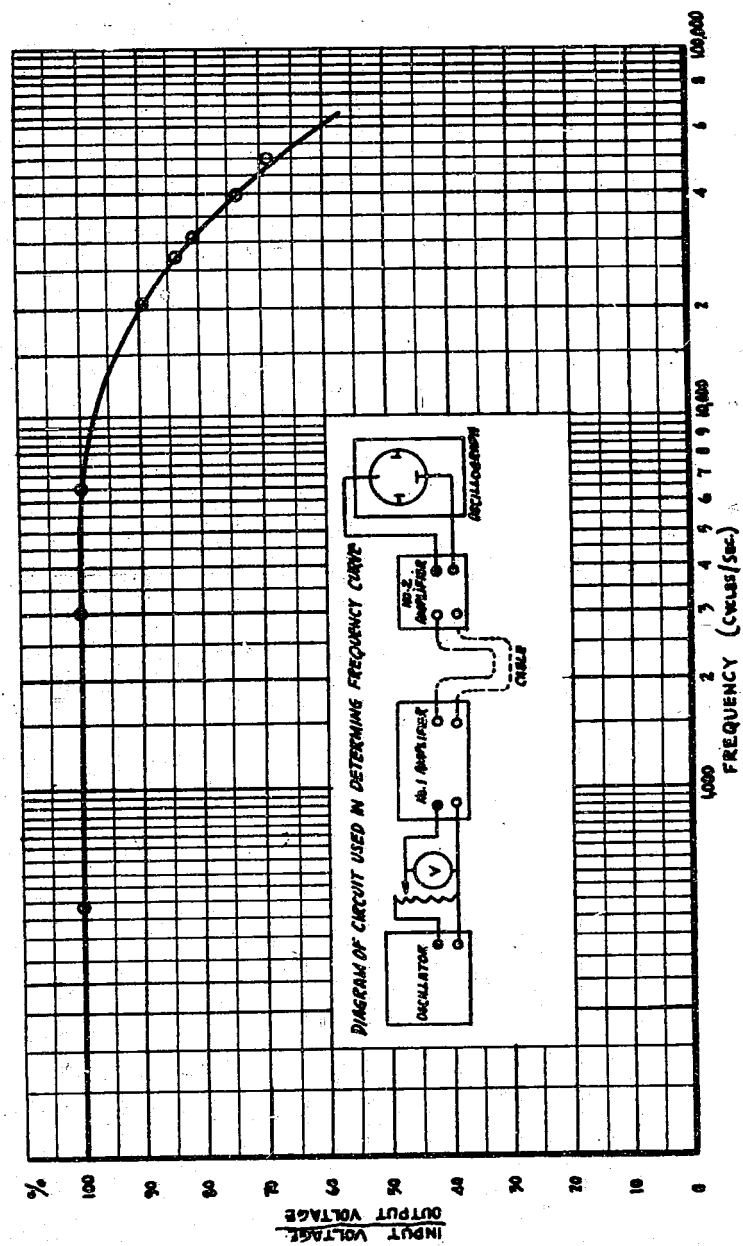


Figure 40
FREQUENCY CURVE OF AMPLIFIER

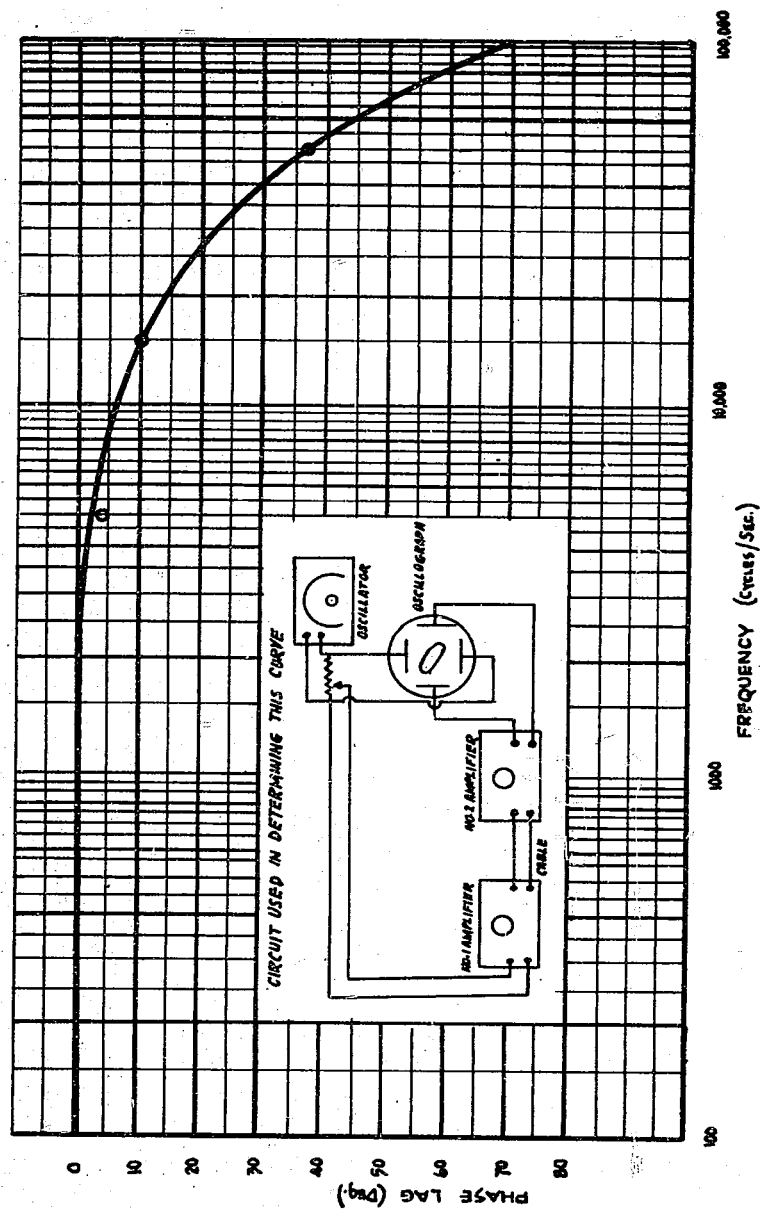


Figure 21
RELATIONSHIP BETWEEN FREQUENCY AND LAG

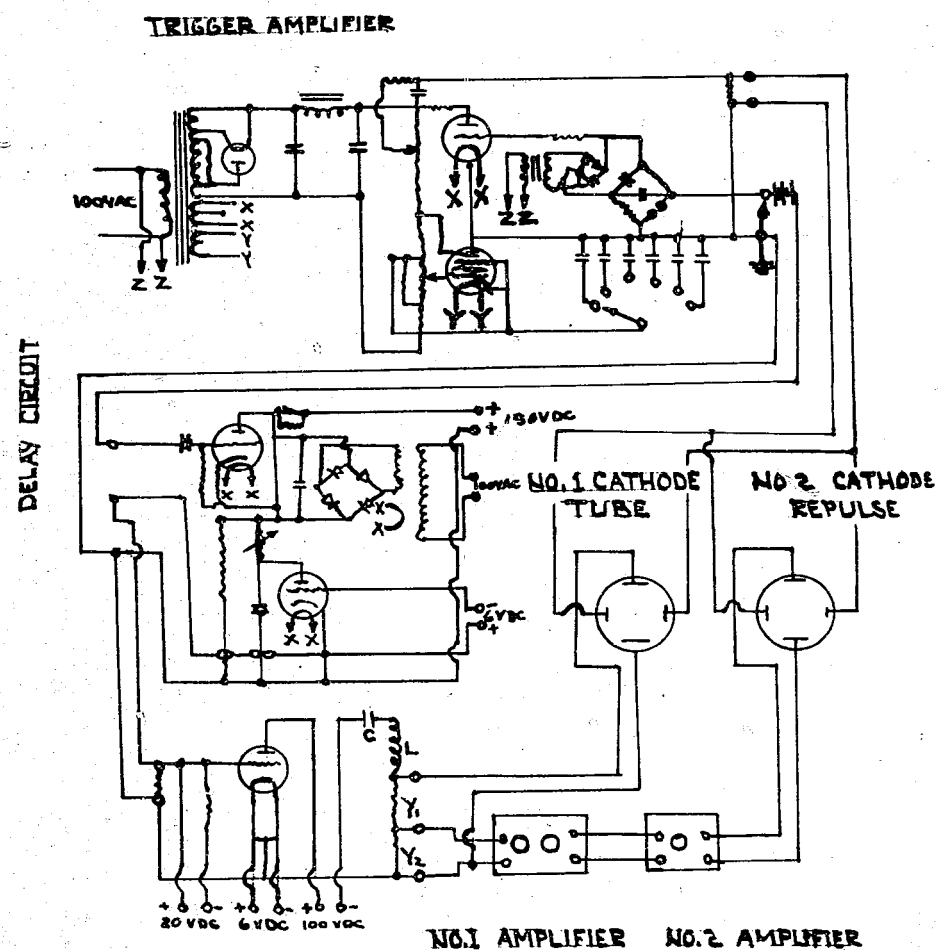


Figure 22
WIRING CIRCUIT OF ARTIFICIAL EXPLOSION SIGNAL GENERATOR

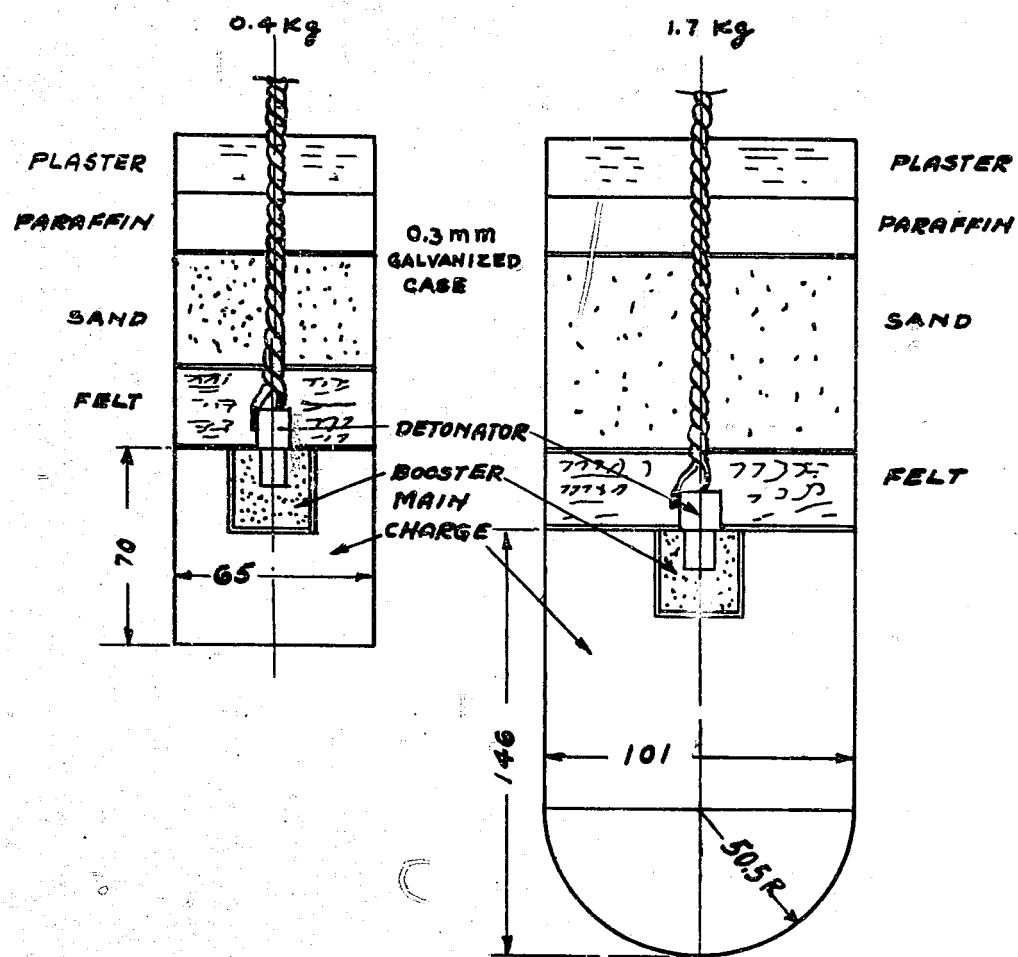


Figure 23
DIAGRAM OF EXPLOSIVE CHARGES

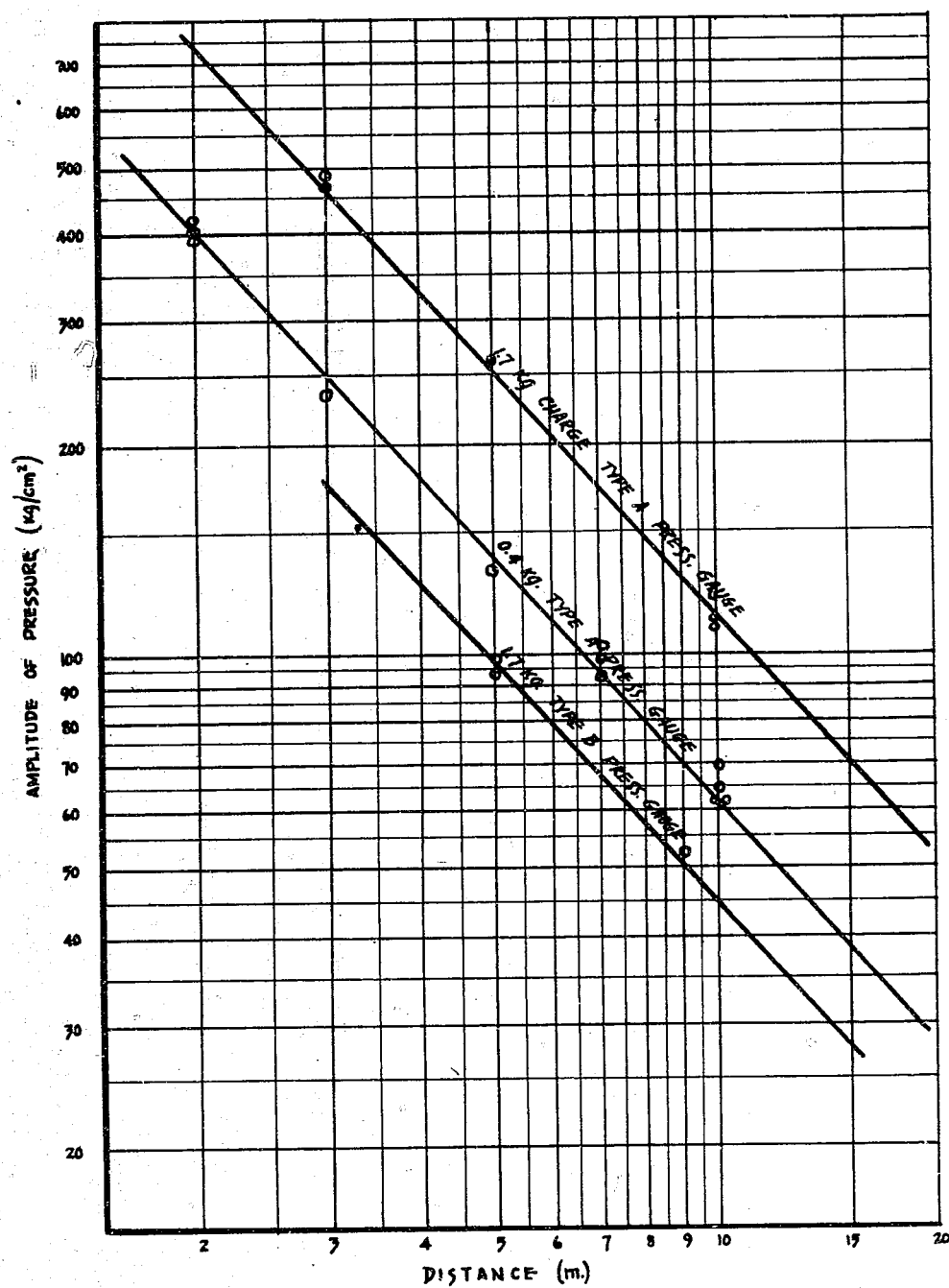


Figure 24
PRESSURE DAMPING CURVE

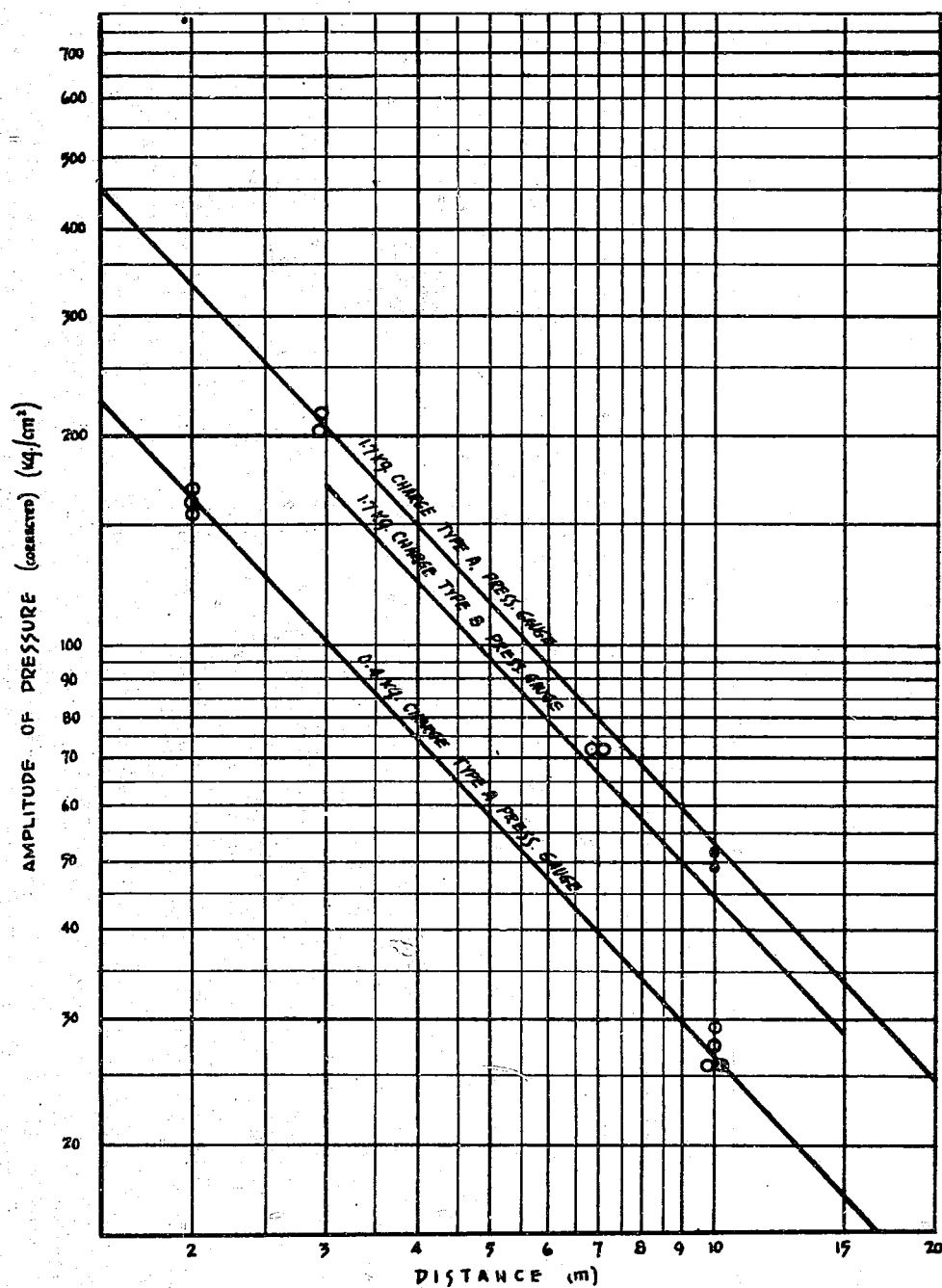


Figure 25
PRESSURE DAMPING CURVE

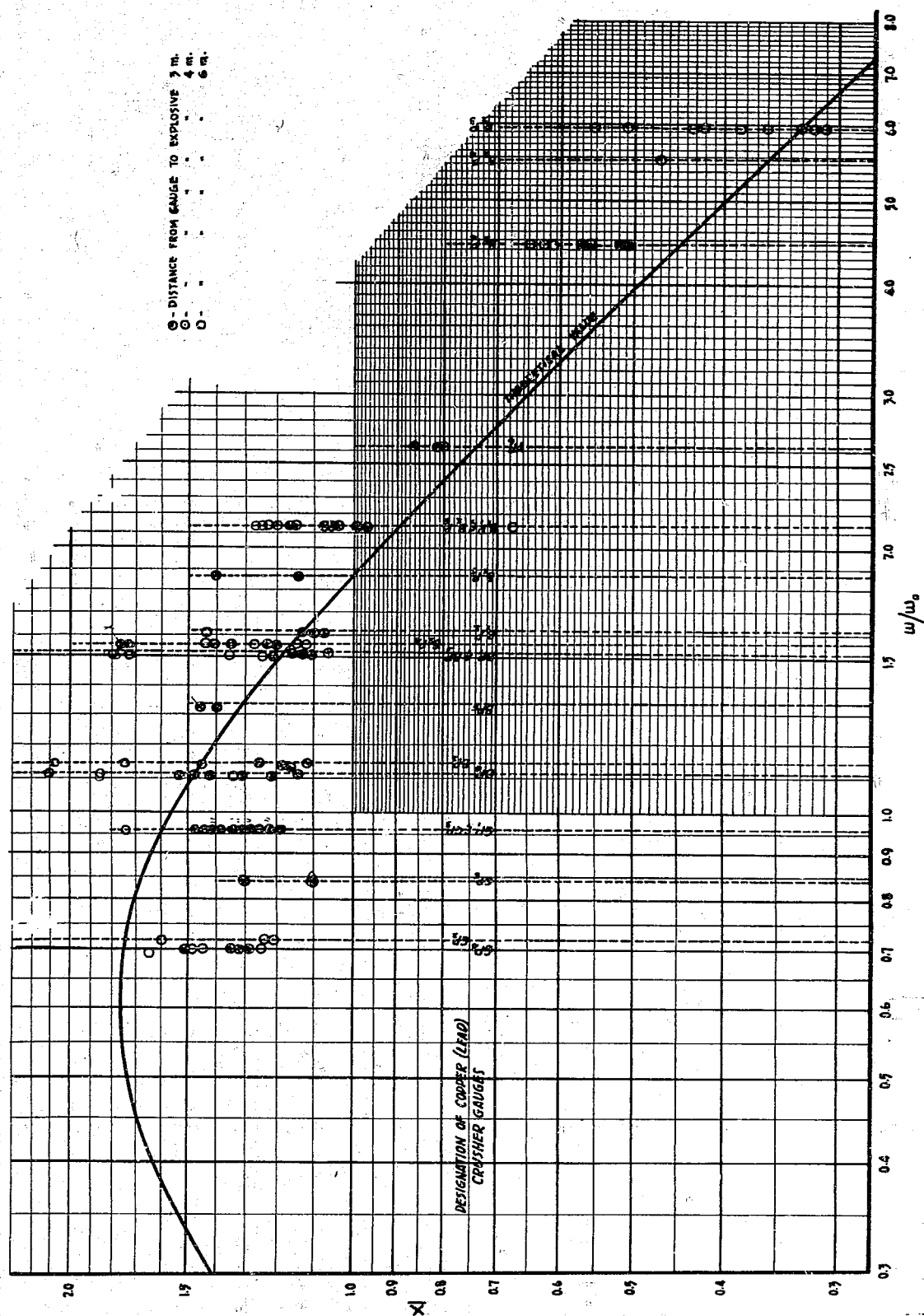


Figure 26
GRAPH OF X vs. w/w_0

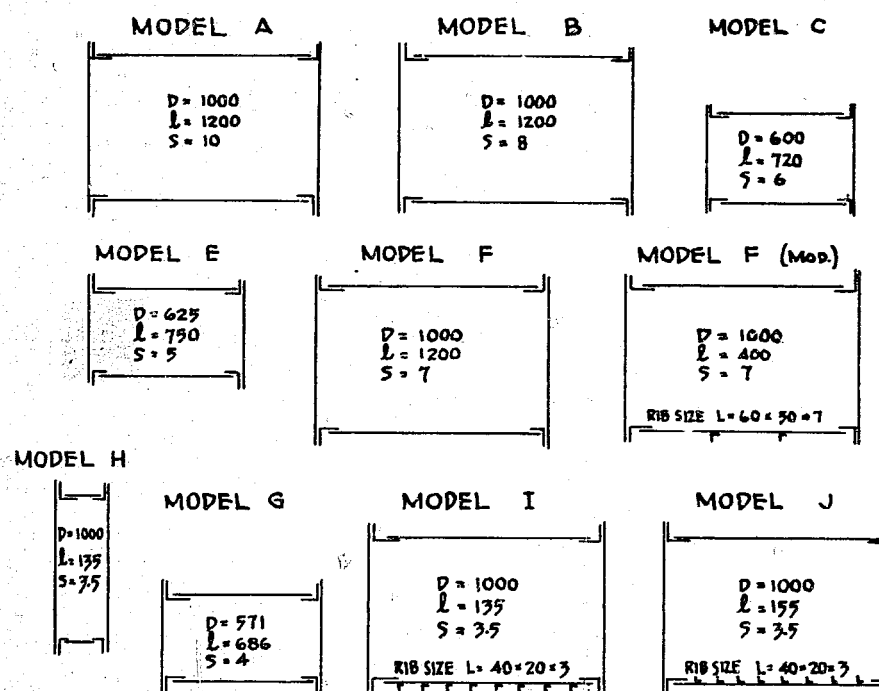
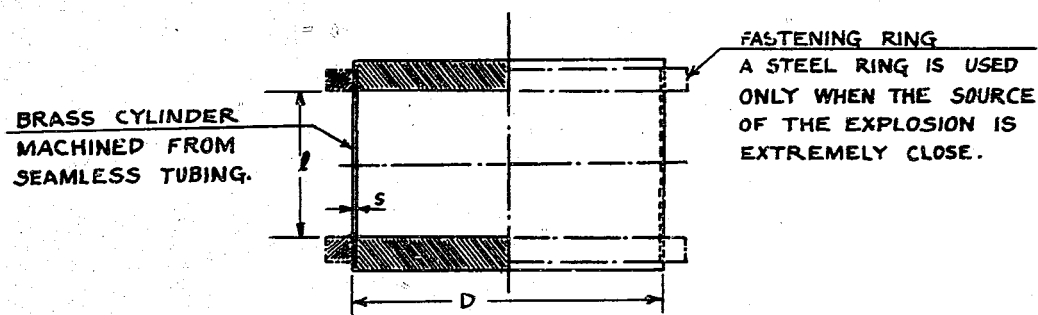


Figure 27
CONSTRUCTION OF BRASS AND MILD STEEL MODELS

MILD STEEL MODELS				BRASS MODELS			
MARK	D (mm)	S (mm)	L (mm)	MARK	D (mm)	S (mm)	L (mm)
A	1000	10	1200	A ₁	100	1.0	120
D	1000	8	1200	A ₁₁	50	0.5	60
F	1000	7	1200	A ₁₂	24	0.25	34
G	571	4	684	A ₁₃	100	0.5	120
H	1000	3.5	135	A ₁₄	50	0.25	60
J	1000	3.5	155	A ₁₅	100	1.0	90
				A ₁₆	100	1.0	25
				A ₁₇	100	1.0	12.5
				V	100	0.5	50
				V ₁	100	0.5	25
				V ₁₂	100	0.5	12.5

O 1/2 kg. Charge
 ● 0.4 " "
 ○ 0.8 " "
 △ 1B " "
 □ 400 " "

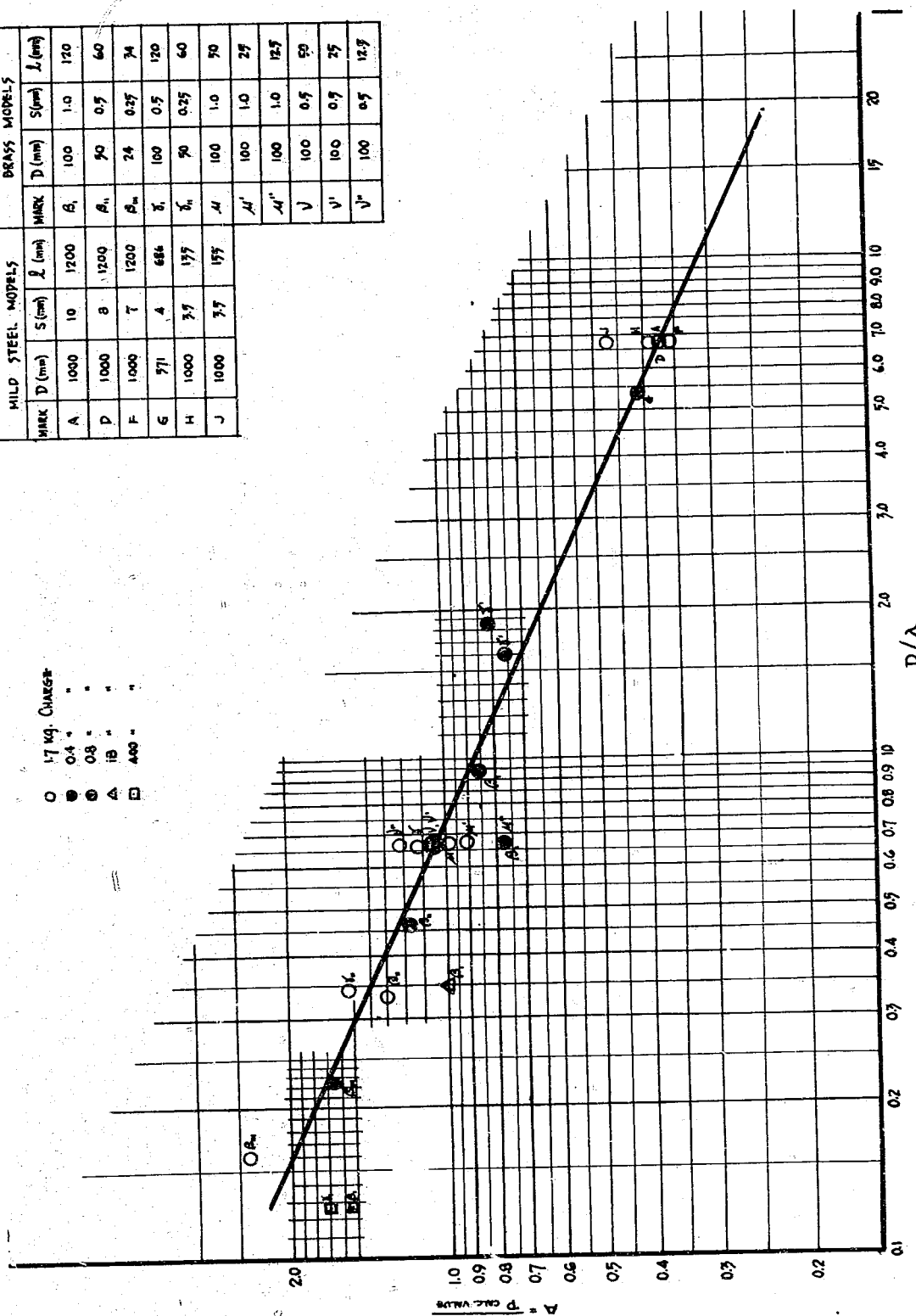
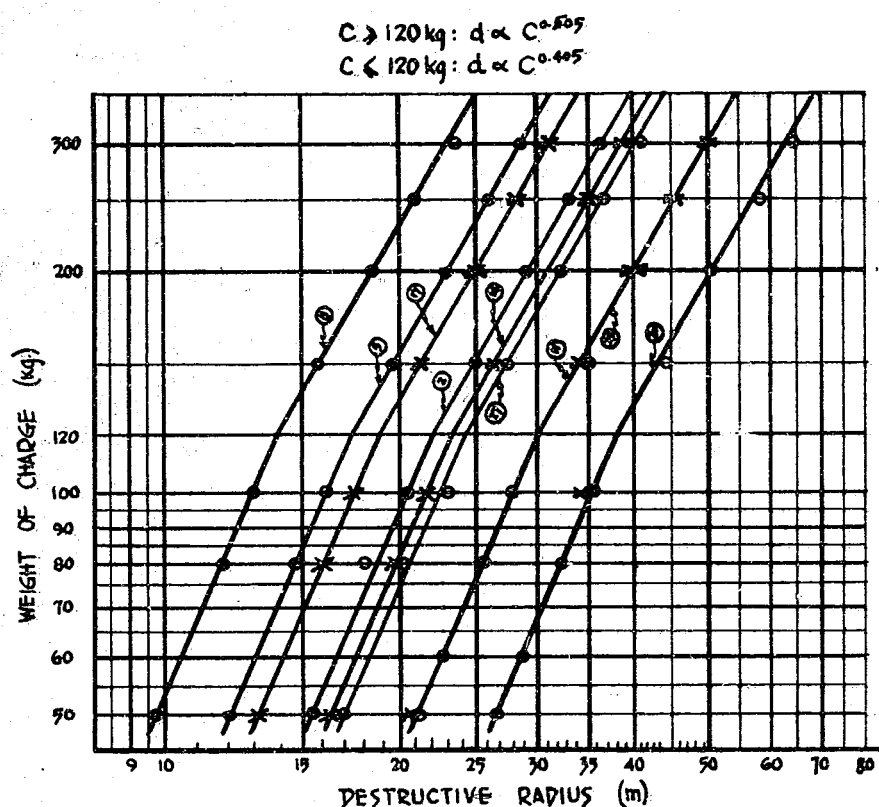


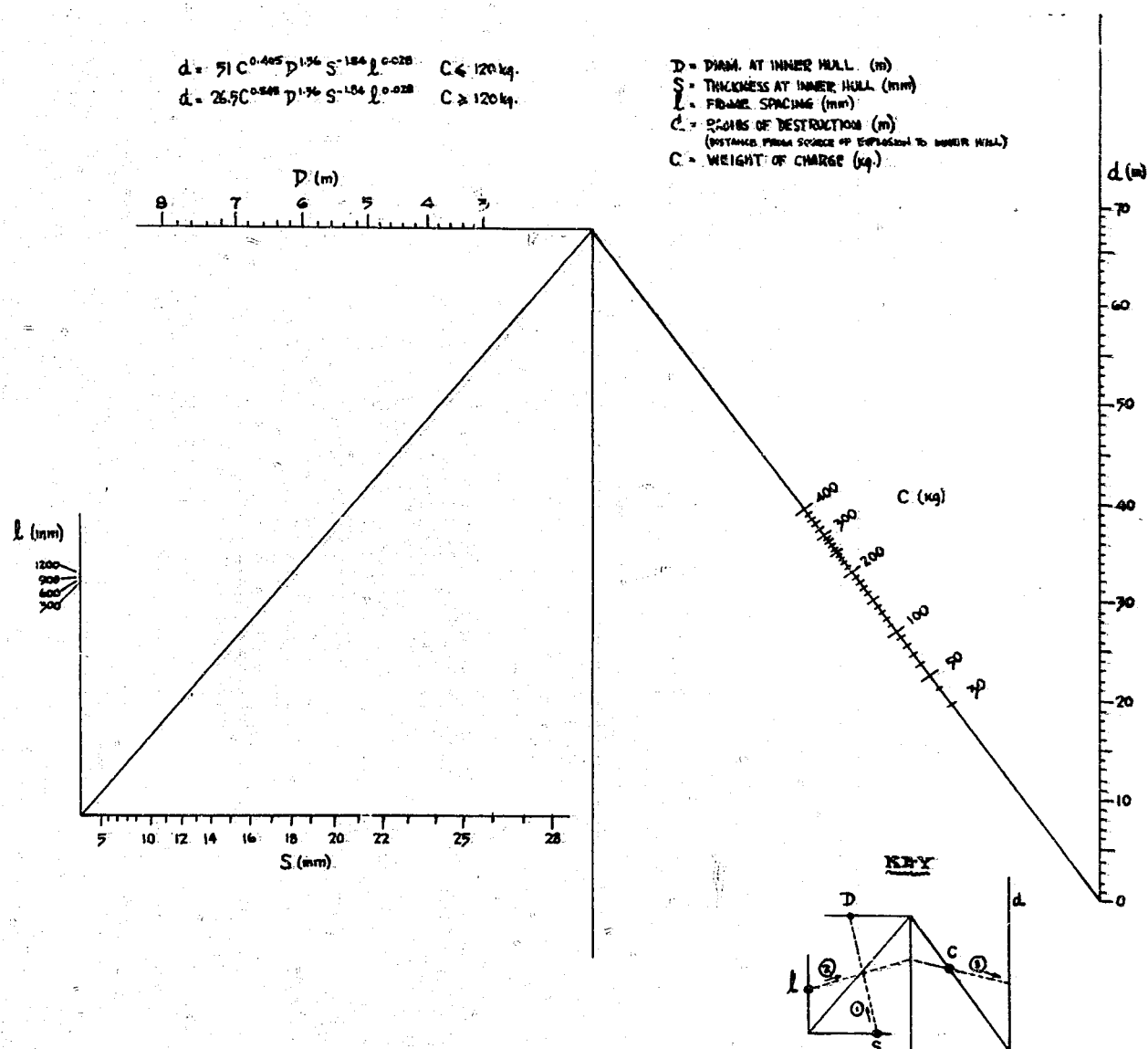
Figure 28
CORRECTION FACTOR 'A'



MARK	D (m)	l (mm)	S (mm)	MARK	D (m)	l (mm)	S (mm)	MARK	D (m)	l (mm)	S (mm)
1	4.0	400	14	10	5.0	400	14	19	6.0	400	14
②	"	600	"	⑪	"	600	"	②②	"	600	"
3	"	800	"	12	"	800	"	21	"	800	"
4	"	400	16	13	"	400	16	22	"	400	16
⑤	"	600	"	⑬	"	600	"	②③	"	600	"
6	"	800	"	15	"	800	"	24	"	800	"
7	"	400	18	16	"	400	18	25	"	400	18
⑧	"	600	"	⑮	"	600	"	②④	"	600	"
9	"	800	"	18	"	800	"	27	"	800	"

Note: Calculations have been made for all dimensions appearing on the chart above. Since the influence of "l" upon the destructive radius is very slight, in order to avoid trouble only those values which are circled are entered upon the curve.

Figure 29
CURVE OF WEIGHT OF CHARGE VS. DESTRUCTION RADIUS

**Caution:**

1. This chart should be used only when the inner hull is constructed of MS.
2. This chart cannot be used with any explosive but picric acid.
3. Considerable errors will appear if dimension (of model) or weight of charge is not to scale.

Figure 30
 NOMOGRAPH: RADIUS OF DESTRUCTION

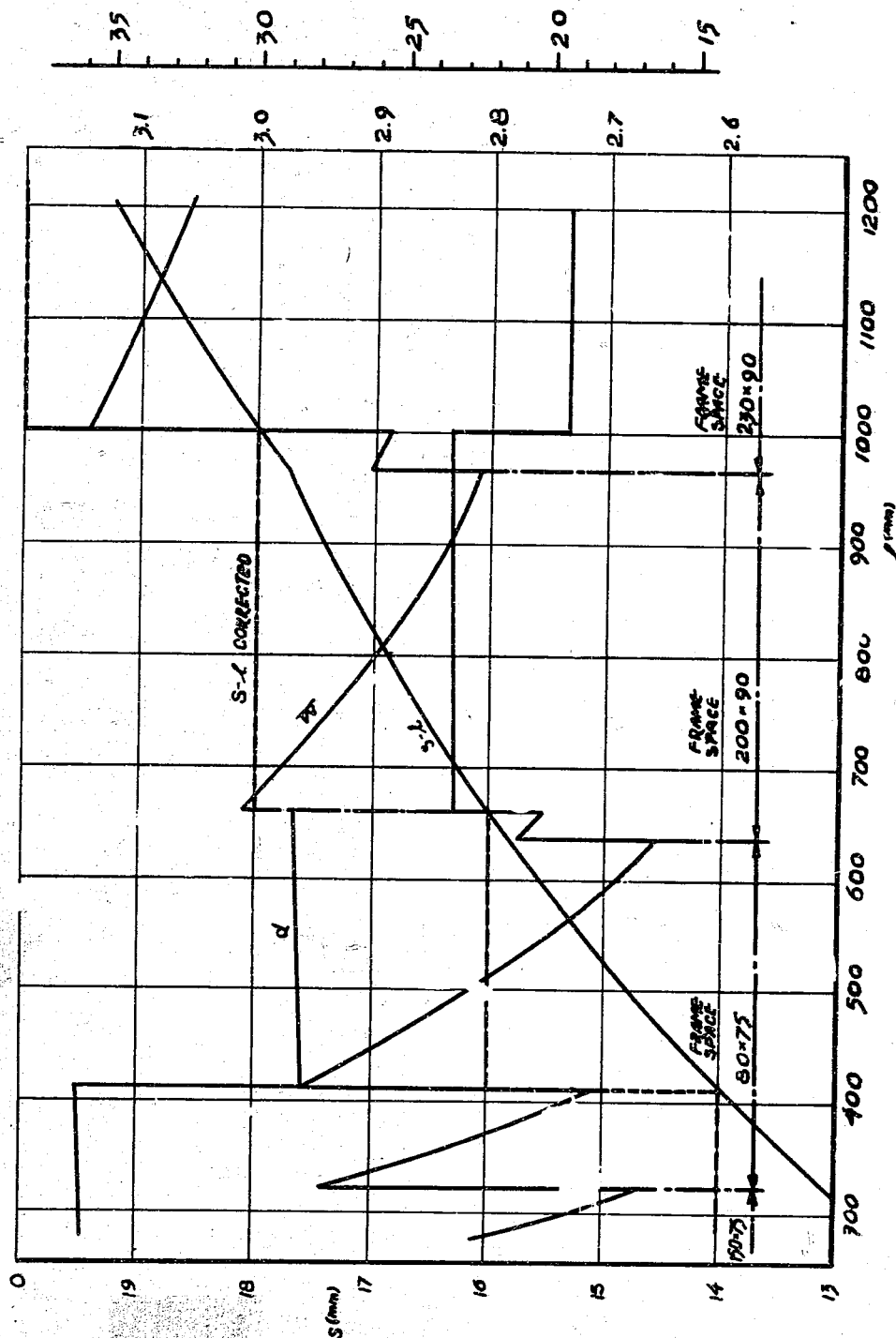


Figure 31
GRAPH - S vs. L

- Q, Q₂ QUARTZ
 B BEESWAX
 M STEEL FOLDER OF QUARTZ
 A₁ AMBEROID INSULATION TUBE
 A₂ AMBEROID INSULATOR
 C₁ DEAD-WIRE
 C₂ FEEDER LINE
 D INSULATION WAX COVER.
 P PACKING
 SP STEEL PIPE

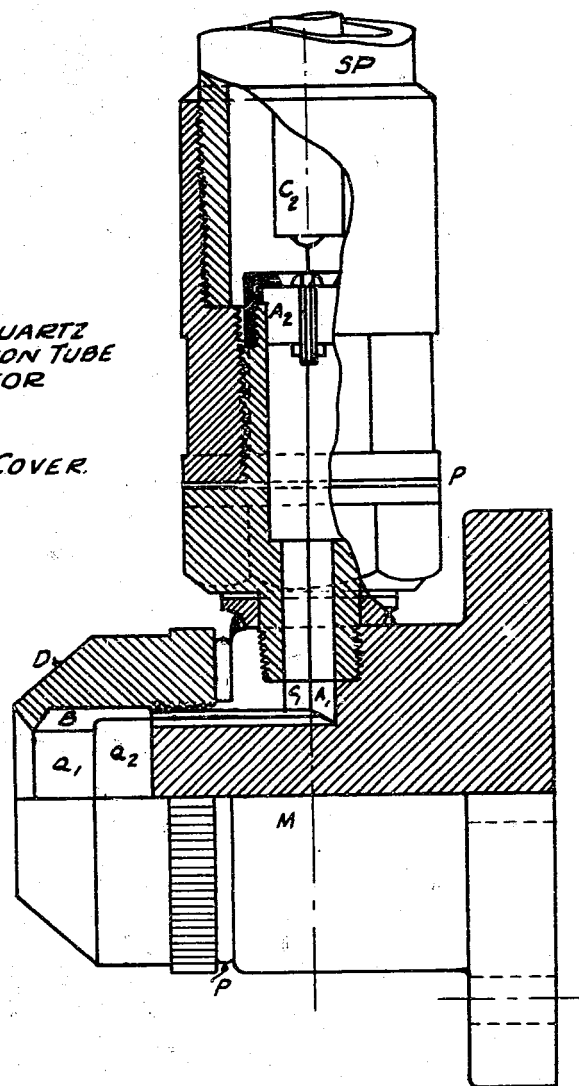


Figure 32
 GIKEN TYPE MODEL A PRESSURE GAUGE

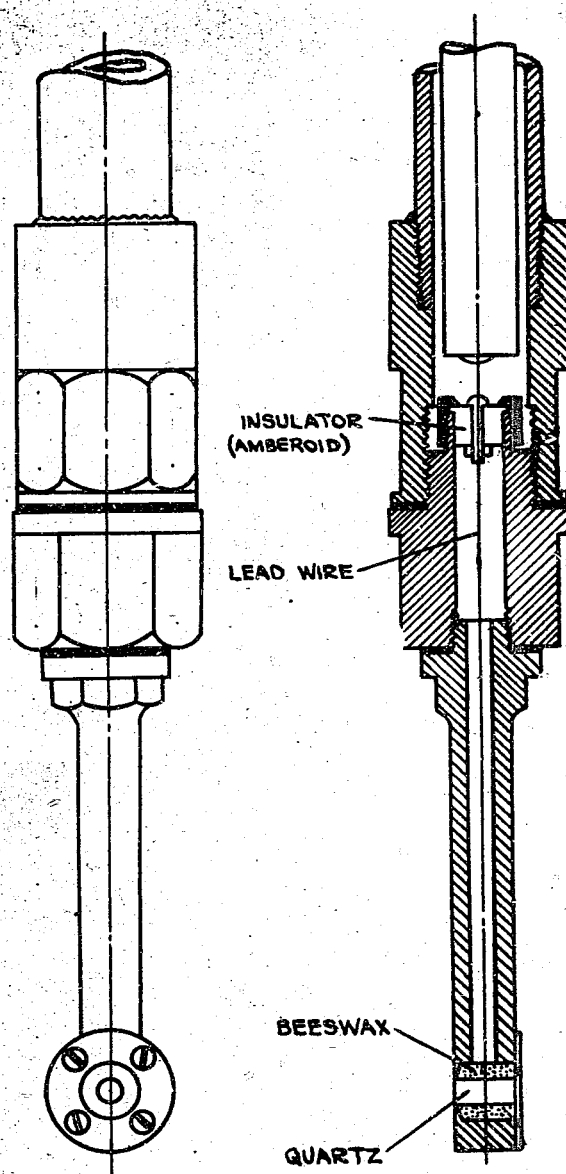


Figure 33
GIKEN TYPE MODEL B PRESSURE GAUGE

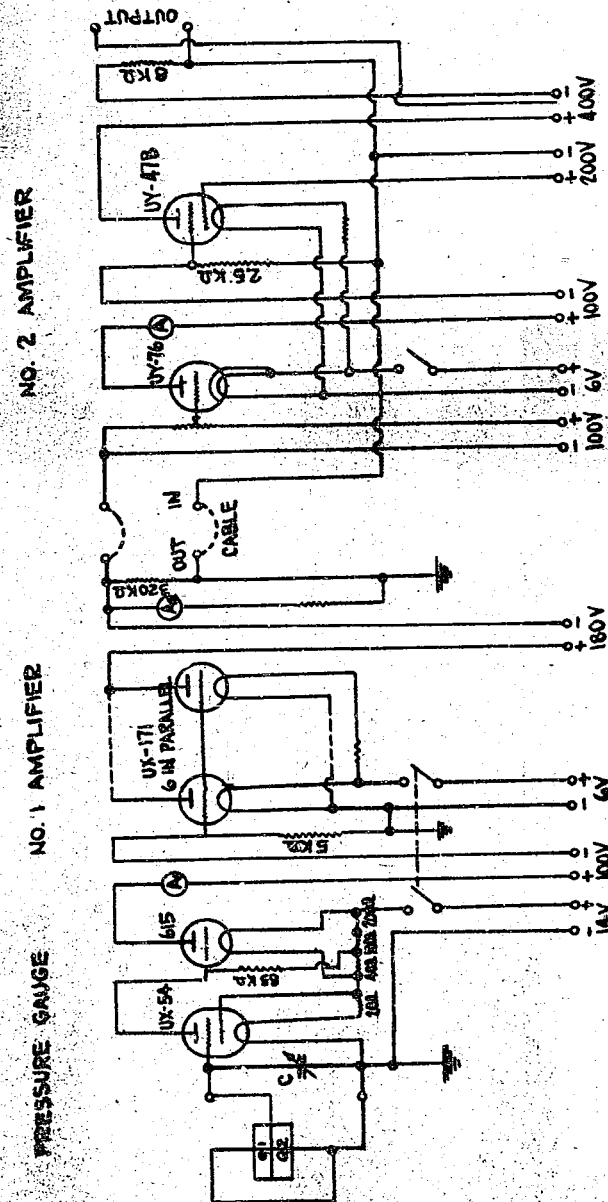


Figure 34
WIRING DIAGRAM OF AMPLIFIERS

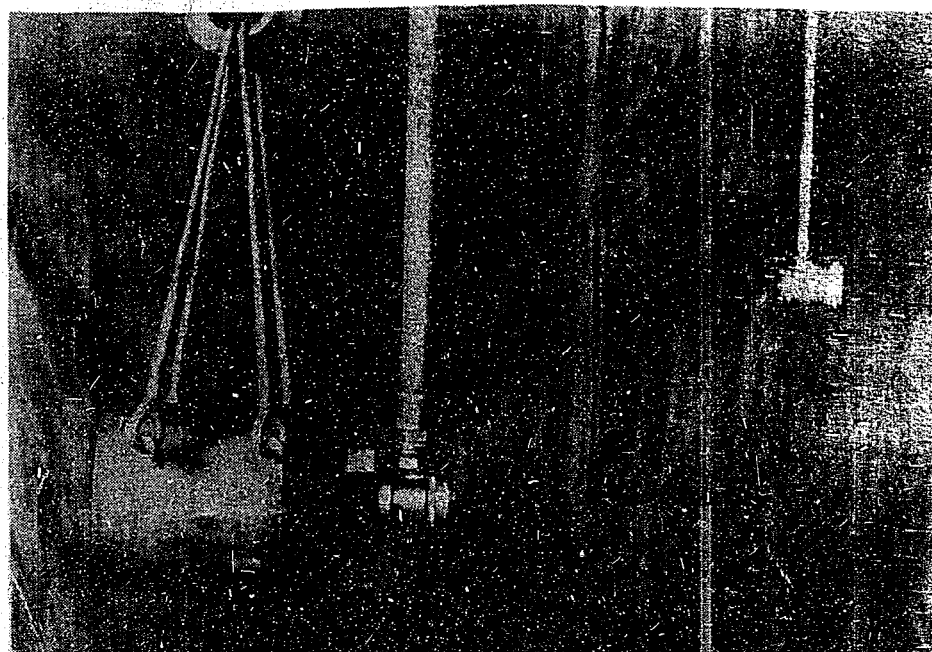


Figure 35
METHOD OF SUSPENSION OF PRESSURE GAUGES
AND ARRANGEMENT OF RECORDING INSTRUMENTS

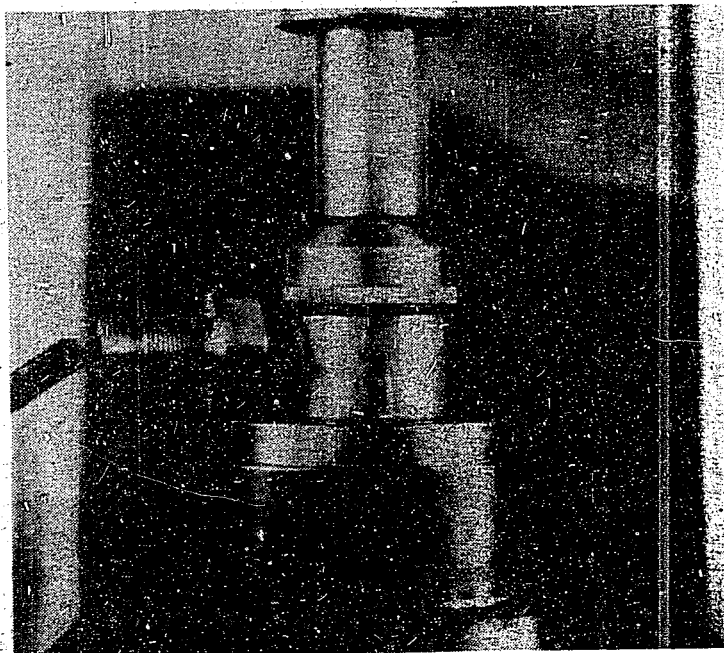


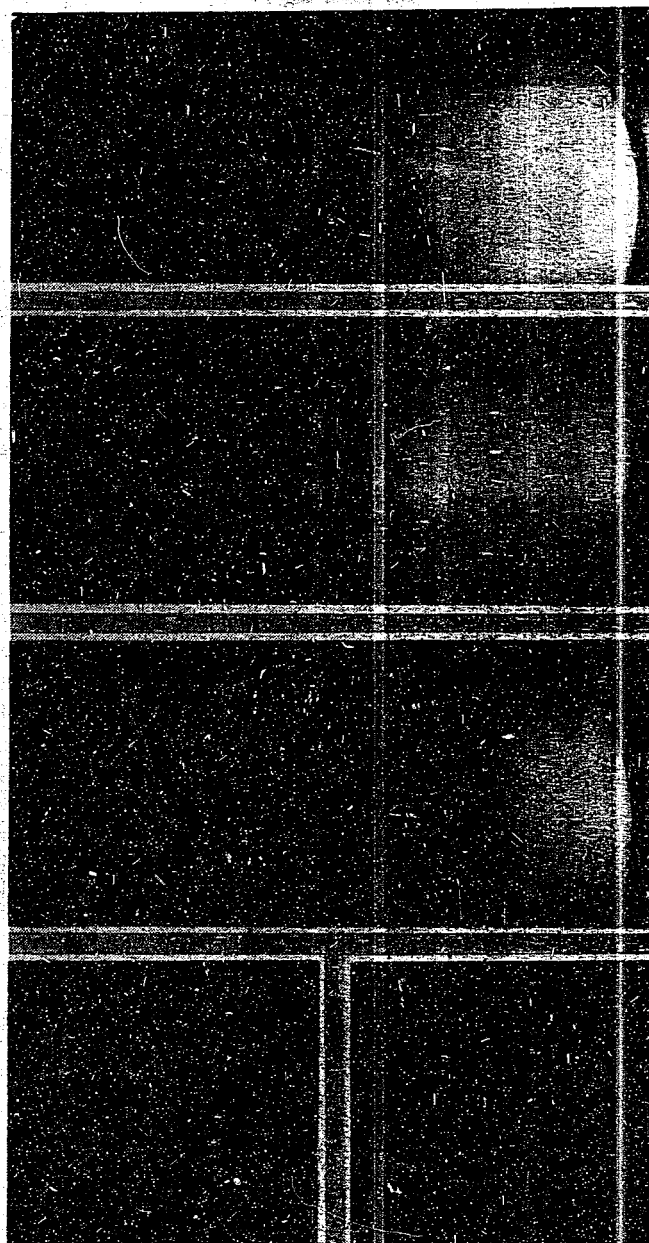
Figure 30
STATIC CALIBRATION OF QUARTZ PRESSURE GAUGE

Shape of Wave
at Input

Shape of Wave
through Amplifier

Time Mark
(20,000 μ)

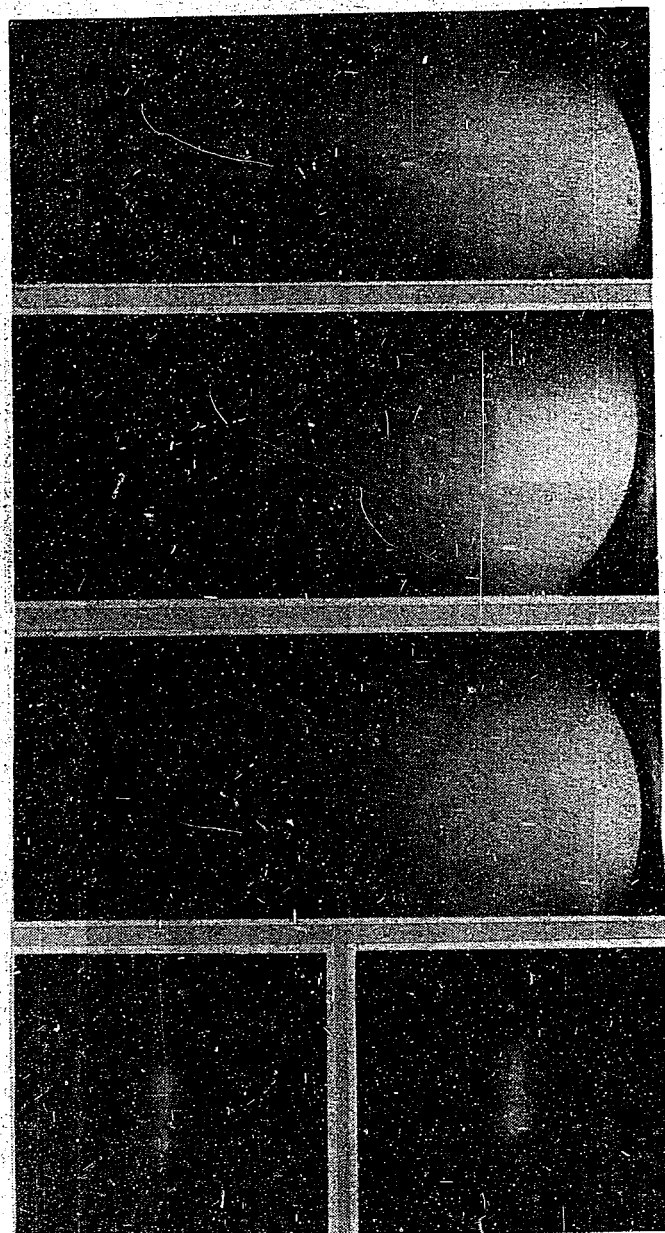
Amplitude
of Point



Direct

Through
Amplifier

Figure 37
TRACES ON C.R. TUBE OF SINGLE SAW-TOOTH WAVE



Shape of Wave
at Input

Shape of Wave
through Amplifier

Time Mark
(20,000 μ)

Amplitude
of Point

Direct

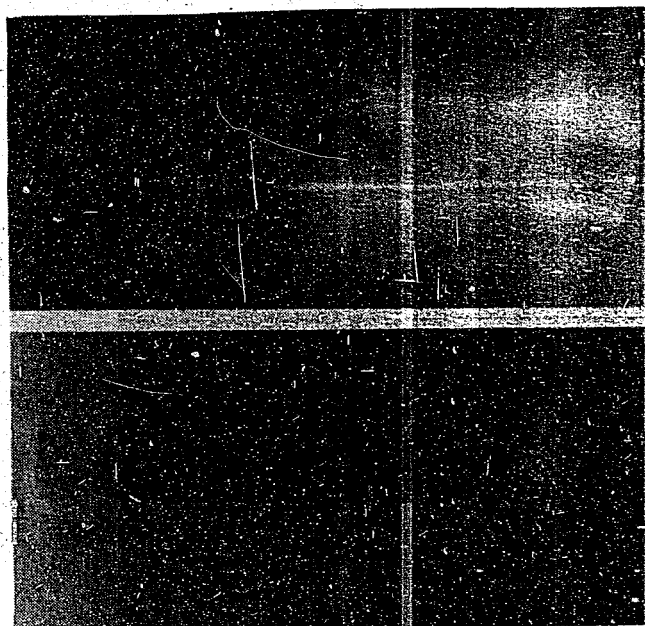
Through
Amplifier

Figure 38
TRACES ON C.R. TUBE OF SINGLE SINE WAVE

Type A

Charge 0.4 kg
Distance 7.0 m

Time Mark
(10,000 ∞)



Type B

Charge 1.7 kg
Distance 7.0 m

Time Mark
(10,000 ∞)

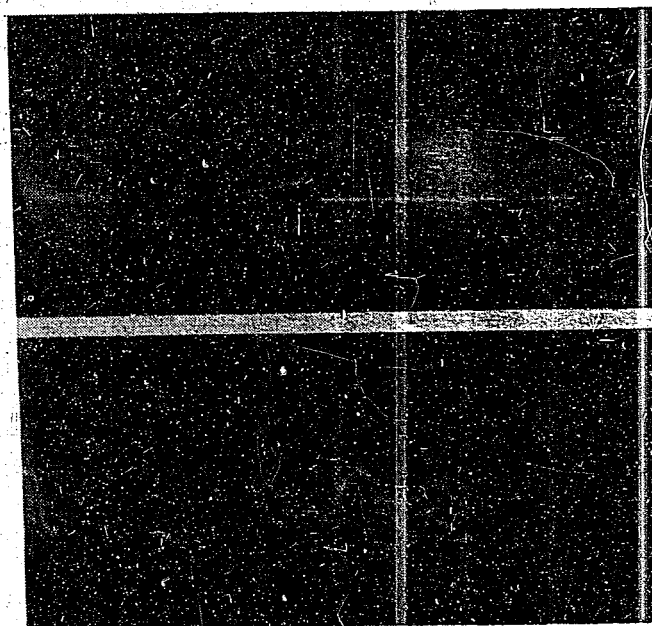


Figure 39
PHOTOGRAPHS OF PRESSURE WAVES - MODEL A PRESSURE GAUGE

Statical collapsing pressure: 31-33 kg/cm²

D 100
L 120
S 1



Charge: 400 kg

Distance (m) between
charge and model

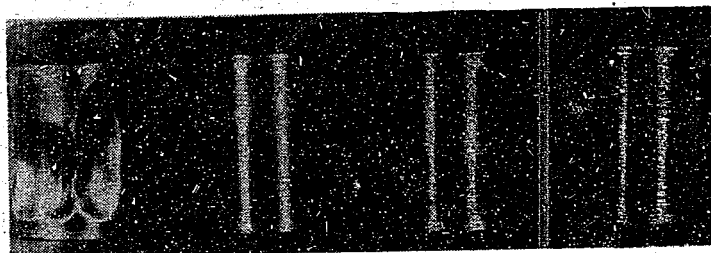
35

45

55

70

D 100
L 120
S 1



Charge: 1.7 kg

Distance (m) between
charge and model

.5

5

6

7

D 100
L 120
S 1

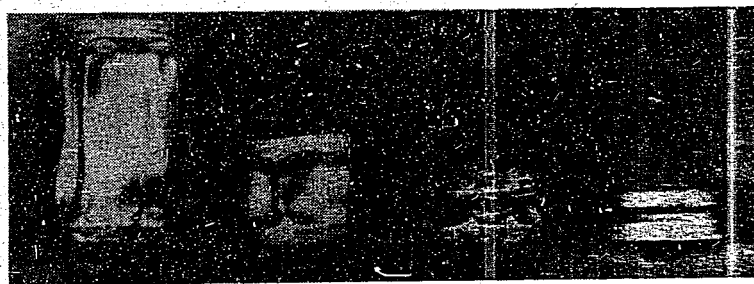


Figure 40
PHOTOGRAPHS OF MODELS

Extent of Collapsing at Various Unsupported Lengths

Charge 1.7 kg
 Diameter 100mm
 Thickness 1.0mm

Unsupported length	120mm	50mm	25mm	12.5mm
Distance from charge	3.5mm	3mm	3mm	3mm



Comparative Strength against Explosion of Similar Models

Charge 1.7 kg
 Distance from charge 2 m

Unsupported length	120mm	60mm	34mm
Thickness	2.0mm	1.0mm	0.5mm
Diameter	100mm	50mm	24.5mm

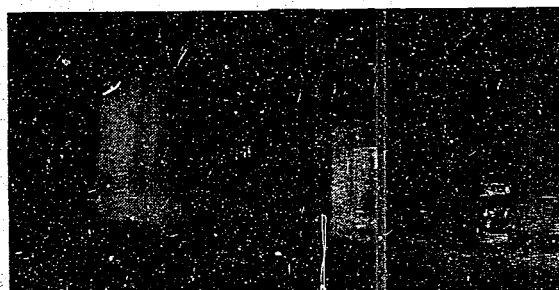
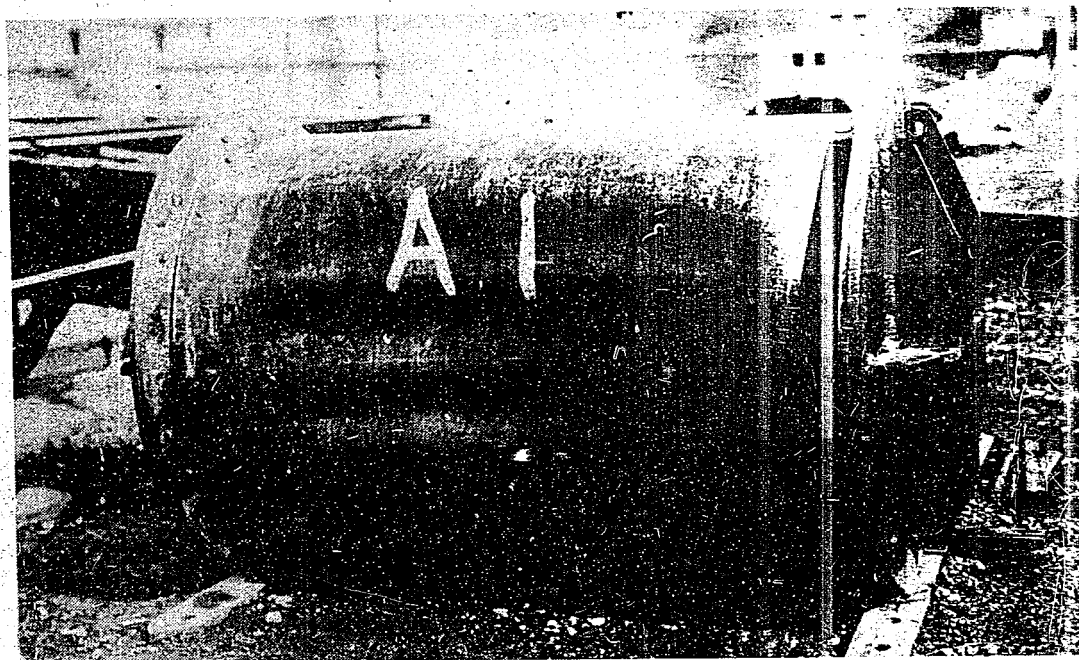
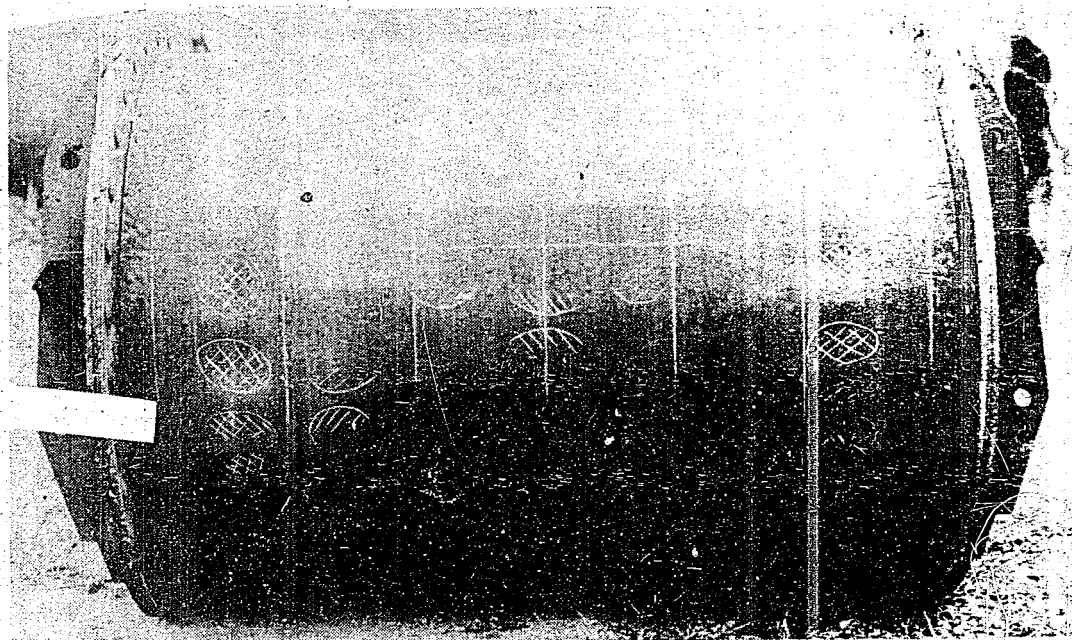


Figure 41
 PHOTOGRAPHS OF MODELS



Charge: 1.7 kg Distance: 0.7 m Assumed peak pressure: 1.100 kg/cm²



Charge: 1.7 kg Distance: 3.5 m Assumed peak pressure: 174 kg/cm²

Figure 42
PHOTOGRAPHS OF MODELS

ENCLOSURE (A)

LIST OF ILLUSTRATIONS

Part I

REPORT OF TORPEDO AND MINE TESTS IN BATTLESHIP TOSA

Figure 1(A)	Plan of Location of Tests - "TOSA"	Page 195
Figure 2(A)	Results of Test at Position (1)	Page 196
Figure 3(A)	Results of Test at Position (2)	Page 197
Figure 4(A)	Results of Test at Position (3)	Page 198
Figure 5(A)	Results of Test at Position (4)	Page 199
Figure 6(A)	Results of Test at Position (5)	Page 200
Figure 7(A)	Results of Tests in Torpedo Room	Page 201

Part II

ANNOUNCEMENT OF TORPEDO AND MINE TESTS

Figure 8(A)	Underwater Explosion Pressure Curve	Page 204
Figure 9(A)	Underwater Explosion Pressure Curve	Page 205

ENCLOSURE (A), continued

Part I

REPORT OF TORPEDO AND MINE TESTS IN BATTLESHIP TOSA

In these tests the draft of the ship was shallower than in normal load condition. Accordingly, the depth of the explosion, too, was shallower. Therefore, the explosive force at the planned depth was thought to be greater than what appeared in the test.

30 June 1936

ENCLOSURE (A), continued

Table I(A)
RESULTS OF TEST ON TOSA

	Charge			Area Damaged			Max. Deflection on Deck Over
	Size	Position	Depth Below W.L.	Hole (ft ²)	Plating (ft ²)	Protective Bulkhead(ft ²)	
6 June	100 kg	Starboard side F57	12' 0"	240	750		
8 June	200 kg	Port side F87	13' 3"	240	1400	900	2' 9"
9 June	300 kg	Starboard side F192	13' 3 1/4"	160	1700	1000	3' 4"
12 June	350 kg	Port side F192	16' 0"	280	1200	1000	2' 4"
13 June	150 kg	Starboard side F87	20' 9 1/2"	190	1300	320	1' 1 1/2"

ENCLOSURE (A), continued

Table I(A) (Continued)

Damage to Protective Bulkhead	Water Taken On	Compartments Flooded			List		
		Immediately	Slowly	Total	Immediately Before	After	Change
	995 T	17	5	22	0° 14'	1° 40'	1° 54'
In the vicinity of center of explosion a hole 4' x 1' was made	1.008 T	19	9	28	1° 40'	4° 36'	6° 16'
In several places in vicinity of center line of concussion, outermast of 3 armor plate seams were torn	1.203 T	26	1	27	2° 51'	5° 22'	8° 13'
Since steel tube was loaded there was no partial damage, nevertheless, along curved upper seam a rent 36' was torn	1.160 T	15	11	26	1° 0'	5° 20'	6° 20'
Here and there around line of center of concussion melting traces were impressed	726 T	10	10	20	3° 50'	0° 48'	4° 38'

RESTRICTED

ENCLOSURE (A), continued

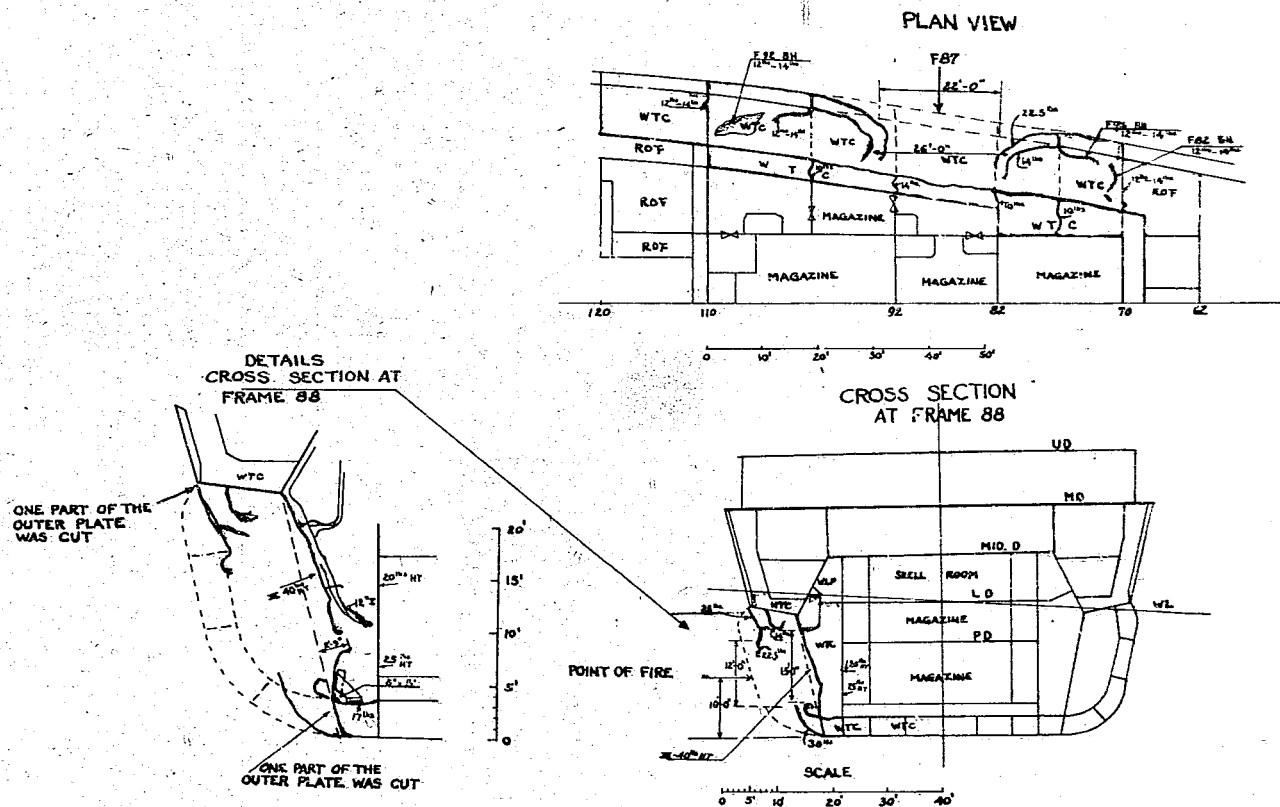
S-01-9

RESULTS OF MEASUREMENTS OF UNDERWATER PRESSURE IN TOSA TESTS (TORPEDOES & MINES)

			EXPECTED		TEST RESULTS		OBSERVATIONS		
NO. OF TEST IN WHOLE SERIES	REL. POSITION OF EXPLOSIVE ON HULL	LOCATION OF PRESSURE GAUGES AND EXPLOSIVES AT SHIP'S SIDE	MEASURED PRESSURE	DATE OF TEST	SIZE OF HOLE	MAXIMUM DEPTH OF HOLE	LIST OF HULL DAMAGE BEFORE TEST	NOTE	
1	STERN MK I MINE 100 KG 14'-0" DEPTH	STARBOARD 22.5 LBS.		6 JUNE 1924	15'-6" x 15'		LIST OF HULL DAMAGE BEFORE TEST	1. BECAUSE HIGHEST LINE OF PRESSURE GAUGES WAS ABOVE WATER, THE PRESSURE WAS GREATLY DECREASED. 2. TABLE 2.	1. ACTUAL MEASURED PRESSURE WAS GREATER THAN CALCULATED PRESSURE. THIS WAS BECAUSE THE EXPLOSIVE CAUSED CUTS AND HOLES IN THE SIDE. 2. IT IS BELIEVED THAT UNEXPECTED PRESSURE RESULTS WERE DUE TO THE UNDERWATER PRESSURE OF THE BOWING OF THE SHIP'S SIDES AND BLUE KEEL, ETC., IN DISSEMINATING PRESSURE. 3. THE PRESSURE GAUGES HIGHEST ON THE SHIP'S SIDES WERE AT TIMES OUT OF WATER, BECAUSE OF DRIFT, LIST, ETC., SO THAT PRESSURE WAS DECREASED. 4. MARINE PRESSURE IN HOLE IN SUBMARINE PRESSURE IN HOLE IN TOSA (INDICATED ON PRESSURE GAUGES LOCATED ON A WIRE BETWEEN THE TOSA AND THE SUBMARINE) WAS GREATER THAN THE PRESSURE FOLLOWING THE SIDE OF THE TOSA. THE FORMER WAS MUCH GREATER THAN THE CALCULATED PRESSURE WHILE THE LATTER WAS LESS. ALTHOUGH THIS EFFECT IN THE OPPOSITE DIRECTION AT RIGHT ANGLES TO THE SIDE INCREASES AS THIS PRESSURE INCREASES, IT IS BELIEVED THAT IN THE DIRECTION OF THE SHIP'S SIDE THE PRESSURE WILL BE COMPARATIVELY SMALL AS DESCRIBED IN (1) AND (2) OF THESE CONCLUSIONS. 5. IN REGARD TO THE TRANSMISSION OF UNDERWATER EXPLOSIVE PRESSURE, WHERE THERE ARE NO OBSTRUCTIONS IT FOLLOWS WITH NO GREAT DISCREPANCIES THE GUNNERY EXPERIMENTAL FORMULA (REPORT OF RESULTS OF UNDERWATER EXPLOSIVE TESTS, KURE NAVAL ARSENAL, FEBRUARY 1923).
2	BOW 4TH YEAR TYPE TORPEDO 300 KG SET DEPTH 14'-0"	PORT 22.5 LBS.		8 JUNE	22' x 12'	2'-9"	PORT 2'-16'	1. BECAUSE HIGHEST LINE OF PRESSURE GAUGES WAS ABOVE WATER, THE PRESSURE WAS GREATLY DECREASED. THE RISE OF THE WATER. 2. TABLE 3.	
3	STERN 8TH YEAR TYPE TORPEDO 300 KG SET DEPTH 14'-0"	STARBOARD 35 LBS.		9 JUNE	16'-6" x 8'	3'-4"	PORT 2'-5'	1. BECAUSE HIGHEST LINE OF PRESSURE GAUGES WAS ABOVE WATER, THE PRESSURE WAS GREATLY DECREASED. 2. TABLE 4.	
4	BOW 8TH YEAR TYPE TORPEDO 300 KG SET DEPTH 14'-0"	PORT 35 LBS.		12 JUNE	18' x 20'	2'-4"	STARBOARD 1'-0'	1. TABLE 5.	
5	STERN 8TH YEAR TYPE TORPEDO 150 KG SET DEPTH 19'-0"	STARBOARD 35 LBS.		13 JUNE	18' x 18'	1'-11/2"		1. TABLE 6.	

Figure 1(A)
PLAN OF LOCATION OF TESTS - "TOSA"

ENCLOSURE (A), continued



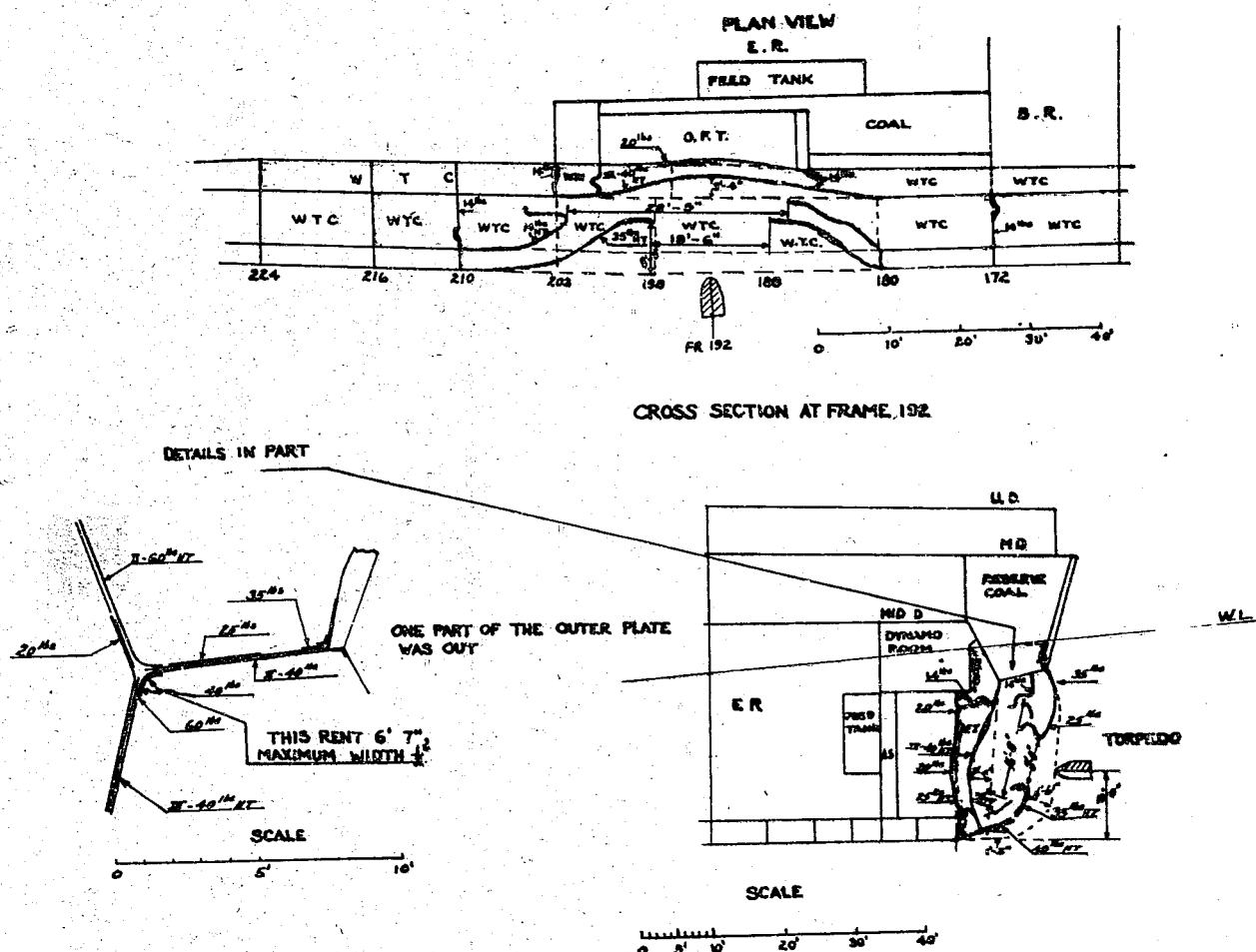
8-June - Year 6 Type Mine Against Submarine Defense (Charge 200 kg)

REMARKS:

- In a hit against the armored part of the hull, the explosive force of this type of weapon is not capable of inflicting vital damage to a battleship of TOSA class.
- As a result of the explosion a hole was observed in the 3" armor plate. Judging from other tests the damage was somewhat more than expected. One cannot say definitely the reason for this but it is thought that one reason was the fact that the upper part of the outer plate was inclined outward.
- In this test there was a 6° port and starboard heel at the time of the explosion. This type of damage is recognized to have given a large shock to the control of the ship and the use of its weapons.

Figure 3(A)
RESULTS OF TEST AT POSITION 2

ENCLOSURE (A), continued



9 June - Year 8 Type Torpedo Against Submarine Defense (Charge 300 kg)

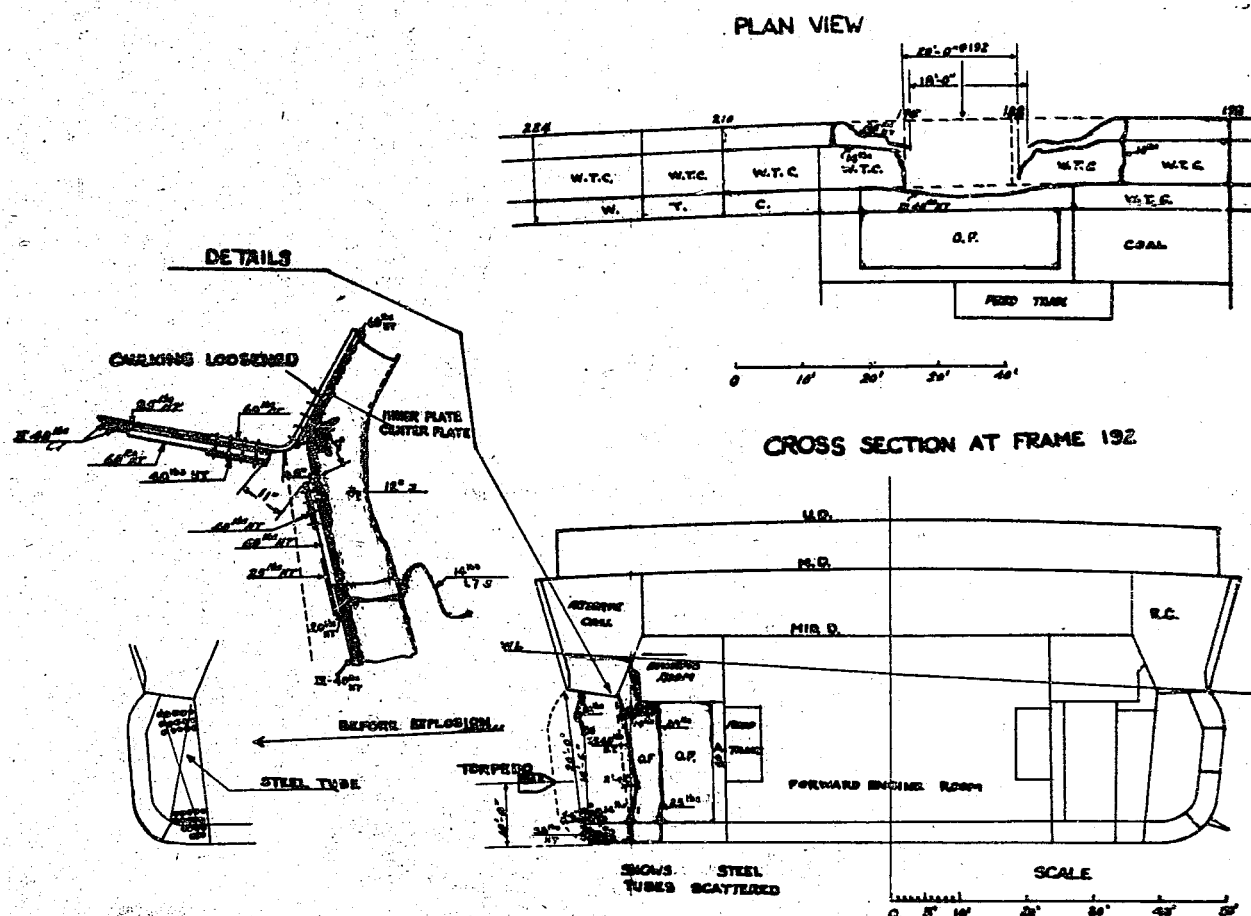
REMARKS:

In this test it is recognized that there was equality between the explosive force of this type of torpedo against a battleship of TOSA class and the ship's submarine defenses.

However, in this test the ship's draft was 23' 3 1/2" which was about 10' shallower than the ideal combat draft. Moreover, the depth of the point of explosion was 13' 3 1/2" and was somewhat shallower than the depth actually used with torpedoes. Because of this the explosive force at the planned depth is somewhat greater. Nevertheless, it is thought necessary to increase the explosive power to damage completely the submarine defenses.

Figure 4(A)
RESULTS OF TEST AT POSITION 3

ENCLOSURE (A), continued



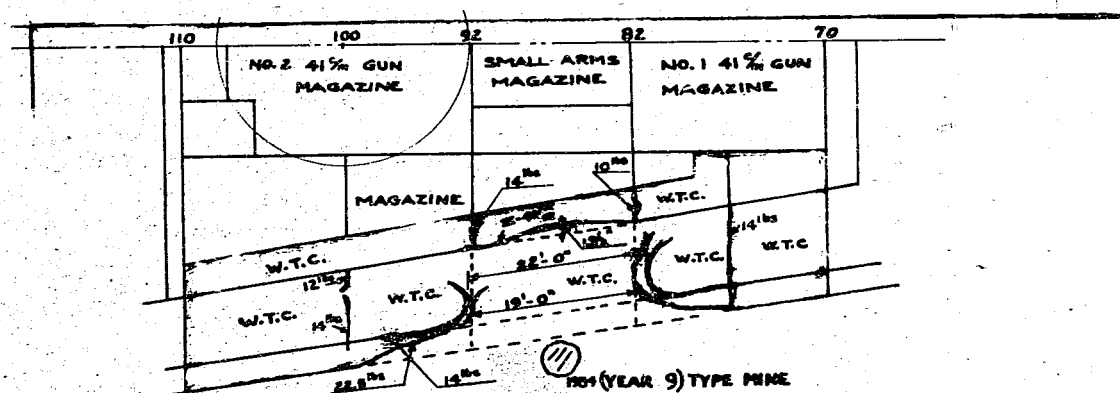
12 June - Year 8 Type Mine Against Submarine Defenses (Charge 350 kg)

REMARKS:

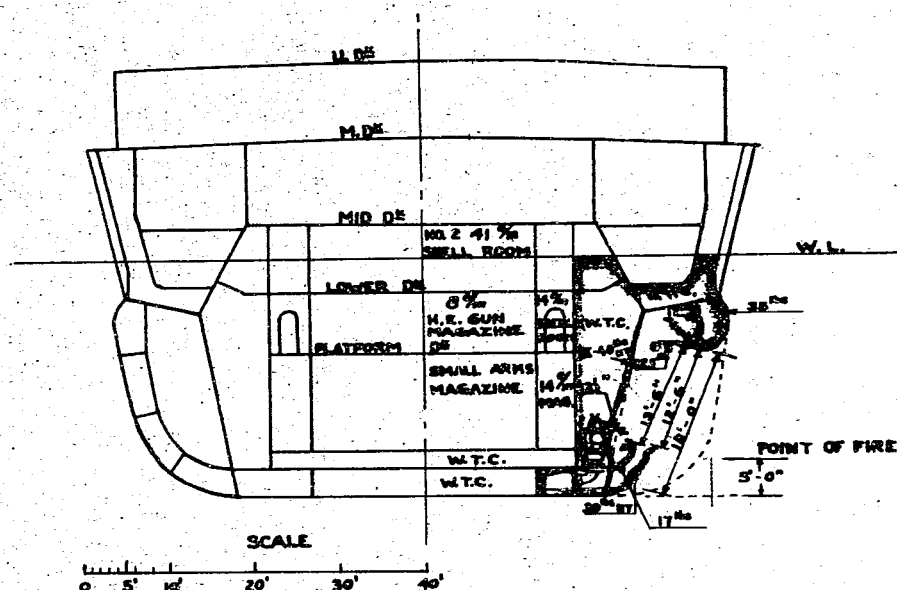
Although it is recognized that the torpedo produced the expected explosive force when the condition of the flooded compartments is as indicated, it is recognized that it cannot produce adequate results against armor or defenses which utilized steel tubes. Further, though the steel tubes are thought to be effective as defensive materials, their weight was 150 kln (TN: 1 kln = 1.32 lbs) for each square foot of bulkhead and is heavier than the longitudinal bulkheads themselves; it is thought that if this much weight is expended, better means of defense can be devised. Experiments and planning are necessary.

Figure 5(A)
RESULTS OF TEST AT POSITION

ENCLOSURE (A), continued



CROSS SECTION AT FRAME 87



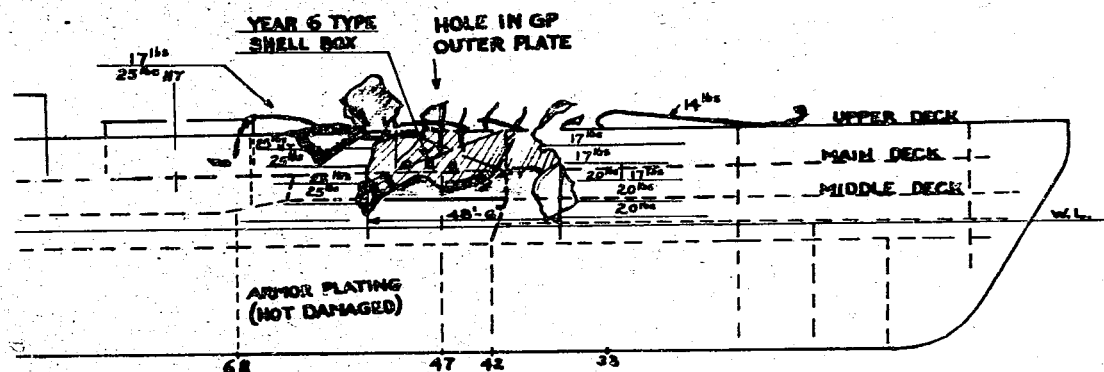
13 June - Year 9 Type Mine Against Submarine Defenses (Charge 150 kg)

Although there was suitable destructive force in the weight of the charge, it is difficult to damage the defensive parts of the sides of a battleship of TOSA class. Moreover, in view of the fact that there are many opportunities to hit the defensive parts of the sides of a ship, it is recognized as necessary to increase as much as possible the amount of the charge, and so increase the explosive force.

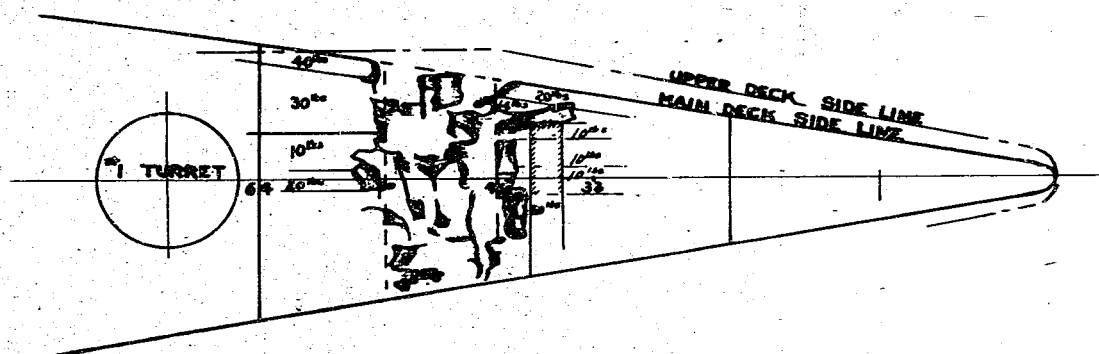
Figure 6(A)
RESULTS OF TEST AT POSITION 5

ENCLOSURE (A), continued

SIDE VIEW



DECK PLAN



16 June - Explosion of War Heads Actually Used on Torpedoes
in the Torpedo Tube Room

REMARKS:

In view of this test it is recognized as necessary to equip the torpedo tube room as indicated below.

- (a) To reduce the damage from the torpedo explosions and protect from fragments from enemy bombs, the torpedo casemates should be armored.
- (b) When this cannot be done it is necessary to use a comparatively strong steel plate on both sides of the torpedo tubes, and by making one side weaker, twist the destructive force in that direction.
- (c) The torpedoes mentioned in the two preceding items have thin warheads pointing outboard and it is necessary to equip the sides of the ship in this vicinity with strong steel plating. Moreover, it is thought suitable to protect the torpedoes which will be fired next with similarly strong steel plates, and the other torpedoes should be stored in the armored compartment.

Figure 7(A)
RESULTS OF TESTS IN TORPEDO ROOM

ENCLOSURE (A), continued

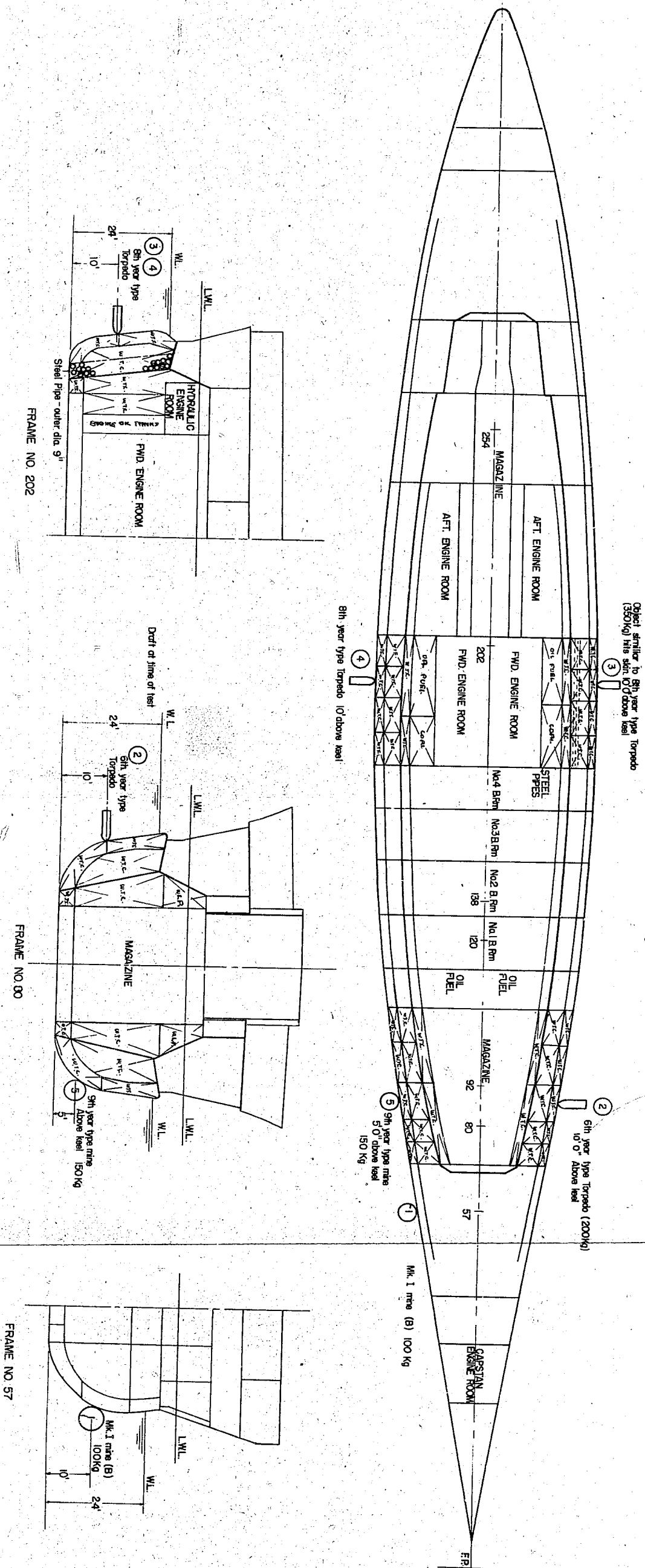
Part II
ANNOUNCEMENT OF TORPEDO AND MINE TESTS

15 Sept. 1937

ENCLOSURE (A), continued

S-01.9

PLAN OF LOCATION OF TESTS



ENCLOSURE (A), continued

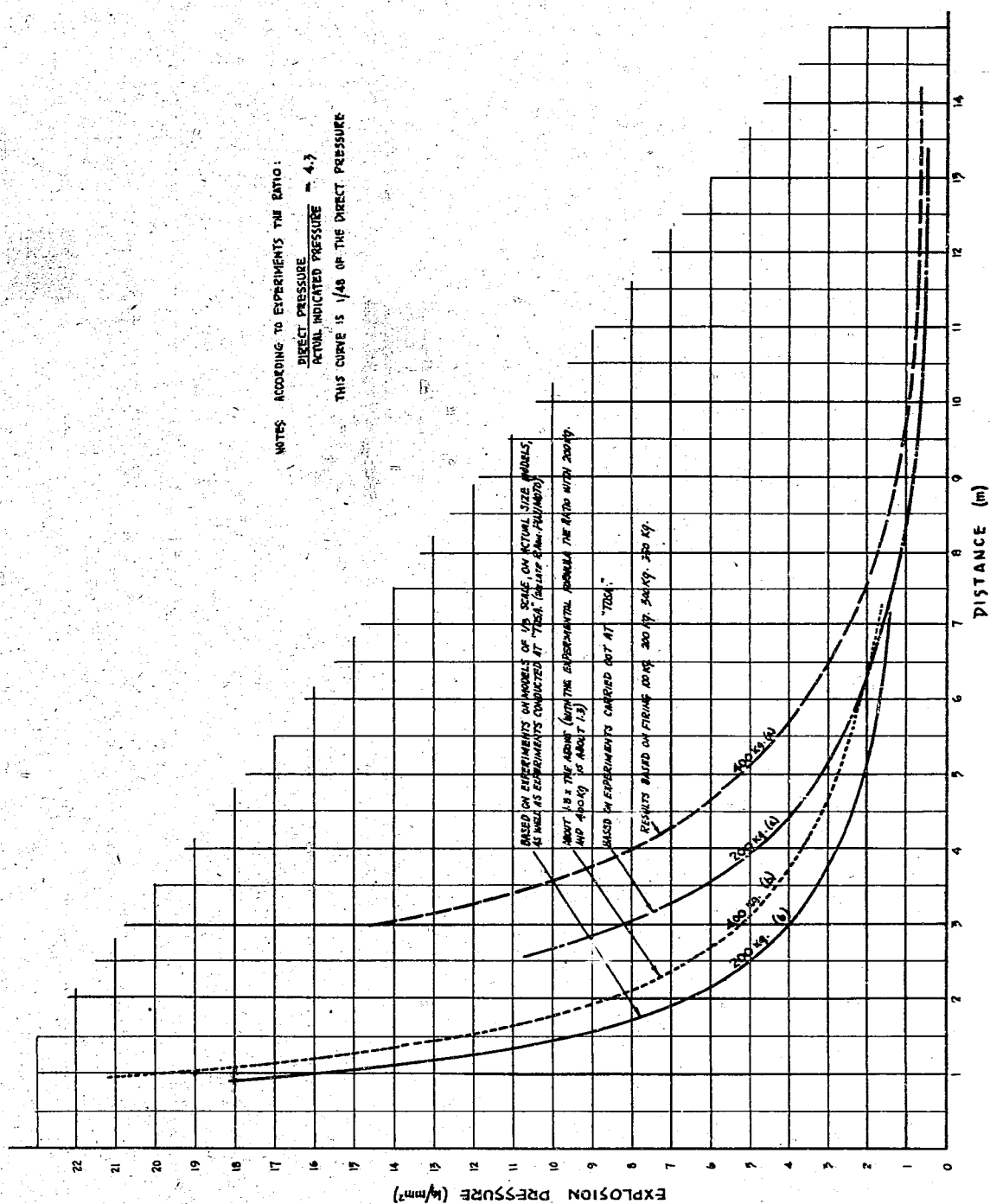


Figure 8(A)
 UNDERWATER EXPLOSION PRESSURE CURVE
 (Measurements made by Copper Crusher Gauge)

ENCLOSURE (A), continued

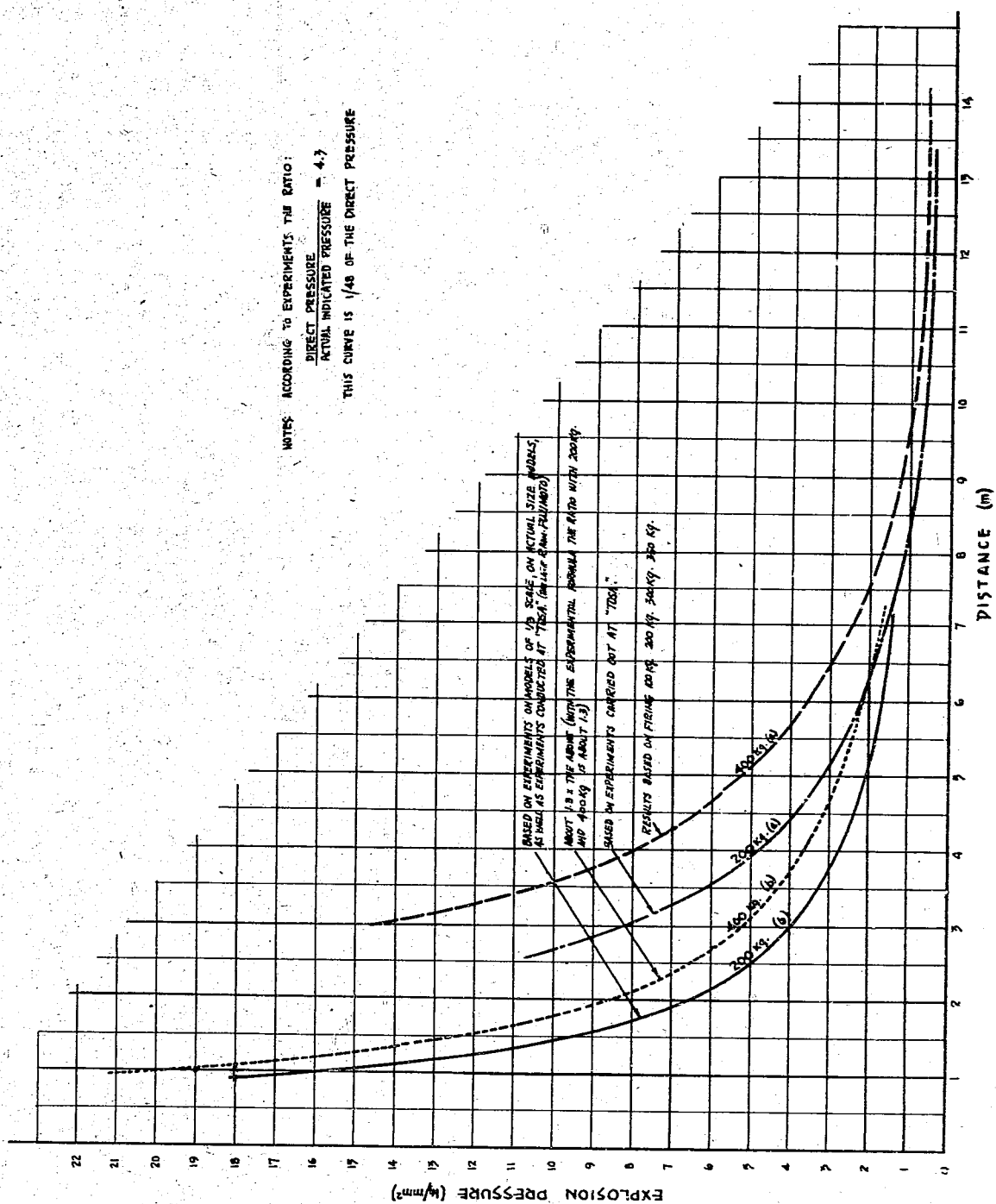


Figure 8(A)
 UNDERWATER EXPLOSION PRESSURE CURVES
 (Measurements made by Copper Crusher Gauge)

ENCLOSURE (A), continued

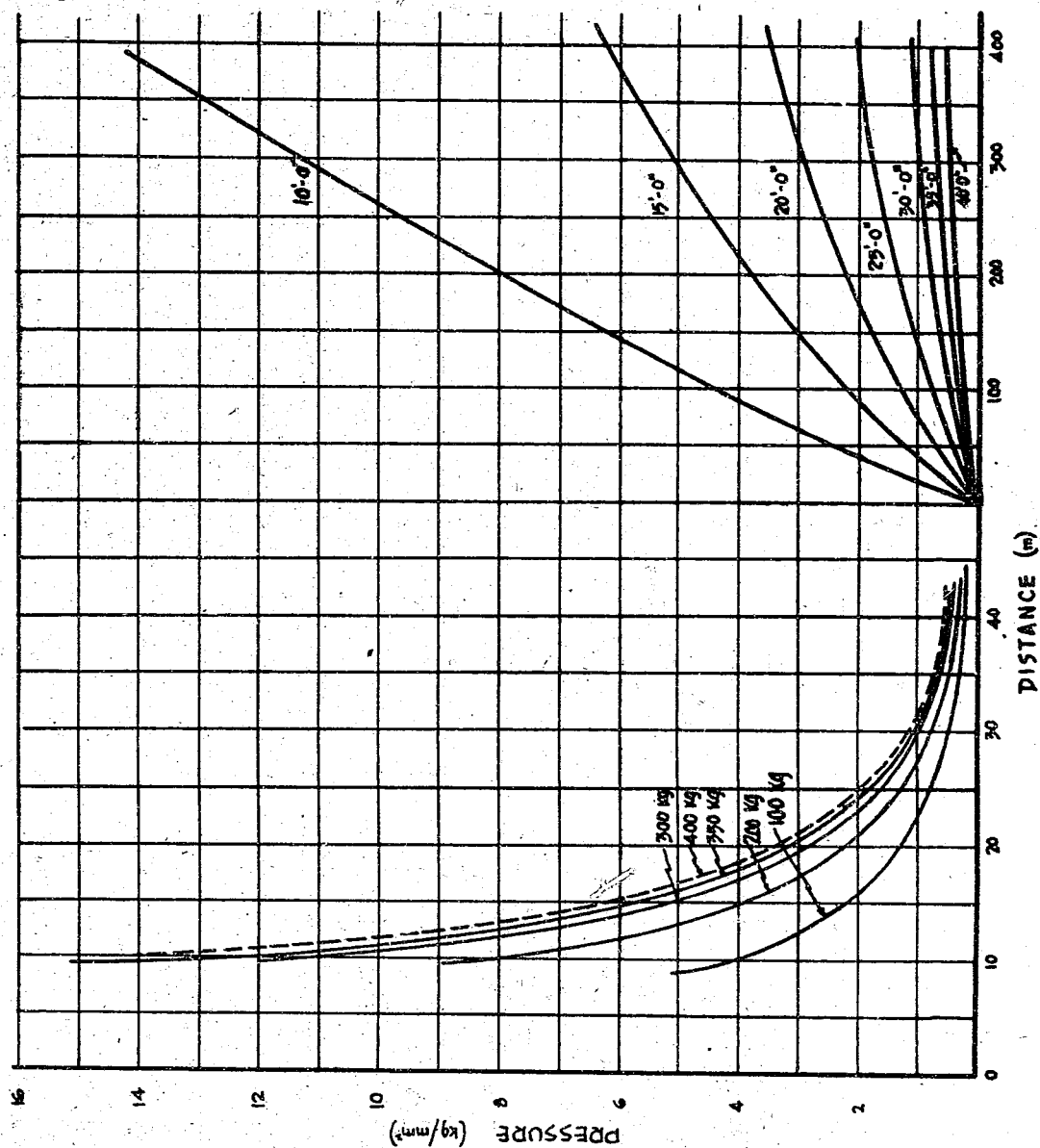
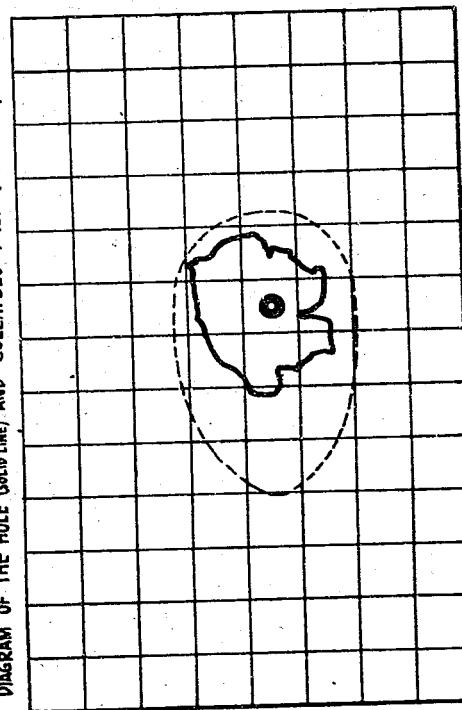
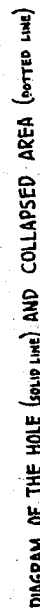
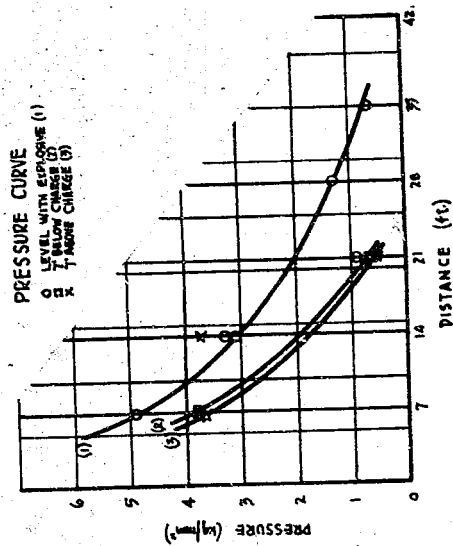
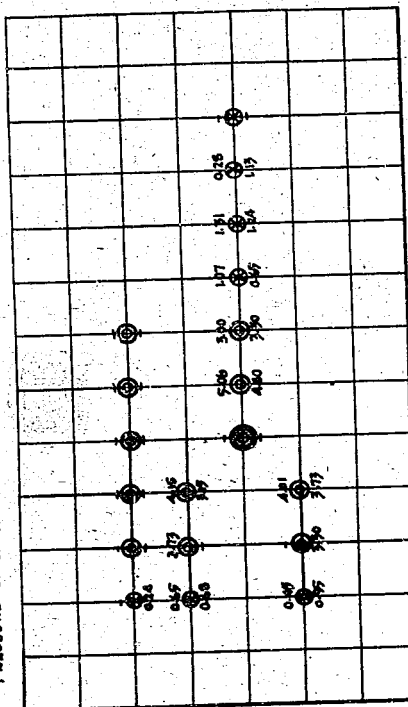
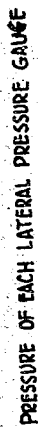


Figure 9(A)
UNDERWATER EXPLOSION PRESSURE CURVE
(Experiments on TOSA at TOSA)
(Copper Gruener Gauge)

ENCLOSURE (A), continued

Table II(A) (Test No. 1)

Position Starboard F. 57, above keel 10'0"
Draft (before test) 22'0"
Mark I {B} Mine (look)
Amt. of explosive Electric firing (double
Detonating method electric fuze for mines).



ENCLOSURE (A), continued

Table V(A) (Test No. 4)

Location Port side F.192, 10' above the keel
 W.L. of place of experiment (before the experiment) 26'0"
 Size of charge 8th year type torpedo (350k)
 Method of detonation .. Fired electrically (2 electric fuses -
 small generator type - in parallel).

PRESSURE OF EACH LATERAL PRESSURE GAUGE

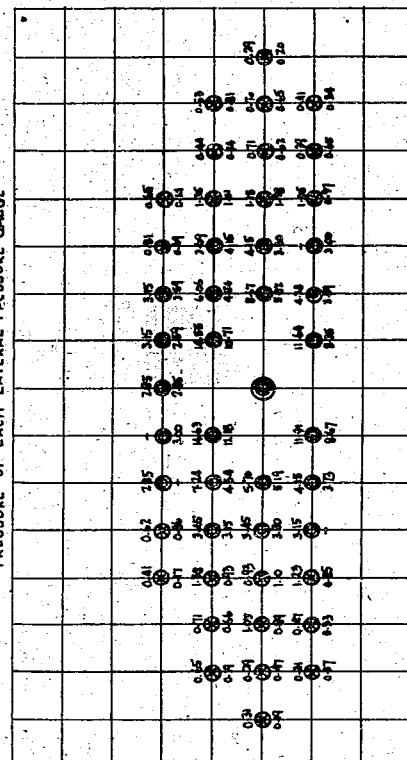
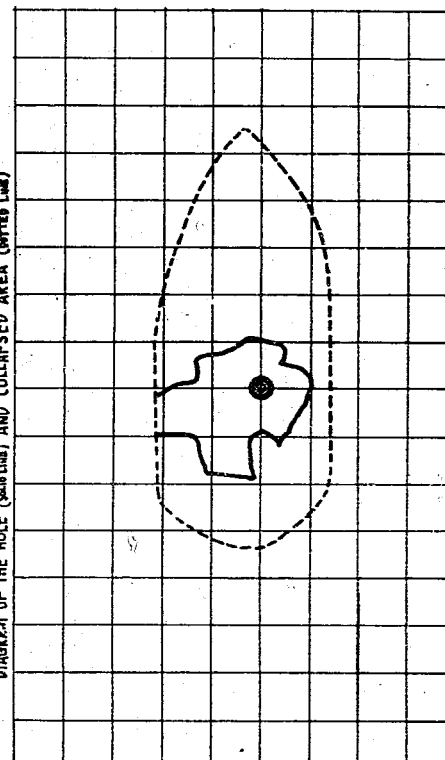


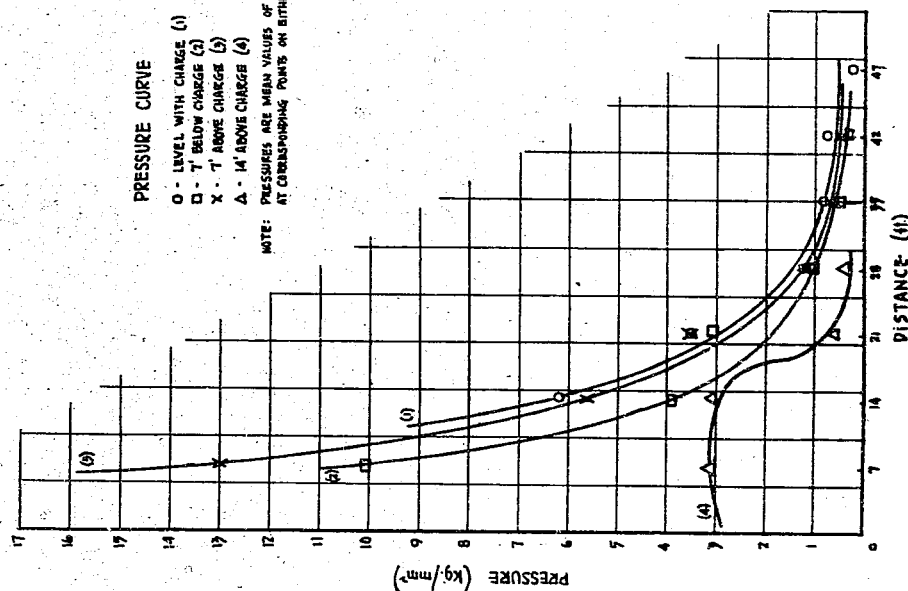
DIAGRAM OF THE HOLE (measured) AND COLLAPSED AREA (water line)



PRESSURE CURVE

- O - LEVEL WITH CHARGE (1)
- - 1' BELOW CHARGE (2)
- X - 1' ABOVE CHARGE (3)
- Δ - 14' ABOVE CHARGE (4)

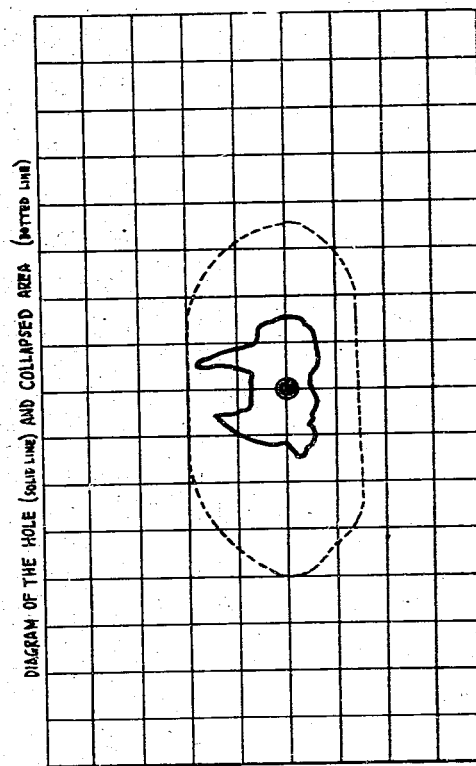
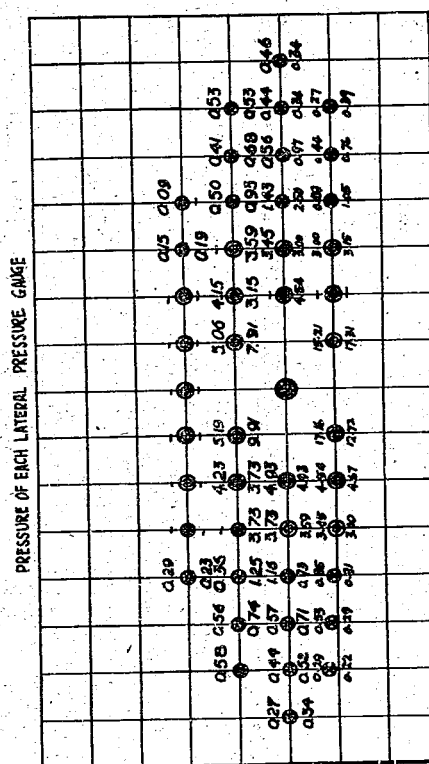
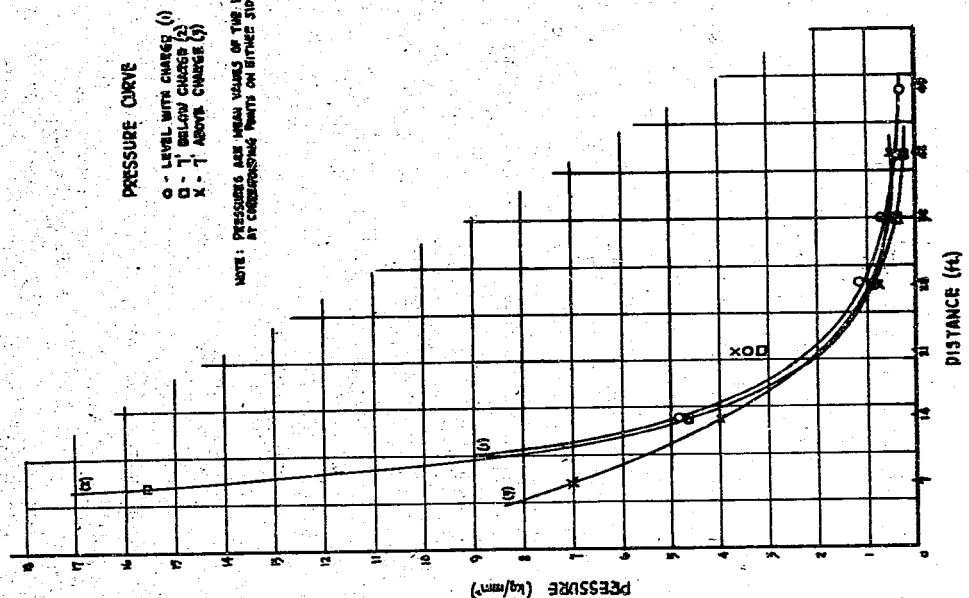
NOTE: PRESSURES ARE MEAN VALUES OF THE MEASURED PRESSURES AT CORRESPONDING POINTS ON EITHER SIDE OF THE CHARGE.



ENCLOSURE (A), continued

Table IV(A) (Test No. 31)

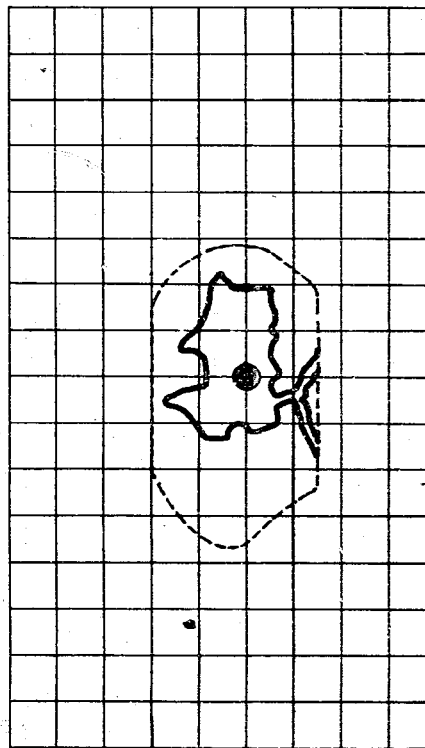
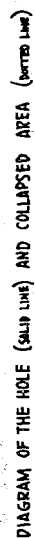
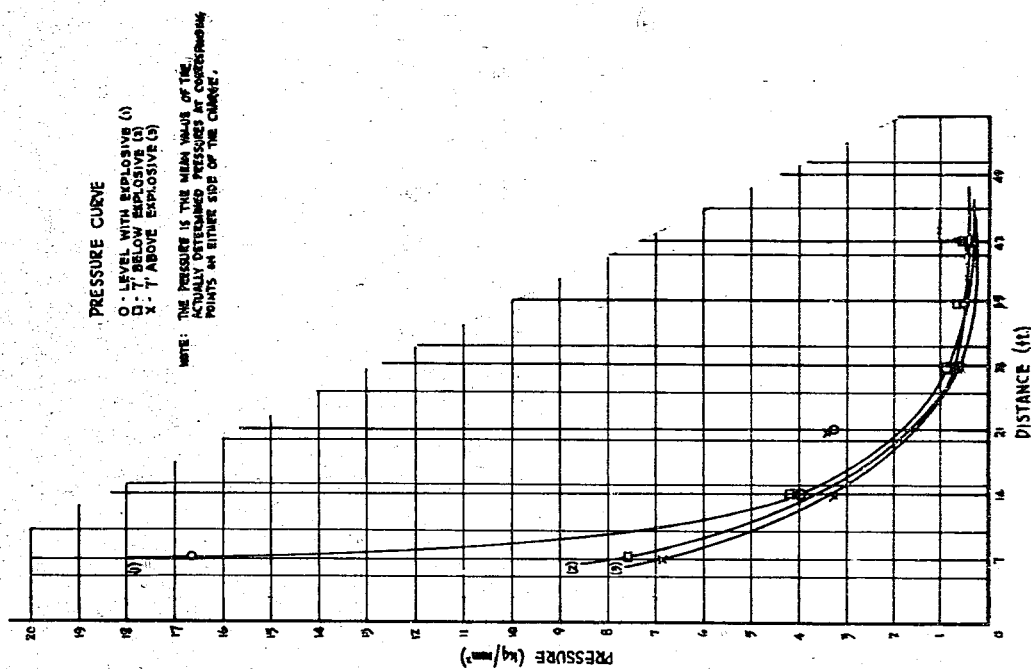
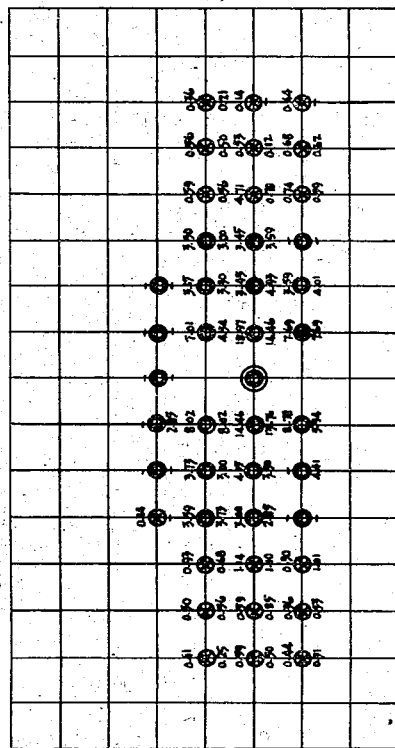
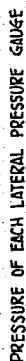
Location	Starboard side F.192, 10'0" above keel
W.T. of place of experiment (before the experiment)	23'3 1/4"
Amt. of charge	8th year type torpedo (300kg)
Method of detonation	Actual firing.



ENCLOSURE (A), continued

Table III(A) (Test No. 2)

Location	Port side F.87. 10'0" above the keel
W.L. of place of experiment 23'3"
Amt. of explosive 6th year type torpedo (200k)
Method of firing Actual firing.



ENCLOSURE (A), continued

Table VI(A) (Test No. 5)

Location Starboard side F.87, 5'0" above keel
 W.L. of place of experiment (before the experiment) 25'9"
 Size of charge 9th year type mine (150k)
 Method of detonation Electrically fired (2 electric fuzes -
 small generator type - in parallel).

PRESSURE OF EACH LATERAL PRESSURE GAUGE

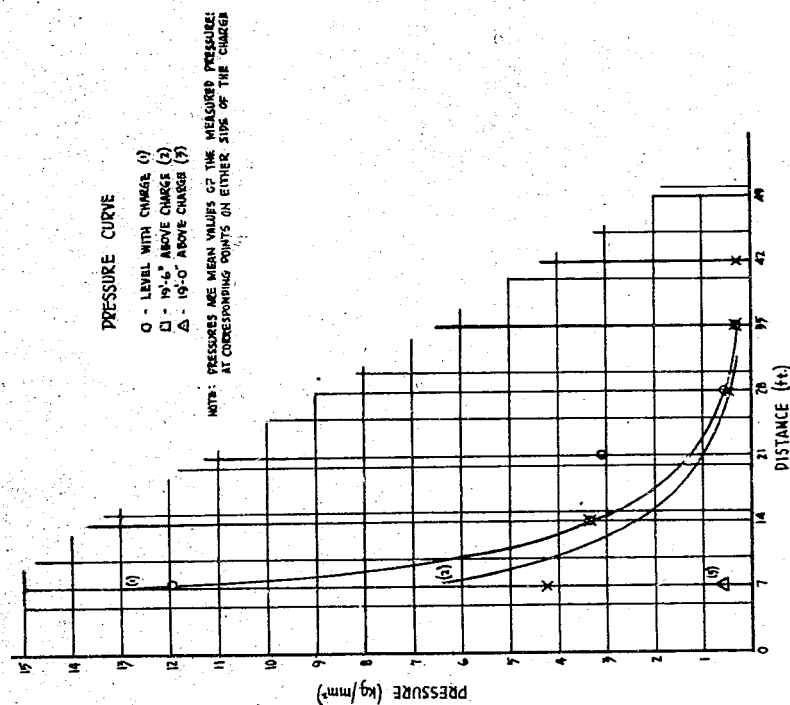
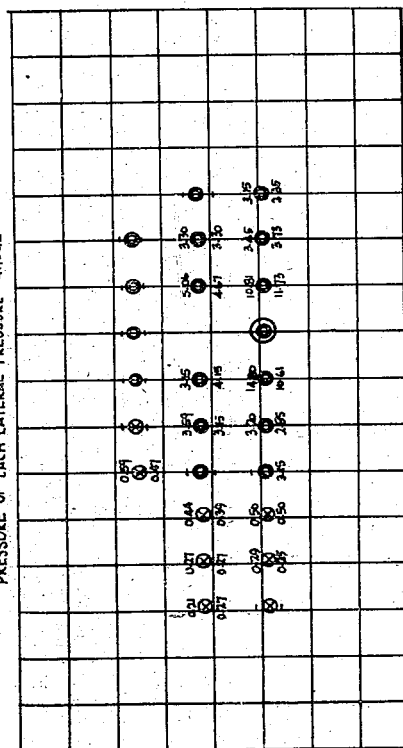
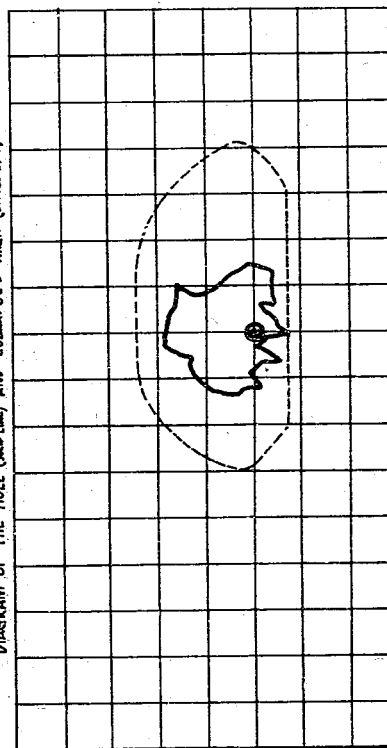


DIAGRAM OF THE HOLE (SEE LINE) AND COLLAPSED AREA (DOTTED LINE)



ENCLOSURE (B)

SUMMARY OF TESTS ON V WARHEAD
(1/5 Test Torpedo Model)

LIST OF ILLUSTRATIONS

Figure 1(B)	V Warhead Test Set-Up	Page	214
Figure 2(B)	V Warhead Test Model	Page	215
Figure 3(B)	Full Charge and Aperture Type Charges	Page	215
Figure 4(B)	A and B Model V Attachments	Page	216
Figure 5(B)	V Attachment Models	Page	216
Figure 6(B)	Damage to 5.36 A Model	Page	216

ENCLOSURE (B), continued

Classified: Top Secret E

Dated: 23 August 1943

By: Technical Lt. NAKADA

With Conical Aperture in Warhead

With Funnel-Shaped Cover on Warhead Conical Aperture

Experiments on the V Warhead, using small scale test models, were made in the Second Naval Powder Depot and the Physics Research Depot of the Technical Research Laboratory. In the light of the results attained there, experiments were then made with the 1/5 test model on 20 and 21 August 1943 in Yokosuka Harbor.

After securely fixing the V Warhead to the center of the target, it was exploded by an electric firing wire which led from a 100 ton floating crane.

The depth of the V Warhead and the center of the target were both 1.4 meters (equivalent to 7 meters).

The plate was DS and without seams. There was one thickness of plate and a layer of water and the distance between plates was 1/5 of the COLORADO type.

Structure of the V Warhead

There are two types: (a) Explosive aperture
(b) V metallic attachment

(a) Explosive aperture: With 3.445 kg of Type 97 explosive the total weight is about 400 kg.

(b) V Metallic attachment: The material for the V metallic attachment is SF54 and is hollowed out. There are two models A and B, but since the results for Model B were not satisfactory, in the small test model experiments, only Model A was experimentally used. For example, 5.36.3 A model was a 1/5 model. Aperture angle on V metallic attachment was 36°. Ratio of input of explosive to total weight was 0.3. Metallic type is the Model A. Moreover, total weight of explosive and V metallic attachment was always 3.5 kg as described above. That is, the weight of the explosive is decreased only by the weight of the metallic attachment.

Experimental Results

(a) Full charge model: Explosive aperture models were substantially alike with no outstanding differences.

- No. 1, 2 Plates: Both burst; scattered without any remains recognizable.
- No. 3 Plate: Openings cut into the plate at the edges of the parts. Do not correspond to the upper void indentations.
- No. 4 Plate: Same as above for void. Frame rivets attached to it were cut. Openings. Indentations.
- No. 5 Plate: Indented.
- No. 6 Plate: Almost no damage.

However, in the target used in the experiments with the full charge model there was an electric contact cord at the section that corresponded to the upper void. By chance, the cord split open. For this reason, the rivets

ENCLOSURE (B), continued

attached to the upper edges of No. 6 plate also were cut.

(b) Warhead, V type metal fitting: Both very similar. Compared with the full charge type of 3.5 kg, the complete damage of the target is decreased. That is to say, the No. 1 and No. 2 plates are damaged and blown off. The No. 3 and No. 4 plates are dented in and the upper perimeter of the hole becomes somewhat smaller. The dent in the No. 5 plate is very small. However, projectiles made with the V type metal fitting made a big hole in even the No. 6 plate and had some penetrating power remaining.

5.36.3 A Model:

- No. 1 and No. 2 Plates: Completely blown off.
- No. 3 Plate: Upper rim blown open and out; dented in. There was hole of about 150mm diam. in center.
- No. 4 Plate: Same as above.
- No. 5 Plate: Center hole about 210mm x 50mm.
- No. 6 Plate: Center hole was 70mm diam. Small melting traces noted around its edges.

After the projectile has penetrated the No. 6 plate, reaches the attached frame and recoils, it scarcely projects from the back of the No. 6 plate. It produces on the attached frame about eight melting traces. When the projectile collides with the frame, the nose changes shape.

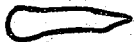
5.36.4 A Model: Almost the same as above. But a piece of wood is affixed to the front of the frame and keeps it from damage.

The projectile penetrates the timber and its tip reaches the frame. The head of the projectile is destroyed and remains in the timber.

Comparing this and 5.36.3 A Model, although the entire damage to the target is about the same, the hole in the No. 3 plate is small. The diameter of the hole in the innermost plate is large.

Opinion

(This is a private opinion on the result of the experiments on the warhead with V metallic attachment).

The A Model projectile shaped by the V metallic attachment was deformed as shown: 

It may have been caused by the projectile reversing its direction. After examining the hole in the plate and comparing it with the projectile of a cannon, it seems to break through after being shattered and the ballistic characteristics are inferior. Furthermore, judging from the great change inflicted upon the shape when striking the frame, and by the destruction of the head, there is some question that it can be developed effectively as a weapon against the thick armor of ships as it had against many layer plates in this experiment. This experiment is only in case of direct attack, and in accordance with technical research, even though it is clear there is no difference in the attacking power in a 1/10 model up to 0 - 30°, there is some question about the attacking power in case of a large attack angle.

Additional Note

It is anticipated that an experiment will be carried out on a small scale model in the near future for the case of large angle firing.

ENCLOSURE (B), continued

Concerning the V metallic attachment materials, although the SF 54 used is thought sufficiently strong and most suited, it would be a good idea to conduct research using various other materials.

In the 1/10 model, the B Model projectile was clearly inferior to the A Model in penetrating power.

Again, the fact that the angle of entry is small has nothing to do with the size or length of the shell. The direction of the trajectory is bad. The projectile from the pressure of the explosion appears solid; and, although it is melted and fused, and shaped as described above, the fact that it leaves a hole in the center about 1/15 the outer diameter is evident in the small A Model.

In regard to the shape of the exploded hole, the results of the research in No. 2 Arsenal are as follows:

"With the impulse wave in a vertical plane to the powder surface, just as if there were a hollow cone-shaped hole, there is a point which might be called a focus. It is clear that in the direction of the hollow cone-shaped hole the impulse wave and the explosion were effective. However, no difference can be found in this test."

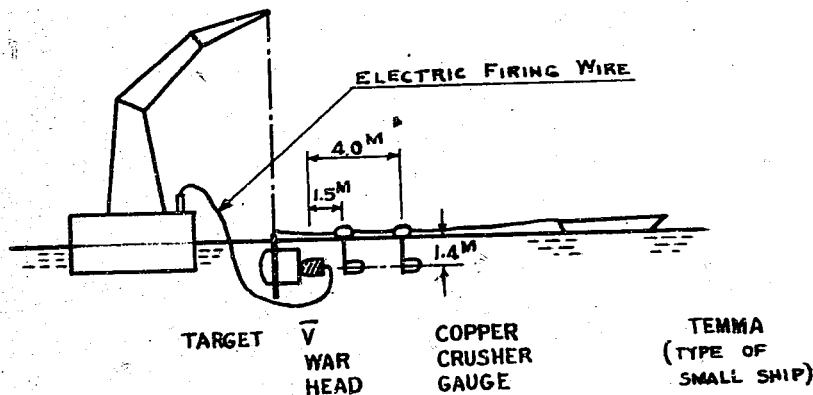


Figure 1(B)
V WARHEAD TEST SET-UP

ENCLOSURE (B), continued

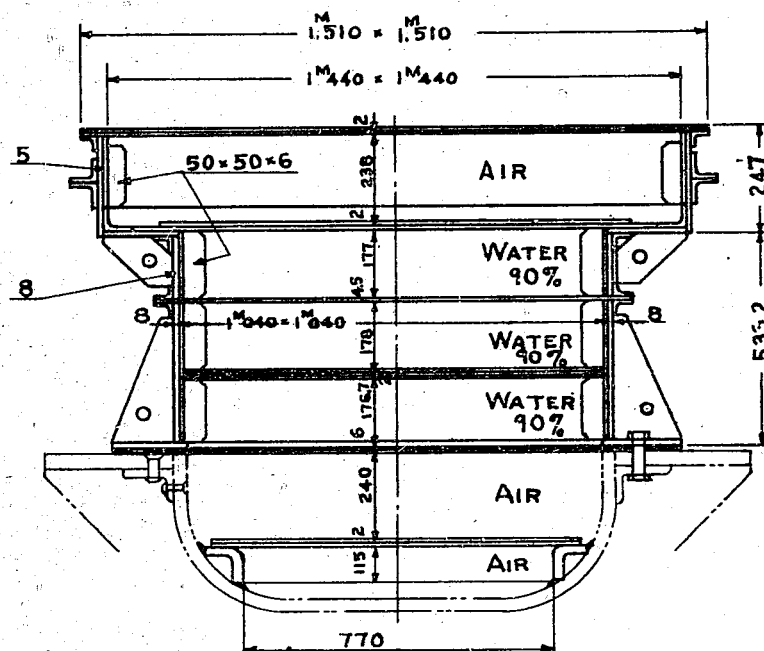
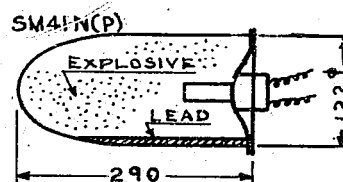


Figure 2(B)
V WARHEAD TEST MODEL



APERTURE TYPE

ALTHOUGH THE WEIGHT OF THE EXPLOSIVE IS THE SAME AS IN THE FULL CHARGE MODEL (3.445 kg), THERE IS A CYLINDRICAL APERTURE ON THE NOSE.

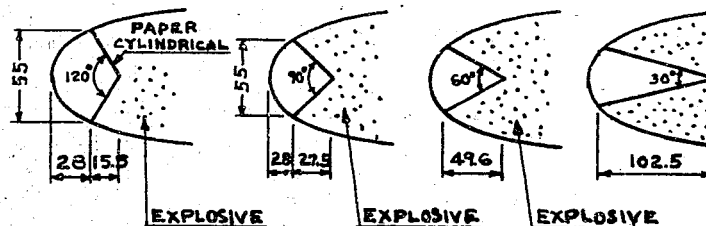


Figure 3(B)
FULL CHARGE AND APERTURE TYPE CHARGES

ENCLOSURE (B), continued

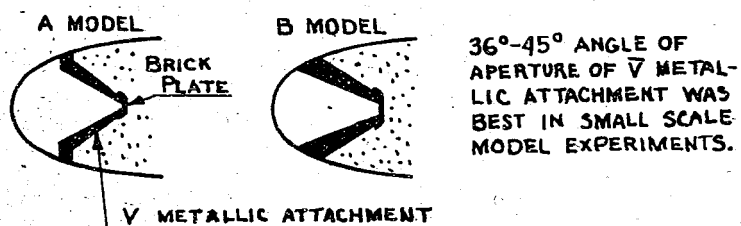
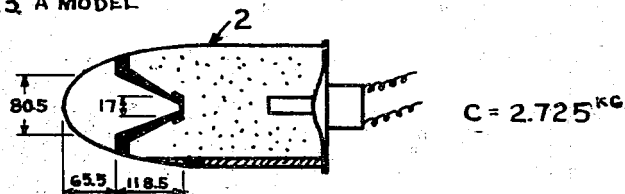


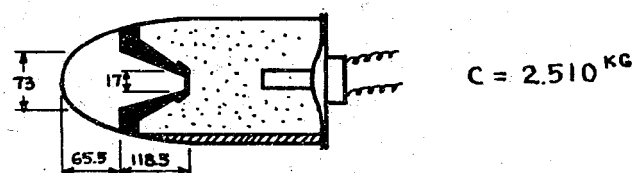
Figure 4(B)

A AND B MODEL V ATTACHMENTS

5.36.3 A MODEL



5.36.4 A MODEL



5.45.3 A MODEL

C = 2.690 KG

Figure 5(B)

V ATTACHMENT MODELS

5.36.4 A MODEL

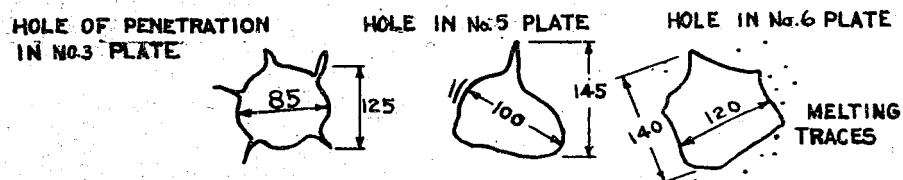


Figure 6(B)

DAMAGE TO 5.36.4 A MODEL

ENCLOSURE (C)

CHART OF DEVELOPMENTS OF TESTS ON UNDERWATER DEFENSE (IN JAPAN) - SHEET 1

Bulletin and Notification No.	Date of Execution	Report* Number	Scale	Explosive** Side or Charge (kg) Bottom	Contact or Distant (m)	Number of Targets	Important Points of Test	Place of Test
23 March 1915 Secretariat, Top Secret No. 385	June 1915		1/1	200	Contact	3	Defensive strength of KMS deck; Defensive strength of outer plates; Effect of defense with air layers.	YOKOSUKA
6 Oct. Secretariat, Top Secret No. 1221	Jan. 1916		1/1	200	Contact	2	Defensive strength of HT plates.	YOKOSUKA
1 Nov. 1916 Secretariat, Top Secret No. 1334	Sept. 1917		1/1	200	Contact	MAGATO Model 1	Defensive strength of MAGATO Class.	YOKOSUKA
25 May 1922 Secretariat, Top Secret No. 792	From July 1922 to Nov. 1923		1/3 1/2	9 (200) 30 (200)	Contact Contact	12 2	Using protective pipes; Cement on 3 sides in front of protective plates; Defensive strength of model 1/3 size of MAGATO Model	YOKOSUKA
12 Nov. 1924 Secretariat, Top Secret No. 1314	Jan. 1925		1/3	9 (200)	Contact	4	Distance between explosive and defensive plate and relation to thickness of defensive plate.	YOKOSUKA
4 Sept. 1925 Secretariat, Top Secret No. 1078	From Nov. 1925 to Feb. 1926		1/3	9 (200)	Contact	4	Thickness of defensive plate when distance between plate and explosive is small.	YOKOSUKA
15 Jan. 1924 Secretariat, Top Secret No. 34	June 1924	Nov. 1924 (No number)	1/1 1/1 1/1	100 mine 150 mine 200 torpedo 250 torpedo 300 torpedo 370 bomb	Contact Contact 5-0 Distant	Discarded vessel (TUSA)	Defensive strength and damage of TUSA.	HIROSHIMA Bay
12 July 1926 Secretariat, Top Secret No. 694	Aug. to Sept. 1927		1/3	9 (200)	Contact	3	Protective strength of outer plates of DS; Effect of DS defensive plate using air layers. (GT with KX)	YOKOSUKA
Navy Technical Dept., No. 2 section in charge	From Nov. 1929 to August 1930		1/3	9-5.431 (200-121)	Contact	20	Special torpedo head test. Conducted by changing the oblique angle on the standard made English and American types.	YOKOSUKA
16 Jan. 1935; Navy Tech. Dept., Top Secret No. 411 and 2 April 1936 Navy Tech. Dept., Top Secret No. 4396	From Feb. 1936 to Sept. 1936		1/5.35	1.7 (200)	Contact	69	Measurement of model and amount of explosives. Volume of air space between outer plates and defensive plates and its protective effect.	Technical Research
			1/5.83	1.7 (200)	Contact	6	Research on ship-sides protective methods using layers of water.	Technical Research
Sept. 1935 Secretariat, Top Secret No. 2137	Dec. 1935	May 1936 Colonel Arsenau, Top Secret No. 158	1/3	9 (200)	Contact	1	Defensive strength of shell and powder magazine floor of BB's.	YOKOSUKA
			1/3	9 (200) 5.35 (200) 3.25 (20)	Distant 1,600 (4,74)	3	Defensive strength of boiler room of BB's (60% water in inner bottom)	YOKOSUKA

ENCLOSURE (C), continued

CHART OF DEVELOPMENTS OF TESTS ON UNDERWATER DEFENSE (IN JAPAN) - SHEET 2

Bulletin and Notification No.	Date of Execution	Report* Number	Scale	Explosive** Charge (kg)	Side or Bottom	Contact or Distant (m)	No. of Targets	Important Points of Test	Place of Test
28 July 1936 Secretariat, Top Secret No. 1873	Nov. 1936	Sept. 1937 Yokosuka Arsenal, Top Secret No. 177 (*1)	1/3	9 (200)	Side	Distant 2,000	1	Underwater defensive strength against bombs of American BB (laminated protective plates)	YOKOSUKA
	Dec. 1936	Sept. 1937 Yokosuka Arsenal, Top Secret No. 177 (*1)	1/3	9 (200) bomb	Side	Distant 1,500	1		
	Feb. 1937	Sept. 1937 Yokosuka Arsenal, Top Secret No. 177 (*1)	1/3	9 (200) bomb	Side	Distant 0,500	1		
	May 1937		1/3	18 (400) bomb	Side	Contact (Depth) 1,500	1		
	July 1937		1/3	18 (400) bomb	Side	Contact (Depth) 2,180	1		
23 Aug. 1937 Secretariat, Top Secret No. 3316	Jan. 1937		1/7.35	0.7 (200)	Bottom	Contact	3	Ship-bottom contact using water layers.	Technical Research
	Feb. 1937		1/7.35	0.7 (200)	Side	Contact	3	In order to compare with Jan. 1937 test.	
	From 1937 to 1939	From Research No. 643 (*1) Tech. Research No. 114	1/5.35	1.7 (200)	Side	Contact	26	Defensive strength of water layers. Quality and strength of protective plates. Effect of laminated protective plates. Depth of target. Methods of equipping targets. Adjacent compartments and protective strength. Defense of ship's bottom.	Technical Research 25 YOKOSUKA
			1/2.97	9 (200)	Side	Contact	11		
			1/5.35	1.7 (200)	Bottom	Contact and Distant	5 3		
5 Dec. 1939 Secretariat, Top Secret No. 7535	April 1940	20 May 1941, Yokosuka Arsenal, Top Secret No. 6139 (*1)	1/2.97	18 (400)	Side	Contact	2	Investigation of the relation between the amount of explosive charge and the effective thickness of the water layers	YOKOSUKA
	June 1940		1	200	Side	Contact	1	Real vessels using water layers.	
	Aug. 1940		1	400	Side	Contact	1		
			1/5.35	1.7 (200)	Bottom	Distant	2	Distant explosions using water layers	YOKOSUKA
	Sept. to Oct. 1940								
13 June 1940 Secretariat, Top Secret No. 4125	From Jan. 1941 to April 1941	28 Aug. 1941, Tech. Report No. 0113 (*1) Tech. No. 140	1/7.31	0.7 (200)	Bottom	Distant	1	Distant explosions using water layers (preliminary of first test to be held in 1941).	Technical Research
			1/7.31	1.24 (350)	Bottom	Distant	1		
			1/7.31	1.75 (500)	Bottom	Distant	1		
	June, July 1941		1/2.97	15.75 (350)	Bottom	Distant	3	Escape from explosion using water layers.	YOKOSUKA
			1/2.97	20.25 (450)	Bottom	Distant	1		
6 May 1941 Navy Tech. Report No. 3974 of No. 1 (1st phase in 1941)			1/2.97	18.0 (400)	Bottom	Distant	3		
			1/2.97	11.25 (250)	Bottom	Distant	1	Escape from explosion using water layers. (Distance is 1/2).	YOKOSUKA
			1/2.97	13.50 (300)	Bottom	Distant	1		
			1/2.97	15.75 (350)	Bottom	Distant	1	Escape from explosive not using water layers.	YOKOSUKA

ENCLOSURE (C), continued

CHART OF DEVELOPMENTS OF TESTS ON UNDERWATER DEFENSE (IN JAPAN) - SHEET 3

Bulletin and Notification No.	Date of Execution	Report* Number	Scale	Explosive** Charge (kg)	Side or Bottom	Contact or Distant	No. of Targets	Important Points of Test	Place of Test
3 May 1941 NavTech Dept., Top Secret Report No. 3895 of No. 4 (2nd phase in 1941)	Aug., Sept. 1941		1/2.97	22.14 (490)	Side	Contact	3	Investigation of the effect of different type of torpedo warheads while using water layers.	YOKOSUKA
			1/2.97	21.15 (470)	Side	Contact	1		
			1/2.97	9 (200)	Side	Contact	2	Effect in defensive plates, using water layers (one bow-shaped and one straight model).	
26 April 1941 NavTech Dept., Top Secret Report No. 3740 of No. 4 (3rd phase in 1941)	Incomplete		1/5.35	1.7 (200)	Bottom	Distant	2	Effect on main sea-water pipe valves and condensers according to differences in condition of main sea-water connecting pipes.	Tech. Research
24 June 1941 NavTech Dept., Top Secret Report No. 5708 of No. 4 (4th phase in 1941)	Sept., Oct., Nov., Dec. 1941 Jan., Feb. 1942		1/2.97	4.5 (100)	Side	Contact	2	Effect of method of using several water layers when the air layers are fired. Comparison of defensive strength when the explosive force passes through air layers in front of protective plates and into the ocean and when construction is such that the effects are not so dissipated.	YOKOSUKA
			1/2.97	6.5 (150)	Side	Contact	2		
			1/2.97	9.0 (200)	Side	Contact	2		
			1/2.97	11.25 (250)	Side	Contact	1		
			1/2.97	15.75 (350)	Side	Contact	2		
			1/2.97	20.25 (450)	Side	Contact	2		
28 Feb. 1942 NavTech Dept., Top Secret Report No. 1094 of No. 4 (5th phase in 1941)	April 1942		1/2.97	27.0 (600)	Side	Contact			YOKOSUKA
25 Feb. 1942 NavTech Dept., Top Secret Report No. 2002 of No. 4 (6th phase in 1941)	May 1942		1/2.97	9.0 (200)	Bottom	Contact	3	Investigation of the effect of flooding the heavy deck under the powder magazine against setting off the charge in the powder magazine.	YOKOSUKA
			1/2.97	3 (66.7)	Side	Contact	2	Things which will affect protection of light oil tanks against under-water explosion.	

*The number in parenthesis is the custody No. of the Naval Tech. Dept., Dept. 4.

**The number in parenthesis is the full scale charge.

ENCLOSURE (D)

DISCUSSION ON THE USE OF PROTECTIVE PLATING AGAINST TORPEDO ATTACK

LIST OF ILLUSTRATIONS

Figure 1(D)	Failure in Plate Near Lap Joint.....	Page 223
Figure 2(D)	No. 1 - No. 5 Cross Sections.....	Page 226
Figure 3(D)	Case 1 - Water Inboard of Protective Bulkhead.....	Page 227
Figure 4(D)	Case 2 - "Sandwich" Protection.....	Page 227
Figure 5(D)	Example 4.....	Page 229
Figure 6(D)	Solution to Example 4.....	Page 229
Figure 7(D)	Example 5.....	Page 230
Figure 8(D)	Example 6.....	Page 233
Figure 9(D)	Positions of Charges.....	Page 234
Figure 10(D)	Test Model Structural Features	Page 235
Figure 11(D)	Relation Between Volume, Thickness of Protective Plate and Bulge Width.....	Page 238
Figure 12(D)	Effective Charge vs. Utilization Coefficient.....	Page 239
Figure 13(D)	Anti 200 kg Depth Charge Armor.....	Page 240
Figure 14(D)	Anti 250 kg Depth Charge Armor.....	Page 241
Figure 15(D)	Anti 350 kg Depth Charge Armor.....	Page 242

ENCLOSURE (D), continued

These views are not the result of organized research, but are simply based on past experience. They are not, therefore, necessarily accurate but have been gathered together before the material is lost.

CHAPTER IA. Relation Between the Strength of the Protective Plating and Izod Value

It is stated in the report of the Naval Technical Laboratory on protective plating that plating with a low Izod value is very easily destroyed by the force of an explosion. Therefore, impact tests are always made on any steel to be used for protective bulkheads, and those materials which fail to reach a certain standard are naturally rejected. In particular, if the impact test is omitted, it is extremely difficult to determine the most suitable plate thickness as the errors may be introduced into the experimental results.

H T steel has an Izod value of 30 ft - lbs or more. There are, however, many steels with an Izod value of 6 ft - lbs but which cannot be distinguished as far as ultimate tensile strength and elasticity are concerned. Material for protective bulkheads should have an Izod value of over 30 ft - lbs. Material with Izod values below 16-18 ft - lbs is useless for protective bulkheads.

B. Suitability of Welding for Protective Plating

Although it has been claimed that welding is stronger than riveting for resistance to explosion, experience at the Kure Arsenal indicates that the opposite is probably true. This has recently been tested there. Welded sections have extremely low Izod values and blowholes must not occur or a stress may be induced. For these reasons, welding will always have a weakness against an impact such as an explosion, which makes it difficult to believe that it is better than riveting. In plating in actual use the explosive force might be reduced, or else it may be possible to make arrangements to apply a certain amount of elasticity before the plating is destroyed. Where there is any difference in the characteristics of protective plating, it certainly cannot be said that welded plate is better.

To summarize it is certainly advisable to use riveting on protective plating under present conditions.

C. Destruction of the Protective Bulkhead

1. Plating which shatters like glass or from which a piece breaks cleanly, or which cracks like glass is in general of low impact value and useless.
2. The outer bottom etc. does not always break at the point of weakest strength, when attacked by an explosion. Instead it often breaks at unforeseen places such as the laps where two plates join (see Figure 1(D)). In other words the weak points are the joints which may be opened unexpectedly.

ENCLOSURE (D), continued

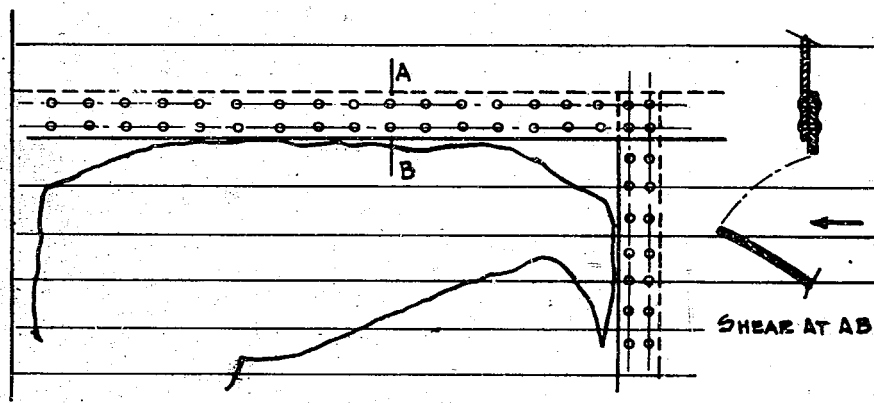


Figure 1(D)

FAILURE IN PLATE NEAR LAP JOINT

3. At the time of the explosion the surrounding structure may be broken up into fragments which may cause dents, blisters or small holes in the protective bulkhead.

In general, when the distance between the outer bottom and the protective bulkhead is about 4 ft 6 in, the latter is damaged by explosive pressure; when the distance is 10 ft small holes are caused by splinters. It would, therefore, appear that between 4 ft 6 in and 10 ft damage to the protective bulkhead would be caused by both explosive pressure and splinters. However, the effect of splinters is fairly small in general.

In order to reduce damage to the protective bulkhead by flying splinters, rows of pipes may be installed and thus permit reduction of the thickness of the plating. When water or oil is used instead of pipes, not only is splinter damage prevented, but transmitted pressure is weakened by diffusion, permitting a great reduction in protective plating thickness. If the space between the outer bottom protective bulkhead is 10 ft 10 in and is empty, a thickness of 3 in is necessary to withstand the explosion of 200 kg. of picric acid. However, if water or oil is contained in a tank about 3 ft thick outside the protective bulkhead, the thickness of the bulkhead can be reduced to 1.5 in. Furthermore, if a similar tank of water or oil is located inboard of the protective bulkhead, the thickness of the plate may be further reduced or the width of the bulge decreased.

Further research should be carried out on liquid layer protection.

4. According to the experience on TOSA, the size of the hole made in the skin of a ship with the present form of bulge is as follows:

<u>Explosive Charge (kg)</u> (Picric Acid)	<u>Area of Hole (Ft²)</u>
100	240
150	190
200	240
300	160
350	280

ENCLOSURE (D), continued

Table I(D)
RESULTS OF MODEL TESTS

Model No.	Depth of Explosion	Distance Between Outer Bottom & Protective Bulkhead	Double Bottom Thickness	Thickness of Protective Bulkhead	Damage Condition	Dimension of Target			Volume of Air Space per kg of Explosive
						Length	Width	Vol. Ft. ³	
9 kg, A	15'0"	1'4 1/2"	None	60 lbs	Best 5-1/8" Left Margin	7'0"	7'0"	67.5	8.8
9 kg, B	7'6"	2'1 1/2"	None	60 lbs	Small rip Small holes Splintering	9'0"	9'0"	172.0	22.3
9 kg, A	14'4"	3'3"	5 lbs	40 lbs	Hole	7'0"	7'0"	159	20.6
9 kg, B	5'0"	3'3"	5 lbs	40 lbs	3 1/2" O K	7'0"	7'0"	159	20.6
9 kg, 3-2	5'0"	8 1/2"	None	70 lbs	6 1/2" O K	7'0"	6'6"	31.3	5.95
9 kg, 3-3	5'0"	4'3-1/8"	5 lbs	35 lbs	2 small holes	6'6"	7'0"	194.5	25.2
9 kg, 3-4	5'0"	5'3-3/8"	5 lbs	27 lbs	5 small holes	6'6"	7'0"	240.0	31.2
9 kg, 4-1	5'0"	4"	None	90 lbs	Large tears	6'6"	7'0"	15.2	19.2
9 kg, 4-2	5'0"	0	None	120 lbs	Large tears	6'6"	7'0"	0	0
9 kg, 4-3	5'0"	4"	None	100 lbs	9 1/2" O K	7'0"	6'6"	15.2	19.2
9 kg, 4-4	5'0"	0	None	160 lbs	8-5/4" O K	7'0"	6'6"	0	0
9 kg, Special 3	5'0"	1'9"	None	with pipes 40 lbs	4-9/16"	4'6"	7'0"	55.0	7.15
9 kg, Special 2	5'0"	2'3 1/2"	None	with pipes 30 lbs	4"	5'3"	7'0"	83.5	10.9
1.7 kg	3'4"	5'8 1/2"	2mm	with water 8mm	Perfect	40"	40"	18.88	14.8
1.7 kg	4'0"	2'0"	None	13.9mm	2 small holes	40"	40"	22.22	17.5
1.7 kg	4'0"	2'0"	None	21.69mm	Destroyed	40"	40"	12.93	10.4
100 gr.	3'3"	172mm	None	5.1mm	Perfect	320mm		3.00	
100 gr.	3'3"	172mm	None	6mm	Perfect	320mm		2.50	
9 kg	5'0"	3'3 1/2"	5	34 lbs	Small 4" holes	7'0"	7'0"	160	20.8
Special 1	15'0"	2'3 1/2"	None	with pipes 30 lbs	Great Destruction	5'0"	7'0"	79.5	10.4

ENCLOSURE (D), continued

D. Relation Between Explosive Force and Column of Air Space

Experiments have shown that there is a very close connection between explosive force and volume of the space between outer bottom and protective bulkhead. For a charge of 17 kg if the volume of the air space is 17.5 cubic feet, a plate 14.2mm thick can resist it; but if the air space is reduced to 10.4 cubic feet 21.6mm of plate will be defeated by it.

If the distance between the outer bottom and protective bulkhead is increased, keeping the volume of the air space constant, the necessary thickness of the protective bulkhead is not reduced. If, however, the air space volume is simultaneously increased, the thickness of the bulkhead may be materially reduced.

If the air space volume is increased without a proportionate increase in thickness of bulge, little effect is observed. For example: If the distance is 3 ft there will be almost no difference in the thickness of the bulkhead if the air space volume is increased from 300 to 600 cubic feet.

Further work on this subject is necessary.

CHAPTER II

A. Use of Bulge as a Protection Against Torpedoes

This bulge was 21.8 ft across with each compartment 16 ft long and provided 50% protection against a 200 kg charge. In practice even though three compartments may be destroyed, the explosive gases are more or less restricted by rupturing the transverse bulkhead of one compartment. Therefore, when this bulge is used, if the transverse bulkheads are of ordinary thickness plate the following volumes are suitable against one kg of powder.

Table II(D)

Transverse Bulkhead Spacing (ft)	Length of Bulkhead Determining Volume of Space per kg of Charge		
	L. (ft) (200 kg)	1.077 L (250 kg)	1.205 L (350 kg)
12	29	31.2	35.0
16	32	34.4	38.6
20	35	37.7	42.2
24	38	41.0	45.8
28	41	44.1	49.5

When there are full tanks on both sides or when the transverse bulkheads are specially thick, the explosive gases are further restricted. Therefore, when these compartments are not as long as those just described the volume should be computed from their length.

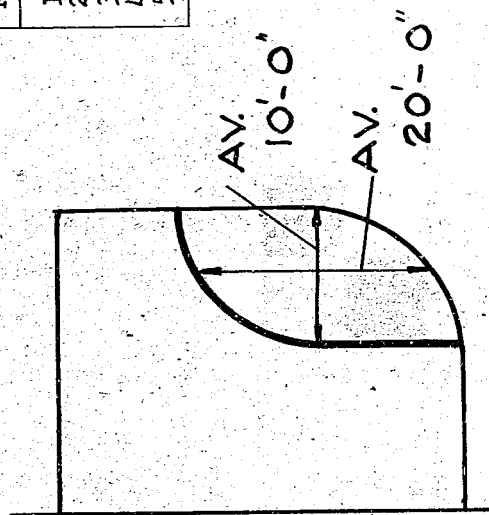
Example 1. What thickness of protective bulkhead of the type shown in Figure 2(D) will withstand 200 kg and 350 kg torpedoes?

Volume per kg explosive at No. 1 is shown in Table II(D).

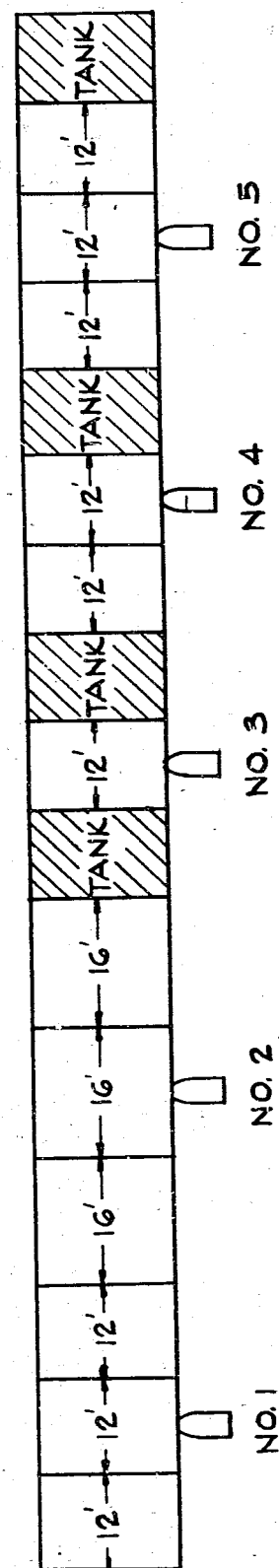
$$\text{Against 200 kg explosive} = \frac{10 \times 20 \times 29}{200 \text{ kg}} = 29 \frac{\text{ft}^3}{\text{kg}}$$

Table III(D) - SOLUTION FOR EXAMPLE 1

Shot No.	Explosive Weight 200 kg		Explosive Weight 350 kg	
	Vol./kg (ft ³ /kg)	Thickness of Protective Bulkhead (lbs)	Vol./kg (ft ³ /kg)	Thickness of Protective Bulkhead (lbs)
1	29	114	20	146
2	35	113	22	145.5
3	12	128	6.9	166
4	24	116	13.8	154
5	29	114	20	146

Figure 2(D)
NO. 1 - NO. 5 CROSS SECTIONS

NO. 1 - NO. 5 CROSS SECTION



ENCLOSURE (D), continued

$$\text{Against 350 kg explosive} = \frac{10 \times 20 \times 35}{350 \text{ kg}} = 20 \frac{\text{ft}^3}{\text{kg}}$$

Necessary thickness of plate: For 200 kg when the distance between skin and protective bulkhead is 10 ft 0 in at 29 cubic feet per kg, the thickness is 114 lbs.

Similarly from Figure 15(D) thickness is 146 lbs per 360 kg. Volume of air space for shot No. 2 is similarly computed from Table II(D).

No. 3 and 4 are smaller than the values based on Table II(D) because they are bounded on both sides by tanks and a corresponding reduction will be made.

In the case of No. 5, there are tanks on both sides, but as the three compartments total 36 ft 0 in the value for both 200 kg and 350 kg will

be greater than that given in Table II(D). The value is, therefore, the same as No. 1.

Example 2. What thickness of protective bulkhead will be necessary to resist 200, 250, or 300 kg torpedoes when the distance between the skin and the plate is 2 ft 0 in and fitted with a splinter preventative?

Using the curves in Figures 13(D), 14(D) and 15(D) we find:

<u>Charge (kg)</u>	<u>Thickness of Protective Bulkhead (lbs)</u>
200	225
250	250
350	290

Example 3. What thickness of protective bulkhead will be necessary to resist 200, 250, or 300 kg torpedoes when the bilge thickness is 9 ft 0 in and fitted with splinter preventative (three rows of pipes or 600mm of water or oil)?

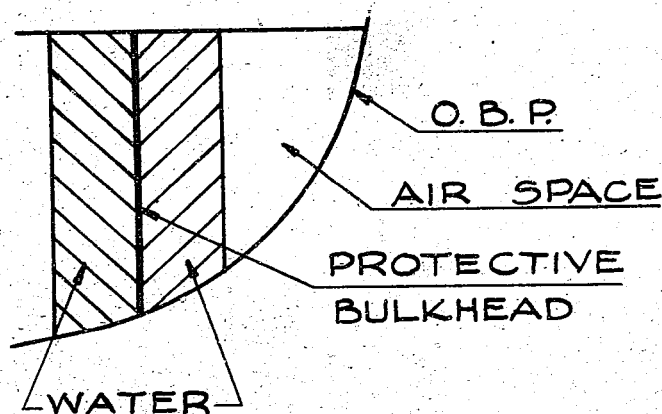


Figure 3(D)

CASE 1 - WATER INBOARD OF PROTECTIVE BULKHEAD

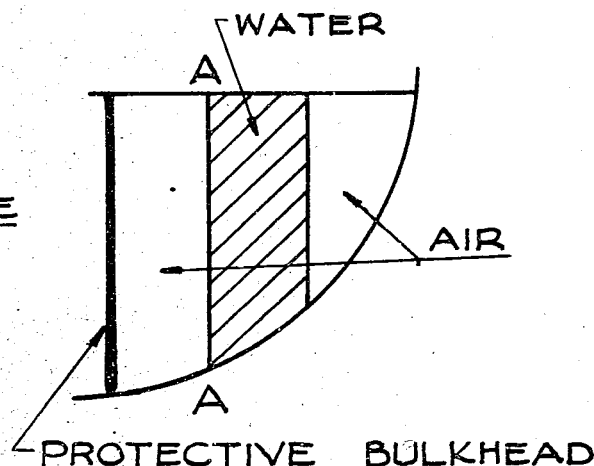


Figure 4(D)

CASE 2 - "SANDWICH" PROTECTION

ENCLOSURE (D), continued

Thickness is found from curves in Figures 13(D), 14(D) and 15(D) as follows:

<u>Charge (kg)</u>	<u>Thickness of Protective Plate (lbs)</u>
200	69
250	79
350	98

Note: These curves should not be used in cases such as the following:

1. Where there is water inboard as well as outboard of the protective bulkhead. In this case the thickness may be reduced to a fraction of the value found from these curves. (See Figure 3(D).)
2. When there is a form of sandwich protection, the thickness of the protective bulkhead must be increased somewhat because splinters may arise from bulkhead AA. (See Figure 4(D).)

CHAPTER IIISCALE MODELS

As has already been described, in making scale models the scale must first be decided with regard to their dimensions. In cases where they are not in contact with oil or water tanks, they may range from one compartment to volumes greater than those shown in Table II(D).

Regarding the scale of the model, provided the distance of the explosion from the protective bulkhead and the volume of the air space are correctly adjusted, small changes in length, height and other measurements may be made.

Example 4. What is the correct charge and thickness of protective bulkhead in a 1/3 scale model of a bulge attacked by a 200 kg charge? (Figure 5(D).)

To determine the amount of charge:

$$\text{Effective charge} = 200 \times (1/3)^3 = 7.407 \text{ kg}$$

According to Figure 12(D) this charge is 0.85 effective. Therefore:

$$\text{Charge to be used} = 7.407 \times \frac{1}{0.85} = 8.75 \text{ kg}$$

$$\begin{aligned} \text{Where: Height } H &= 20' \times 1/3 = 6.67' \\ \text{Length } L &= 16' \times 1/3 = 5.33' \\ \text{Mean Width } B &= 9' \times 1/3 = 3.00' \end{aligned}$$

$$\begin{aligned} \text{Distance between charge and protective bulkhead,} \\ C &= 10' \times 1/3 = 3.33' \end{aligned}$$

$$\text{Volume of one full-scale compartment} = 20 \times 16 \times 9 = 2880 \text{ ft}^3.$$

$$\text{Volume of outer compartment necessary from Table II(D)} = 20 \times 9 \times 32 = 5760 \text{ ft}^3.$$

ENCLOSURE (D), continued

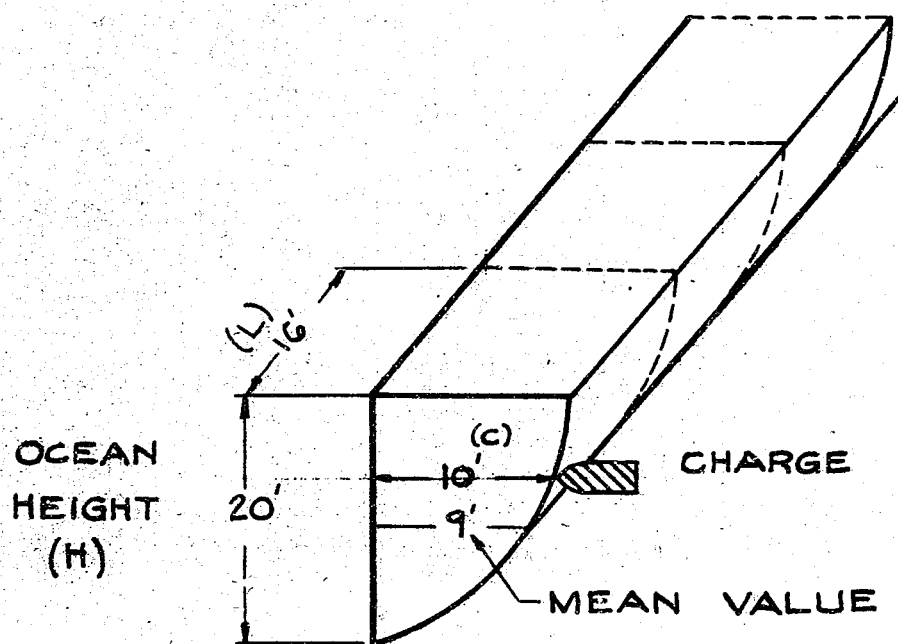


Figure 5(D)
EXAMPLE 4

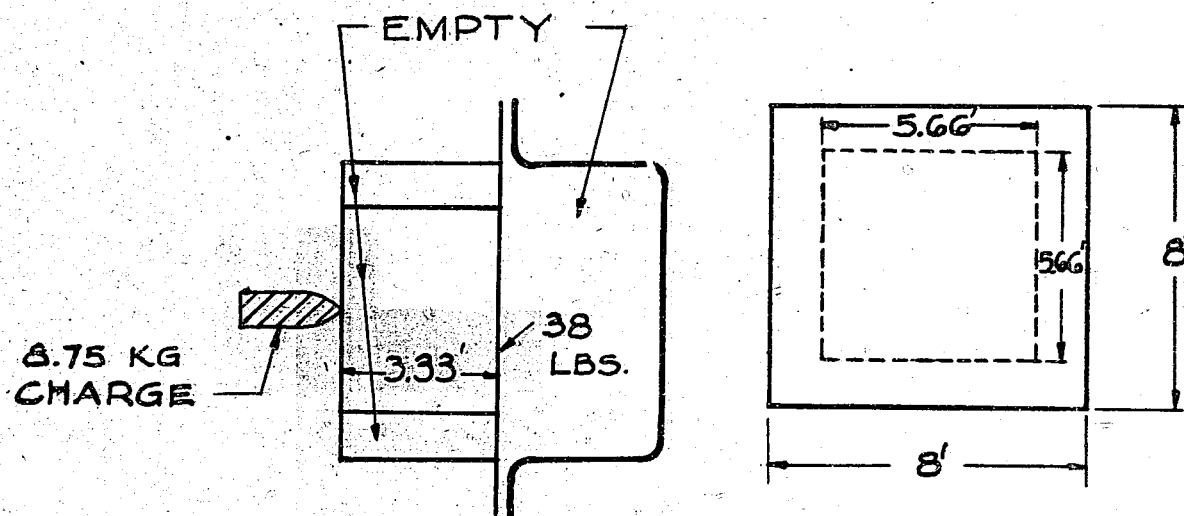


Figure 6(D)
SOLUTION TO EXAMPLE 4

ENCLOSURE (D), continued

Accordingly, the volume for a one kg charge = $\frac{5760}{200} = 28.8 \text{ ft}^3$.

If the model is square, the measurement C is determined as 3.33 ft. Therefore, the height and length of one side of the inner compartment

$$\sqrt[2]{\frac{2880}{10}} \times 1/3 = 5.66'$$

The volume of the outer compartment is 28.8 cubic feet since the charge is one kg and, therefore, for 7.407 kg it will be $28.8 \times 7.407 = 213 \text{ ft}^3$, although a larger volume would be satisfactory. Accordingly, the length of one side of the outer compartment would be:

$$\sqrt[2]{\frac{213}{3.33}} = 8.0' \text{ or more.}$$

As for the thickness of the protective bulkhead, the curve in Figure 13 (D) shows 114 lbs for a distance of 10 ft and a volume of 28.8 cubic feet per kg. Therefore, the scale thickness should be $114 \div 3 = 38 \text{ lbs}$.

Example 5. What are the charge, thickness of protective bulkhead, and size if 1/4 scale model (Figure 7(D)) against a 250 kg charge?

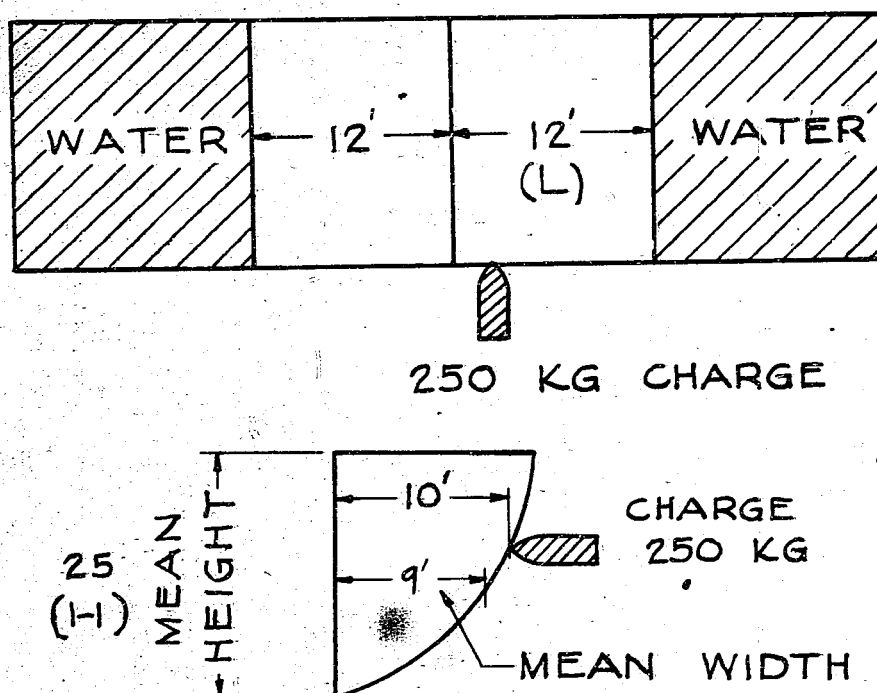


Figure 7(D)
EXAMPLE 5

ENCLOSURE (D), continued

(In this case, since the distance between the water tanks is small, as shown in Table II (D), no outer compartment is necessary.)

$$\text{Effective charge} = 250 \times (1/4)^3 = 3.9 \text{ kg}$$

The charge to be used from Figure 12(D) = 4.8 kg

The distance between the portion of the charge and the protective plating
 $= C = 10 \times 1/4 = 2.5'$

$$\text{Volume of scale model} = 24 \times 25' \times 9 \times (1/4)^3 = 84.5 \text{ ft}^3.$$

Hence, for a square model the side will be

$$\sqrt[2]{\frac{84.5}{2.5}} = 5.82'$$

The volume for a one kg charge = $\frac{24 \times 25 \times 9}{250} = 21.6 \text{ ft}^3/\text{kg}$

Figure 14(D) for 10 ft width of bilge gives 128 lbs thickness of protective bulkhead, which in the model becomes $\frac{128}{4} = 32 \text{ lbs.}$

Example 6. What is the thickness of protective bulkhead on models with the following measurements when a 1.7 kg charge is used corresponding to a 200 kg charge (Nos. 1-6, Figure 8(D))?

The reduction ratio, depending on the charge will be as follows:

If the charge proportionate to 200 kg is 1.7 kg and, according to Figure 12 (D) the effective ratio for 1.7 kg is 0.783, the effective charge is $1.7 \times 0.783 = 1.33 \text{ kg.}$

$$\text{The reduction ratio will be } \sqrt[3]{\frac{200}{1.33}} = 5.32$$

See Table IV(D).

Notes

1. For the same amount of explosive, the effect on the protective bulkhead will vary if the form of the charge or its direction varies. A fixed charge will have different effects if placed as shown in the following illustrations in Figure 9(D). Therefore, in making model experiments a definite method of charge placing should be used.

2. Even though the form and measurements of the scale model are defined by the calculations described above, it is necessary in actual tests for the treatment of the plates, the position of the frames etc. to be uniform or nearly so. For example:

In (A) of Figure 10(D) the method of securing the protective plate is too weak so that it can bend freely. In (B) however, the support is stronger than should be used. In (C) if concrete is used in part "a" the characteristics of the air space will be different from that in use which is unsuitable. Part "b" is strong enough so that it will not break at the time of the explosion.

ENCLOSURE (D), continued

TABLE IV(D)

Model No. (Fig 8(D))	Effective Volume ft ³ /kg	Calculated Bulge Width (Full size) (ft)	Required Thickness of Protective Bulkhead (From* Fig 13(D)) (lbs)	Calculated Thickness Required in Model lbs - mm	Tested Thickness (lbs)	Results of Tests*
1	17.5	10.64	120	22.5 - 14.1	14.2	Resisted for a short time.
2	10.4	10.64	132	24.8 - 15.5	21.6	Broke unexpectedly probably because of low Izod value.
3	14.7	8.42	(+9) 127	(25.5 - 16.0) 23.9 - 14.9	16.0	Margin of safety at bulge (68mm). However 2 small holes appeared. 16.5mm would be sufficient.
4	8.8	8.42	(+9) 139	(27.8 - 17.4) 26.1 - 16.3	16.0	Considerable damage 18mm necessary.
5	22.7	8.42	(+9) 120	(24.3 - 15.2) 22.5 - 14.1	16.0	Bent 55mm leaving some margin but 4 holes appeared.
6	With water for anti-splinter protection.	8.42	73	13.7 = 8	8.0	Resisted perfectly with no cracks or holes even though it bent 96mm.

*(Figures in parenthesis in the 4th column of this table are for the case of a 9 lb double bottom added.)

ENCLOSURE (D), continued

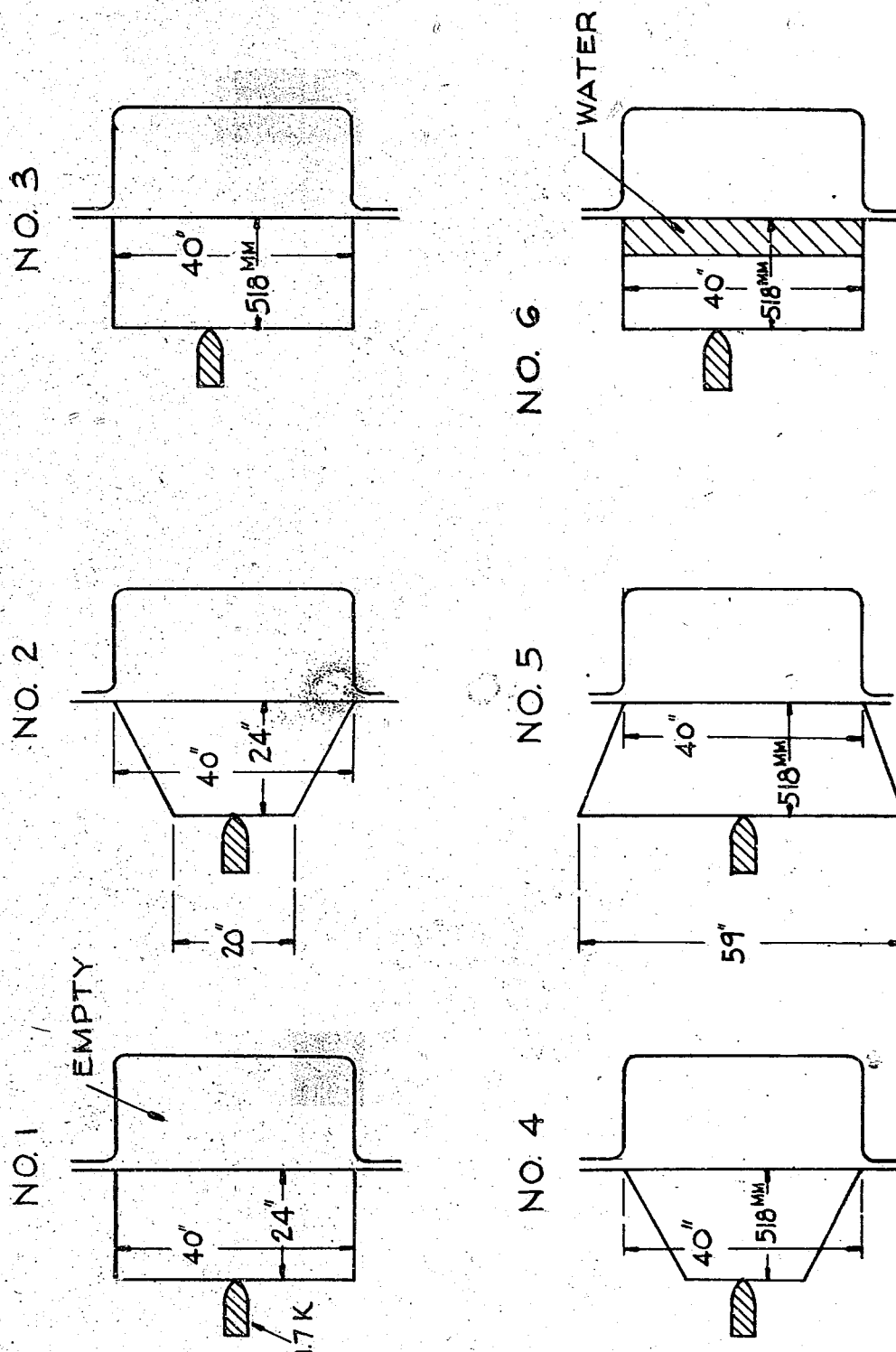
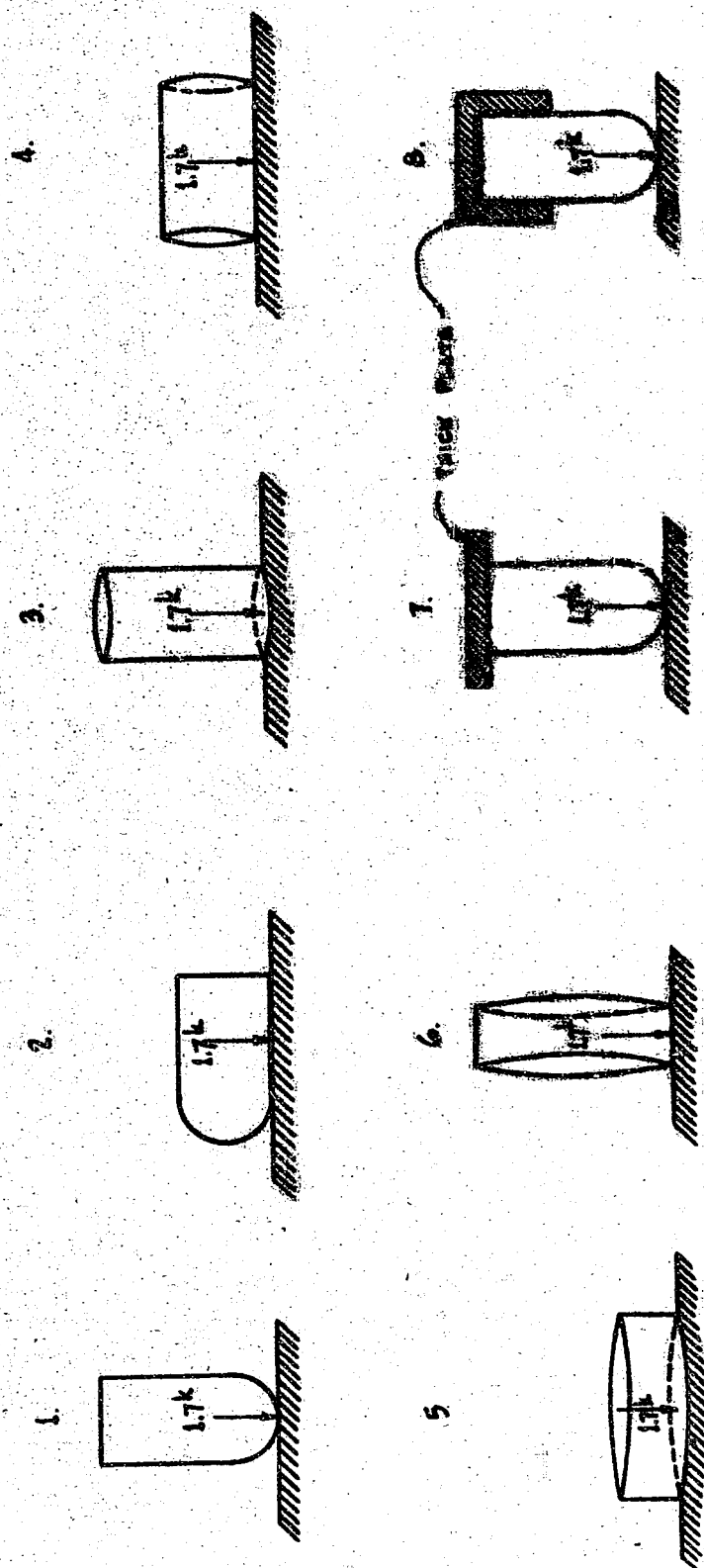


Figure 8(D)
EXAMPLE 6

ENCLOSURE (D), continued

Figure 9(D)
POSITIONS OF CHARGES

ENCLOSURE (D), continued

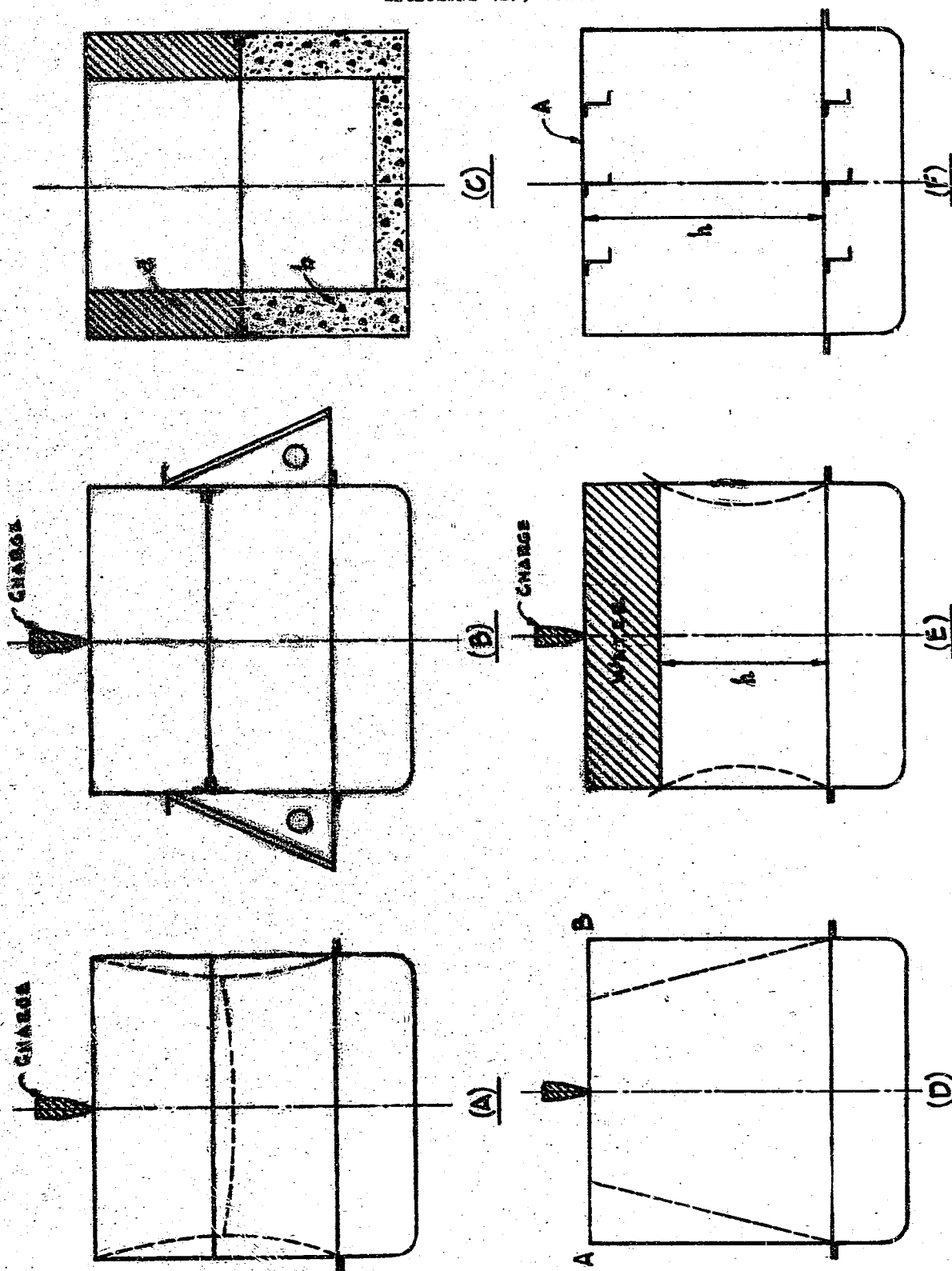


Figure 10(D)
TEST MODEL STRUCTURAL FEATURES

ENCLOSURE (D), continued

In (D) AB as it stands is satisfactory but if its shape is changed as shown by the dotted lines, the volume of the air space is reduced, which is unsuitable.

In (E), the height "h" is changed at the time of the explosion, changing the volume of the air space. This method is, therefore, unsuitable.

In (F), there are some stiffeners in actual use. If these are omitted in the model, plate A will bend because of the water pressure, changing height "h". The whole structure will therefore differ from the actual case and it would be unsatisfactory.

CHAPTER IV

The basic description of torpedo protection already given is based on the coordinated results of tests with sealed projectiles weighing 9 kg and 1.7 kg. As Table I(D) shows, there are several sizes of 9 kg targets but for the most important tests the length was 6 ft 6 in and width 7 ft 0 in. When the distance between the outer skin and the protective plating was 2 ft 9 in or more, the test was always conducted with a double bottom attached.

The volume of the 1.7 kg targets (see Table I(D)) was not in proportion with that of the 9 kg targets which are taken as a standard here.

1. 9 kg Projectiles

a. Reduction of scale: The 9 kg projectile is a 1/3 scale model of 200 kg torpedoes.

b. Size of charge: Theoretically, charge = effective charge = $200 \times (1/3)^3 = 7.407$ kg.

$$\text{Charge used} = 7.407 \times 1.212 = 9 \text{ kg}$$

It was felt that this charge might be too large for 1/3 scale test, but the experiments showed it to be generally suitable.

The scale is actually 1/2.97 since from Figure 12(D) ratio of effectiveness = 0.88 and effective charge = 7.65 kg.

$$\text{The scale} = \sqrt[3]{\frac{200}{7.65}} = 2.97.$$

c. Thickness of protective plate: The thickness of the protective plate has been defined as the minimum thickness which will fully withstand explosions. It must be thick enough so that it is not lacerated and so that splinters will not make any small holes. The bulkhead is satisfactory if no "throughs" are found. Deep strikes are permitted.

2. The Relation of the Full-Scale Charge to the Scale Model

Reduction error in the charge: As a result of previous tests at the Technical Research Laboratory using charges of 62 gr, 100 gr, 125 gr, and 1.7 kg, it was found that with the reduction of the charge used there was a successive diminution of the explosive force against the protective

ENCLOSURE (D). continued

plating. Therefore, calculating conversely on the basis of the force on the plating, we obtain, in seeking the ratio of the charge used to the effective charge (ratio of effectiveness) the curve shown in Figure 12(D).

Because this curve is for a full-scale charge of 200 kg it cannot be used for other full-scale charges.

For example, for an effective charge of 7.407 kg with a full-scale charge of 200 kg, the charge used is 8.75 kg, but when the full-scale charge is 350 kg a charge of 9 kg must be used.

The reduction error has been determined by taking the error for a full-scale charge of 200 kg as a base, and taking the same ratio for 250 kg and 350 kg.

(This is not theoretically correct but the errors are not considered to be large.)

For example: $1/3$ scale model 200 kg charge = 9 kg charge

Ratio of effectiveness = 0.85

Charge ratio = $9/200 = 0.045$

Therefore: 350 kg charge = $350 \times 0.045 = 15.75$ kg

3. Relation of the Volume of Bulge to the Thickness of the Protective Bulkhead.

The changes in force due to changes in volume have been plotted in Figure 11(D) in which:

⊙ Indicates the thickness of the protective bulkhead with double bottom attached, as obtained from experiments conducted at the Yokosuka Navy Yard using a 9 kg scale model.

△ Indicates the volume (V) of the space between the outer bottom and protective bulkhead with an effective charge of one kg when the thickness is ⊙. The line B in the graph connects the points.

□ Indicates the thickness of the protective bulkhead and volume of space (ft^3/kg) found by converting the volume for a one kg effective charge and the thickness of the protective bulkhead tested in the Technical Research Laboratory with a 1.7 kg charge to a 9 kg charge.

The broken lines ——— are curves describing the thickness of the protective bulkhead for a fixed volume so as to conform to the volumes at □, the volumes at ⊙ and the volumes at the points which are intersected by the line A.

These lines (broken lines) correlate Figures 13(D), 14(D) and 15(D) which illustrate the relations between the volume of the explosion space, the thickness of protective bulkhead, and the bulge width.

ENCLOSURE (D), continued

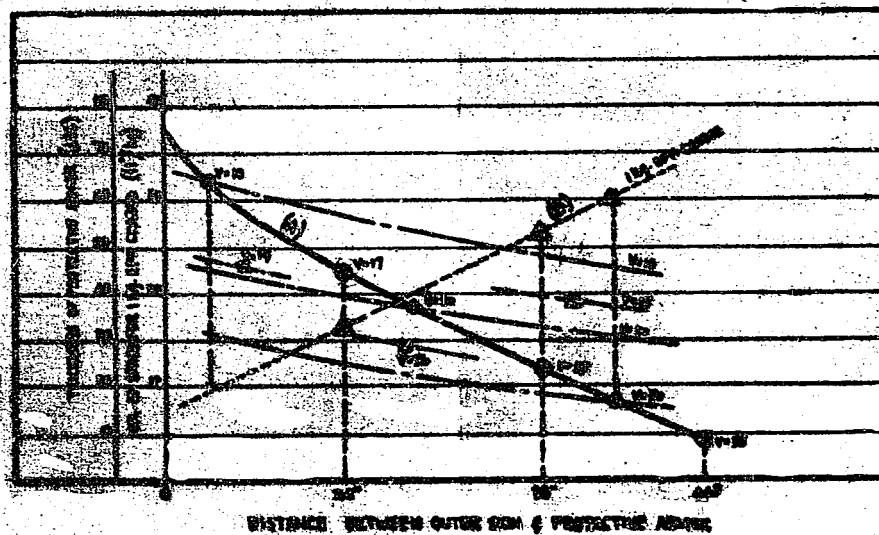


Figure 11(D)
RELATION BETWEEN VOLUME, THICKNESS
OF PROTECTIVE PLATE AND BULGE WIDTH

This graph is only applicable to side explosions. Further tests are necessary regarding hits on the bottom and topside.

ENCLOSURE (D), continued

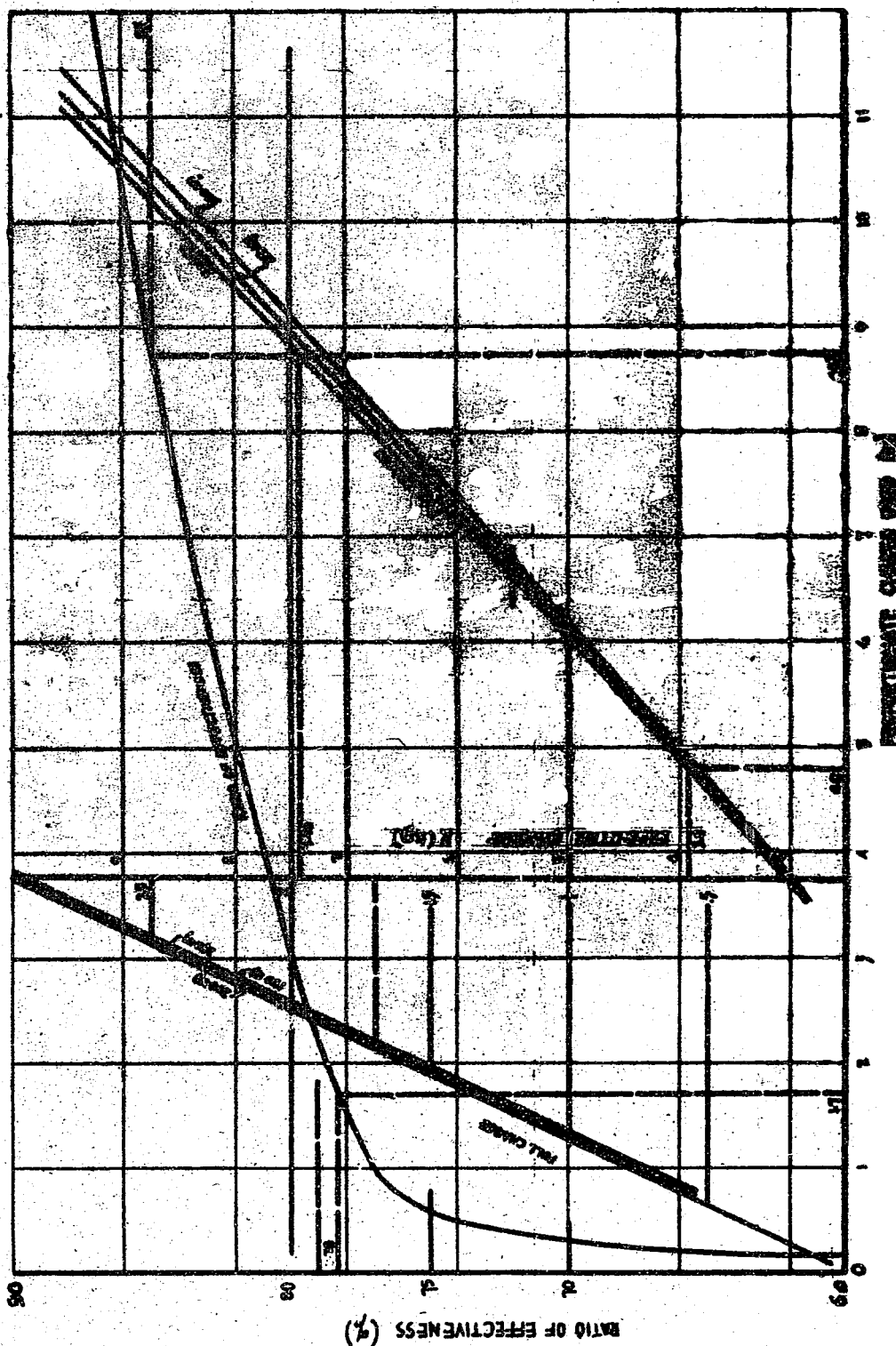


Figure 12(D)
EFFECTIVE CHARGE VS. UTILIZATION COEFFICIENT

ENCLOSURE (D), continued

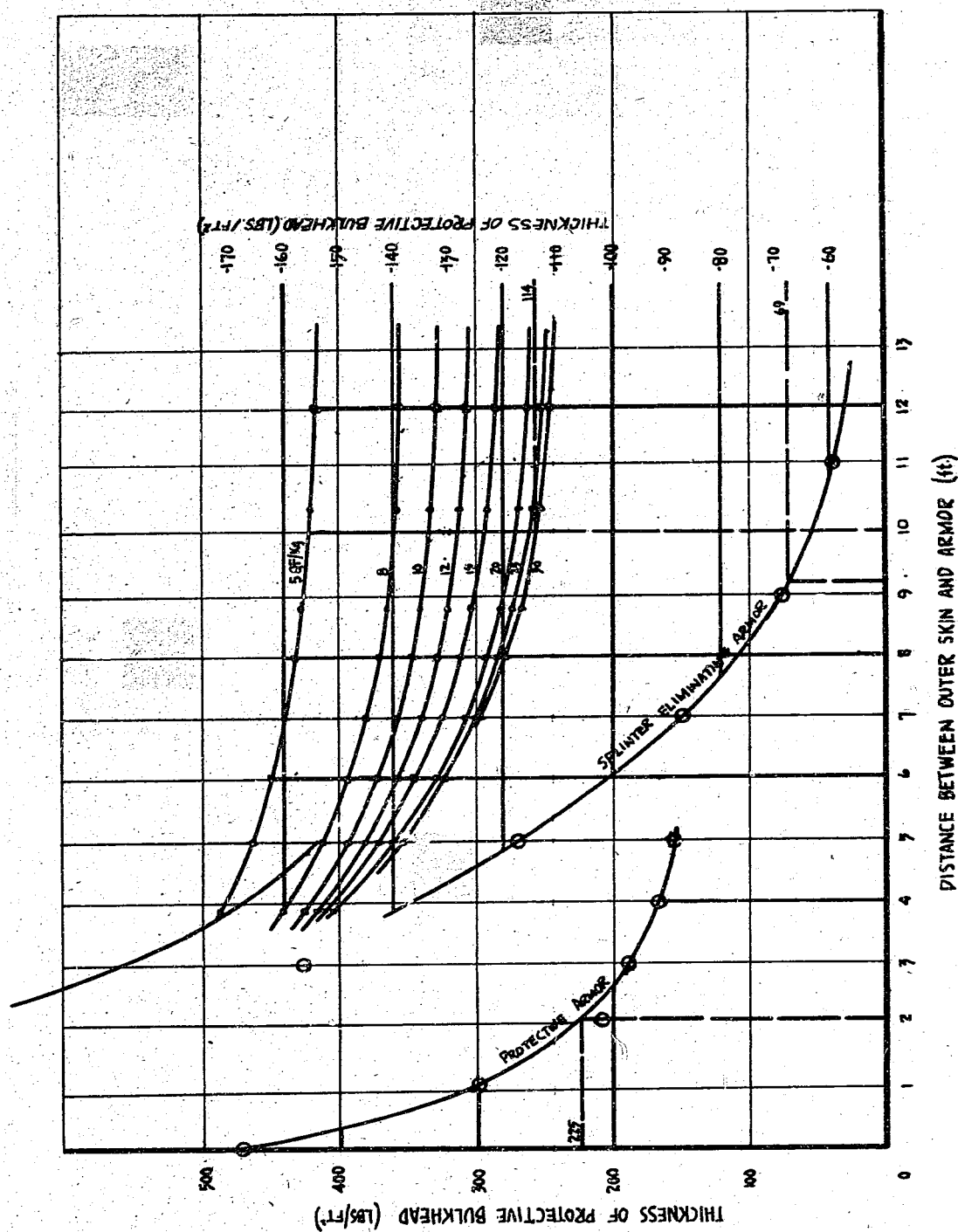


Figure 13(D)
ANTI 200 kg DEPTH CHARGE ARMOR

ENCLOSURE (D), continued

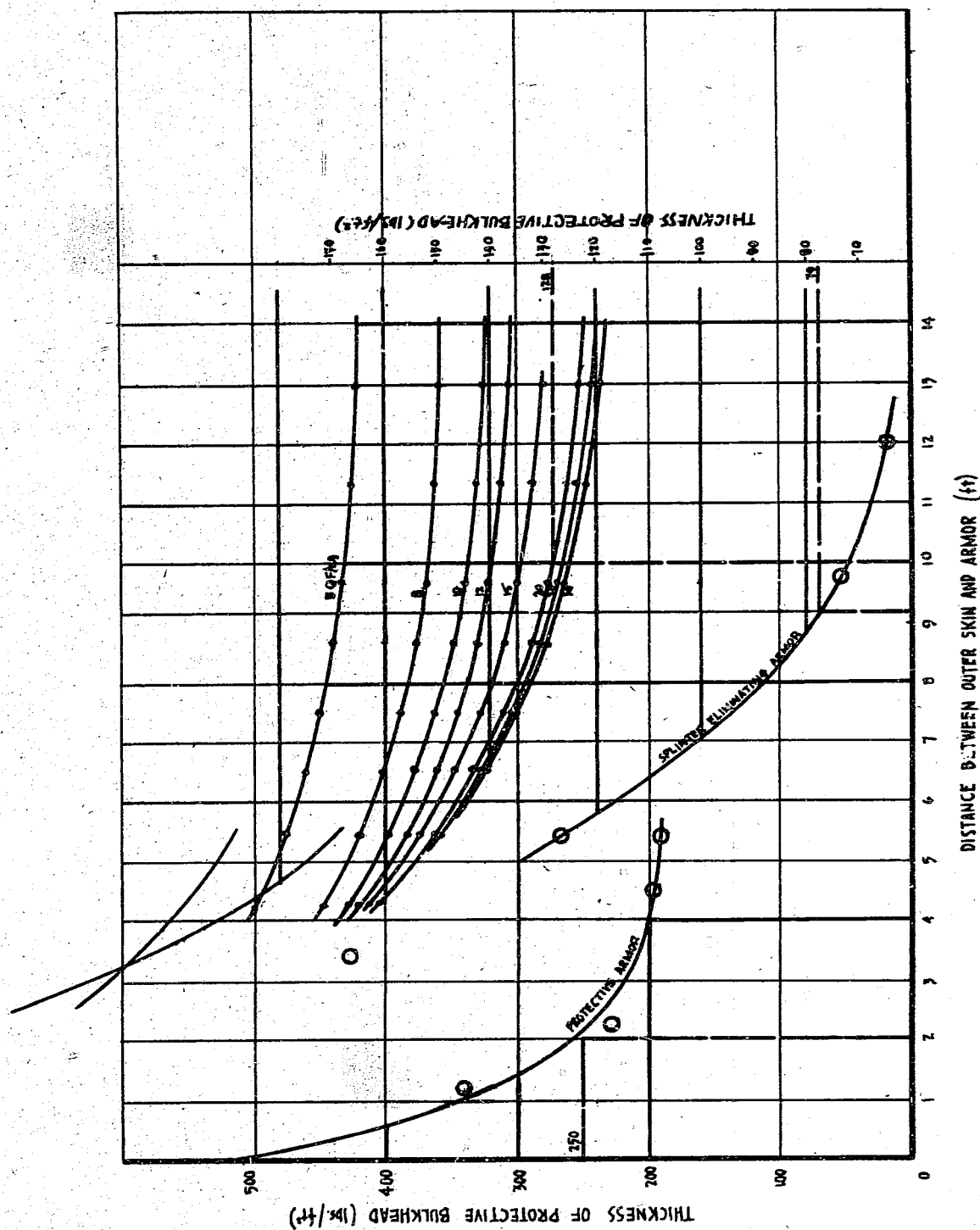


Figure 14(D)
ANTI 250 lb DEPTH CHARGE ARMOR

ENCLOSURE (D), continued

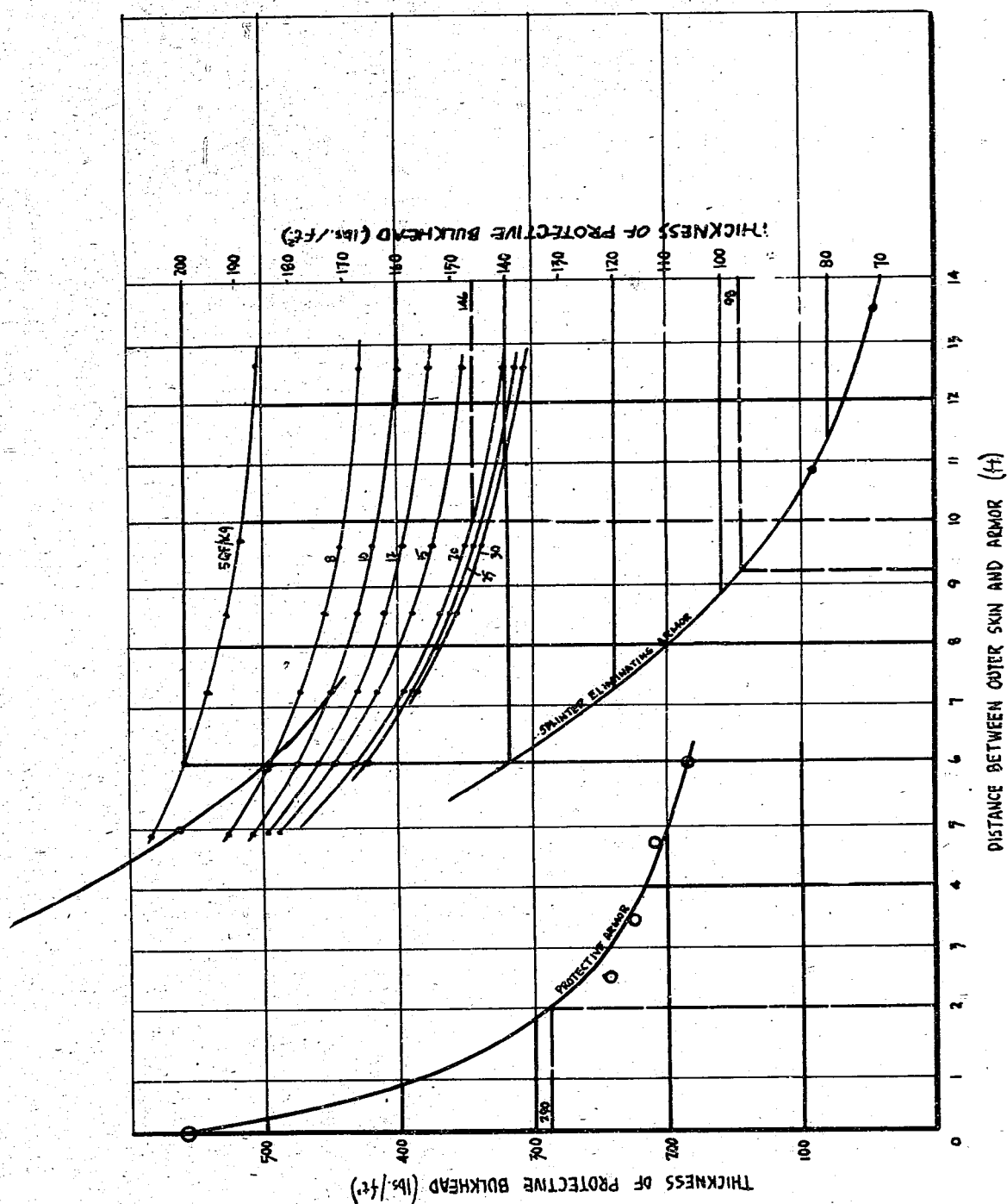


Figure 15(D)
ANTI 350 kg DEPTH CHARGE ARMOR

ENCLOSURE (E)

EXPERIMENTS FOR DETERMINING THE STRENGTH OF SUBMARINE
HULL MODELS AGAINST DEPTH CHARGES AT GREAT DEPTHS

(Ship Construction Research Department)

21 November 1944

LIST OF ILLUSTRATIONS

Figure 1(E)	Experimental Set-Up for Determination of Submarine Hull Resistance at Great Depths	Page 248
Figure 2(E)	Curve Showing Relationship of Explosive Pressure-Distance of Depth Charge	Page 249
Figure 3(E)	Pressure Ratio - Safe Depth Curve	Page 250

ENCLOSURE (E). continued

1. Purpose

To investigate the resistance of submarines against depth charge at safe diving depths, and to determine the relation between the diving depth and radius of damage in accordance with Secretariat Secret #6179 of 11 October 1944.

2. Results and Remarks

a. The strengths of resistance of a reinforced pressure-resistant circular hull model with planned collapsible depth of 50 meters (actually between 44-55m), when tested at depths of 45m, 30m, 25m, and 15m against depth charges with 800 grams of Shimose Powder (41grams of tetryl booster charge) are as shown in Table I(E). The radius of damage determined from the above are as follows:

Depth at Which Static Collapse Takes Place. (Computed value) A (kg/cm ²)	Depth B (m)	Pressure Ratio B/A	Estimated Radius of* Damage (m)	Percentage of Radius of Damage
44- 48	15	0.34 - 0.31	13 - 11	1
44	25	0.57	15 - 14	1.36 - 1.08
45- 48	30	0.67 - 0.62	17 - 16	1.54 - 1.23
48- 55	45	0.94 - 0.83	25 - 22	2.28 - 1.69

*Based on the formation of lobes

b. It is believed from the results of this experiment that for a submarine to escape to great depths in event of depth charge attacks will only invite opportunity for greater damage, considering the increased adjustable depths of present day depth charges.

c. The crusher gauge used showed far less variance in its indicated values than the standard pressure meter. Consequently it has greater practical value in computing low explosion pressures.

3. Outline of Experiment

a. Date: 17, 18, and 19 November 1944

b. Location: MITARAIJIMA, Toyotagun, Hiroshima Ken, 2100m off shore, depth 82m.

c. Experiment: Ten models of the reinforced pressure-resistant circular hulls (plate thickness 2mm, diameter 700mm, reinforcement strip length 235mm) with a collapsible depth of 50m were constructed. Two of these were tested for strength of resistance against static pressure and the remaining eight were used in the depth charge experiments. Four depths 45, 30, 25, and 15 meters were selected. The relative distances between the depth charges and the hulls were kept at 8-22 meters and the differences in the radii of damage at each depth investigated. Two hulls used in the initial test, being only slightly distorted, were used again. So in

ENCLOSURE (E), continued

effect, the depth charge tests were conducted ten times.

The depth charges used were cylindrical types with powder charges of 800 grams of Shimose and 41 grams of tetryl boosters.

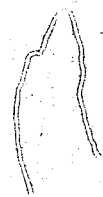
The hull construction and the arrangement of the experiment are shown in Figure 1(E).

4. Results of Experiment

Table I(E): Results of experiments on hull resistance against depth charges at great depths.

Figure 2(E): Pressure - Distance Curve.

Figure 3(E): Pressure Ratio - Safe Depth Curve.



ENCLOSURE (E), continued

Table I(E)
RESULTS OF EXPERIMENTS ON HULL RESISTANCE AGAINST DEPTH CHARGES AT GREAT DEPTHS

Depth of Depth Charge & Hull (Meters)		Distance Between Depth Charge & Hull (Meters)	Calculated Collapsing Pressure (Actual)	Pressure Ratio	Mechanical Properties of Hull						Explosive Pressure* (Standard Pressure Meter)				Explosive Pressure* Counter Gauge				
					Yield Pt (kg/mm ²)		Tensile Strength (kg/mm ²)		Elongation (%)		Experiment Number	Surface Facing Explosion	Opposite Surface Explosion	Top Surface Explosion	Bottom Surface Explosion	Surface Facing Explosion	Opposite Surface Explosion	Top Surface Explosion	Bottom Surface Explosion
					T	C	L	C	L	C									
45	12		5.5	8.2	33.3	33.1	42.0	44.4	13.9	14.9	1	17.00 11.00	5.50 6.00	22.00 17.00	14.00 8.00	15.40	9.50 8.80	14.60 10.20	13.00 14.60
45	18		5.3	8.5	34.3	35.5	41.6	45.1	10.6	13.1	1	9.90	7.00 4.40	8.50 7.00	9.40 9.40	13.00 8.20	2.20 6.40	7.40 6.40	3.90 11.60
45	22		4.8	9.4	35.9	31.6	45.3	46.4	13.3	16.9	1	5.60 5.30	5.60 3.20	3.90 3.20	9.40 6.30	4.40 5.40	2.50 1.40	2.80 4.40	4.40 4.40
30	12		4.5	6.7	44.8	45.9	52.5	60.8	12.5	11.9	1	11.40 10.90	10.40 7.70	12.40 16.00	23.00 8.50	16.20 14.60	13.60 13.00	13.60 10.20	12.30 13.00
30	14		4.5	6.7	35.3	33.6	42.7	45.4	11.7	13.2	1	8.50 8.00	5.60 2.90	10.90 7.40	9.90 9.00	16.20 14.60	7.00 7.40	7.40 10.20	8.00 7.40
30	18		4.8 (3.9)	6.3	45.9	45.0	58.8	59.2	14.2	12.6	1	7.00 8.50	7.70 6.30	6.30 7.40	7.00 7.20	7.00 7.60	6.40 8.20	6.40 7.60	4.40 7.00
25	8		4.4	5.7	50.5	47.1	66.1	64.0	12.9	10.3	1	38.00 30.00	11.00 27.00	8.00 51.00	15.50 22.00	25.60 32.60	17.80 23.60	16.20 23.60	18.70 23.60
25	12		4.4	5.7	53.3	42.5	67.2	66.8	10.6	9.6	1	9.50 17.00	5.50 15.50	8.00 11.00	11.00 5.00	19.60 24.60	13.00 10.90	13.80 19.60	19.60 19.60
15	8		4.8 (3.9)	3.1	45.9	45.0	58.8	59.2	14.2	12.6	2	29.20 16.30	14.00 13.40	18.20 20.20	30.10 8.90	30.20 25.60	16.20 30.20	22.60 28.90	24.60 18.70
15	12		4.4	3.4	53.3	49.5	67.2	66.8	10.6	9.6	2	15.00 8.10	5.60 14.30	13.00 13.00	18.00 6.30	21.60 16.20	13.00 18.70	14.60 16.20	20.90 16.20

*Top figure, Starboard
Bottom figure, Port

ENCLOSURE (E), continued

Table I(E) (Cont.)
RESULTS OF EXPERIMENTS ON HULL RESISTANCE AGAINST DEPTH CHARGES AT GREAT DEPTHS

Maximum Distortion (in)	Instant Distortion	Variation of Height	Variation of Length	Number of Lobes		State of Collapsing			Calculated Number of Lobes	Number of Experiments	Model Designation	Date of Experiment	Location	Description of Weather and Sea Surface	Current and Wind	East West
				Near Weld	Center of Weld	P1 1/2 Cross Section	P2 1/2 Cross Section	P3 1/2 Cross Section								
7.6	7.0	2.1	7.6	7	4				13	3	1 A	Nov. 17	OFF MIYAKAWI JIMA, Toyota Gun, Hiroshima Ken	Clear White Caps	□ → 2.5	East West
7.1	7.0	1.8	7.1	3	1				13	4	1 B	Nov. 18		Clear Calm	□ → 0.5	East West
7.5	7.0	0.6	7.5	7	14				9	7	1 A	Nov. 19		Clear Few Caps	□ → 1.6	None
18.5	5.0	0.9	18.5	4	3				14	6	1 B	Nov. 18		Clear Calm	□ → 1.3	None
12.5	9.0	0.9	12.5	5	6				20	5	1 A	Nov. 18		Clear Calm	□ → 1.0	None
4.0	7.0	0.8	4.0	Section where collapse occurred according to Stat. Pres.					28	8	1 B	Nov. 19		Clear Few Caps	□ → 0.7	None
15.0	10.0	1.6	15.0	21	12				14	1	1 A	Nov. 17		Clear White Caps	□ → 1.4	East West
6.8	4.0	1.7	6.8	3	1				12	2	1 B	Nov. 17		Clear Caps	□ → 1.0	East West
12.9	8.0	0.6	12.9	9	1				11	10	1 B	Nov. 19		Clear Few Caps	□ → 0.7	None
9.0	4.0	0.5	9.0	2	2				17	9	1 B	Nov. 19		Clear Few Caps	□ → 1.2	None

Note: The symbol "A" shows the surface facing the blast

ENCLOSURE (E), continued

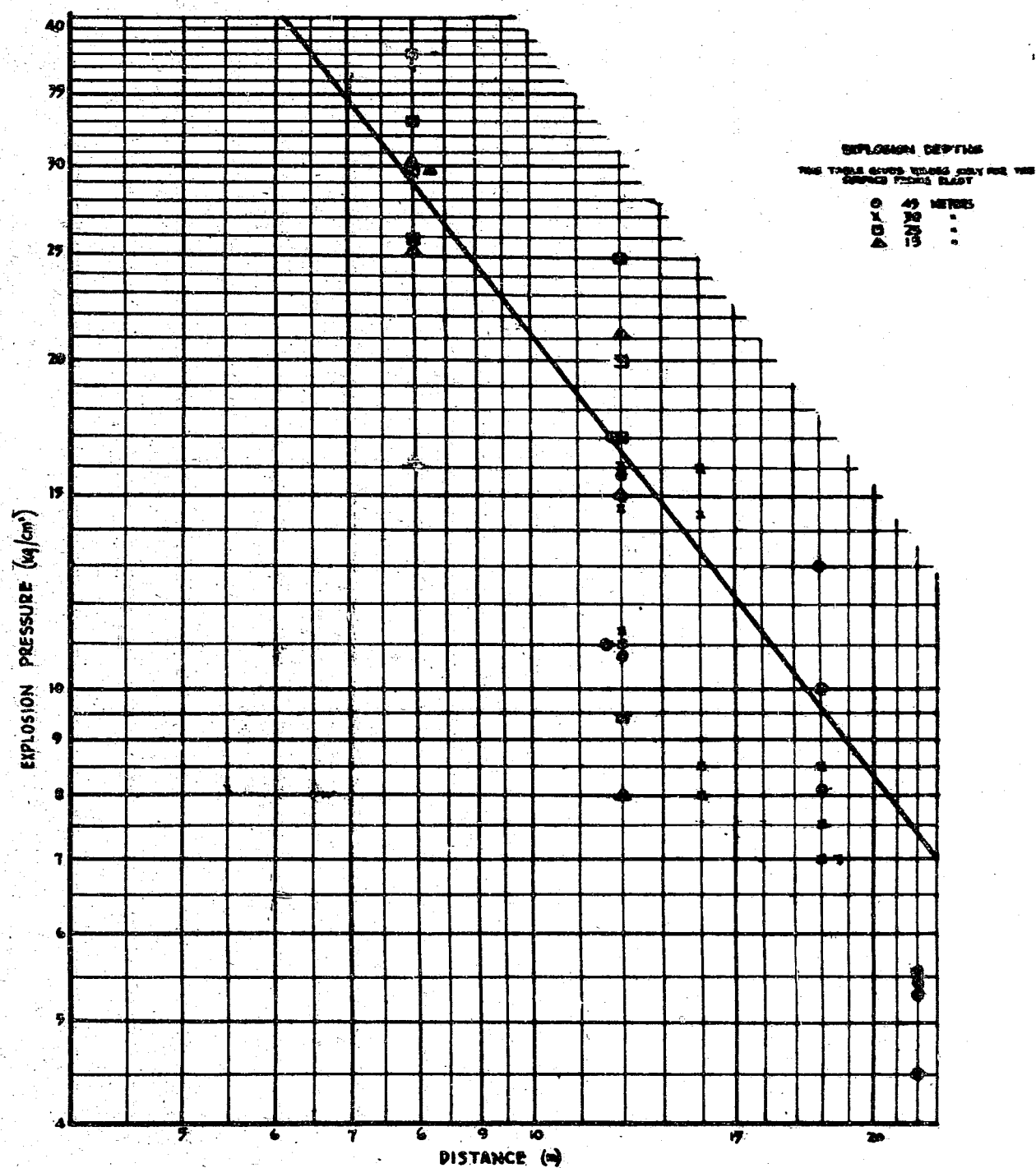


Figure 2(E)
CURVE SHOWING RELATIONSHIP OF EXPLOSIVE
PRESSURE - DISTANCE OF DEPTH CHARGE

ENCLOSURE (E), continued

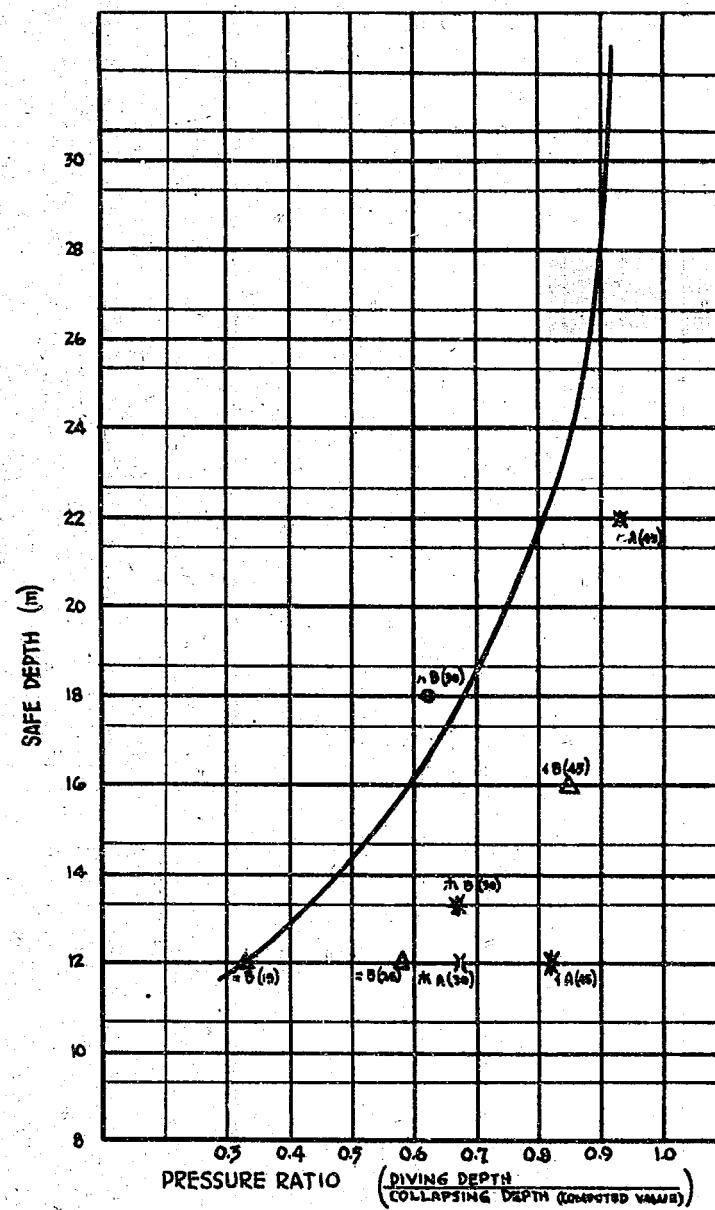


Figure 3(E)
PRESSURE RATIO - SAFE DEPTH CURVE

ENCLOSURE (F)

THE EFFECT OF OPENING AND CLOSING OF KINGSTON VALVES ON THE
RESISTANCE OF SUBMARINE PRESSURE HULLS TO DEPTH CHARGES

(Experiments on Double Cylindrical Containers Relative to
Concussion Collapse with the Effect of Aperture in the Outer
Container)

LIST OF ILLUSTRATIONS

Figure 1(F)	Construction of Models.....	Page 257
Figure 2(F)	Test Set-Up.....	Page 257
Figure 3(F)	Bursting Charge Container.....	Page 258
Figure 4(F)	Effect of Aperture in Outer Container (A).....	Page 259
Figure 5(F)	Effect of Aperture in Outer Container (B).....	Page 260
Figure 6(F)	Effect of Aperture in Outer Container (C).....	Page 261
Figure 7(F)	Effect of Strength of Outer Container.....	Page 262

ENCLOSURE (F), continued

1. INTRODUCTION

Although the mechanisms involved in the collapse and destruction of the inner and outer hulls of a submerged submarine as the result of the concussion of a depth charge are unknown, the inner and outer hulls by mutually resisting the concussion give greater resistance than they would individually. From this we may suppose that they may be made to resist large concussions.

The outer hull receives the concussion first and reflects part of it; but inside the shell the pressure is sluggishly transmitted (corresponding to the speed of the compression wave in water), and, therefore, the seawater between the shells is compressed. However, only the pressure equivalent to the elasticity of the outer shell is transmitted to the inner shell. Therefore it must be better for the inner shell if, instead of the outer shell not having any apertures, the outer shell had an aperture with some sort of Kingston valve to relieve the pressure.

On the other hand, after the concussion passes through the outer shell (of course with a certain amount of it reflected), the seawater between the shells transmits the compression wave to the inner shell, and unless the aperture in the outer shell functions as a buffer, as mentioned above, there will be no difference with or without an outer shell.

Recently, in order to study this problem, small double containers of brass were constructed, and the space between the containers was filled with water, in one case with an aperture in the outer shell and in the other case with no aperture in the outer shell. They were subjected to concussion and the relative state of destruction for the two were studied. From these results, it was decided that the mechanism of the collapse in the latter case was very similar to the others. Accordingly, further consideration was given to the advantages and disadvantages of the opening and closing of a Kingston valve by a submerged submarine under depth charge attack.

2. PURPOSE

To find the effect of the opening and closing of a Kingston valve of a submarine on the degree of resistance to underwater concussion, and thus to acquire some data to counter the effect of depth charge attacks.

3. RESULTS AND OPINIONS

The following results were obtained after subjecting small double containers of copper to underwater concussion:

- a. For a given inner container, the damage was smaller when it had an outer container than when it did not. Further, the stronger the outer container, the more conspicuous this difference becomes.
- b. The damage to the inner container was not lessened when the outer container had an open aperture. However, the part facing the source of the concussion was more badly damaged.
- c. The concussion on the inner shell of a submerged submarine from a depth charge exploding at a distance is that of the compression pressure wave which has passed through the outer shell as well as the water between the containers. Therefore, the opening or closing of the Kingston valve had almost no effect on the concussion resistivity. However, if the case when the Kingston valve is facing the explosion is considered, leaving the Kingston valve shut is somewhat more advantageous to the concussion resistivity of the submarine's hull. However, it is thought

ENCLOSURE (F), continued

safer to leave the valve open to avoid the possibility of the valve not functioning if it is left shut.

4. ESSENTIALS OF THE EXPERIMENT

Double cylindrical containers of copper, shown in Figure 1(F), were made the object of this experiment and the space between the two cylinders was completely filled with water. The inner container was filled with air. In a pond, 3.5 meter depth, as shown in Figure 2(F), the containers were suspended at a depth of 2 meters, and subjected to concussion from bursting charge containers of 0.4 kg and 1.7 kg, as shown in Figure 3(F). The bursting charge containers were at the same depth as the double containers and at a fixed distance.

As a model of the Kingston valve, a long slit 4.5mm wide was cut extending the full length of the outer container. One part was bent back in a flange to give greater strength to the edge of the aperture. In submarines the relationship of the width of a Kingston valve to the diameter of the inner hull is about 0.09, and in this experimental container the relationship of the slit in the outer container and the diameter of the inner container is 0.10. Furthermore, the ratio of the tank capacity to the area of the Kingston valve in a submarine is 50-70 metric tons/meter², while in the experimental object the ratio of the equivalents, the water capacity between the inner and the outer containers to the area of the slit, is 56.7 metric tons/meter².

The experiment was conducted with the slit either directly facing or at right angles to the concussion.

5. EXPERIMENTAL RESULTS

The results of the experiment are given in Table I(F). Figures 4(F) through 7(F) show the damage to the containers.

6. ANALYSIS

As Sections I-IV of Table I(F) on the results of this experiment show the degree of damage to the inner container is clearly less when the outer container is used than when it is not. Moreover, as Sections VII, XI, and XII show, this tendency becomes more conspicuous as the outer container is made stronger.

Although in a submarine the strength of the outer hull is markedly less than that of the inner hull, it is a question worthy of consideration as to whether it contributes to the concussion resistivity of the inner shell. (Note: At Kure Naval Arsenal a partial scale model of the I-57 submarine was subjected to the explosion of a Type 88 depth charge (148 kg bursting charge) at a depth of 15 meters and a distance of 609-19 meters. The ratio of the concussions inside the main tank and at the gunwhale of the vessel were reported to be about 2/3 by rock crystal type pressure recorder and a copper post type pressure recorder.)

From this reasoning, it would be best for the inner hull if the valve were left closed in a case where the depth charge explosion is directly opposite the Kingston valve. However, in regard to the effect of the opening of the Kingston valve when the depth charge explosion is elsewhere than directly opposite the valve, as shown from V through X in Table I(F), the damage to the whole object and the part facing the source of the explosion is exceedingly pronounced. At the same time, it is shown that the damage was very much smaller when the outer container had no aperture. When there is an aperture

ENCLOSURE (F), continued

in the outer container the damage is about the same no matter how unrelated the angle of incidence of the concussion and the position of the aperture.

One may then reason that the damage to the inner container was smaller when the outer container had no aperture. In spite of the fact that a flange was added on the edge of the aperture to strengthen it, the degree of strength is less than in the case where there is no aperture; thus, allowing more damage to the inner container.

In the case where the outer container had a slit, no matter how unrelated the positions of the source of the explosion and the slit are, the part facing the explosion was always by far the most damaged while generally the degree of damage was about the same.

The concussion on the inner container is the compression pressure wave which has passed through the outer container; therefore, it must be reasoned, that even though an aperture is cut in the outer container, it is not the source of any concussion-relieving action. However, due to the fact that the ratio of the hull measurements and the width of the water layer inside the main hull to the anti-depth charge resistivity in an actual submarine is clearly greater than the ratio of the container measurements and the width of the water layer between the inner and outer containers in this experiment to the anti-bursting charge resistivity, the concussion distribution in a submarine must be more concentrated than in the objects used in this experiment.

It may be reasoned from the results of this experiment that in a case where the depth charge exploded directly opposite an open Kingston valve, the concussion will come through the valve and reach the inner shell causing comparatively heavy damage to the inner shell. That is to say, that there are no advantages to leaving the Kingston valve open.

Then again, the ratio of the strength of the inner and outer containers of the object of this experiment are clearly comparable to cases where the inner container has a low degree of strength. Furthermore, the bursting charge used was large. That is to say, if a case is considered where the concussion waves are long, it may be inferred that compared to the results of this experiment, in actual cases, the damage to the outer hull will be greater. (Note: According to the Mine Experimental Department's #108, classified top secret, dated 31 November, when a Type 88 depth charge was used against a Type 3 large submarine, the damage caused was as follows (on a 1/3 scale model):

- a. At a distance of 12 meters both the inner and the outer shells of the hull were crushed.
- b. At a distance of 17 meters both the inner and outer hulls showed deformation. Rivets were loosened and scattered in a large portion of the single-hulled part.
- c. At a distance of 23 meters one part of the outer hull was deformed and rivets scattered.
- d. At a distance of 32 meters, the outer hull was slightly deformed.
- e. At a distance of 50 meters there was no change in the ship's hull. This shows that the outer hull is more easily damaged than the inner hull.

Therefore, in cases where the outer hull is damaged and deformed and the damage to the inner hull is not necessarily fatal, if the possibility of functional damage and ultimate failure of the Kingston valve is considered, it is thought safer to leave the valve open.

*ENCLOSURE (F), continued*6. CONCLUSIONS

The concussion from the distant explosion of a depth charge on the inner hull of a submerged submarine is the compression pressure wave which has passed through the outer hull and the layer of water between the hulls. Therefore, the opening or closing of the Kingston valve has almost no effect on the concussion resistivity. However, in a case where the explosion is directly opposite the Kingston valve, leaving the Kingston valve closed had a somewhat advantageous effect on the concussion resistivity of the submarine. It is thought best to leave the Kingston valve open because of the possibility of the valve being unable to function if left closed at the time of the concussion.

ENCLOSURE (F), continued

Table I(F)
SUMMARY OF EXPERIMENTAL RESULTS

Symbol	Experimental Models						Bursting Charge (kg)	Distance between Object and Bursting Charge (m)	Direction of Concussion	Amount of Damage to Object	
	Outer Container			Inner Container						Outer Container	Inner Container
	Thickness of Sides (mm)	Aperture	Static Pressure Strength kg/cm ²	Thickness of Sides (mm)	Static Pressure Strength kg/cm ²						
I	0.5	No	15.5	0.5	54	1.7	6		A slight indentation of one part. Maximum indentation - 0.05	Collapse on side toward explosion and the rear. Maximum indentation - 0.57 I in Figure 4(F)	
II	No Outer Container			0.5	54	1.7	6			Complete collapse, especially bad on side toward explosion. Maximum indentation - 0.26. II in Figure 4(F)	
III	0.5	No	15.5	0.37	6.7	1.7	6		A slight deformation covering the whole surface. Maximum projection - 0.03 (on the side). Maximum indentation - 0.02 (on the side toward explosion and on the side diagonally to rear).	Collapse on side toward explosion. Maximum indentation - 0.09. Expansion of sides. Maximum projection - 0.03 III in Figure 4(F)	
IV	No Outer Container			0.37	6.7	1.7	6			Great collapse. The driven collapse out off both edges. IV in Figure 4(F)	
V	0.3	Aperture		0.3	15.4	0.4	4.5	In direction of outer container's aperture	Slight indentation on side toward explosion (near aperture). Indentation - 0.16. V in Figure 5(F)	Collapse on side toward explosion. Maximum indentation - 2.2. V in Figure 5(F)	
VI	0.3	Aperture		0.3	15.4	0.4	4.5	At right angle to aperture in the outer container	Collapse on side (near aperture). Maximum indentation - 1.39. VI in Figure 5(F)	Collapse on side toward explosion and on side toward aperture in outer container. Maximum indentation - 2.19. VI in Figure 5(F)	
VII	0.3	No	3.6	0.3	15.4	0.4	4.5		Collapse on side toward explosion and diagonally to rear. Maximum indentation - 0.40 VII in Figure 5(F)	Collapse on side toward explosion and part diagonally to rear. Maximum indentation - 0.68 VII in Figure 5(F)	
VIII	0.3	Aperture		0.3	15.4	1.7	10	In direction of outer container's aperture	Collapse on side toward explosion (near aperture). Maximum indentation - 2.99 VIII in Figure 6(F)	Collapse on side toward explosion. Maximum indentation - 0.82. VIII in Figure 6(F)	
IX	0.3	Aperture		0.3	15.4	1.7	10	At right angle to aperture in outer container.	No change detected. IX in Figure 6(F)	Collapse on side toward explosion. Maximum indentation - 1.08. IX in Figure 6(F)	
X	0.3	No	3.6	0.3	15.4	1.7	10		No change detected. X in Figure 6(F)	No change detected X in Figure 6(F)	
XI	0.4	No	8.0	0.3	15.4	0.4	4.5		No change detected. XI in Figure 7(F)	Collapse on side toward explosion. Maximum indentation - 0.25. Great collapse as compared to XII. XI in Figure 7(F)	
XII	0.5	No	15.5	0.3	15.4	0.4	4.5		No change detected. XII in Figure 7(F)	Collapse on side toward explosion. Maximum indentation - 0.26. Collapse is less than in XI. XII in Figure 7(F)	

Notes:

1. Damage to inner container is less, if an outer container is used.
2. Damage to inner container is much less when there is no aperture in the outer container. In the one with the aperture it seemed to make no difference from what direction the explosion came.
3. From VII, XI, XII, the stronger the container, the less damage to the inner container.

ENCLOSURE (F), continued

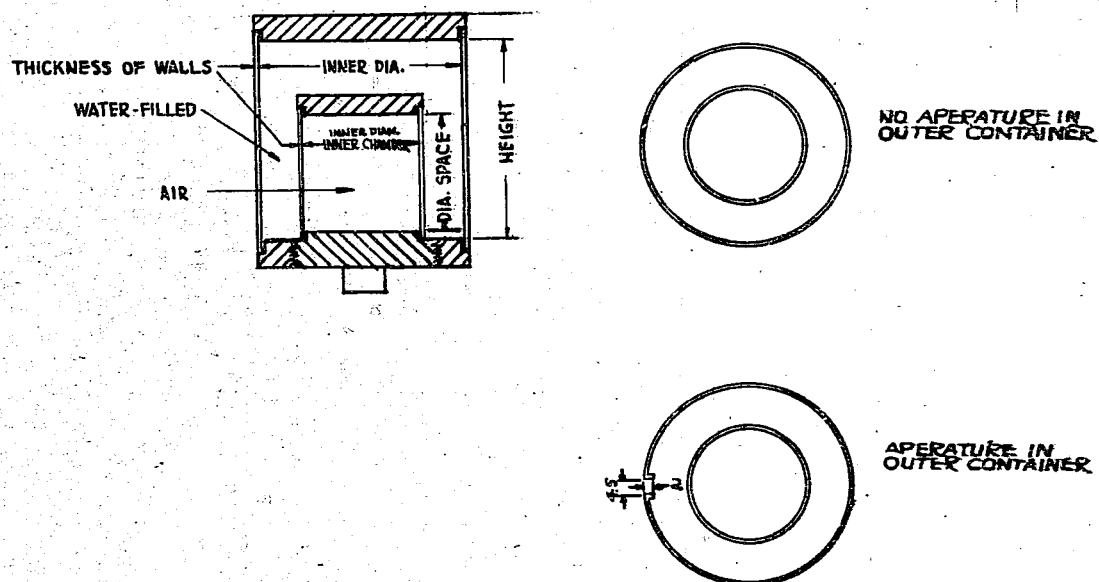


Figure 1(F)
CONSTRUCTION OF MODELS

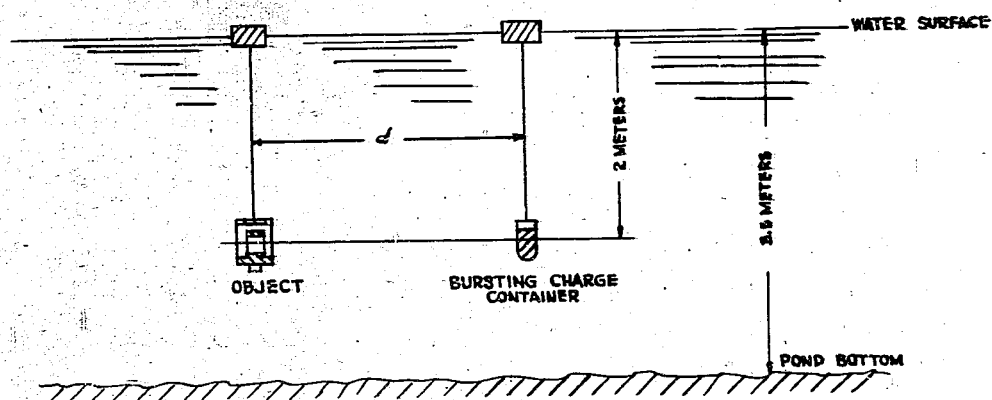


Figure 2(F)
TEST SET-UP

ENCLOSURE (F), continued

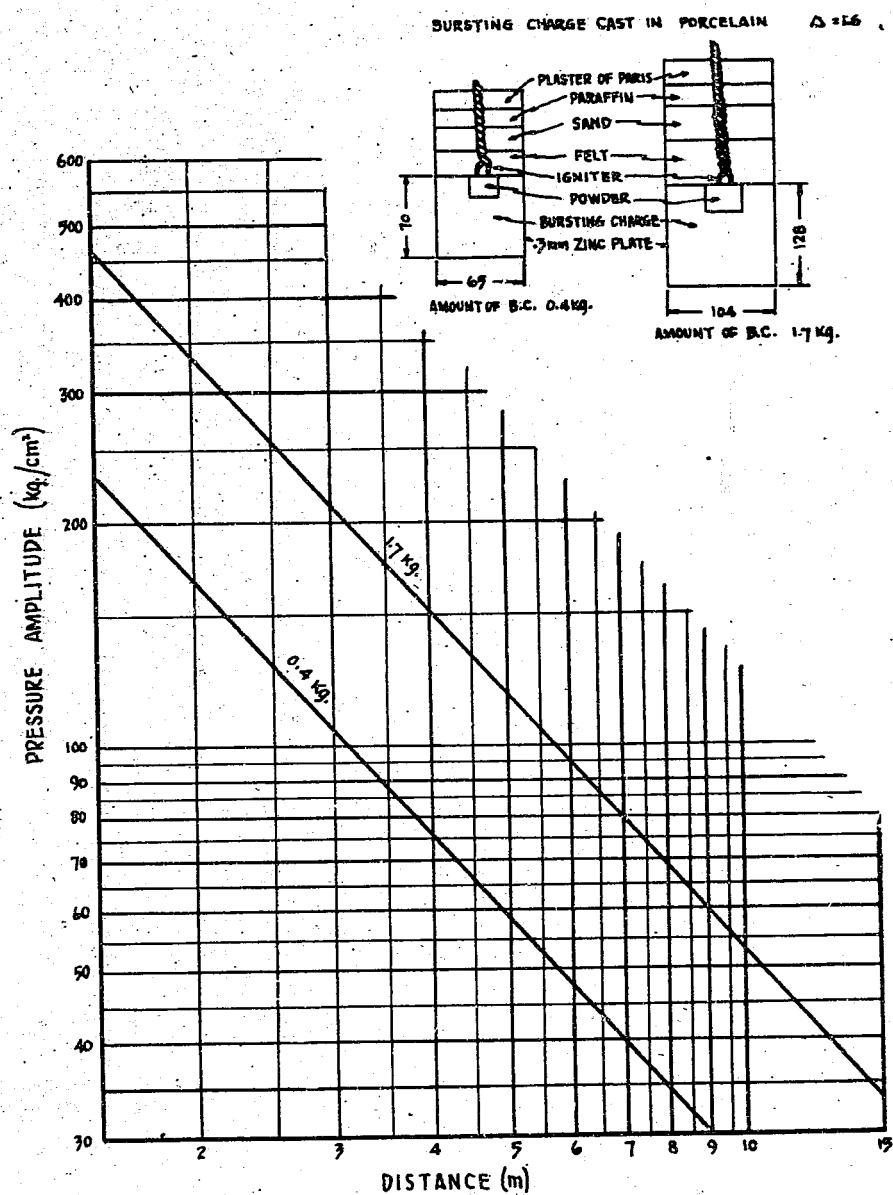
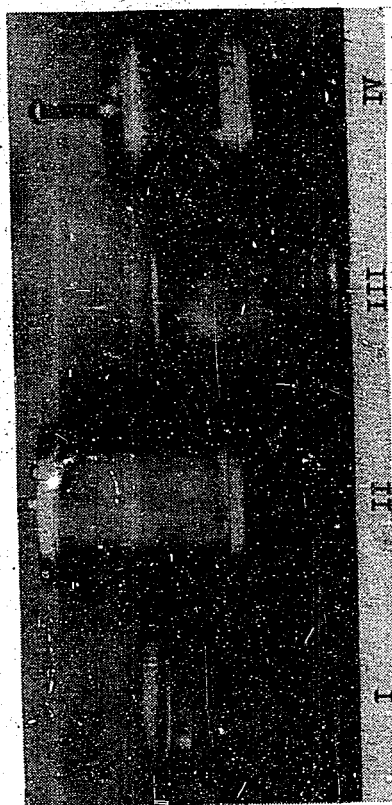


Figure 3(F)
BURSTING CHARGE CONTAINER

ENCLOSURE (F), continued



Model	Dimensions (mm)			Bursting Charge (kg)	Distance between Bursting Charge and Object (m)	Notes
	Thickness of Walls	Length	Inner Chamber			
I	0.5	36	43.5	1.7	6	Space between two container filled with water
II	0.5	36	43.5	1.7	6	No outer container
III	0.37	36	43.5	1.7	6	Space between two container filled with water
IV	0.37	36	43.5	1.7	6	No outer container

Fig. 1 (F)
EFFECT OF APERTURE IN OUTER CONTAINER (A)

ENCLOSURE (F), continued



	Dimensions (mm)			Amount of Bursting Charge (kg)	Distance be- tween Bursting Charge and Object (m)
	Thickness of Sides	Length	Inner Diameter		
Outer Container	0.3	60	72	0.4	4.5
Inner Container	0.3	36	43.5		

Notes:

1. Width of aperture in outer container of V, VI is 4.5mm.
2. The measurements on the drawings below were taken on a cross-section at mid-length.
3. In all sketches the direction of the concussion is from the bottom of the page.

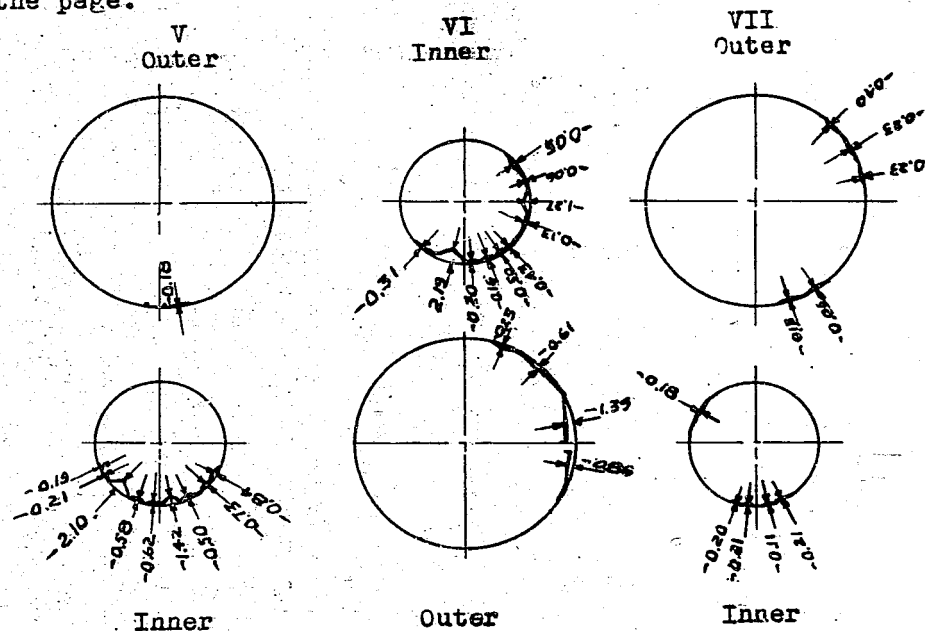


Figure 5(F)
EFFECT OF APERTURE IN OUTER CONTAINER (B)

ENCLOSURE (F), continued

	Dimensions (mm)			Amount of Bursting Charge (kg)	Distance be- tween Burst- ing Charge and Object (m)
	Thickness of Sides	Length	Inner Diameter		
Outer Container	0.3	60	72	1.7	10
Inner Container	0.3	36	43.5		

Notes:

- VIII and IX have a 4.5mm wide slit in the outer container.
- Shows a cross-section of mid-length.
- In all sketches direction of concussion is from bottom of the page.

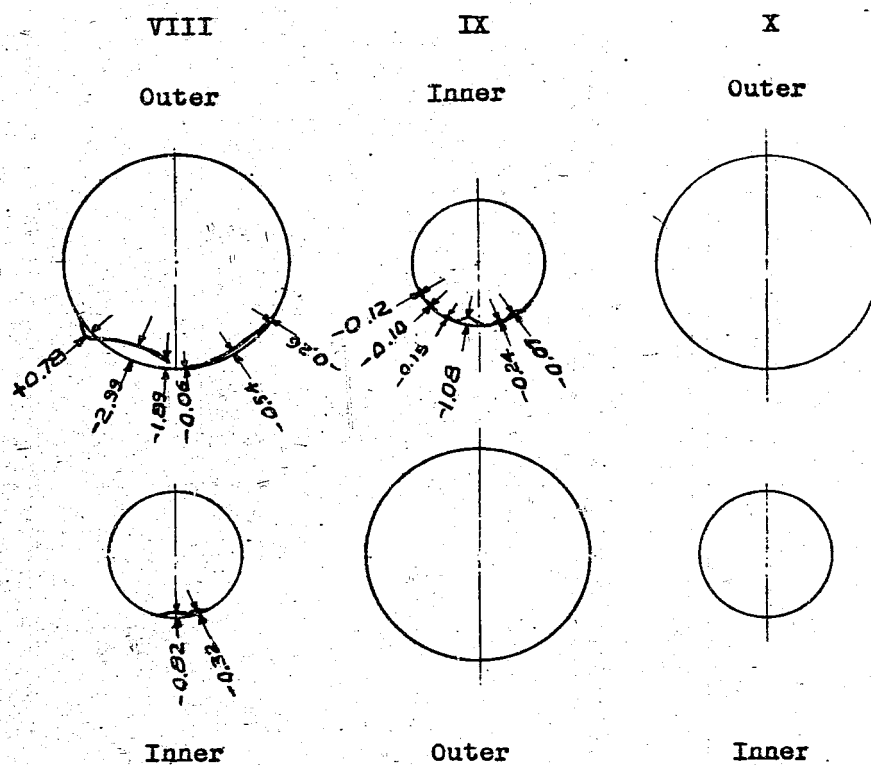
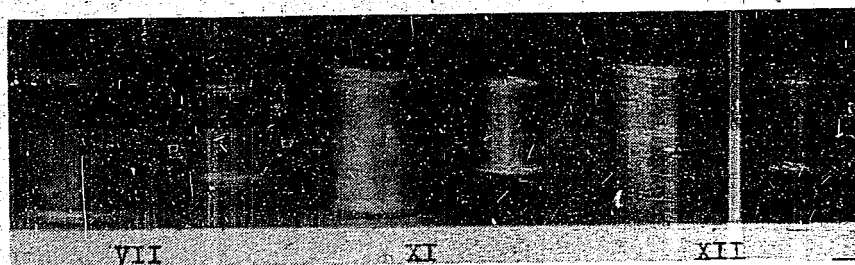


Figure 6(F)
EFFECT OF APERTURE IN OUTER CONTAINER (C)

ENCLOSURE (F), continued



	Dimensions (mm)			Amount of Bursting Charge (kg)	Distance be- tween Burst- ing Charge and Object (m)
	Thickness of Sides	Length	Inner Diameter		
Outer Container	VII...0.03	60	72	0.4	4.5
	XI....0.4				
	XII...0.5				
Inner Container	0.3	36	43.5		

Note: Almost no change in all outer containers. However, there was a slight indentation in VII the thinnest (refer to Figure 5(F)). Direction of concussion in all cases from bottom of page.

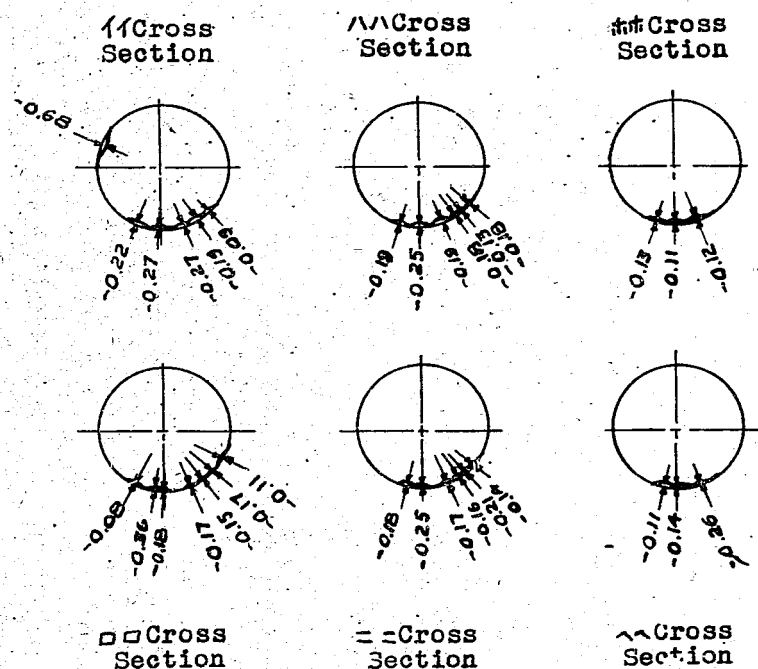


Figure 7(F)
EFFECT OF STRENGTH OF OUTER CONTAINER

ENCLOSURE (G)

TESTING STRENGTH OF SUBMARINE TANKS AGAINST UNDERWATER EXPLOSIONS

(The Collapse of Double Cylindrical Containers
Under Concussion)

October 1943

LIST OF ILLUSTRATIONS

Figure 1(G)	Test Set-up.....	Page 271
Figure 2(G)	Construction of Explosive Container	Page 271
Figure 3(G)	Concussion Amplification Range.....	Page 272
Figure 4(G)	Plumb Tester.....	Page 273
Figure 5(G)	Experiment Concerning Effect of Free Liquid Surface and Rubber Covering.....	Page 274
Figure 6(G)	Experimental Results Concerning Effects of Free Liquid Surface and Rubber Covering.....	Page 275
Figure 7(G)	Experimental Results Concerning Effects of Free Liquid Surface and Rubber Covering.....	Page 276
Figure 8(G)	Experiment on Cylinders Enclosed with Various Shaped Tanks.....	Page 277
Figure 9(G)	Experimental Results on Cylinder Enclosed with Tanks...	Page 278
Figure 10(G)	Results of Brass Tube Tensile Test.....	Page 279
Figure 11(G)	(A) Target.....	Page 280
Figure 12(G)	(B) Target.....	Page 281
Figure 13(G)	(C) Target.....	Page 282
Figure 14(G)	(D) Target.....	Page 283
Figure 15(G)	(E) Target.....	Page 284
Figure 16(G)	(F) Target.....	Page 285
Figure 17(G)	(G) Target.....	Page 286
Figure 18(G)	(H) Target.....	Page 287
Figure 19(G)	(I) Target.....	Page 288
Figure 20(G)	(J) Target.....	Page 289
Figure 21(G)	(K) Target.....	Page 290
Figure 22(G)	Effects of Outer Cylinder upon the Damage of Inner Cylinder.....	Page 291

ENCLOSURE (G), continued

FOREWORD

When a submarine navigating underwater is attacked by depth charges, some effect will be produced upon the inner and outer hulls. The walls of the inner tanks may expand or the second series battery case may be damaged.

To prevent such a phenomenon, research is necessary on the construction of the submarine hull, the battery case or on the methods of attaching the battery case. However, the effect of the concussion from a depth charge on the hull of a submarine, excluding an explosion at close range, depends upon the underwater elastic compression waves. It has been assumed to be a sudden striking pressure with an endurance time of 10-4 seconds. First of all, it is important to know the characteristics of both the exterior force and the damages which it produces upon the inner tank walls and battery case of a submarine. However, such theoretical research problems are at present unsolved and too much cannot be anticipated.

This report covers the research conducted on the characteristics of an exterior force striking the small brass model double layer cylinder used in this experiment, as well as on the strength of the model itself, surrounded as it is by a thin plate and a liquid layer. It is thought that there is room for further study before this can be suited to practical use. In regard to the characteristics of this force, it is an underwater elastic compression wave passing through the outer and inner wall and through the liquid layer between them. The strength of this model as compared to that of the inner tank walls of a submarine, is considerably greater, so it may be reasoned that the reinforcing of the submarine walls is necessary. For this reason, this report covers the advisability of establishing an air layer over the dorsal surface of the inner hull to completely intercept the compression wave.

PURPOSE

To investigate the swelling of the inner tank of submarines subjected to depth charge attacks, and to obtain countermeasures for preventing damage to the battery case by improving the construction of the submarine hull.

SUMMARY OF RESULTS

A. The following results were obtained when the small, brass model, double layer cylinders were subject to concussion.

1. When the space between the inner and the outer cylinders was filled with water, due to the increased thickness of the wall, the inner cylinder was more dented, even though its static strength was much greater.
2. When a free liquid surface was established between the inner and outer cylinders, the damage to the inner cylinder which had part touching the air layer, and of course part adjacent to the liquid surface, was lessened.
3. The effect of encircling the inner cylinder with rubber was hardly noticeable and was inferior to that of the free liquid surface.
4. An inner cylinder encircled by an outer cylinder with water between the two cylinders endured more than an inner cylinder by itself.

ENCLOSURE (G), continued

B. When a small brass model of an inner tank filled with water was subjected to concussion the following occurred:

A cylindrical inner tank wall had greater concussion resistivity than a flat wall of the same thickness.

OPINIONS

A. The exterior force which strikes the inner tank wall consists of the impact transmitted when it hits the inner hull, and the underwater elastic compression wave which has a comparatively large compression amplitude although it has been lessened by passing through the two hulls and the water layer between them.

B. If construction were such that the compression waves propagated within the liquid layer in the inner submarine tank could be intercepted, deformation of the tank wall could be prevented.

C. A cylindrical surfaced inner tank wall would be advantageous in that deformation would be decreased.

D. The pressures received by the inner tank walls of the submarine can be obtained only through experiments with models. Although conditions will differ from those for the submarine, and the results will not be immediately applicable, they can be accepted as data for the modification of hull construction to prevent the destruction of the battery cases.

TESTS AND ANALYTICAL RESEARCH

It may be presumed that, because of the outer and inner hulls, the pressure received by the inner tank wall of the submarine due to a depth charge explosion would be less than if it received the concussion directly. However, it is difficult to deal with this mathematically. Conditions will vary according to the submarine, the size of the depth charge and the strength of the concussion. For this reason, with purpose of obtaining results for general conditions, a target was constructed of brass pipe, placed in a testing pool and subjected to the concussion from a 1.7 kg cast picric acid charge. It was also tested with an experimental plumb tester, the aim being to obtain a striking pressure of long duration. Data on the test, construction of the target, construction and specifications for the explosive container, and the construction of the plumb tester are shown in the attached diagrams.

The extent of the concussion produced by the 1.7 kg cast picric acid container is as shown in Figure 3(G). It is a single attenuated sine wave of about 10,000 ∞ . The striking pressure of the plumb tester produces about a 700 ∞ single wave form. Compared to the former, it takes about fourteen times longer to build up this pressure. The targets and their results are produced in Table I(G). The results of the tests are shown in Figures 11(G) to 22(G).

A. Tests and Analysis relative to the Pressure Striking the Wall of a Submarine Inner Tank.

1. Tests applying to exterior forces of differing endurance times to an outer and inner cylinders with space between them filled with water:

As shown in A and B of Table I(G), when the space between the outer and inner cylinder is filled with water, the damage to the inner container is more marked, with the varying endurance time having no

ENCLOSURE (G), continued

effect. In the case of A and B, the static strength of the outer cylinder is greater than that of the inner cylinder. However, in the same way it can be said that, in the case of the inner and outer cylinder of C and D, they have an equal static strength.

2. Test conducted with the static strength ratio of the inner and outer cylinders changed:

B, E, F, and G of Table I(G) are all filled with water. However, the static strength of the inner cylinder of B is less than that of the outer cylinder. Both cylinders of E are of the same shape and of equal strength. The static strength of the inner cylinders of F and G are greater than that of the outer cylinders. In all instances, the damage on the inner cylinder appeared more marked. The outer cylinder was hardly changed.

3. Test conducted with inner and outer cylinder of equal static strength but differing wall thickness:

In Table I(G), the shapes of the inner and outer cylinders are the same and the static strengths are equal with only the wall thicknesses differing. Furthermore, the space between both cylinders is filled with water. Even at that the damage to the inner cylinder appeared more marked.

4. The influence of the outer cylinder upon the damage to the inner cylinder:

It is easy enough to imagine that the concussion received by the inner cylinder would be less when there is an outer cylinder. When a 0.55mm and 0.37mm thick cylinder, each with a 0.5mm thick outer cylinder with the space between the two cylinders filled with water were subjected to the explosion from the 1.7 kg charge from a distance of 6 meters, the results as shown in Figure 22(G), proved that the ones with outer cylinders were less damaged.

5. Analysis:

Even when the static strength of the inner cylinder is considerably greater than that of the outer cylinder, the damage to the inner cylinder was still more marked, and had no apparent relation to the thickness of the cylinder wall or the endurance time of the concussion. It is pointed out that there is considerable difference between the construction of the inner hull and the tank wall of the submarine and the target model.

a. The actual tank walls are flat while the inner cylinder of this target model is pillar-shaped so there will be a difference in the effects of the damage.

b. The lengths of depth charge concussion waves (Converting the depth charge to a spherical body whose diameter is thought to be about 60cm, the length of an underwater concussion wave is approximately the same as the diameter of the explosive charge container. For this reason, it is presumed that the concussion wave from the depth charge would be about 60cm.) are approximately 60cm, with the distance between the inner hull and the tank wall averaging 30-50cm. On the contrary, in this test

ENCLOSURE (G), continued

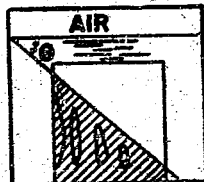
the length of the concussion waves from the 1.7 kg explosive charge is about 15cm with the distance between the two cylinders being 1.6cm. It can be concluded, therefore, that the ratio of the wave length to the water layer thickness differs. Regarding B above, this target was made similar to a submarine but it is difficult to judge as to its safety. However, upon observing the static strength ratio of the inner and outer cylinders, the static strength of the inner hull of the submarine was about 10-20 kg/cm² and that of the tank wall about 3 kg/cm². The ratio was 0.15-0.3. On the other hand, in this target the ratio of the static strength of the inner cylinder to that of the outer cylinder was 0.42-2.28. In spite of this, when it is considered that the inner cylinder is damaged more greatly, in general, it can be supposed that the concussion applied to the submarine tank wall will be considerably greater than the strength of the wall.

For this reason, in order to reinforce the submarine tank wall and equalize its strength to that of the inner hull, so as to have a stronger concussion resistance, considerable reinforcing would be necessary. However, as it was expected, to obtain data mathematically is very difficult and tests must be conducted on models.

B. Test and Analytical Research on the Effectiveness of the Free Liquid Surface and the Rubber Covering.

1. Effectiveness of a free liquid surface:

In Table I(G), B and J, D and K are the same targets with the former in each case filled with water. The latter are provided with a free liquid surface. The inner cylinder of the latter is less damaged. Damage to the cylinder with the free liquid surface is practically negligible. The lower edge, that is, the cylinder end opposite the bottom water layer, was damaged as it had been before. Moreover, that portion of the inner cylinder facing the source of the explosion was damaged markedly along its whole length. It can be said, however, that upon nearing the dorsal surface, the extent of the damage gradually lessened in the direction of the height of the axis. Just as in the sketch, if the inner cylinder were intersected by a surface formed by the water level and an established angle θ , the lower portion, that is, the portion in the sketch shaded by diagonal lines, only would be damaged. Because of such a phenomenon, when it is reasoned that the striking force reaching the inner



cylinder is an elastic pressure wave (even in the test being carried out at the present time at the No. 2 Powder Factory, the underwater pressure wave was able to pass through a thin plate) which has passed through the liquid layer, the free liquid surface must buffer the force of the compression wave. However, it is considered that the effective scope will be localized to within the surface formed by the water level and the fixed angle θ as shown in the sketch.

2. The comparative effectiveness of a free liquid surface and a rubber covering:

L, M, and N of Table I(G) have the same dimensions. One has an air

ENCLOSURE (G), continued

layer at the upper portion, between the inner and the outer cylinders (the volume of the air layer is the same as that of the rubber layer). The inner cylinder of another is enveloped by a 1.5mm thick rubber layer with the space between the two cylinders filled with water, while the space between the inner and outer cylinders of the last is completely filled with water. It was made clear from the results that the effect of the rubber layer is practically negligible, the free liquid surface being the more effective. The construction of the targets and the test results are given in Figures 5(G) through 7(G).

3. Analytical research:

It is supposed that the striking force reaching the submarine tank wall is the compression wave which has passed through the inner and outer hulls and the liquid layer. Even if the submarine tank wall was protected by a rubber layer, good results could not be anticipated. In the case of the free liquid surface, the effect was seen to be great, but the extent of its effectiveness was limited to the vicinity of the free liquid surface. In the broadside tank of a submarine the height is so great and the shape smaller in length; consequently the effective scope is small and it is thought that the objective could not be accomplished.

C. Test and Analytical Research Relative to the Change in Shape of the Submarine Tank Walls.

1. The outer cylinders O, P, and Q of Table I(G) are of the same dimensions. They were fitted with three differently shaped submarine tanks having a wall thickness of 0.3mm and filled with water. They were subjected to concussion from the side to which the tank is fitted. Construction of these targets and results of the test are shown in Figures 8(G) and 9(G).

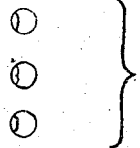
As compared to the flat walled tank, the cylindrically surfaced tank wall had a greater concussion resistivity.

CONCLUSION

The compression and pressure waves which have passed through the outer and inner hulls and the liquid layer are the main causes of the expansion of the submarine wall. It would be difficult to obtain data on these pressures unless we use model targets. However, even though the pressure amplitude decreases between the two hulls, it is still comparatively large. It will take substantial reinforcing to maintain the equilibrium in both hulls with the inner tank wall in its original form. Furthermore, we recognize that the effect of a free liquid surface is considerable, but in cases such as that of a tank on the side of a hull in which there is a large height and narrow width the effect is small, and we are not able to attain our objective. Consequently we can prevent the shock pressure on the wall of the tank by constructing an empty space behind the inner hull which will completely absorb the propagation of the compression wave. However, this will sacrifice simplicity of construction. In this way we can prevent the expansion or rupturing of the tank wall itself, and may be able to decrease the degree of damage to the battery case.

ENCLOSURE (G), continued

Table I(G)
TABLE OF EXPERIMENTAL RESULTS

Target	Outer Cylinder				Inner Cylinder				Comparison of Static Pressure	Conditions Met for Liquid Between Inner and Outer Cylinder
	L (mm)	D (mm)	S (mm)	Static Pressure For ** (see 2) (kg/cm ²)	L (mm)	D (mm)	S (mm)	Static Pressure For ** (see 2) (kg/cm ²)		
A	50	72	0.5	15.5	36	43.5	0.22	6.5	0.42	Completely Filled With Water
B	60	72	0.5	15.5	36	43.5	0.22	6.5	0.42	Completely Filled With Water
C	60	72	0.37	6.7	36	43.5	0.22	6.5	0.97	Completely Filled With Water
D	60	72	0.37	6.7	36	43.5	0.22	6.5	0.97	Completely Filled With Water
E	60	72	0.5	15.5	36	43.5	0.3	15.4	0.99	Completely Filled With Water
F	60	72	0.5	15.5	36	43.5	0.37	24.0	1.55	Completely Filled With Water
G	60	72	0.5	15.5	36	43.5	0.45	35.3	2.28	Completely Filled With Water
H	60	72	1.0	66.0	36	43.5	0.6	64.5	0.98	Completely Filled With Water
I	60	72	1.5	150.0	36	43.5	0.9	150.0	1.00	Completely Filled With Water
J	60	72	0.5	15.5	36	43.5	0.22	6.5	0.42	Free Liquid Surface
K	60	72	0.37	6.7	36	43.5	0.22	6.5	0.97	Free Liquid Surface
L	60	72	1.0	66.0	36	43.5	0.22	6.5	0.01	Free Liquid Surface
M	60	72	1.0	66.0	36	43.5	0.22	6.5	0.01	Inner Cylinder covered with 1.5mm thickness rubber plate. Filled completely with water.
N	60	72	1.0	66.0	36	43.5	0.22	6.5	0.01	Completely Filled With Water
O	50	100	0.5	10.4	 Thickness of tank wall 0.03mm					Completely Filled With Water
P	50	100	0.5	10.4						Completely Filled With Water
Q	50	100	0.5	10.4						Completely Filled With Water

NOTES:

- *Target is of brass construction, and results of its tension and compression tests are shown in Figure 10(G)
- ** (Static pressure For) refers to the calculation obtained by TOKUGAWA's formula and shows the static pressure damaging intensity after passing the elastic limit and the yield point.
- # (PLUMB 2 kg-1m) refers to the plumb tester dropping a kg plumb weight from a height of 1 meter.
- ## (Bursting charge 1.7 kg-6m) refers to 1.7 kg cast picric acid explosive container placed at a range of 6 meters from target. Experiment conducted at depth of 2m from surface of a pond 3.5m deep.

⊖ (TH - Evidently a symbol representing deflections or hollows in cylinder).

ENCLOSURE (G), continued

Table I(G), continued
TABLE OF EXPERIMENTAL RESULTS

Applied Pressure	Results		Photographs
	Outer Cylinder	Inner Cylinder	
Plumb # (see 3) 2 kg-1m	No Change	$\bar{u} = 1.52$ max $n = 12-12$ 27-15	1
Bursting Charge## (see 4) 1.7 kg-6m	Slightly Concave $\bar{u} = 0.96$ Two Dents $\bar{u} = 0.09$	$\bar{u} = 3.37$ max $n = 12-24-21$	2
Plumb# (see 3) 2 kg-0.75m	No Change	$\bar{u} = 1.29$ max $n = 9-$	3
Bursting Charge## (see 4) 1.7 kg-10m	No Change	$\bar{u} = 0.38$ max $n = 21-21-$	4
Bursting Charge## (see 4) 1.7 kg-6m	Slightly Concave $\bar{u} = 0.28$ One Dent $\bar{u} = 0.28$	$\bar{u} = 0.87$ max $n = 12-15-27$ 24-15	5
Bursting Charge## (see 4) 1.7 kg-6m	Slightly Concave $\bar{u} = 0.05$ Two Dents $\bar{u} = 0.03$	$\bar{u} = 0.38$ max $n = 18-18$	6
1.7 kg-6m	Slightly Concave $\bar{u} = 0.53$ Two Dents $\bar{u} = 0.41$	$\bar{u} = 0.21$ max	7
1.7 kg-3m	Surface Facing $\bar{u} = 0.16$ Explosion max Slightly Flattened	$\bar{u} = 0.54$ max $n = 21-18$ 24-18	8
1.7 kg-2m	Surface Facing $\bar{u} = 0.24$ Explosion max Slightly Flattened	$\bar{u} = 0.61$ max $n = 15-$	9
1.7 kg-6m	Air Space $\bar{u} = 0.60$ Section max Damaged $n = 27-12$	Section Facing Explosion and Lower Water Layer Section Damaged $\bar{u} = 1.01$ max	10
1.7 kg-10m	Air Space $\bar{u} = 0.30$ Section max Damaged $n = 30-$	No Change	11
1.7 kg-5m	Section Facing Explosion and Rear Section Slightly Dented $\bar{u} = 0.08$ $\bar{u} = 0.01$	Section Facing Explosion and Lower Water Layer Section Damaged $\bar{u} = 0.68$ max $n = 39-$	13
1.7 kg-5m	No Change	$\bar{u} = 0.96$ max $n = 30-30-24-$	
1.7 kg-5m	No Change	$\bar{u} = 1.25$ max $n = 30-27-30-18$	
1.7 kg-14m	Outer Section of Tank Receiver and Rear Section Damaged	No Change	14
1.7 kg-14m	Outer Section of Tank Receiver Damaged	No Change	
1.7 kg-14m	Outer Section of Tank Receiver Damaged	Blistered Out $\bar{u} = 1.93$ max	

ENCLOSURE (G), continued

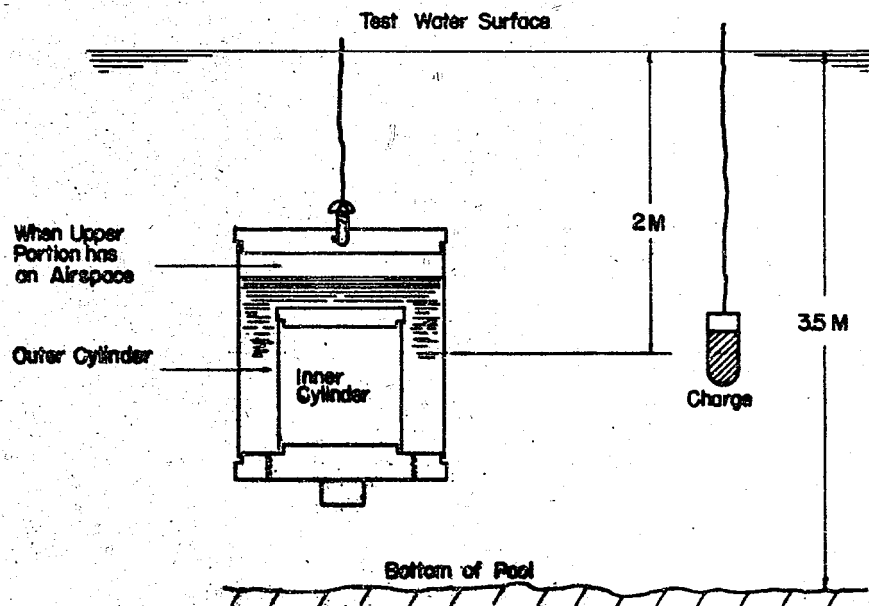


Figure 1(G)
TEST SET-UP

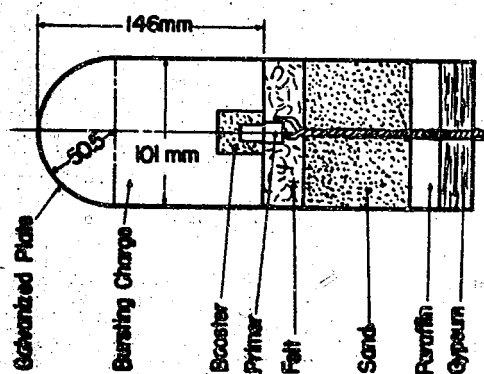


Figure 2(G)
CONSTRUCTION OF EXPLOSIVE CONTAINER

ENCLOSURE (G), continued.

Measured by Tech Research Type Model A Crystal Manometer
Bursting charge: 1.7 kg cast picric acid

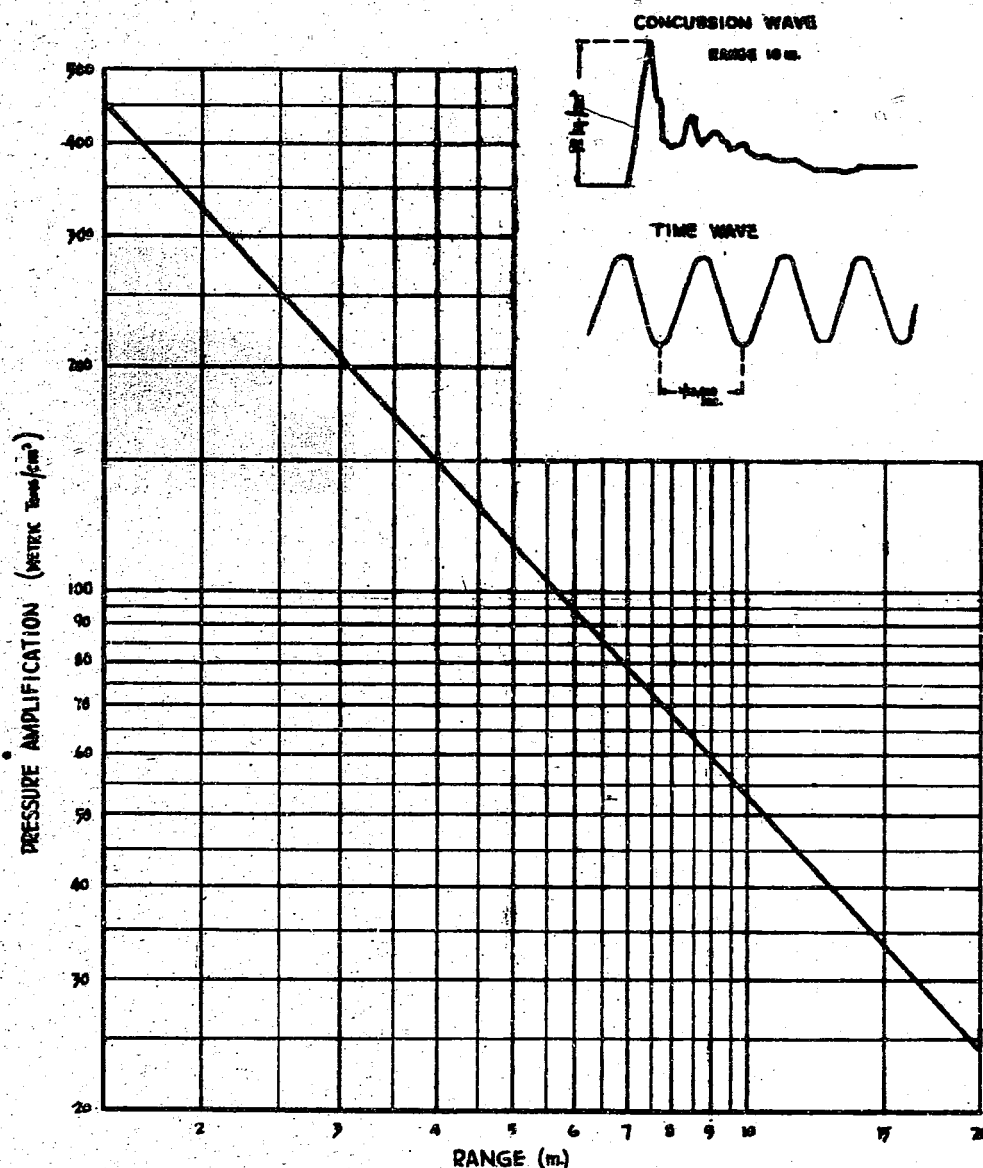
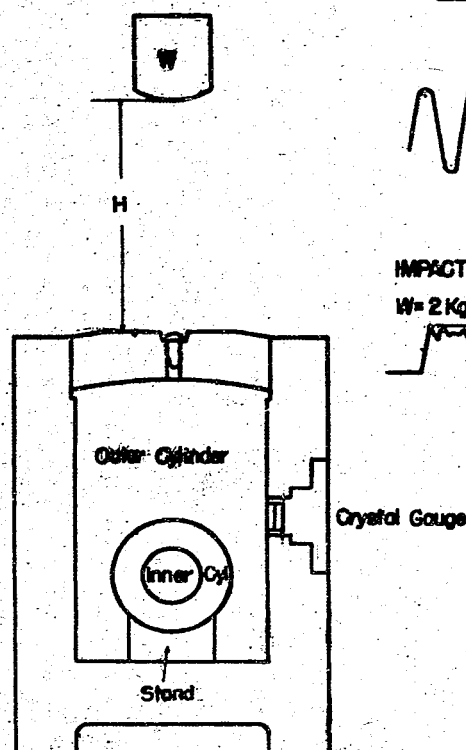


Figure 3(G)
CONCUSSION AMPLIFICATION RANGE

ENCLOSURE (G), continued

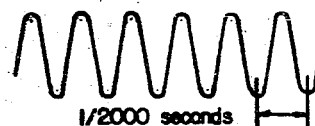
W= Plumb
H= Height of Drop
The Plumb is Dropped
Perpendicularly



IMPACT PRESSURE WAVE
Measured by Crystal Manometer

W= 2 Kg. H= 75 cm
Equal to 35 Kg/cm²

TIME WAVE

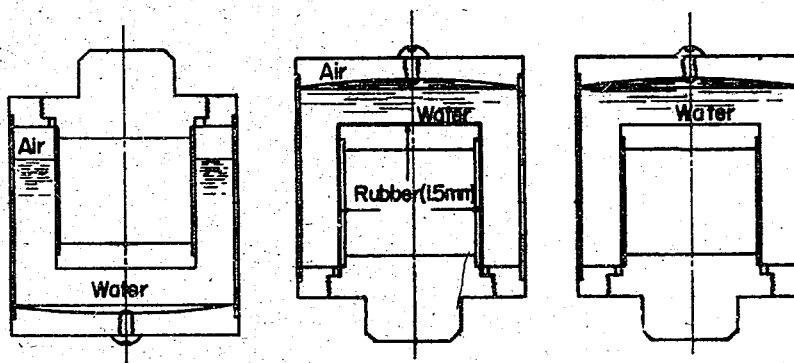


IMPACT PRESSURE WAVE

W= 2 Kg. H= 1.0 m
Equal to 40 Kg/cm²

Figure 4(G)
PLUMB TESTER

ENCLOSURE (G), continued



Outer cylinder (meters)

D 72
 L 60
 S 1.0

Inner cylinder (meters)

D 43.5
 L 36
 S22

Thickness of rubber covering: 1.5mm

Volume of air space: equivalent to bulk of rubber covering

Bursting charge: 1.7 kg cast picric acid

Range between explosive and target: 5 meters
 (amplified concussion: 115 kg/cm²)

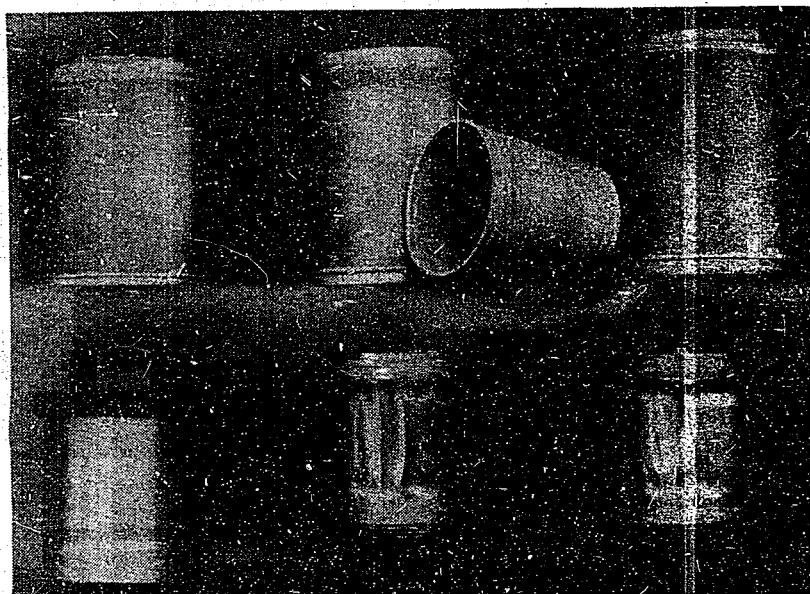


Figure 5(G)
 EXPERIMENT CONCERNING EFFECT OF FREE LIQUID SURFACE
 AND RUBBER COVERING

ENCLOSURE (G), continued

(L) Target - With free liquid surface.

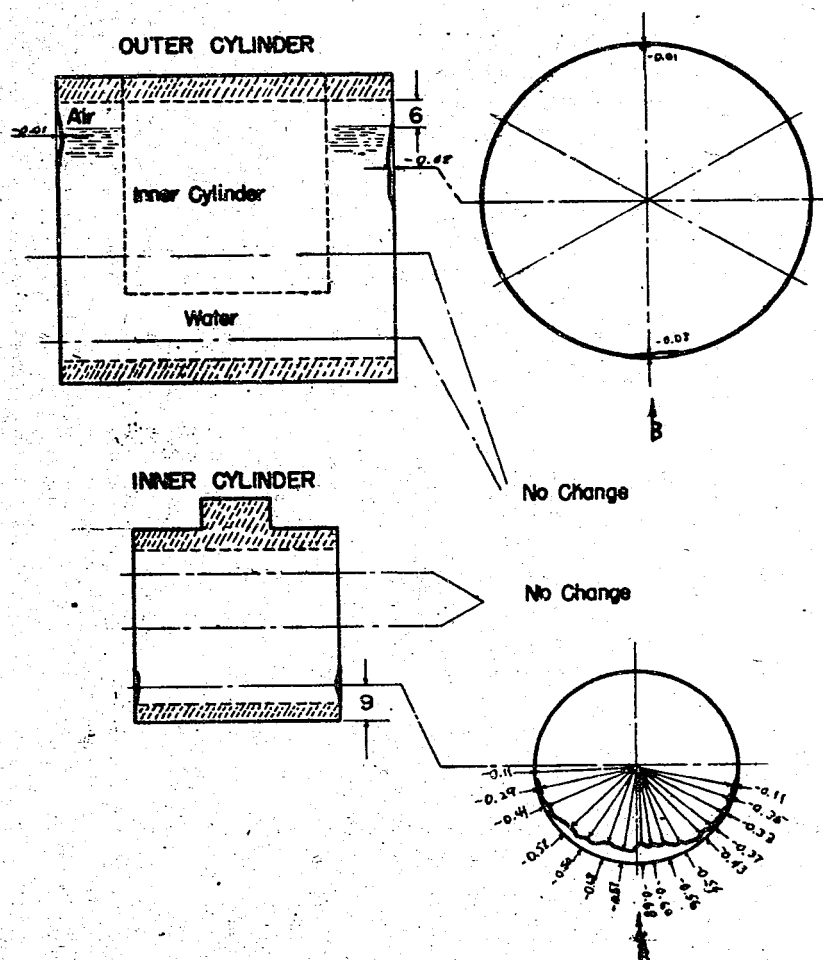
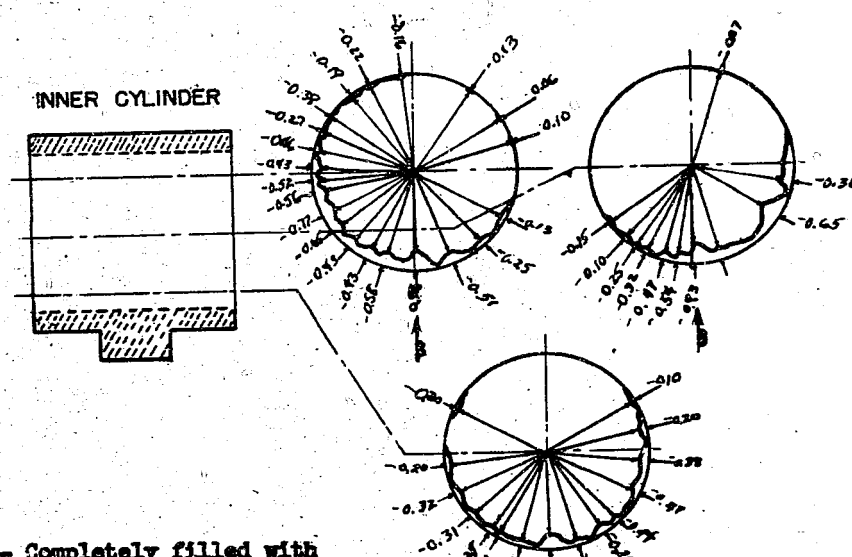


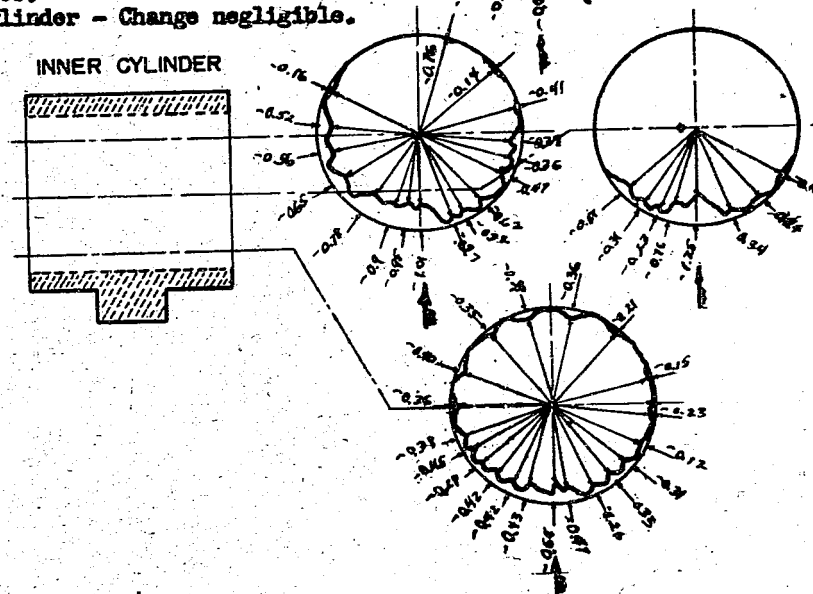
Figure 6 (G)
EXPERIMENTAL RESULTS CONCERNING EFFECTS OF FREE LIQUID SURFACE
AND RUBBER COVERING

ENCLOSURE (G), continued

- (M) Target - With rubber covering.
Outer cylinder - Change negligible.



- (N) Target - Completely filled with water.
Outer cylinder - Change negligible.



Notes: \uparrow indicates incident direction of concussion wave.
Dimensions within arrows indicate denting measured on radius.

Figure 7(G)
EXPERIMENTAL RESULTS CONCERNING EFFECTS OF FREE LIQUID SURFACE
AND RUBBER COVERING

ENCLOSURE (G), continued

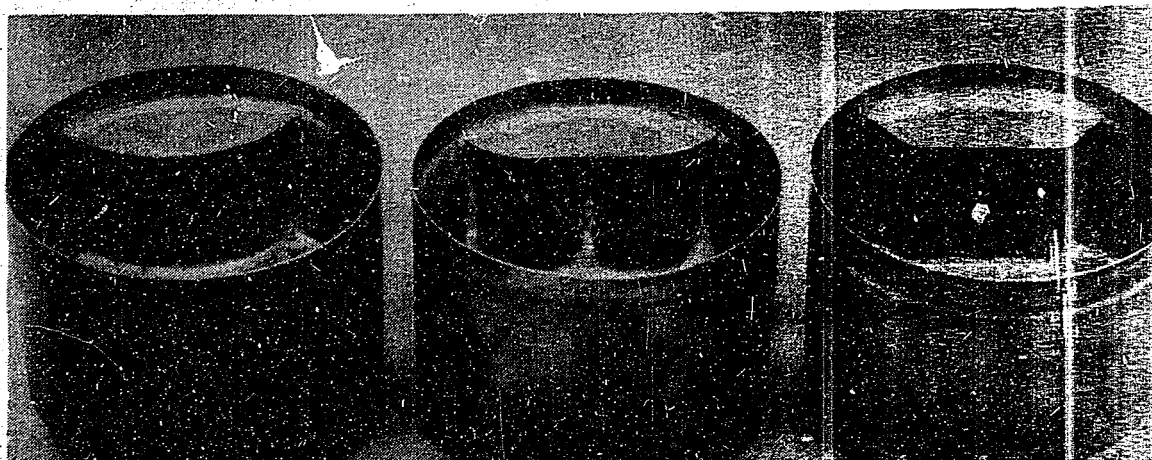
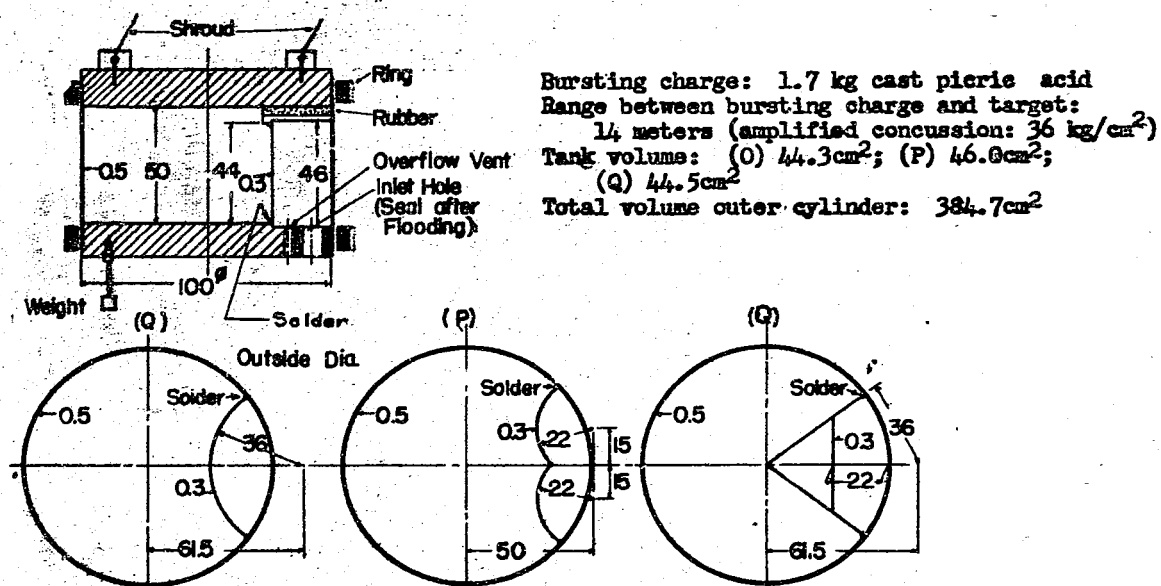
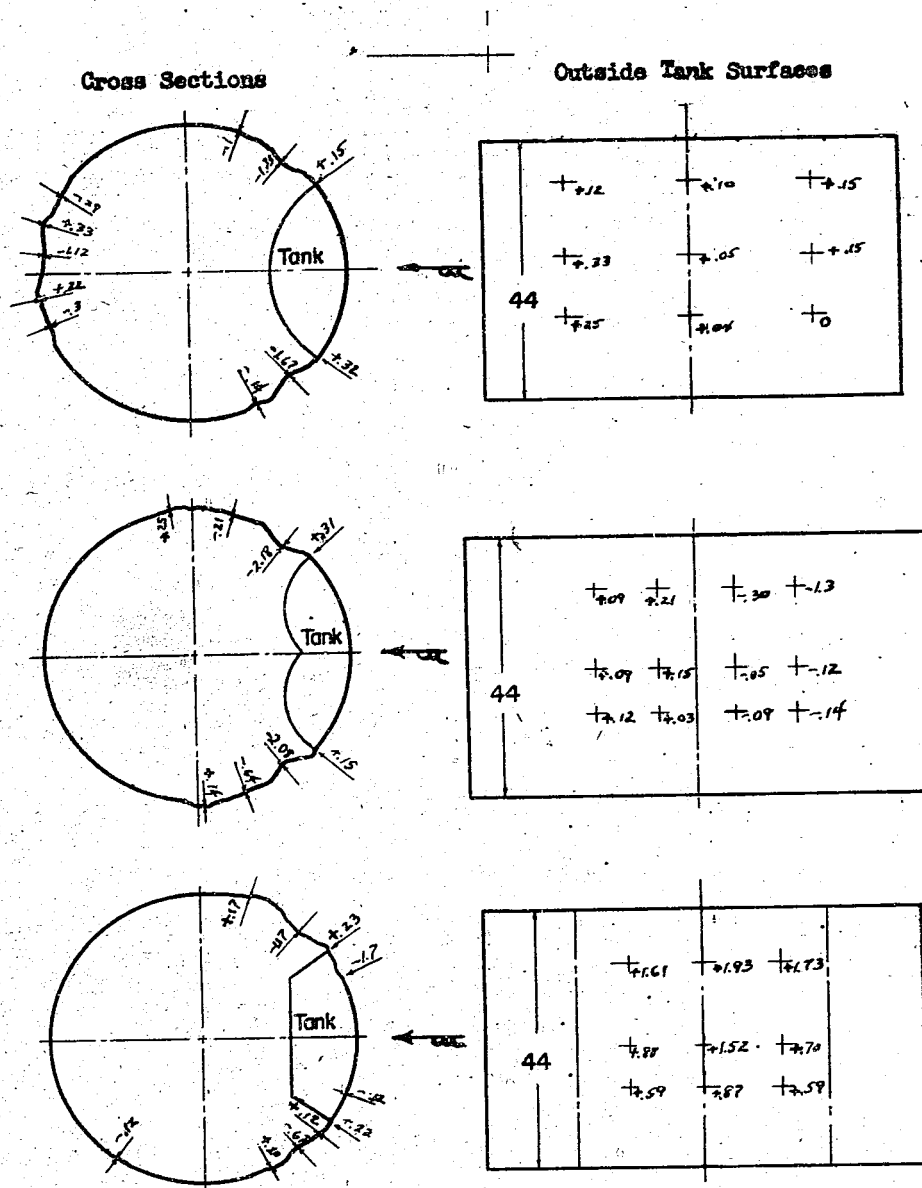


Figure 8(G)
 EXPERIMENT ON CYLINDERS ENCLOSED WITH VARIOUS SHAPED TANKS

ENCLOSURE (G), continued



Notes: Dentings of cross section view taken from mid-section.
 Outside tank surface drawing shows denting measured from direction indicated by \leftarrow .

Figure 9(G)
 EXPERIMENTAL RESULTS ON CYLINDER ENCLOSED WITH TANKS

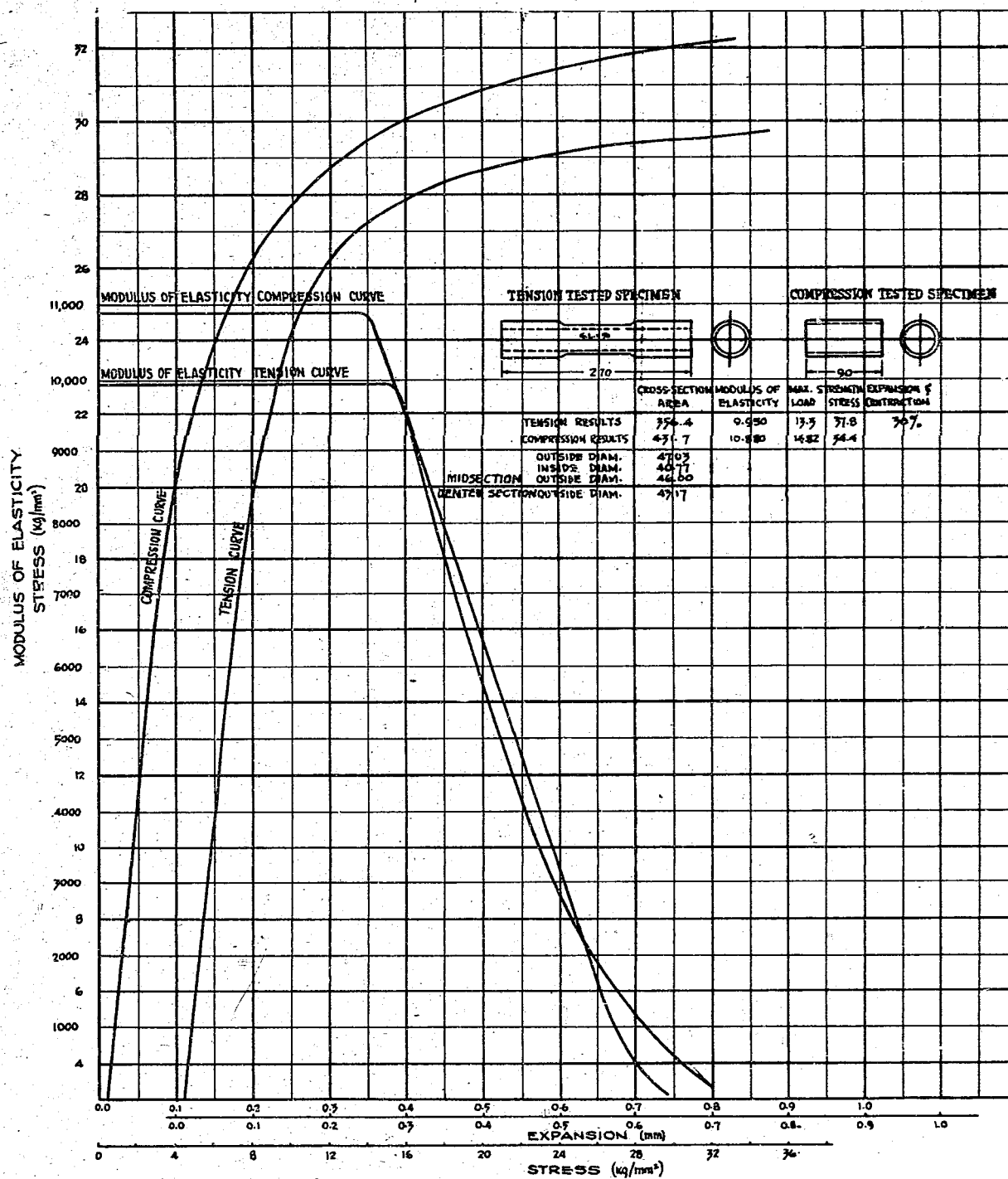
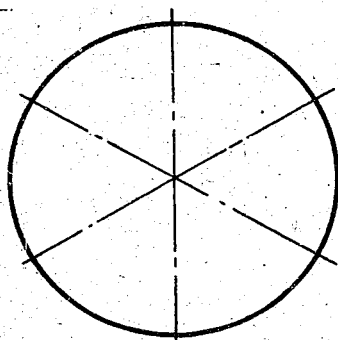
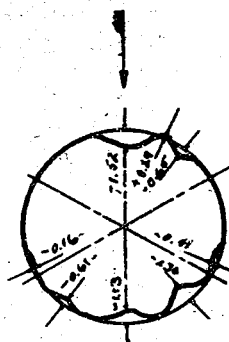


Figure 10 (G)
RESULTS OF BRASS TUBE TENSILE TEST
(May 17, 1943)

ENCLOSURE (G), continued

Outer Cylinder
(No change)

Inner Cylinder

 $n = 12 \sim 12$

Outer cylinder (mm)

L 60
 D 72
 S 0.5

Inner cylinder (mm)

L 36
 D 43.5
 S 0.22

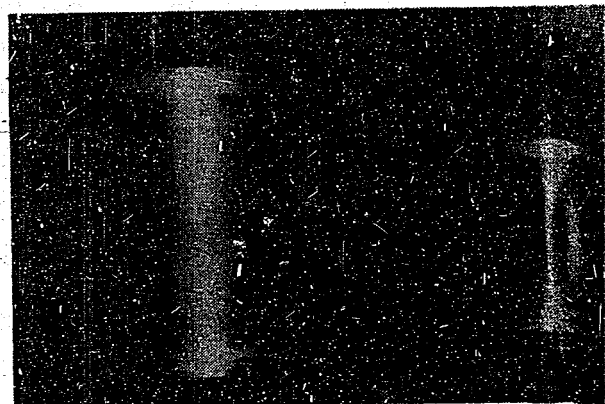
Concluded amplified impact pressure: 40 kg/cm²

Time duration impact pressure: 1/650 sec

W 2 kg

H 1.0 m

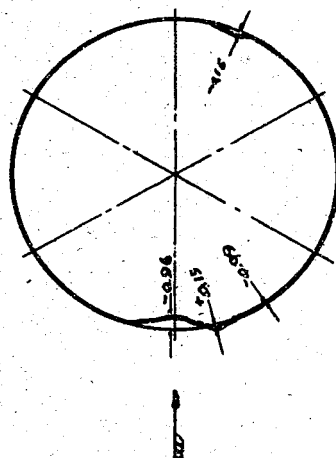
Space between inner and outer cylinders completely filled with water.



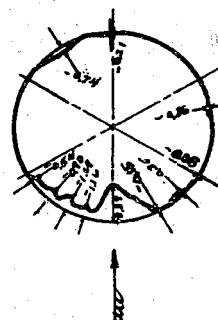
Notes: ↓ indicates direction of applied pressure.
 Cross section drawing shows entire middle section except those specifically mentioned.

Figure 11(G)
 (A) TARGET

ENCLOSURE (G), continued

Outer Cylinder
11 Cross Section

Inner Cylinder



27 ~ 15
 $n = 12 \sim$
 24 ~ 21

Outer cylinder (same as (A) Target)
 Inner cylinder (same as (A) Target)
 Bursting charge: 1.7 kg picric acid
 Range: 6 meters
 Concluded amplified concussion: 94 kg/cm²
 Time duration of concussion: 1/20,000 sec
 Water completely filled between inner and
 outer cylinders.

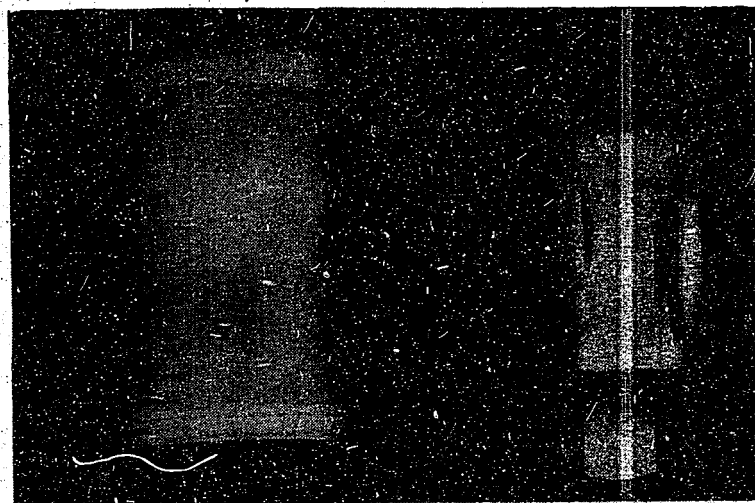
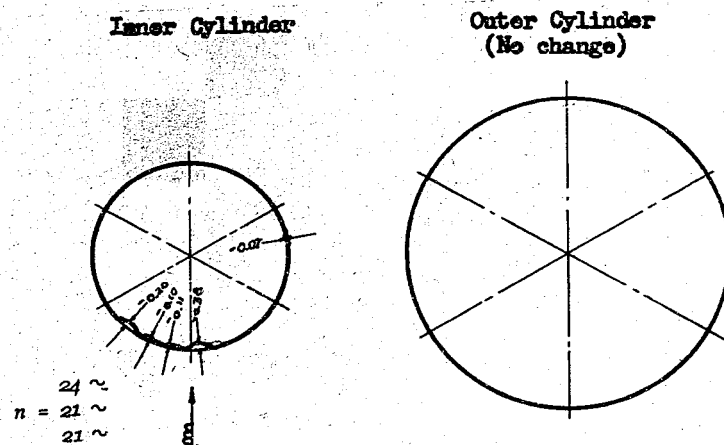


Figure 12(G)
 (B) TARGET

ENCLOSURE (G), continued



Outer cylinder (same as (C) Target)
Inner cylinder (same as (C) Target)
Bursting charge: 1.7 kg picric acid
Range: 10 meters
Concluded amplified concussion: 52 kg/cm²
Time duration of concussion: 1/20,000 sec
Space between inner and outer cylinders
completely filled with water

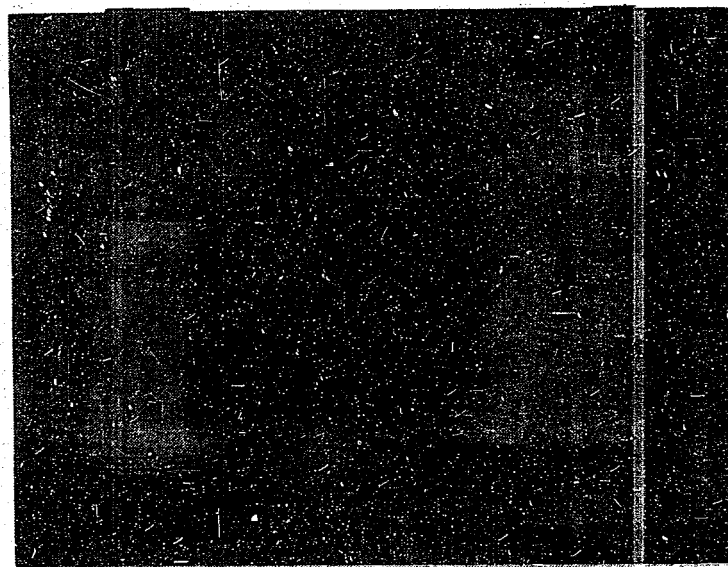
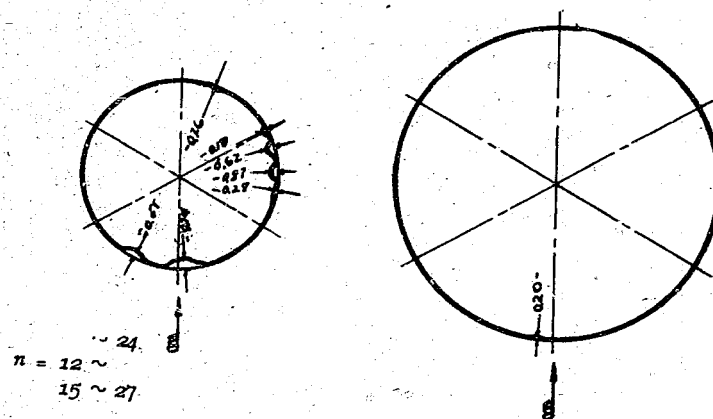


Figure 14(G)
(D) TARGET

ENCLOSURE (G), continued

Inner Cylinder

Outer Cylinder
11 Cross Section

Outer cylinder (mm)

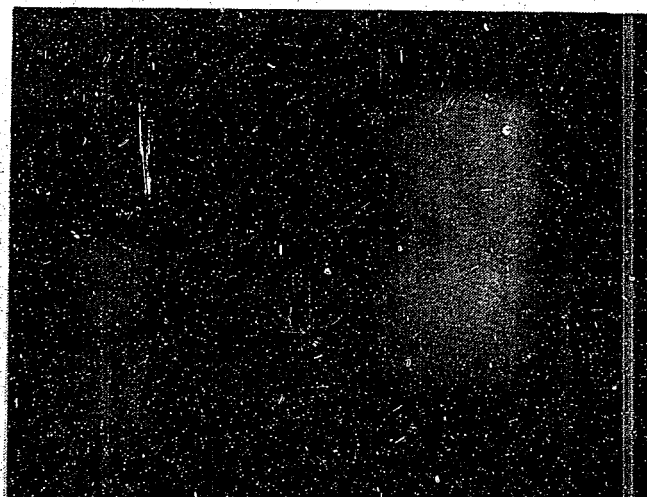
L 60
 D 72
 S 0.5

Inner cylinder (mm)

L 36
 D 43.5
 S 0.3

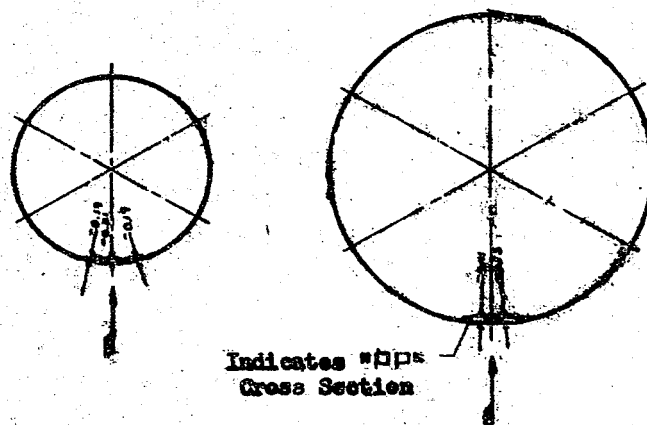
Bursting charge: 1.7 kg picric acid

Range: 6 meters

Concluded amplified concussion: 94 kg/cm²Space between inner and outer cylinders
completely filled with waterFigure 15(G)
(E) TARGET

ENCLOSURE (G), continued

Inner Cylinder

Outer Cylinder
1/1 Cross Section

Same as (F) Target except:
Inner cylinder - 3 0.45

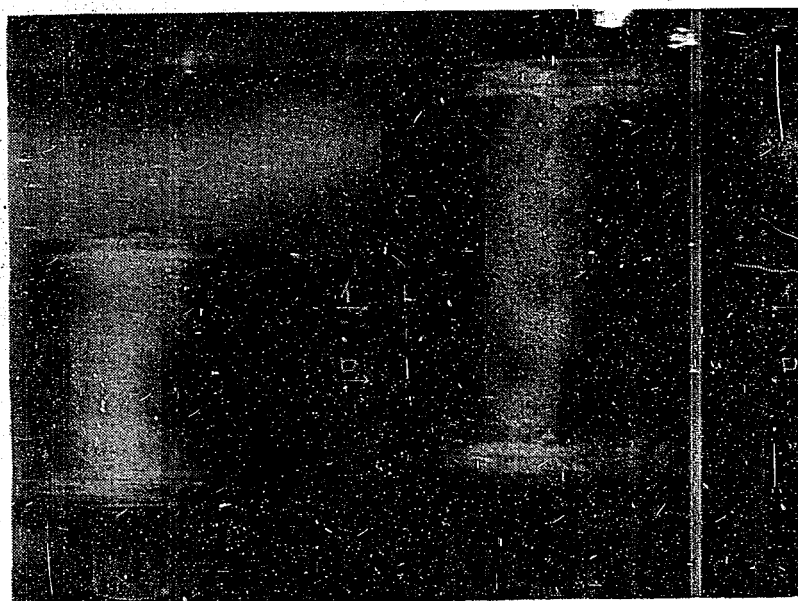
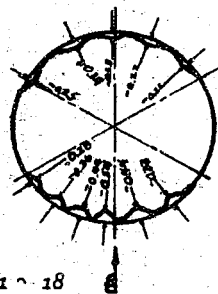
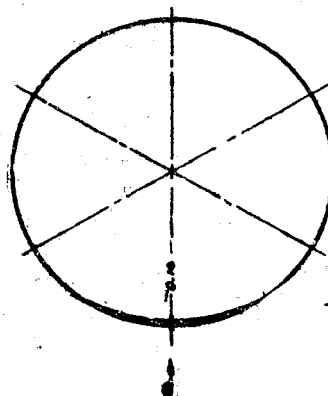


Figure 17(G)
(G) TARGET

ENCLOSURE (G), continued

Inner Cylinder
44 Cross Section

Outer Cylinder



Outer cylinder

L 60
D 72
S 1.0

Inner cylinder

L 36
D 43.5
S 0.6

Bursting charge: 1.7 kg picric acid

Range: 3 meters

Concluded amplified concussion: 210 kg/cm²

Space between inner and outer cylinders
completely filled with water

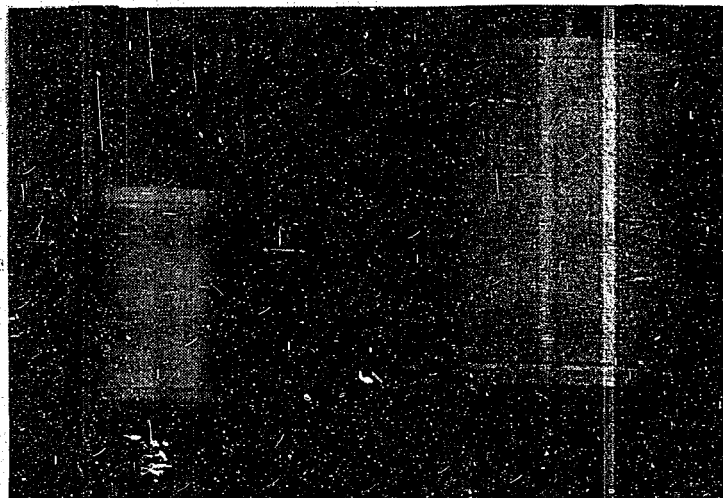
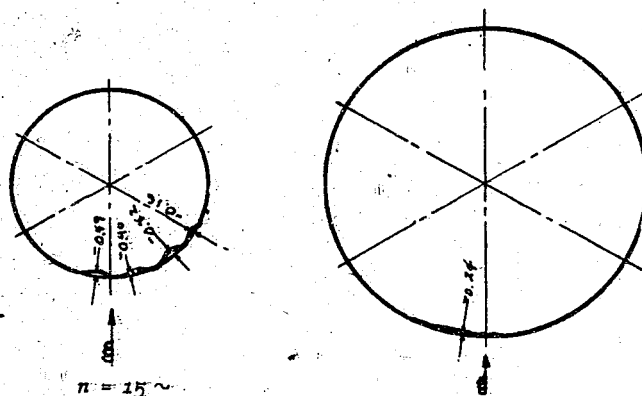


Figure 18(G)
(H) TARGET

ENCLOSURE (G), continued.

Inner Cylinder

Outer Cylinder



Outer cylinder

L 60
 D 72
 S 1.5

Inner cylinder

L 36
 D 43.5
 S 0.9

Bursting charge: 1.7 kg picric acid

Range: 2 meters

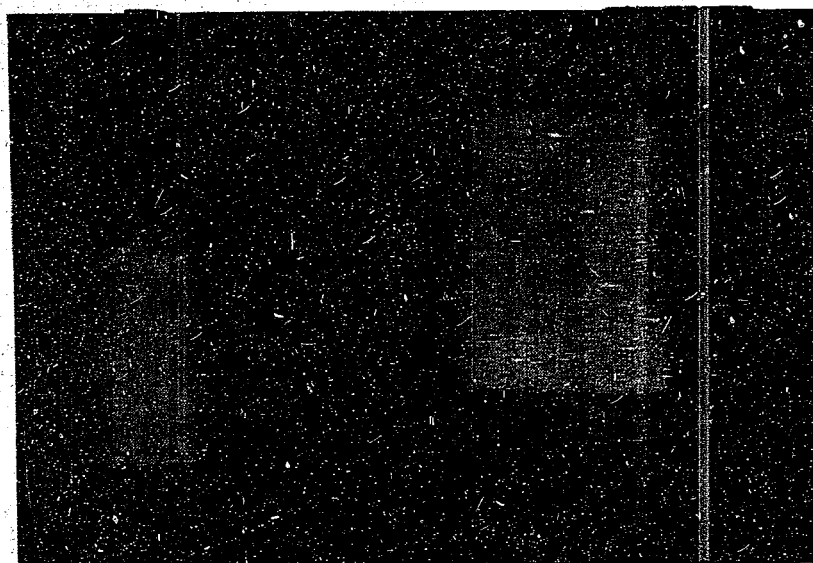
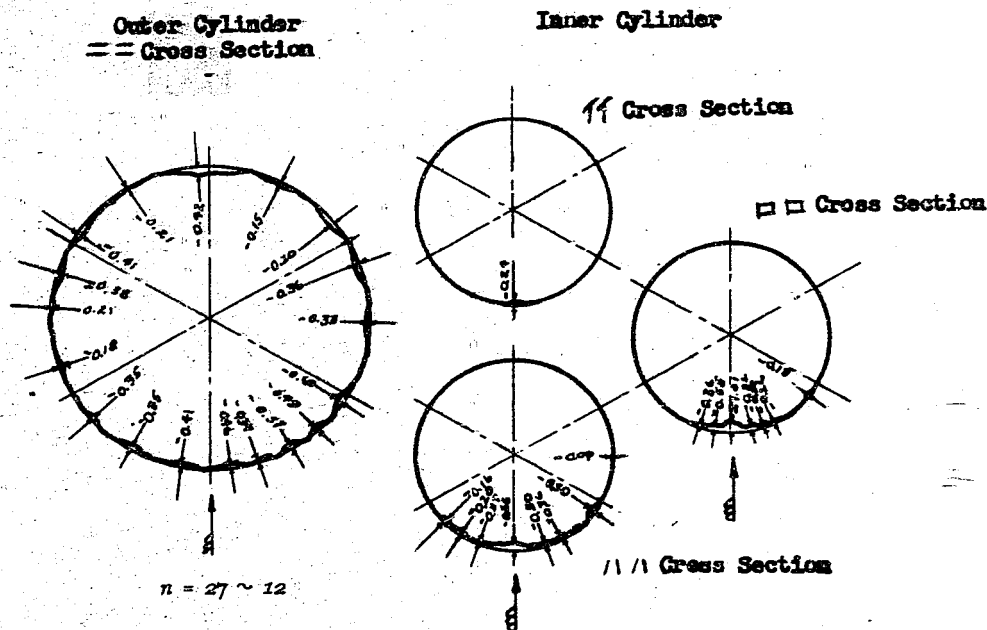
Calculated amplified concussion: 325 kg/cm²Space between inner and outer cylinders
completely filled with water

Figure 19(G)
 (I) TARGET

ENCLOSURE (G), continued



Outer cylinder

L 60
D 72
S 0.5

Inner cylinder

L 36
D 43.5
S 0.22

Bursting charge: 1.7 kg picric acid

Range: 6 meters

Concluded amplified concussion: 94 kg/cm²

Free liquid surface, that is, air space of
7mm thickness above water surface
between inner and outer cylinders

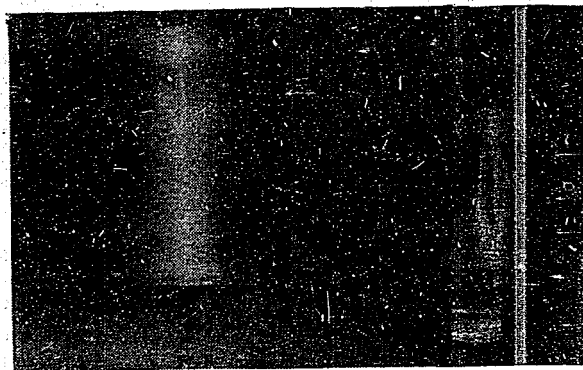
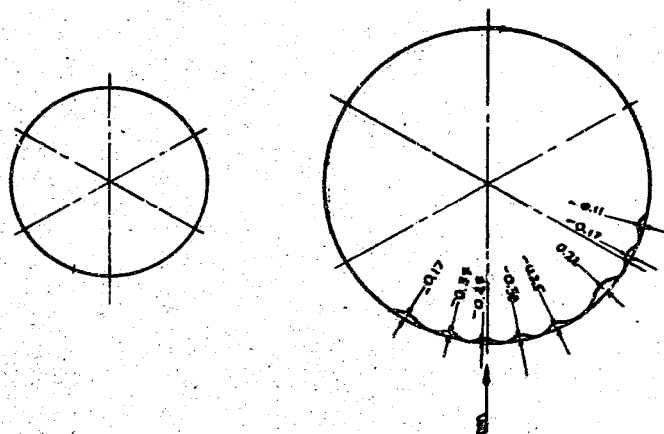


Figure 20(G)
(J) TARGET

ENCLOSURE (G), continued

Inner Cylinder
(No change)

Outer Cylinder
11 Cross Section



ENCLOSURE (G), continued

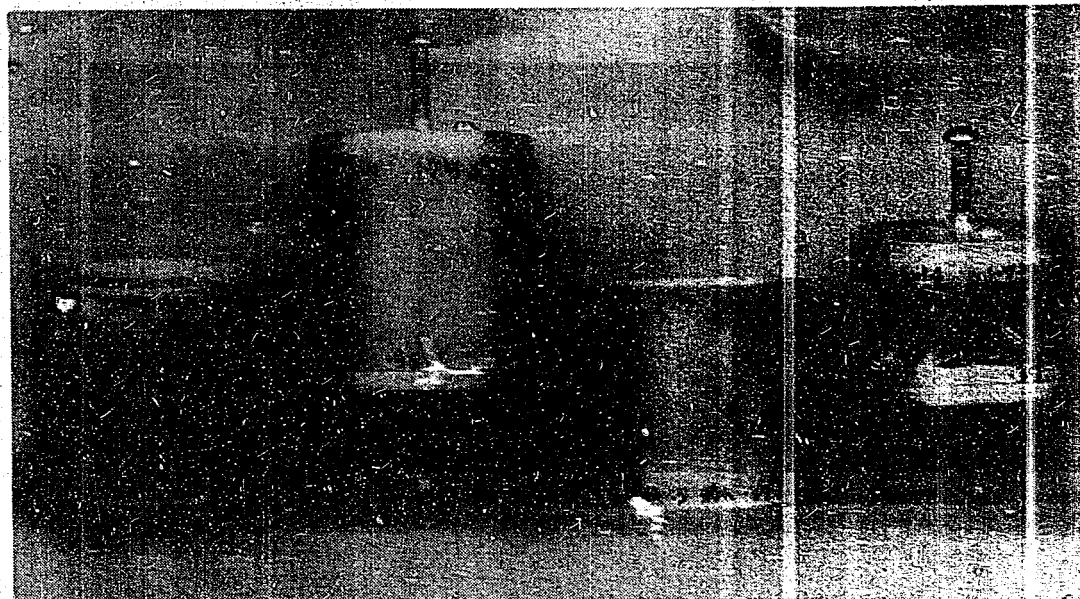


Figure 22(G)
EFFECTS OF OUTER CYLINDER UPON THE DAMAGE OF INNER CYLINDER

The above illustrates the effect on cylinders of the concussion produced by 1.7 kg bursting charge at range of 6 meters. The cylinder in the extreme left (thickness 0.55mm) and the cylinder third from left (thickness 0.37mm) respectively are enclosed in outer cylinders of 0.5mm thickness. The space between the outer and inner cylinders is completely filled with water. In this experiment, no change was produced in the outer cylinder. However, when the cylinder on the extreme right and the cylinder third from the right were subjected to the same concussion as above, without an outer cylinder, the resulting degree of damage was strikingly evident compared with the experiment where the outer cylinder was used.

ENCLOSURE (H)

MODEL EXPERIMENTS TESTING THE STRENGTH OF SUBMARINE HULLS
AGAINST UNDERWATER EXPLOSIONS

Second Report - 28 June 1943

Study of the Copper Crusher

LIST OF ILLUSTRATIONS

Figure 1(H)	Compression Wave	Page 295
Figure 2(H)	Diagram Giving Essentials of Underwater Explosion Pressure Test	Page 300
Figure 3(H)	1.7 kg Bursting Charge Explosion Pressure One Dimensional Curve	Page 301
Figure 4(H)	Amplitude Magnification Curve for Independent Sine Wave Form External Force	Page 302
Figure 5(H)	Amplitude Magnification Curve for Independent Sine Wave Form External Force	Page 303
Figure 6(H)	Pressure Sphere Gauge Details	Page 304
Figure 7(H)	Copper Rod Pressure Sphere Determination Curve, Type P ₁	Page 305
Figure 8(H)	Copper Rod Pressure Sphere Determination Curve, Type P ₂	Page 306
Figure 9(H)	Copper Rod Pressure Sphere Determination Curve, Type P ₃	Page 307
Figure 10(H)	Copper Rod Pressure Sphere Determination Curve, Type P ₄	Page 308
Figure 11(H)	Copper Rod Pressure Sphere Determination Curve, Type P ₅	Page 309
Figure 12(H)	Copper Rod Pressure Sphere Determination Curve, Type P ₆	Page 310
Figure 13(H)	Copper Rod Pressure Sphere Determination Curve, Type P ₇	Page 311
Figure 14(H)	Comparison of Calculated and Static Load Determinations of T _t (max) vs. w/w ₀	Page 312

ENCLOSURE (H), continued

Introduction

The number of people who actually understand the theory of the copper crusher are comparatively few, in spite of the fact that it is a simple and commonly used instrument for determining explosive pressures. Colonel RAI in his "Basic Research on Underwater Explosions" reports that when triangular explosive compression waves with only the maximum pressure varying are applied successively for 2×10^{-5} seconds on a fixed copper crusher gauge, the depth of indentation on the copper rod indicates the proportion between the time element of the explosion compression wave and the degree of maximum pressure. After comparing the results of the numerous experiments and considering the pressure gauge as a vibratory system, it has been found that the indentations will differ if the pattern of time fluctuations varies, even though the maximum pressure of the compression wave is constant. Furthermore, the varying patterns of the load speed of the copper rod have to be taken into consideration and studied as factors affecting the theoretical conclusions.

Since the copper crusher gauge used may not necessarily be the exact type used in the above report, and since the actual curve and time period of the compression wave may vary, the experiment must be conducted by using several copper rods in several pressure gauges.

If the source of the explosion is a considerable distance away, compression waves may be treated as decreasing, crescent-shaped, independent and isolated waves. Some variations must be expected due to the reciprocal relationship between the outside wave form and the vibrational peculiarities of the vibrational system, when the copper crusher gauge is regarded as a vibrational system.

When compression waves register excessively on the copper rod pressure gauge in the form of an underwater compression force, the force received by the piston, the force transmitted to the pressure sphere along the piston, the viscous drag of the copper rod, the resistance offered by the pistons and the walls of the instrument etc. must be taken into consideration.

However, since it eventually becomes just a matter of theoretical accuracy, these factors may be largely disregarded and only their trend considered. As expected the scattering will be great as a result of the experiment. However, looking at it from a broad perspective, it can be said that the trend is as indicated in the theory.

Purpose

The purpose of this investigation is to study the trend of the pressure gauge reading by inquiring into the mutual relationships between the induced vibrational models of the pressure gauge and the frequency of the compression waves. Thereby, a study of the method for pressure measurements with a copper rod pressure gauge can be made.

Summary of Results

The relationship between the natural frequency ($2\pi/a$) of the copper crusher gauge and the time period (π/w) of the compression wave is one factor determining the magnitude of the gauge reading. Although it has been ascertained that the reading of the same compression wave which is in the boundary of $0.7 < w/w_0 < 6.0$ has a tendency to decrease as the ($\frac{w}{w_0}$) increases, a definite conclusion cannot be drawn.

Opinions

Although the impact received by the piston from the compression wave, the

ENCLOSURE (H), continued

viscous drag, the friction resistance, etc. of the copper rod pressure gauge are factors that must be taken into consideration, it is thought that an inquiry should be made into the general theory of the copper rod pressure gauge.

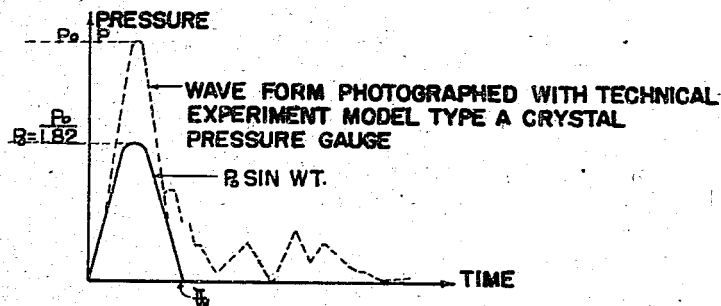
Theory

In the usual vibratory system, when in compression, displacement is caused by the outside kinetic force of an independent wave. The maximum amount of displacement is controlled by the relationship between the natural frequency of the vibratory system and frequency of the outside kinetic force.

The crusher gauge is regarded as a vibratory system. That is to say, the pressure piston and the pressure sphere are considered as one mass, and the copper rod as an elastic spring (the coefficient of the spring utilizes the fact that the actual P-H curve becomes almost straight and the P which causes the unit quantity H is regarded as the said coefficient). Consequently, when the maximum displacement of the pressure sphere is considered as determining the depth of the pressure scar, it is because of the above reason. When the maximum value of the outside kinetic force is statically added periodically, it must be considered that at that time the depth of the pressure scar made on the copper rod is a multiple of the vibrational amplitude (SHINPUKI BAIRITSU) (comparable to the maximum displacement caused by the outside kinetic force and the static displacement in the case when the maximum value of the outside kinetic force is applied statically periodically). When the depth of the pressure scar made by the static load is read off as the depth of the pressure scar made by the outside kinetic force an accidental error in the magnitude of the multiple of the vibrational amplitude (SHIMPUKU BAIRTSU) cannot be avoided.

Although the crusher gauge is to be regarded as a vibrational system, it is understood that the natural frequency includes various factors such as the mass of the movable parts (pressure piston, pressure sphere, the spring coefficient of the copper rod, the coefficient of viscous drag of the copper rod, the friction between the piston and the walls of the instrument etc.). In this report all such coefficients will be omitted.

Furthermore, the amplitude coefficient will vary with the shape of the wave over the same time period as that of the outside force.



RESEARCH IN REGARD TO UNDERWATER PRESSURE WAVE.
RESEARCH REPORT. TECHNICAL REPORT NO. 0320
26 JAN. 1946

Figure 1(H)
COMPRESSION WAVE

ENCLOSURE (H), continued

In this study, a 1.7 kg bursting charge of cast picric acid was used, as shown in Figure 2(H). An example of a wave form was photographed with a Type "A" Technical Experimental Model Crystal Pressure Gauge at a distance of three to ten meters from the source of the explosion as shown in Figure 3(H). (Research in Regard to Underwater Pressure Waves, Research Report, Technical Report 0320, dated 26 January 1943.)

It is thought that the shape of the compression wave changes with the distance from the source of the explosion. Moreover, it is thought that there are some differences in the compression wave forms and the periodic changes in the outside force received by the surface of the pressure gauge. However, for the sake of simplicity, the outside force on the surface of the pressure gauge will be regarded as an independent sine wave as shown in Figure 1(H). Its maximum pressure will be the periodic maximum force of the pressure wave as reported in a previous report of these experiments. Also, differences in readings caused by the different pressure gauge mounting methods, and by disturbances in the pressure waves in front of the pressure receiving surface will not be referred to. The entire body of the pressure gauge does not move at all. The pressure wave hitting the pressure receiving surface will be considered to be equally distributed on the entire surface. It is permissible to make these omissions when observing only the tendencies of the pressure gauge readings. However, at times the movements of the movable parts of the pressure gauge can be formulated as follows:

$$\begin{aligned} m\ddot{x} + kx &= P_0 A \sin wt & \left. \begin{aligned} 0 \leq t \leq \pi/w \\ 0 > t, t > \pi/w \\ t = 0 \end{aligned} \right\} \dots (1) \\ &= 0 \\ x = 0, \dot{x} &= 0 \end{aligned}$$

where: x = displacement of the movable parts
 m = mass of the movable parts
 k = spring coefficient of the copper rod
 P_0 = maximum periodic pressure of the pressure wave
 A = area of pressure receiving surface
 w = angular frequency caused by the pressure wave

The following result is obtained by solving the equation

$$\left. \begin{aligned} X &= \frac{P_0 A}{MW_0^2} \frac{W_0}{W^2 - W_0^2} [W \sin W_0 t - W_0 \sin Wt], \quad 0 \leq t \leq \pi / w \\ \frac{P_0 A}{MW_0^2} \frac{2WW_0}{W^2 - W_0^2} \cos \frac{W_0 \pi}{2W} \sin W_0(t - \frac{\pi}{2W}), \quad t > \frac{\pi}{W} \end{aligned} \right\} \dots (2)$$

The first item obtained in formula (2) is the displacement of the movable parts (piston and pressure sphere) when a static load of $P_0 A$ is added; that is, it shows the depth of the pressure scar on the copper rod.

$$\frac{P_0 A}{MW_0^2} = \frac{P_0 A}{M k/m} = \frac{P_0 A}{k}$$

ENCLOSURE (H), continued

Therefore, it is found that the depth of the pressure scar made by the dynamic pressure is the product of the depth of the pressure scar made by the static load and the value $T(t)_{\max}$.

$$\left. \begin{aligned} T(t) &= \frac{W_0}{W - W_0} \left[W \sin W_0 \sin Wt \right], 0 \leq t \leq \pi/W \\ \frac{2WW_0}{W^2 - W_0^2} \cos \frac{W_0\pi}{2W} \sin W_0 \left(t - \frac{\pi}{2W} \right), t > \pi/W \end{aligned} \right\} \dots\dots\dots (3)$$

Because $T(t)$ changes according to the relation between w_0 and w , it means $T(t)_{\max}$ is controlled by the w_0 and w relation, which is the variation in the peculiar vibration cycle of the pressure gauge and in the time period of the outside force. Therefore, the relation between $T(t)_{\max}$ and w_0/w is obtained it is as shown in Figure 4(H). If w/w_0 is used as the abscissa to assist in expressing the result within the scope of this experiment, Figure 5(H) can be obtained from Figure 4(H). Therefore, even when the same explosion pressure wave strikes, if the peculiar vibration cycle that is the combination of the spring coefficient of the copper rod, the mass of the piston and the pressure sphere vary, the depth of the pressure scar will also vary. In other words, even though the wave forms are similar, if different wave lengths of the compression wave are measured with the pressure gauge, since the amplitude multiple differs, the deepness of the pressure scar will not be proportional to the actual value of the static load corresponding to the periodic maximum force of the pressure wave.

Essentials of the Experiment

One method of changing the value of w/w_0 is to change the wave length on the explosion pressure. However, because this experiment is conducted incidentally to experiments intended for other purposes in which a 1.7 kg cast picric acid bursting charge is being used, we changed the characteristic frequencies of the gauge. As shown in Table I(H), in order to change the weight of the pressure gauge piston, duralumin pistons were used in place of the usual brass pistons. On one hand, in order to change the spring coefficient of the copper rod, one type of lead rod was used in addition to the six types of copper rods. The static load determination curve of these copper or lead rods is shown in Figures 7(H) to 13(H). The spring coefficient was determined by making use of the observation that the depth of the pressure scar is almost a linear function of the static load as shown in the determination curve.

As shown in Figure 2(H), the essentials of the experimental setup of the bursting charge and the pressure gauge were as follows:

The bursting charge and pressure gauge were hung by strings at a depth of 2 meters (the depth of the pond in which experiments were carried out was 3.5 meters) in such a way that the front of the pressure gauge faced the explosive. We carried out three experiments in which the distances between the explosive and the pressure gauge were 3, 4, and 6 meters respectively.

We did not determine the wave form of the explosion pressure wave nor the pressure itself since we thought it unnecessary to the accuracy of the theory developed in this report. It seems quite possible that these will differ according to each experiment.

ENCLOSURE (H), continued

Table I(H)
COPPER ROD MANOMETER ASSEMBLY CHART

Manometer Symbol	Manometer	Cu Rod	\bar{w} (kg)	\bar{K} (kg/cm)	$w_0 = \frac{\bar{K}}{\bar{w}}$ (1/sec)	Remarks
B ₀ P ₁	B ₁	P ₁	8.67×10^{-6}	0.750×10^4	2.94×10^4	
B P ₁	B	P ₁	4.38×10^{-6}	0.750×10^4	4.14×10^4	
G P ₁	G	P ₁	1.75×10^{-6}	0.750×10^4	6.56×10^4	Pressure sphere = 3/8", Area upon which Pressure acts (=) - 1.131 cm ²
B ₂ P ₂	B ₂	P ₂	8.67×10^{-6}	1.333×10^4	3.92×10^4	
B P ₂	B	P ₂	4.38×10^{-6}	1.333×10^4	5.52×10^4	
G P ₂	G	P ₂	1.75×10^{-6}	1.333×10^4	8.73×10^4	
B ₃ P ₃	B ₃	P ₃	8.67×10^{-6}	0.750×10^4	2.95×10^4	
B P ₃	B	P ₃	4.38×10^{-6}	0.750×10^4	4.14×10^4	
G P ₃	G	P ₃	1.75×10^{-6}	0.750×10^4	6.55×10^4	
B ₄ P ₄	B ₄	P ₄	8.67×10^{-6}	1.410×10^4	4.03×10^4	
B P ₄	B	P ₄	4.38×10^{-6}	1.410×10^4	5.66×10^4	
G P ₄	G	P ₄	1.75×10^{-6}	1.410×10^4	8.99×10^4	
B ₅ P ₅	B ₅	P ₅	8.67×10^{-6}	0.972×10^4	3.35×10^4	
B P ₅	B	P ₅	4.38×10^{-6}	0.972×10^4	4.71×10^4	
G P ₅	G	P ₅	1.75×10^{-6}	0.972×10^4	7.46×10^4	
Y P ₆	Y	P ₆	20.4×10^{-6}	1.165×10^4	2.39×10^4	Pressure sphere = 2 mm, Area upon which pressure acts = 2.0 cm ²
B ₇ P ₇	B ₇	Lead rod P ₇	7.14×10^{-6}	0.0776×10^4	1.04×10^4	A = 0.95 cm ²
B ₈ P ₇	B ₈	P ₇	6.12×10^{-6}	0.0776×10^4	1.13×10^4	A = 0.866 cm ²
B ₉ P ₇	B ₉	P ₇	3.96×10^{-6}	0.0776×10^4	1.41×10^4	A = 0.283 cm ² Pressure sphere = 3/8"

We carried out seven experiments. The copper crusher gauge, the copper rod assembly, and the distance between the explosive and the pressure gauge for each experiment are as indicated in Table 2(H).

w/w_0 has the range $0.7 < w/w_0 < 2.6$ in the case of the copper rods, and the range $4.4 < w/w_0 < 6.0$ in the case of the lead rod. According to our theory $T(t)_{\max}$ should decrease in the range $w/w_0 < 0.62$ (approximate), but because it would require a copper crusher gauge with an extremely high frequency once the weight of the explosive had been fixed, we could not actually carry out the experiment.

Results of the Experiment and Analysis

In this experiment we treated all waves as simple sine waves of $10,000\omega$, read from Figure 4(H) the pressure amplitudes for corresponding distances from the explosive source, and concluded that this is the maximum value of the explosion pressure to which the copper rod was subjected. The reasons for this are two-fold: (1) As was stated in the first report, in the case of a 1.7 kg explosive, the explosion pressure wave is a simple damped sine wave of approximately $10,000\omega$; (2) The relationship between the distance from the explosive source and the pressure amplitude is known to be as in Figure 4(H).

The results of these experiments are shown in Figure 14(H). $T(t)_{\max}$ is defined as the ratio of the depth of the pressure scar actually registered on the pressure gauge to the depth of the pressure scar (as found from Figures 7(H) to 13(H)) in the case of a static load equivalent to the product of the periodic maximum value to the compression (obtained from Figure 4(H) and the area of the area of the pressure surface of the piston.

ENCLOSURE (H), continued

As is seen from Figure 14(H), within our experimental range, namely $0.7 < w/w_0 < 6.0$, we can say that there is a tendency for the value indicated on the copper crusher gauge to decrease steadily as w/w_0 increases, although the same explosion pressure wave is added. Moreover, in the range of our experiments it can be recognized quantitatively that the experimental values are very near to the values computed by our simple theory, but since the scattering was rather great we could not come to any quantitative conclusion. It is obvious, however, that in general the values are less than the theoretical values in the neighborhood where $T(t)_{\max}$ is large, and great where $T(t)_{\max}$ is small. Further, by observing in more detail the tendency of the scattering, it can be found that at a distance of three meters (at which the explosive pressure is larger) the experimental values of $T(t)_{\max}$ is smaller than at the distance of six meters (at which the pressure is smaller). We can say that there is a tendency for the experimental values of $T(t)_{\max}$ to be less than the theoretical values in cases where the pressure scar is shallow. We believe that the reason for this lies in the fact that we neglected the elasticity of the copper rod, and the friction between the copper rod and the cylinder etc.

Table II(H)
DISTANCE BETWEEN THE EXPLOSIVE AND THE PRESSURE GAUGE
FOR EACH EXPERIMENT

No. of Experiment	Pressure and Copper Rod Assembly Utilized	Distance between Bursting Charge and Gauge (m)	Water Temp. (°C)
1	BXP ₁ , BXP ₂ , HP ₁ , HP ₂ , GP ₁ , GP ₂ BXP ₁ , BXP ₂ , HP ₁ , HP ₂ , GP ₁ , GP ₂	3 6	10
2	BXP ₄ , BXP ₅ , HP ₄ , HP ₅ , GP ₄ , GP ₅	4	11
3	BXP ₃ , BXP ₄ , HP ₃ , HP ₄ , GP ₃ , GP ₄ BXP ₃ , BXP ₄ , HP ₃ , HP ₄ , GP ₃ , GP ₄	3 6	11.5
4	BXP ₃ , BXP ₄ , HP ₃ , HP ₄ , GP ₃ , GP ₄ BXP ₃ , BXP ₄ , HP ₃ , HP ₄ , GP ₃ , GP ₄	3 6	21
5	BXP ₃ , BXP ₄ , HP ₃ , HP ₄ , GP ₃ , GP ₄	3	18
6	YP6	3 4 6	12
7	BYP ₇ , BZ ₁ P ₇ , BZP ₇ , BZ ₁ P ₇	3 4	28

ENCLOSURE (H), continued

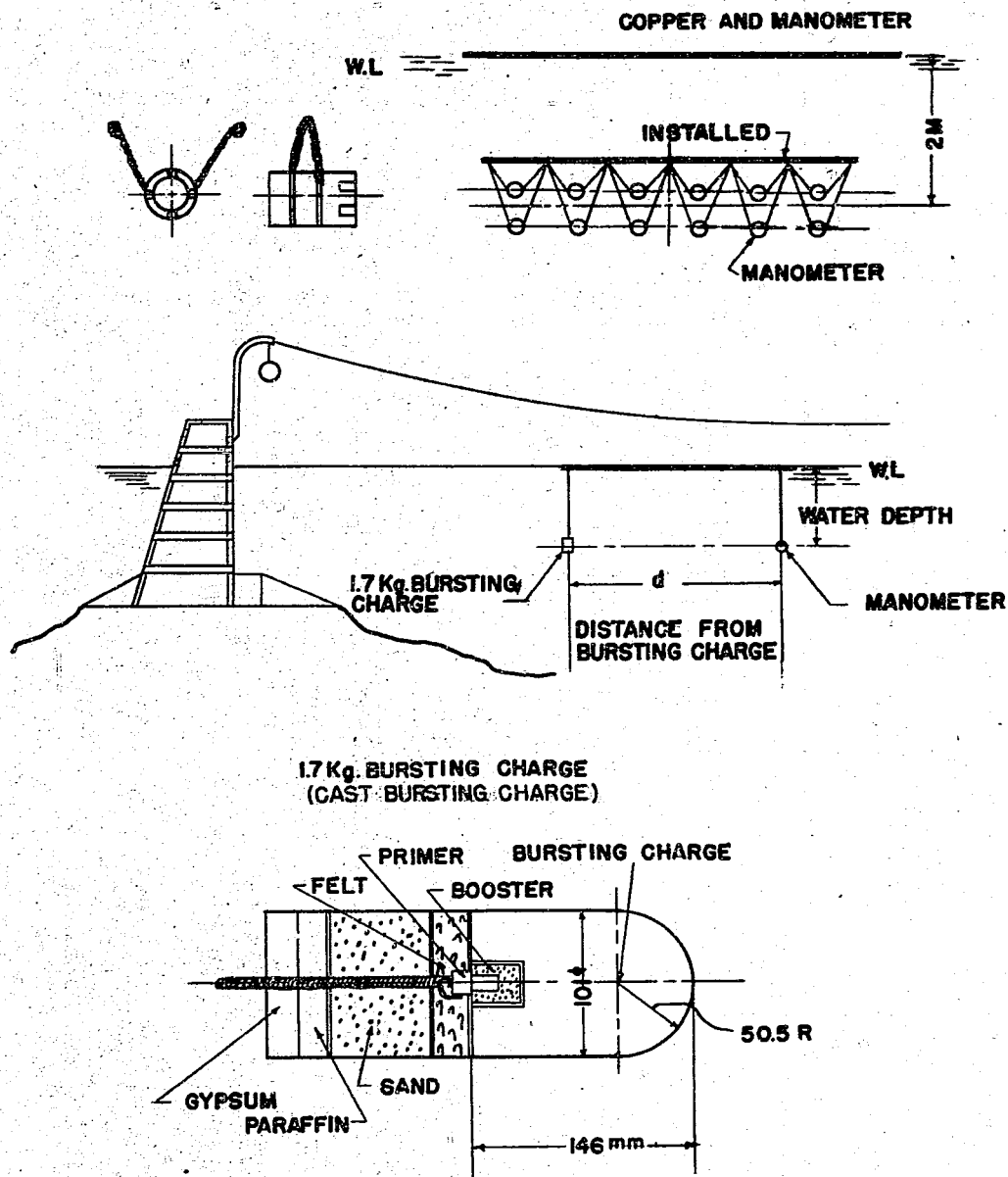


Figure 2(II)
 DIAGRAM GIVING ESSENTIALS OF UNDERWATER EXPLOSION PRESSURE TEST

ENCLOSURE (H), continued

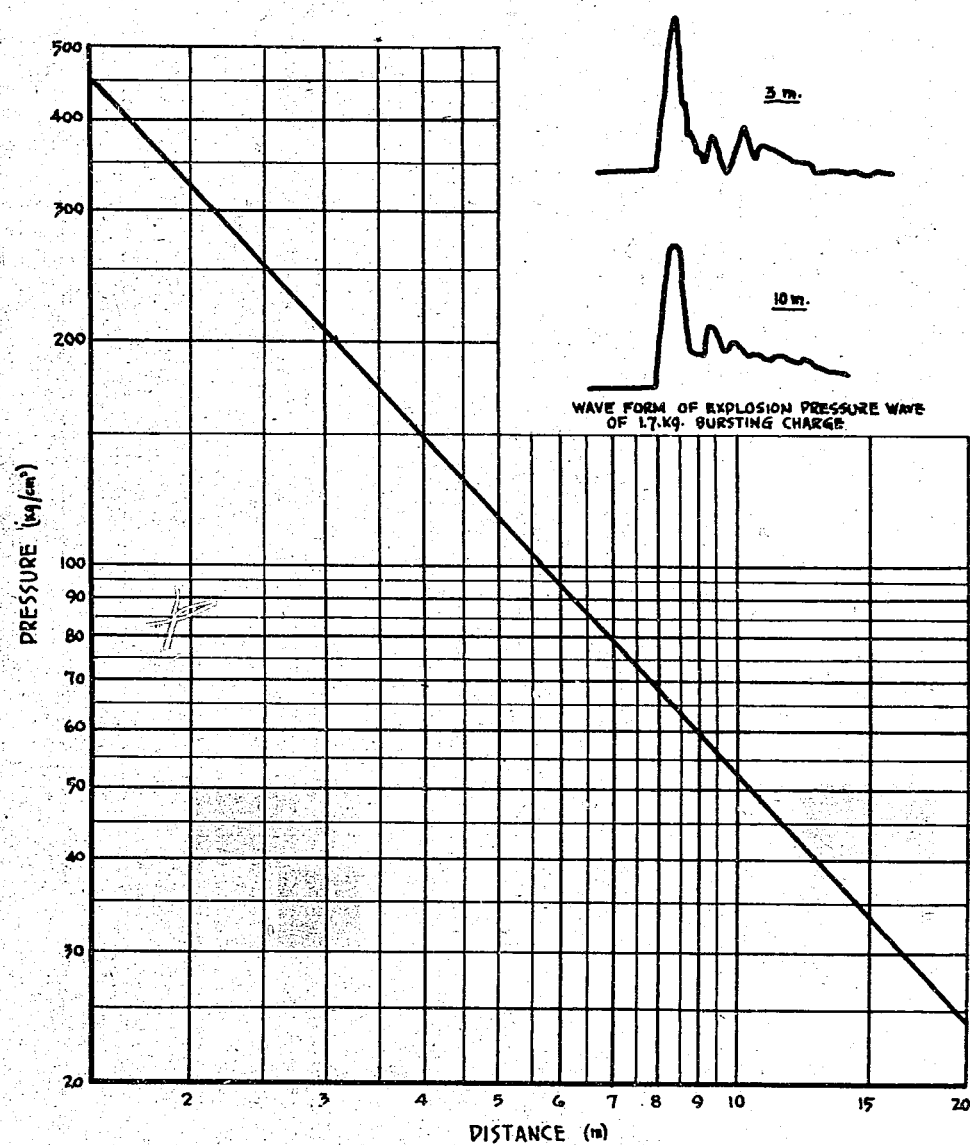


Figure 3(H)
1.7 kg BURSTING CHARGE EXPLOSION PRESSURE ONE DIMENSIONAL CURVE

ENCLOSURE (H), continued

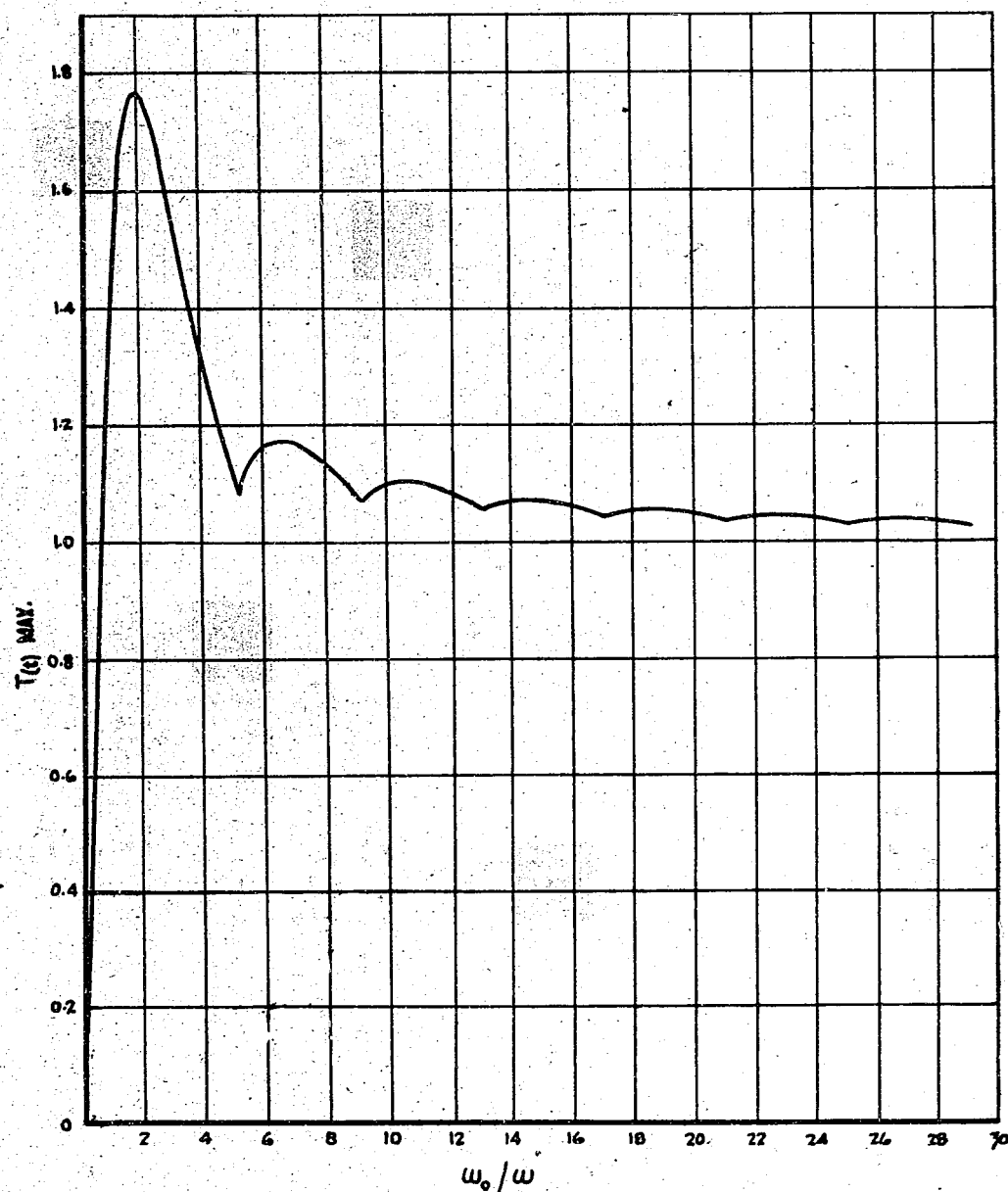


Figure 4(H)
AMPLITUDE MAGNIFICATION CURVE FOR
INDEPENDENT SINE WAVE FORM EXTERNAL FORCE

ENCLOSURE (H), continued

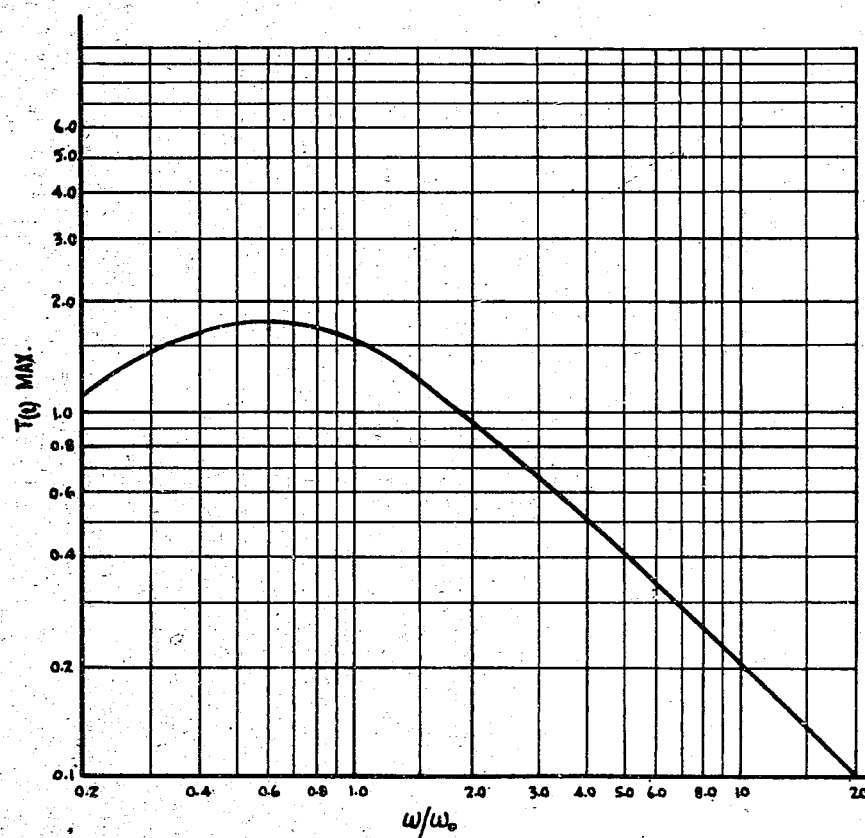


Figure 5(H)
AMPLITUDE MAGNIFICATION CURVE FOR
INDEPENDENT SINE WAVE FORM EXTERNAL FORCE

ENCLOSURE (H), continued

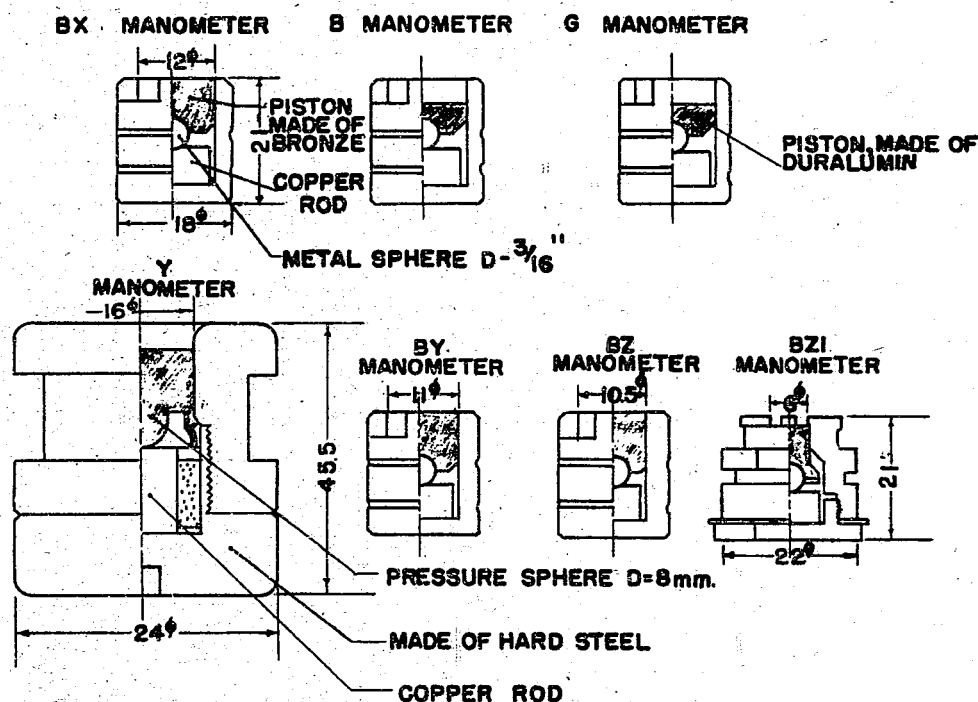


Figure 6(H)
PRESSURE SPHERE GAUGE DETAILS

Type	BX	B	G	Y	BY	BZ	BZI
Diameter of Piston (mm)	12.0	B	G	16.0	11.0	10.5	6.0
Area of Piston Section (cm ²)	1.131	B	G	2.0	0.950	0.866	0.283
Wt. of Piston and Sphere (gm)	8.5	4.29	1.71	20.0	7.0	6.0	3.9
Wt. of Cu Add (Pb) (gm)	4.1	4.29	1.71	10.2	5.2	6.0	3.9
Outer Diameter of Cylinder (mm)	18.0	4.29	1.71	24.0	18.0	6.0	22.0
Wt. of Cylinder (gm)	25.3	4.29	1.71	326.0	27.3	28.8	43.0
Height of Cylinder (mm)	21.0	4.29	1.71	45.5	21.0	28.8	43.0
Wt of Cylinder and Cu Rod (gm)	29.4	4.29	1.71	350.0	31.4	32.9	42.8
Total Wt. (gm)	37.9	33.7	33.1	370.0	38.4	38.9	51.1

ENCLOSURE (H), continued

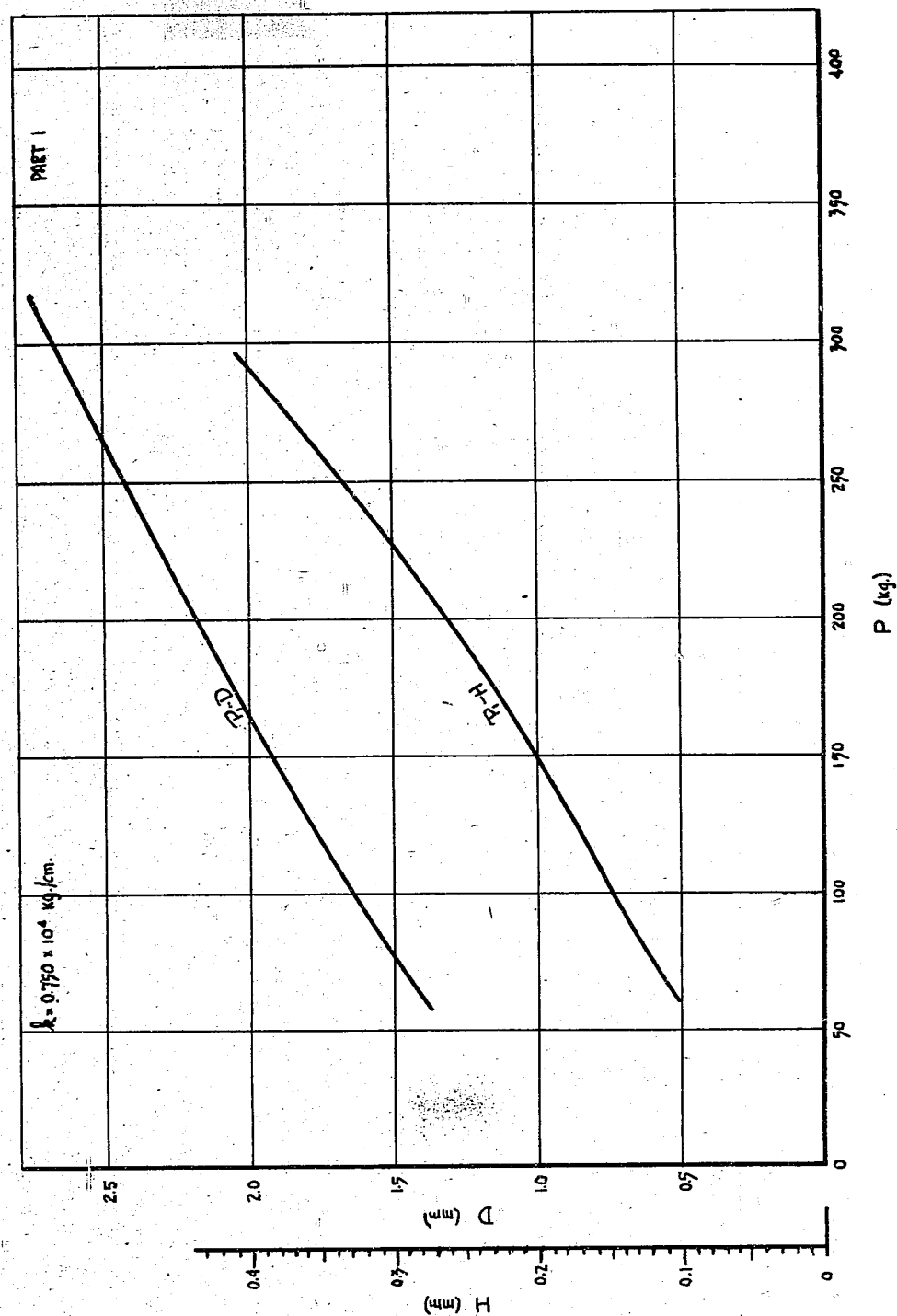


Figure 7(H)
COPPER ROD PRESSURE SPHERE DETERMINATION CURVE TYPE P1

ENCLOSURE (H), continued

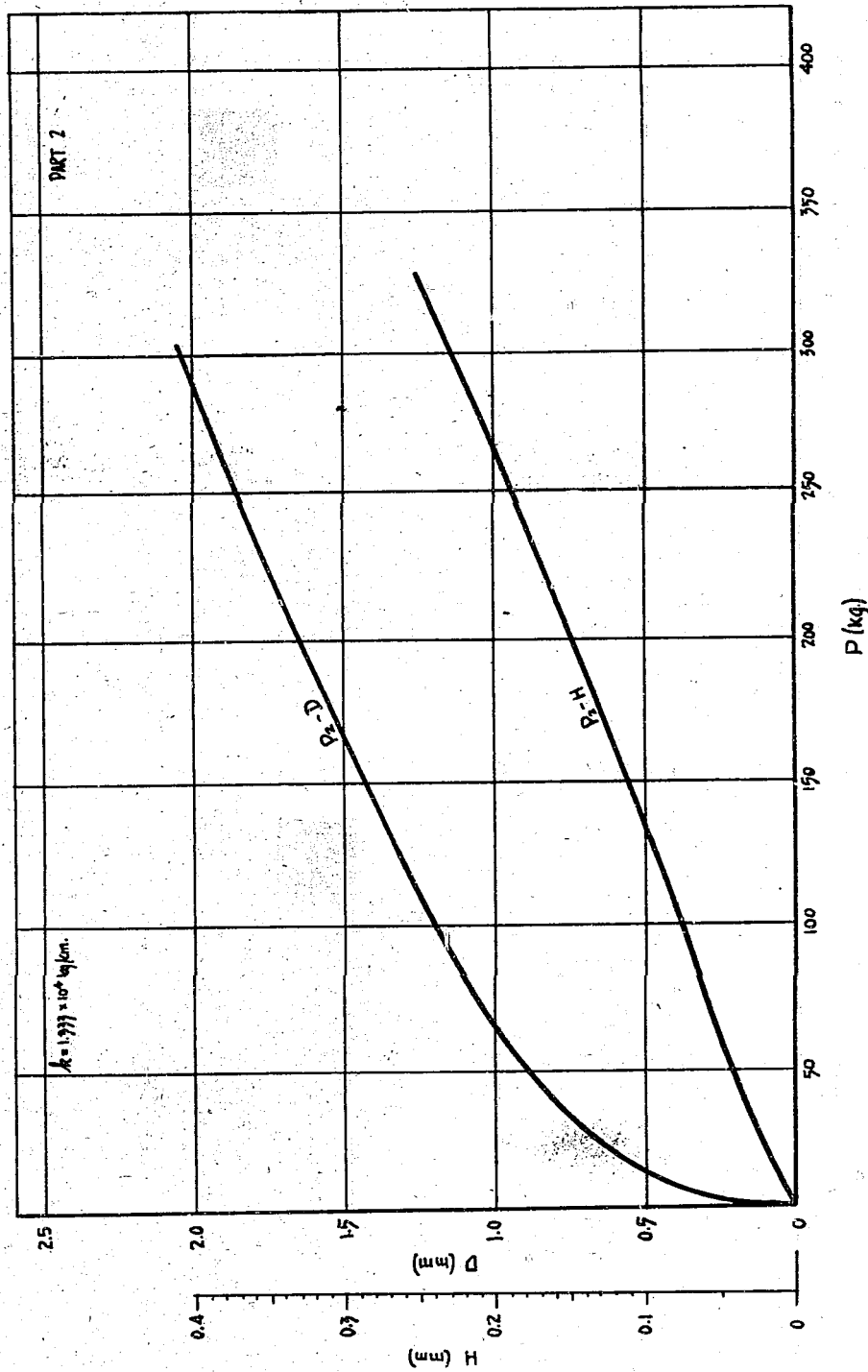


Figure 8(II)
COPPER ROD PRESSURE SPHERE DETERMINATION CURVE TYPE P2

ENCLOSURE (H), continued

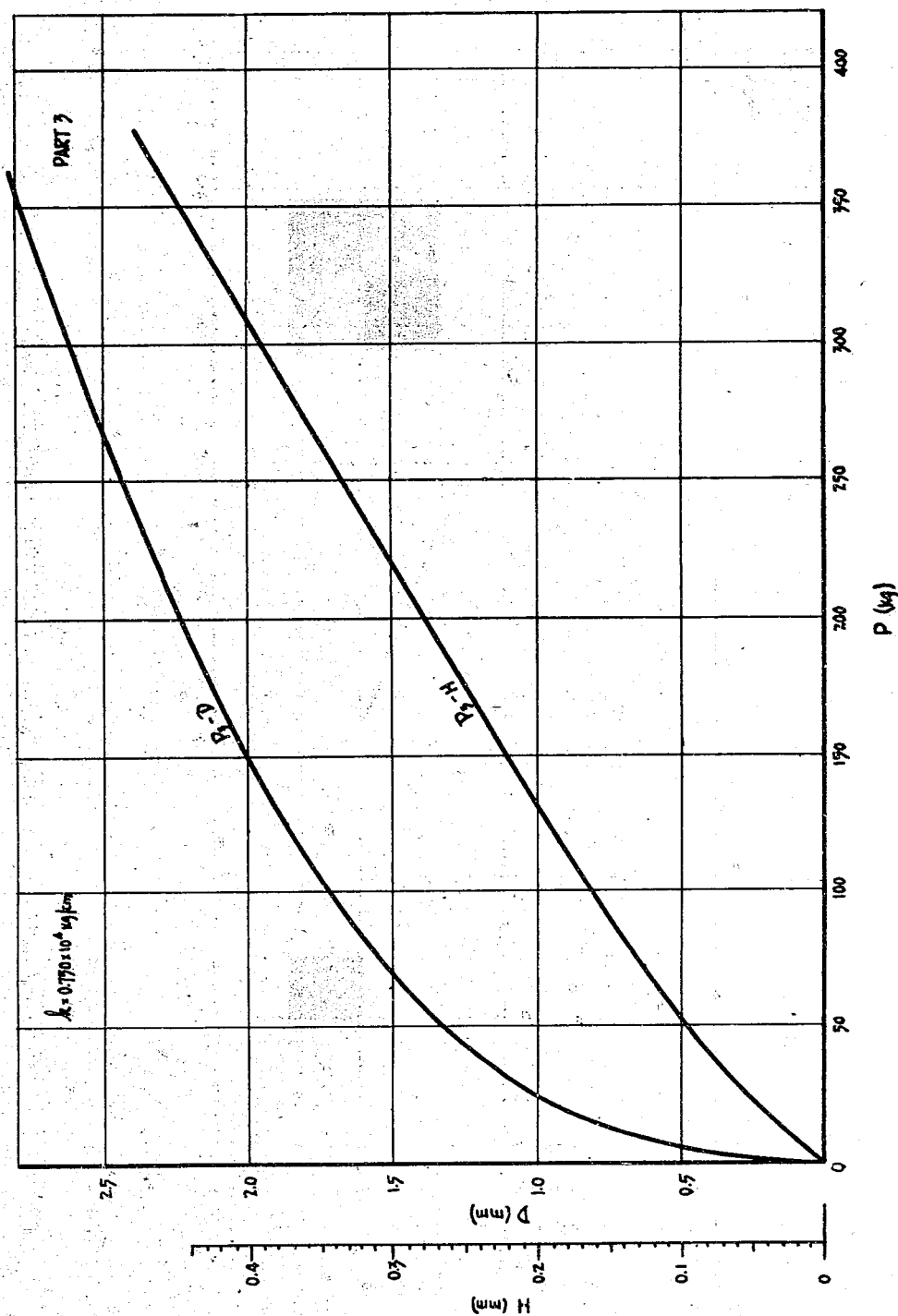


Figure 9(H)
COPPER ROD PRESSURE SPHERE DETERMINATION CURVE TYPE P3

ENCLOSURE (H), continued

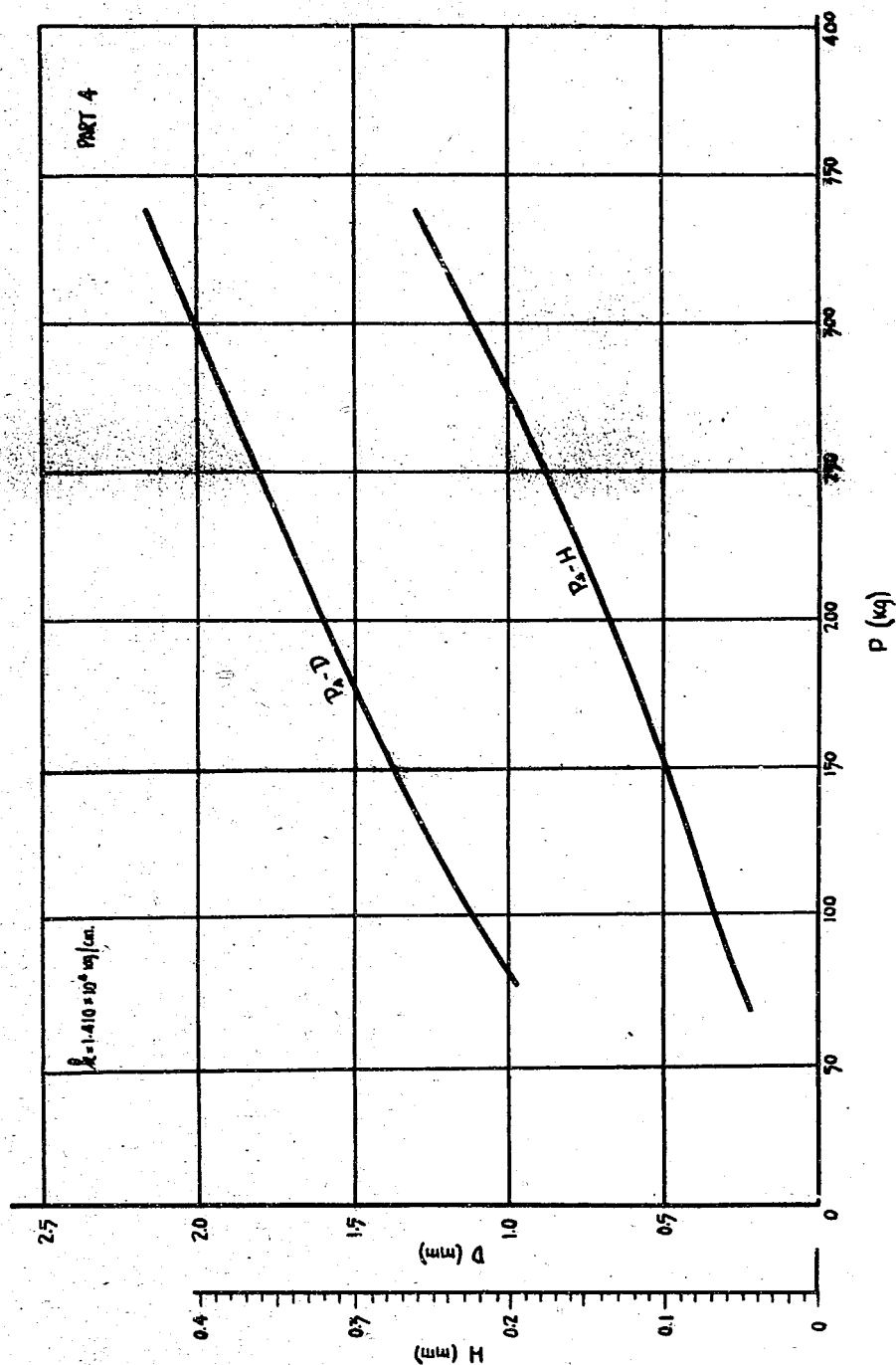


Figure 10(H)
COPPER ROD PRESSURE SPHERE DETERMINATION CURVE TYPE P_4

ENCLOSURE (H), continued

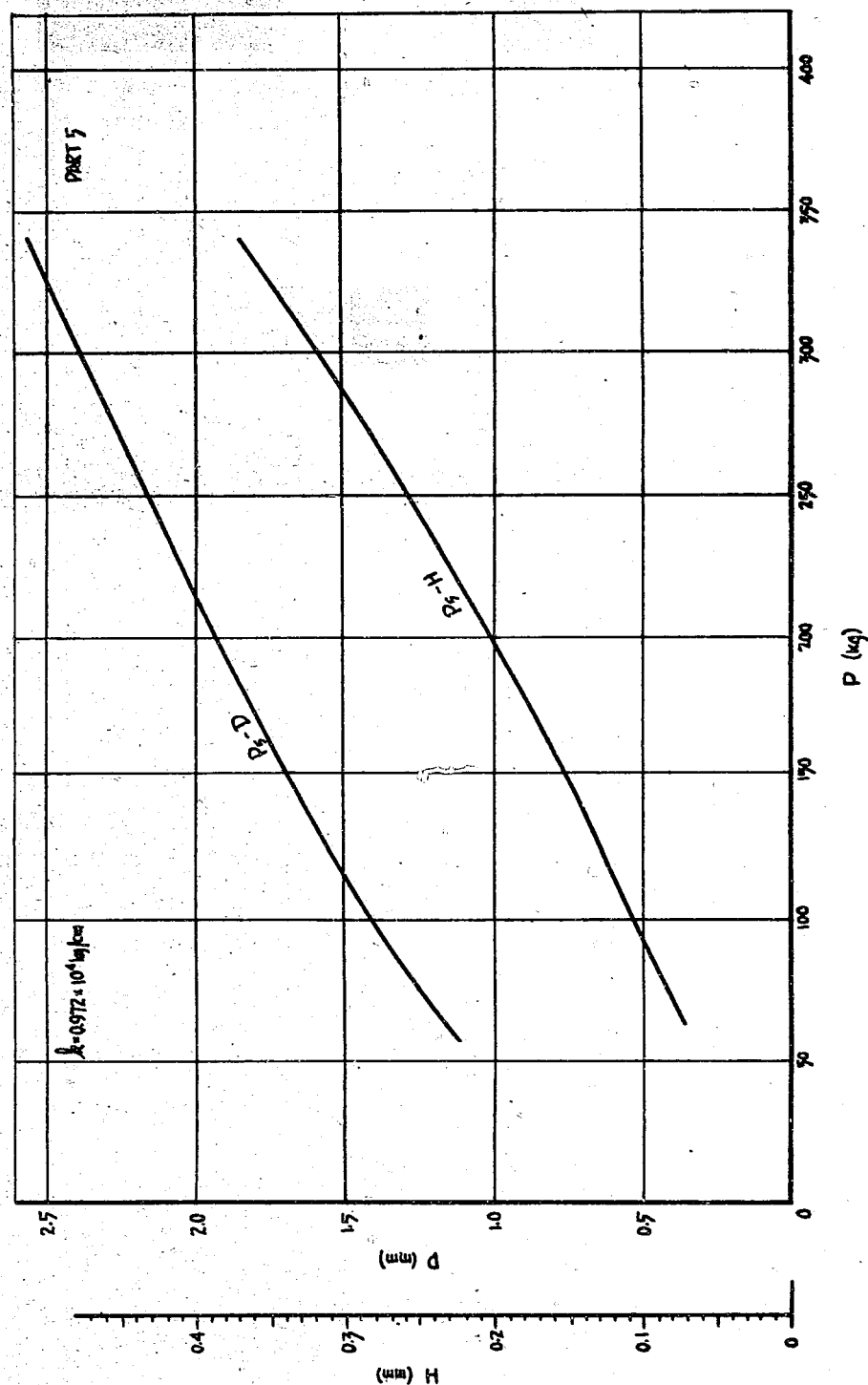


Figure 11(H)
COPPER ROD PRESSURE SPHERE DETERMINATION CURVE TYPE P5

ENCLOSURE (H), continued

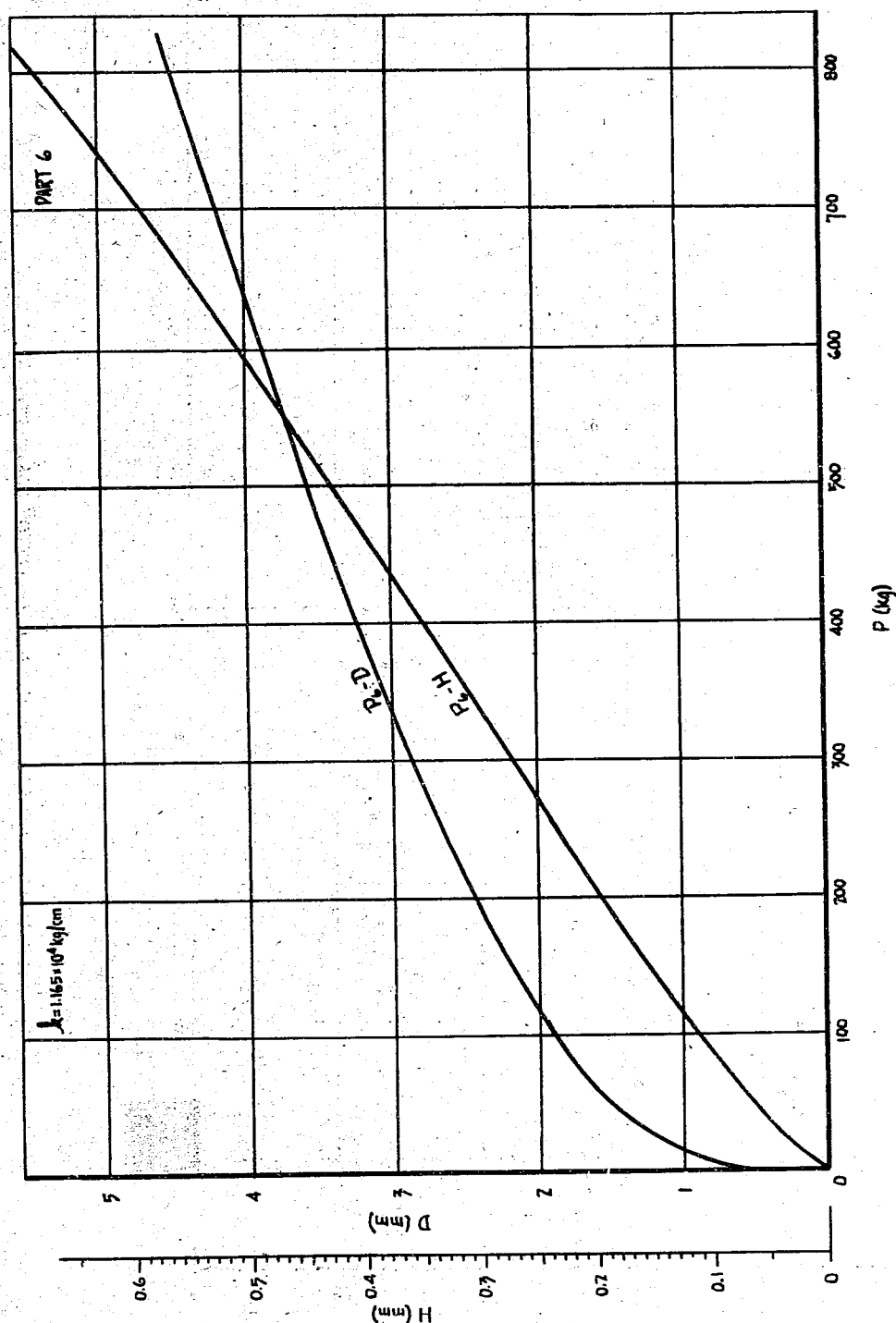


Figure 12(II)
COPPER ROD PRESSURE SPHERE DETERMINATION CURVE TYPE P 6

ENCLOSURE (H), continued

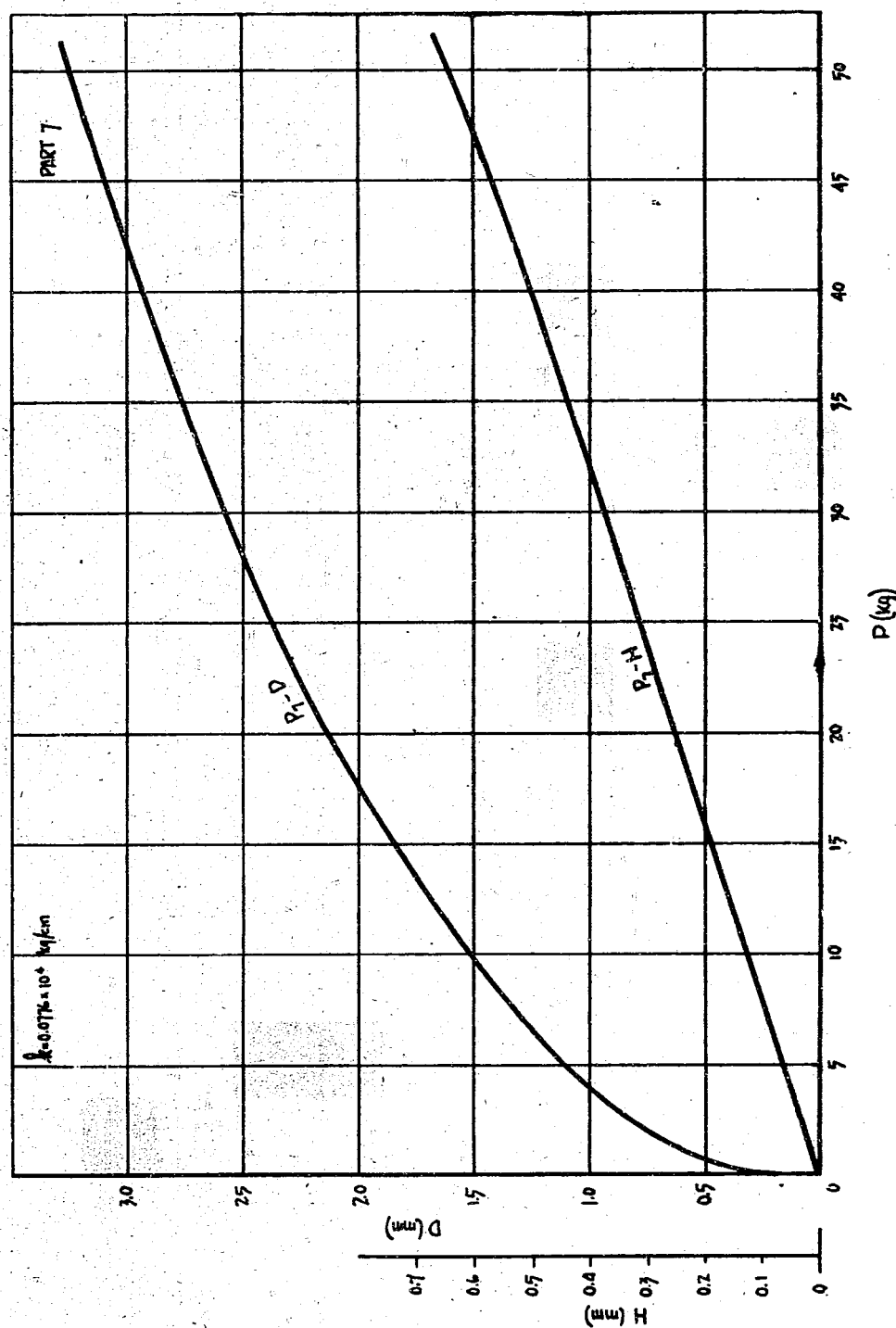


Figure 13(H)
COPPER ROD PRESSURE SPHERE DETERMINATION CURVE TYPE P7

ENCLOSURE (H), continued

KEY: FIRST NUMBER INDICATES TEST NO. (1007)
 LETTER INDICATES TYPE OF ROD (ALUMINUM, STEEL, COPPER)
 SECOND NUMBER INDICATES DISTANCE TO EXPLOSIVE (3.0, 6 METERS)

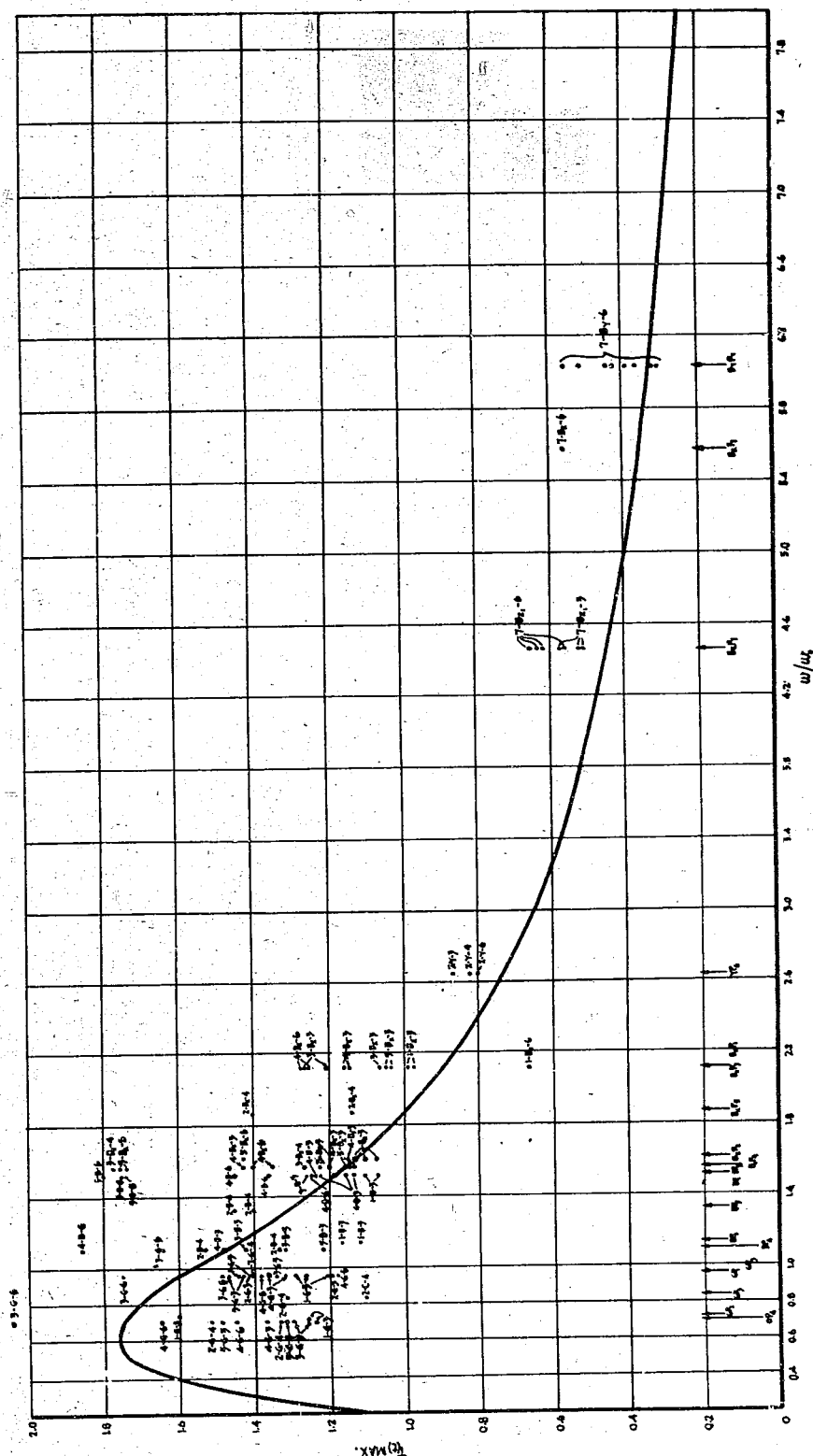


Figure 14(II)
 COMPARISON OF CALCULATED AND STATIC LOAD DETERMINATIONS
 of T_t (max) vs. w/w_0

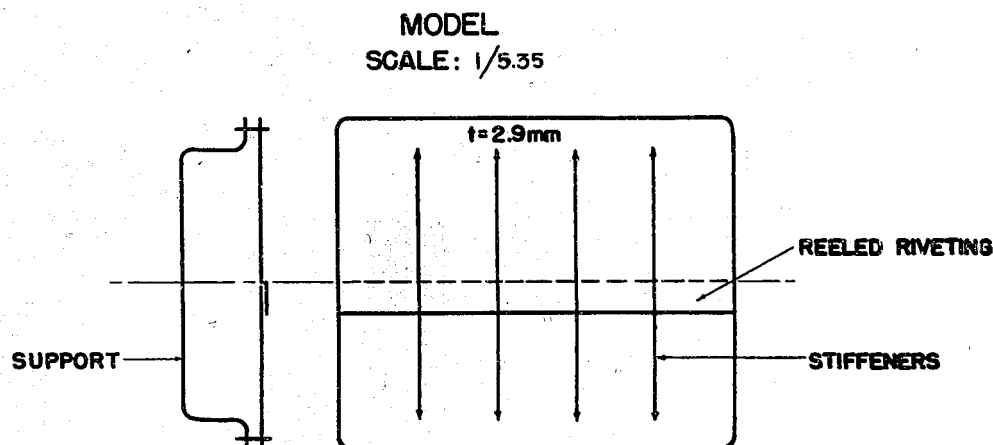
ENCLOSURE (I)

VARIOUS EXPERIMENTS NOT COVERED IN THE TRANSLATED REPORTS

1. Experiments on the Strength of Shell Plating Subject to Non-Contact Underwater Explosions

One series of model experiments was conducted on this subject at the Naval Technical Research Institute, Meguro Ku, TOKYO. Only one thickness of plating was used which was roughly equivalent to the shell plating of a battleship or a merchant ship (25 lbs).

Details of experiment are as follows:



Model	Scantlings of Stiffeners	No. of Stiffeners
A	35mm x 3mm	6
B	50mm x 4mm	4

Charges used : 0.4 kg, 0.9 kg, 1.7 kg. (picric acid)

Depth of charge = 0.8 m (4.28 m full size)

Conclusions:

- Maximum deflection is proportional to volume of deformation
- Maximum deflection is proportional to $W^{0.9} \times D^{-2.1}$

where W = weight of charge

D = distance between the outer shell plating and the point of explosion.

- Critical distances at which the plate can remain tight:

ENCLOSURE (I), continued

Model	Charge	Distance	
	Full Size	Model	Full Size
1.7 kg	200 m	3.7mm	20 m
0.9 kg	107 m	2.6mm	14 m
0.4 kg	47.5 m	1.8mm	9.5 m

2. Photographs of Underwater Explosions at Hiratsuka Arsenal

For some years one man had been working on the photography of the explosion of small underwater charges. He seemed only interested in the theoretical aspects and had not tried to connect his experiments with ship damage. This was another case of the Japanese working in "watertight compartments".

He worked with one gm of explosive in a model tank with two glass sides. He had no cine-camera but used eight fixed cameras which were illuminated by successive sparks. The interval between sparks could be from 2-20 microseconds.

His work was far behind anything done in the United States or Great Britain. He had not even noticed the oscillation of the gas bubble as all his experiments were done too close to a surface.

Two untranslated reports of this work have been forwarded to WDC.

ENCLOSURE (J)

LIST OF DOCUMENTS FORWARDED TO WASHINGTON DOCUMENT CENTER

<u>NavTechJap No.</u>	<u>Title</u>	<u>ATIS No.</u>
ND50-1313	Model Tests on the Strength of Submarine Hulls against Underwater Explosions.	4275
14	Experiments on Watertight Ready Service Lockers for Submarine Ammunition.	4276
15	Record of Bulge Construction ASHIGARA (CA). (NACHI Class)	4277
16	Report of Experiments on the Effective Depth of the Power of Explosives.	4278
17	Comparative Table of Bulge of Battleships (NAGATO Class)	4279
18	Underwater Explosions (Vol I and II) (Experiment in Photography of one gm of Explosure)	4280
19	Strength of Bulge of First-Line Ships.	4281
20	Research on Armor Plate as Protection against Torpedo Explosions.	4282